MANCHESTER 1824
The University of Manchester

Faculty of Engineering and Physical Sciences

School of Mechanical, Aerospace and Civil Engineering

Electrical Supply and Demand in Cyprus:

Optimal use of Renewable Energy Sources in Electricity Production

Written by:

Christos Kettenis, 8113949

Supervised by:

Dr. Rodger Edwards

Temporarily Supervised by:

Dr. Paul Watkins

Dr. Ruth Wood

Dr. Sarah Mander

PhD Thesis

2016

Table of Contents

Word count: 75183

Table of Abbreviations

Initials	Name	Initials	Name
AC	Alternating Current	***LED***	Light Emitting Diode
Bar (a)	Bar (absolute)	***LNG***	Liquefied natural gas
BV	Bypass Valve	***N_2O***	Dinitrogen Oxide
CCHP	Combined Cooling, Heating and Power	***NGB***	Natural Gas Boiler
CCS	Computerized Control Subsystem	***NSC***	Non-Storage Calorifier
CFL	Compact Fluorescent (light bulb)	***ORC***	Organic Rankine Cycle
CHP	Combined Heating and Power	***PCHE***	Phase Changing Heat Exchanger
CH_4	Methane	***PCM***	Phase Changing Material
C_2H_6	Ethane	***PTSC***	Parabolic Trough Solar Collector
CO	Carbon (II) Oxide (Monoxide)	***PV***	Photovoltaic
CO_2	Carbon (IV) Oxide (Dioxide)	***RES***	Renewable Energy Sources
COP	Coefficient Of Performance	***SA***	Steam Accumulator
CP	Condensate Pump	***SCU***	Special Control Unit
CStT	Condensate Storage Tank	***SEC***	Smart Energy Community
CV	Calorific Value	***SEG***	Synchronous Electrical Generator
DC	Direct Current	***SFR***	Steam Flow Regulator
DHW	Domestic Hot Water	***SIM***	Smart Integration Module
DSM	Demand Side Management	***SIS***	Solar Irradiation Sensor
DSG	Direct Steam Generation	***SS***	Steam Separator
EAC	Electricity Authority of Cyprus	***ST***	Steam Turbine
EHS	Environment Hazard and Safety	***STh***	Solar Thermal
FP	Flow Pump	***TB***	Thermal Battery
HE	Heat Exchanger	***tCO_2e***	Tonnes of CO_2 equivalent
HGHE	Horizontal Ground Heat Exchanger	***ThST***	Thermal Storage Tank
HOP	Hot Oil Pump	***TSM***	Thermal Storage Medium
IHE	Internal Heat Exchanger	***TSO***	Transmission Network Operator
LCD	Liquid Crystal Display	***WFV***	Working Fluid Vapour

List of Equations

List of Figures

List of Tables

Abstract

As fossil fuel usage has been proven to have a negative impact on human health and the environment, the world has embraced the usage of renewable energy sources, mainly for energy production. In Cyprus, solar energy is the most potent renewable source and this can be seen by the vast majority of the population using solar water heaters in their households. This thesis explores the usage of solar energy for electricity and domestic hot water production at a residential level by presenting the designs of three solar-thermal concept systems for achieving this task; the first being the basic design of all three without any form of storage, the second is fitted with thermal latent heat storage and the third is fitted with a natural gas boiler instead. The optimal solution is the second concept system that is capable of storing thermal energy around the year thus having a nearly uninterrupted operation, reducing the dependency on fossil fuel produced electricity and emissions. The thesis also explored the usage of siloxane organic compounds as working fluids for a low temperature Rankine cycle, which had a significant impact in the increase of the thermal-to-electrical efficiency of the cycle, raising it to nearly 25%, greater than the efficiency of best acclaimed photovoltaic collector currently available. Lastly, taking into account a typical household's demand profile and by allowing the optimal system to operate as part of the national electrical network continuously, the size of the system's components could be reduced significantly making it more feasible for installing in a typical household's premises. However, due to the non-existence of these components in the within the project's specifications, the thesis could not include a useful economic analysis for a more realistic comparison with a similar sized photovoltaic system.

Declaration

No part of this Thesis has been used for the submission of another degree or diploma of any sort in the University of Manchester nor any other institution.

Copyright Statement

Acknowledgements

I would like to thank my parents, Nicos and Chrysso and my brothers, Aristotelis and Alexandros for their support and motivation in executing this project.

Special thanks and gratitude are due to my supervisor, Dr. Rodger Edwards, for his guidance and advice during the course of this project.

I would also like to thank my three interim supervisors, Dr. Paul Watkins, Dr. Ruth Wood and Dr. Sarah Mander, for their precious assistance during my supervisor's health leave.

Chapter 1: Introduction

Section 1.1: Problem statement

Renewable energy has been the centre of attention for researchers around the world during recent years for numerous reasons. These reasons include the increasing energy demand per capita, the change in climate, the increasing greenhouse gas emissions and the environmental destruction caused by the various ways of acquiring them. Moreover, accidents during the excavation and transportation of fossil fuel, such as leakages and explosions, trigger oil spills and massive fires, which in turn destroy important ecosystems in the oceans, swamps and forests and additionally cause the loss of human lives. Furthermore, the most important reason of all is that fossil fuels exist in limited amounts underground. Oil, coal and natural gas cannot be regenerated by natural processes in short periods of time and as with most of the natural resources, they have to be extracted from mines or the ocean floor which also results in more pollution and environmental destruction. The excavation processes also require large transportation vehicles and sea vessels, drilling equipment, explosives and storage facilities. All these components have high operation and maintenance costs and as a result the end use prices of fossil fuels are increasing every year.

In contrast, Renewable Energy Sources (RES) are considered unlimited and abundant. The reason for this is that they are derived from natural phenomena, such as the wind, ocean waves and tides or the movement of a large mass of water from a high altitude to a low altitude, such in the case of a waterfall. Secondly, these sources produce almost no emissions while they are being harnessed and converted from one form to another, except biomass and only when it is combusted in the atmospheric air. Additionally, the environmental impact of harnessing energy from RES is minimal, compared to the pollution and destruction caused in the case of fossil fuels. However, sustainable and clean energy, provided by natural processes, is not stable relative to fossil fuels. For example, wind speed and solar irradiance are not constant quantities throughout the year, compared to the very controllable flow and calorific value of fossil fuels into a conventional power station's boiler. This intermittent character makes RES not as reliable as fossil fuels and this is another important reason why RES have attracted the scientific interest.

In Cyprus the increasing electricity demand has always been accommodated by the usage of fossil fuels until recently. Space heating and cooling are provided by central heating systems and air conditioning units, respectively, devices that consume large

amounts of energy during operation. In addition, buildings which were constructed prior to 2004 are not fitted with proper thermal insulation and thus the need for space heating and cooling is increasing the electricity and fuel consumption even more. Public transport is almost absent in the country and as a result the citizens do not have any other alternative than to purchase their own automobiles. Even though the automotive technology is constantly evolving, producing more fuel efficient passenger and commercial vehicles and with fewer emissions, the sheer number of passenger automobiles relative to the population in Cyprus is already very large and increasing. Additionally, the three power stations, situated on the south and southeast of the country, still produce electricity using heavy fuel oil and gasoil almost exclusively. However, Cyprus is one of the leading countries in the EU in installed collector surface area for solar water heating systems per capita; wind and solar energy are also being partially exploited for electricity production at national and residential levels respectively. Lastly, natural gas deposits have been discovered in the Exclusive Economic Zone of Cyprus, which may lead to the replacement of heavier fossil fuel with Liquefied Natural Gas (LNG) in the electricity production industry.

Because of the long periods of sunshine in Cyprus, the renewable source with the most potential is solar energy. This is the reason why almost all households in Cyprus are equipped with solar heating systems, which Cypriot citizens consider a sound investment. Wind energy is also considered important in the country; however it does not have the same potential as solar energy. The wind speed is not uniform throughout Cyprus and its strength is marginal in some parts of the country, whilst in others is minimal. Biomass is another a good example of a renewable energy source, as it can partially solve the problem of municipal organic waste when it is combined with the cultivation of specialised crops for energy and biofuel production. For this source to be productive, safe and environmentally suitable a basic infrastructure of irrigation water and land area is needed, which at the present time is inadequate. In addition, there is no infrastructure for recycling the municipal organic waste for harnessing **methane** (**CH_4**) gas and production of biodiesel. Geothermal energy could be used in the country as in other parts of the world, but the high costs prohibit its usage in large scale especially during this period of financial crisis. Hydroelectric power is not suitable for the terrain of Cyprus, as there are no high altitude waterfalls and the cost of constructing artificial reservoirs is also a problem. Lastly, tidal and wave energy are non-exploitable in the small area of Eastern Mediterranean at this point of time.

Section 1.2: Project aims and methodology

Even though Photovoltaic (**PV**) systems are more appealing for installing in individual households at present, a Solar Thermal (**STh**) system is more advantageous in terms of efficiency, energy storage and capability of safe interconnection with the national electrical network. More analytical reasons for choosing to use the STh technology for this thesis instead of PV are presented in Chapter 3. This project's system would also have the capability of exploiting its waste energy for heating up Domestic Hot Water (**DHW**), since almost all residential buildings in Cyprus are currently fitted with solar water heaters and this idea should not be abandoned. Furthermore, the project attempts to explore the case of a domestic scale STh system, as manufacturers today utilize this technology for manufacturing larger scale systems that operate at a metropolitan level. As with solar water heaters, such a system would render its host household into a small power plant capable of entirely covering its electricity demand and also provide the excess to the national network. This would reduce the country's dependency on fossil fuel for energy production, thus providing financial and environmental benefits and it could also allow the national network to operate even if the Electricity Authority of Cyprus (**EAC**) is unable to fully cover the country's electricity demand entirely. The next sections present the aim and objectives of this project in further detail as well as a summary of its chapters and the methodology followed.

Section 1.2.1: Aim, Objectives and Tasks

Project Aim:

This project is set to design a STh system producing electricity and DHW for usage in households or apartment blocks in the Republic of Cyprus with the additional capability of safely injecting electrical energy into the national electrical network in times of need. The system will be based on a modified version of the Rankine cycle that is widely used in modern power plants. The size of this system's components and thermal-to-electrical efficiency will be mathematically calculated and the feasibility of installing such a system in residential units in the country will be examined.

Objective 1: Collect and analyse current background data for Cyprus:

a) **Gather the raw data from various government sources**. The first task is to concentrate data from almost every aspect of Cyprus' economy and way of life from official and reliable state sources so that they can be analysed in the next chapter.

b) **Analyse the gathered raw data**. This meta-analysis allows the identification of possible problems and various other issues that constitute Cyprus' current situation regarding the energy and emissions domains. This task eventually leads to the planning and conception of this project specific system solution that ultimately addresses these problems.

Objective 2: Design and simulate three alternative concept systems:

a) **Make calculations of the hot water and electricity demand of buildings in Cyprus**. These figures represent the demand for electricity and DHW of the building that the optimal system would be installed in.

b) **Design three concept system solutions**. Here, three alternative concept system designs are drawn with the aid of a drawing computer software package. This design step is crucial in the engineering process, as it forms the basis on which the engineer illustrates his thoughts about the project he executes and allows him to optimize his design before it passes to the simulation and/or manufacturing phases, thus reducing its complexity and costs.

c) **Calculate the capacities of the systems**. The purpose of determining the size of the three systems' components is the complete accommodation of the corresponding building's needs, calculated in the first task.

d) **Simulate the designs**. The Engineering Equation Solver (EES) software package (version 6.883-3D) is used for simulating the behaviour of each individual system by using the acquired component data from the literature. Here, the systems' engineering implementation capability is studied and design corrections can be made for optimizing each system.

e) **Acquire system component data and prices**. Information is gathered about the specifications and prices of existing components for implementing the optimal system

of the three. Since this project's goal is not the creation of new technology, rather the usage of existing components, the optimal solution could be implemented immediately while the acquisition and maintenance costs can be calculated and comparisons between the optimal system and a similar sized PV system can be made.

Novelty and contribution:

a) The project is novel in the sense that it attempts to examine the feasibility of electricity producing STh systems at a domestic scale. Currently, STh systems exist medium to large scale producing electrical power between several **MW** to several hundred **MW**.

b) In addition to the domestic scale electricity production, this project's system design also incorporates the production of DHW by exploiting the waste heat of the Rankine cycle.

c) Furthermore, the system design for this project is based specifically on the weather and solar irradiance conditions of Cyprus, although this does not limit its usage in countries with similar or lower latitude north and south of the Equator.

d) Another significant novelty is the examination of alternative organic working fluids for replacing water/steam on the basic Rankine cycle in order to improving its overall efficiency at low temperatures (around **400℃**).

The project's contribution is the examination of whether a STh system solution could become a feasible alternative to residential scale solar Photovoltaics that are currently being used in Cyprus from a technical point of view. In addition, even though it is not a goal of this project to create new technology, after the theoretical design process indicates the optimal system solution, an attempt to realise it using existing components would allow the basic calculation of acquisition and maintenance costs. This would render the system more realistic and financial comparison between it and similar sized PV systems would also be achievable. As a result, the project would be in a position to conclude more confidently whether or not the proposed optimal solution is more economically viable for installing in households instead of Photovoltaics.

Section 1.2.2: Project Breakdown

With all the above in mind, the project is broken down as such:

a) Chapter 2 contains the project's Literature Review with the important background information about energy production and consumption in Cyprus as well as important data about the existing electrical network extracted from various agencies and government services. It also analyses how much energy is been consumed by economic sector and building type and what measures have been proposed for energy saving and conservation. Lastly, it analyses the potential and exploitation of RES in Cyprus today, showing the benefits and problems of each one for the case of this country in particular and setting the foundations on which the project moves into the system proposal. The chapter also includes the work of other scientists in similar scientific directions with this Thesis'.

b) Chapter 3 analyses several fundamental topics of Thermodynamics, as the author's scientific background is not in Mechanical Engineering, rather than in Electrical and Computer Engineering. It also provides the opportunity to any reader interested in the field of renewable energy with a scientific background not deeply associated with Mechanical Engineering to appreciate the content of this project and the idea behind the whole effort.

c) Chapter 4 describes and discusses the main design procedures and results of this project's main research task, developing the three concept systems and determining the preferred choice on the basis of simulation results obtained.

d) Chapter 5 presents the environmental impact that each of the systems would have and compares the financial cost of using Concept System 3 operating on natural gas against the cost of producing electricity in a national power, operating on diesel. Finally, it analyses the load profile of the average household in Cyprus and proposes improvements to the design of the optimal system.

e) Finally, Chapter 6 presents the conclusions of this project. It also contains a discussion section about various issues and future research proposals.

Section 1.2.3: Methodology

Before proceeding into the main body of this Thesis, this section explains in more detail the thought process for the content of Chapter 2, briefly described in the previous section. This important data gathering assists the identification of several underlying problems regarding the energy production, supply and demand in Cyprus that do not allow the country to comply with its renewable energy usage programme and environmental obligations towards the EU.

The data collection for the background information of Cyprus has been conducted either directly from interviews, annual reports of the Electricity Authority of Cyprus (EAC) and other government agencies or by statistical files found on the website of the government's Service of Statistics. The data include historical figures primarily on electricity demand and consumption since 1990 and secondarily on demographics, climate, transports, house stock and emissions of the country. The potential of the various renewable sources in Cyprus is also identified in order to decide which is the most reliable for exploitation in general.

In addition, special and technical information have been collected from journal articles, presentations and other relative websites. Graphs have been generated from the numerical data mentioned in the previous paragraph and discussion is made about the trends of those graphs. In addition, calculations are conducted to determine useful features, needed to support the theoretical approach to various issues discussed.

With all these data collected, the project set to solve the problems derived from the electricity production and demand in Cyprus by proposing three Solar-Thermal concept systems for domestic installation and usage. For this situation several calculations and numerical simulation were conducted in order to optimise the efficiency and ultimately find the best of the three scenarios. Unfortunately, not all of the needed system components exist in the marketplace today. Therefore, the construction of prototypes was not possible and the project remained purely theoretical.

After the calculations indicated the best solution of the three, the project conducted a comparison with the Solar-Photovoltaic technology, which in Cyprus is more appealing for producing electricity. It is proven that Solar-Thermal technology is cleaner and more promising in terms of efficiency, storage and compatibility with the national

electrical network than Photovoltaic technology is. This is important in promoting the Solar-Thermal technology in Cyprus alongside Photovoltaics so that the public and the government is able to evaluate their benefits and disadvantages and use the appropriate one according to the needs and preferences of any given application.

It should be noted that this project is conducted using climate data from the region of Eastern Mediterranean, rendering the best system solution suitable for countries with similar latitudes or closer to the equator. As a result, the project cannot be applied directly to countries that are situated in latitudes larger than Cyprus', without modifications being done.

Chapter 2: Literature Review

Section 2.1: Introduction

This chapter concentrates the literature sources regarding fundamental background knowledge for the project's topic and critically assesses it in an informative manner. The chapter divides the background data into six main sections:

a) Demographics and Geography
b) Demand and Consumption
c) Power Production, Transmission and Distribution
d) Emissions
e) Energy Saving Measures
f) Renewable Energy Sources in Cyprus

The presented information reveals the current state of the energy sector in Cyprus and how demand for energy is met; the reasons why this current state needs to change and what the government is planning for improving the energy domain's operation. The main goal of this review is to identify the energy problems the country currently has, so that the project can propose an appropriate solution and probably motivate the creation of new research topics for completely solving the energy issues of Cyprus.

Section 2.2: Demographics and Geography

Section 2.2.1: Introduction

This section contains quantitative and qualitative data about the geographic location, terrain, climate and population of Cyprus. These elements are crucial in the extraction of useful figures and graphs that will show the growth or reduction rates of the population, building construction, temperature and rainfall density. The purpose is identifying possible problems regarding high pollutant emissions, intensified greenhouse effect, global warming and human health damage.

Section 2.2.2: Population and Demographics

The main sources for acquiring this kind of data are the Cyprus government's services. The Statistical Service of Cyprus provides almost up to date information in Excel files, several of those free of charge. The "Population Summary Data 1995 – 2009" (MF, 2010) file data of 1992 and those from 1995 until 2009 is about the total population

in Cyprus and the number of households. Additionally, a census was performed in 2011 and its results are also available on the website of the Statistical Service, named "Population by District and Urban – Rural Area, 2011" (MF, 2012a). These numbers are presented in the chart of Figure 2.1. As one can observe, the population in the unoccupied areas had a relatively steady growth rate, reaching about **803200** residents for 2009. In the census of 2011 it was revealed that the population reached about **838900** residents during that year. The number of households, shown in green on Figure 2.1, had also a steady growth rate reaching almost **300000** in 2011. As a result, since the country's population and house stock is increasing, the opinion that the demand for energy and pollutant emissions would also increase is completely logical. The data in the following sections strongly confirm this position.

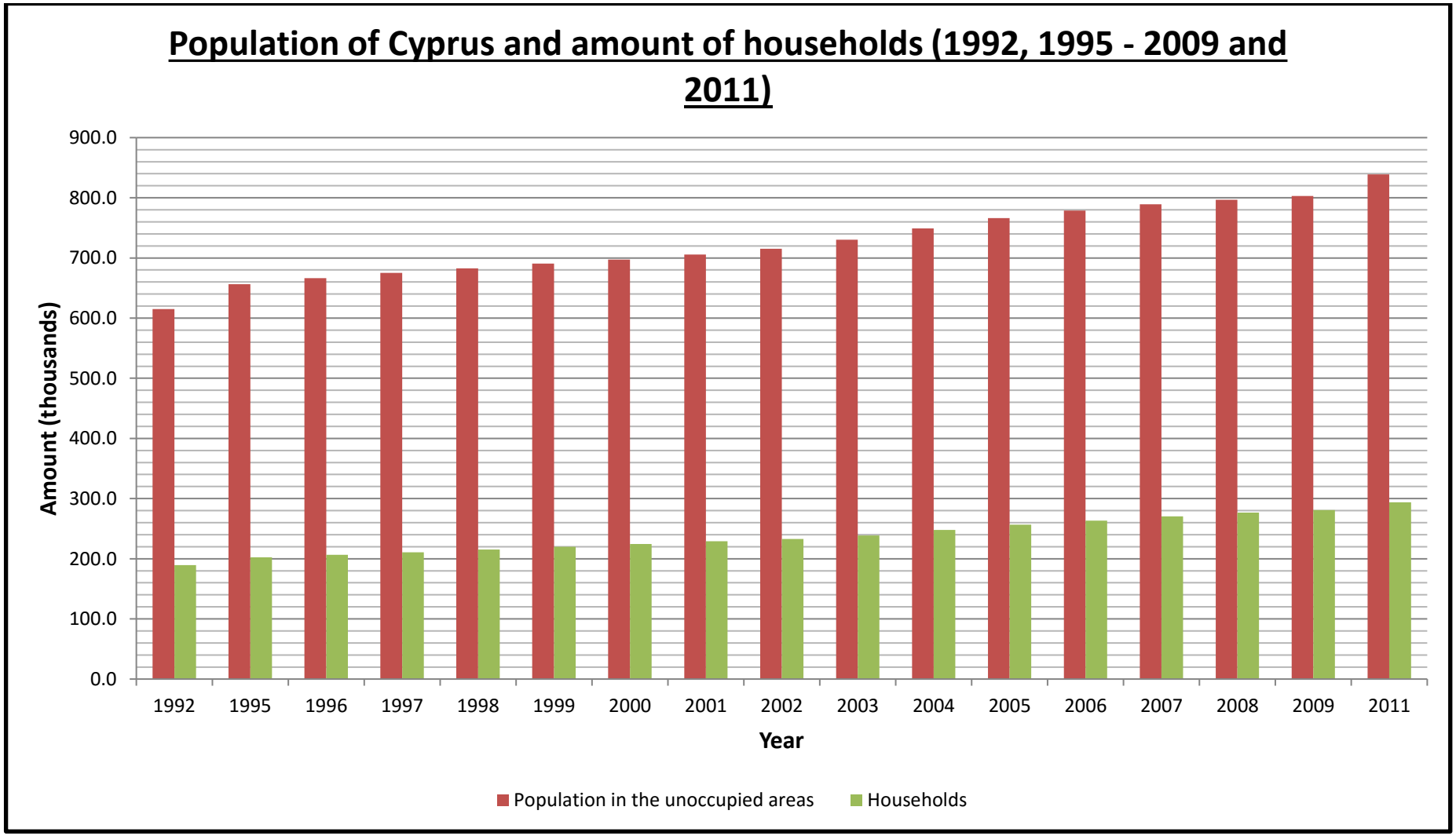

Figure 2.1: Population and household amount in Cyprus in 1992, between 1995 and 2009 and in 2011 (Statistical Service, 2010, 2012a)

Section 2.2.3: Climate and Terrain of Cyprus

Geographical information about the location of Cyprus, climate and water resources can also be found via online sources provided by Cyprus government and its agencies, such as the Electricity Authority of Cyprus (EAC), Statistical Service and the Cyprus Institute of Energy (CIE). High resolution satellite photographs can be retrieved from the Google Maps that show the location of the island relative to its neighbours and they also reveal its terrain's characteristics. Such details are important when investigating the reasons for the residents' increasing demand electricity, heating, cooling and water supply. Koroneos et al. wrote a relevant article in 2005, which contains data regarding the weather conditions of that year and previous periods as well. More specifically it contains charts about the mean temperature change in the country's capital, Nicosia, from 1951 until 1999 shown in Figure 2.2 (Koroneos, 2005: p. 1893) and also about the wind speed frequency distribution in various regions, which appears in Figure 2.3 (Koroneos, 2005: p. 1895). Along with the latter chart, there is a companion map of Cyprus, in Figure 2.4 (Koroneos, 2005: p. 1895) which shows the geographical distribution of the mean annual wind speed at the height of **10 m** above ground. It also indicates the sites of the five wind farms, in the white rhombus markers. Another important graph is the one with the average monthly distribution of solar radiation, shown in Figure 2.5 (Koroneos, 2005: p. 1896) which is measured in hours per day and the final graph presents the mean solar energy density of each month from 0400 hours to 1900 hours. This appears in Figure 2.7 (Koroneos, 2005: p. 1896). Even though the data are relatively old, the mentioned measured quantities are characteristics of the terrain and geographical location of the island. In addition, the great amount of past data in almost all figures is capable of allowing the generation of reliable trend lines for present and future times. The following paragraphs, therefore, analyse the mentioned graphs and comment on their presented information.

Beginning with Figure 2.2, the blue line represents the actual measured variation of Nicosia's average annual temperature, while the solid black line represents a linear trend line of that temperature, during the period between 1951 and 1999. The latter indicates that the mean annual temperature was increased by **1º C** within 48 years.

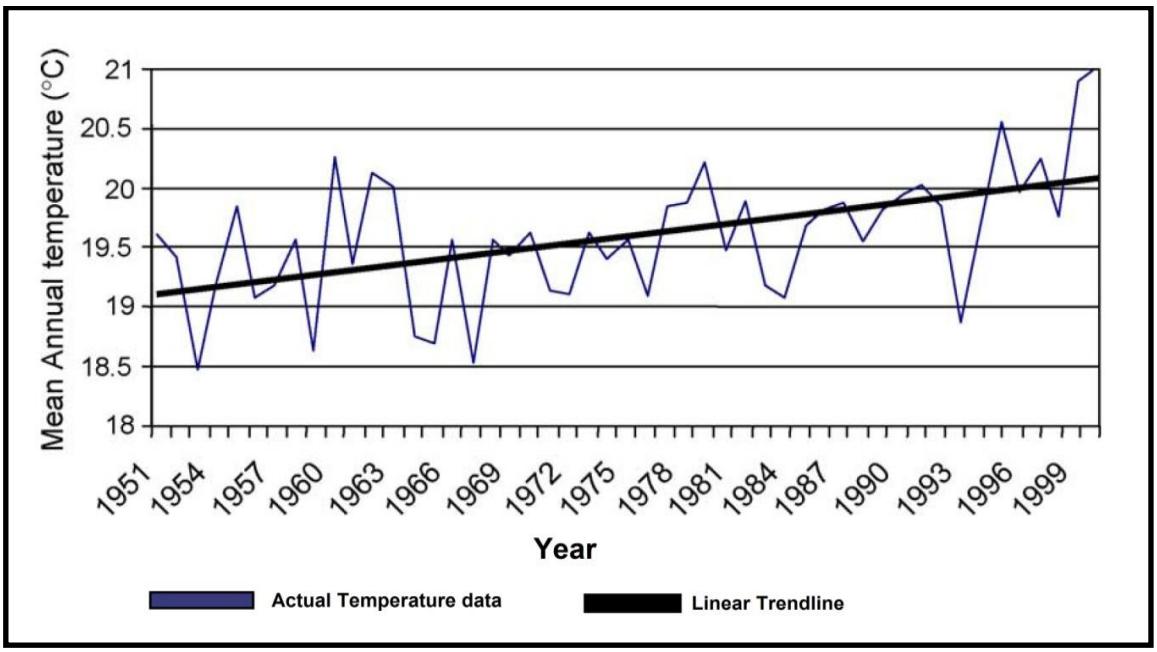

Figure 2.2: Mean annual temperature change in Nicosia during the period 1951 – 1999 (Koroneos et al., 2005: p. 1893)

Following that graph, Figure 2.3 shows the frequency distribution of wind speeds in four districts in the unoccupied areas, Nicosia (Athalassa region), Limassol (Lemesos), Larnaca (Larnaka) and Paphos (Pafos). The most common wind speeds in those territories is between **2** and **4 m/s**, which is the threshold of electricity production of a typical wind generator (NYSERDA, 2005: p. 5).

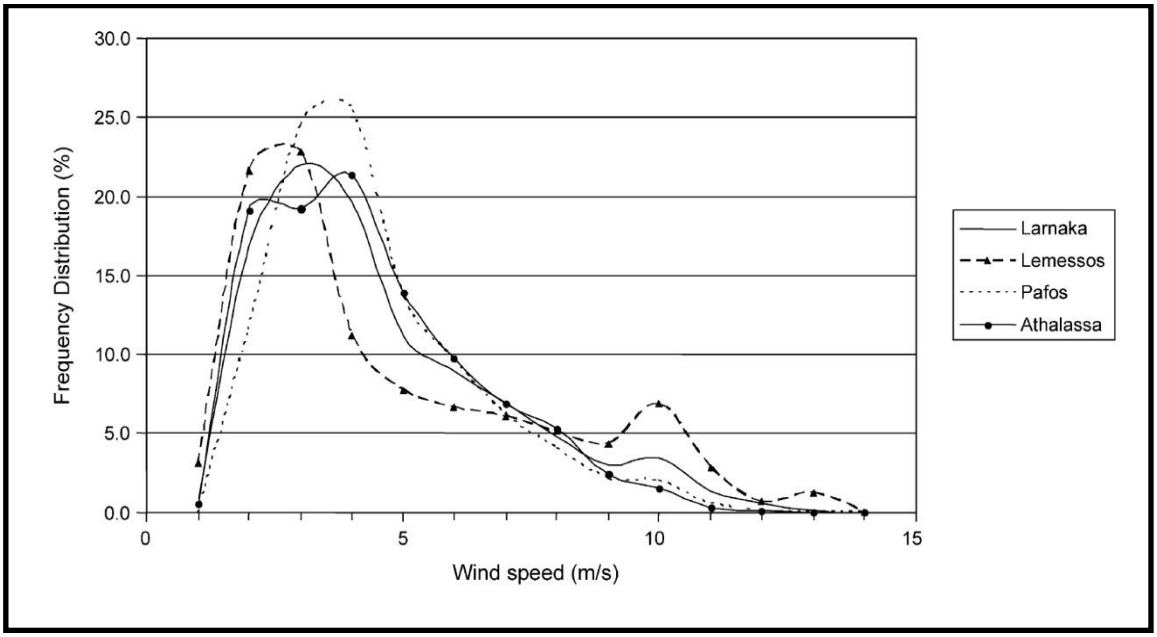

Figure 2.3: Frequency distribution as a function of wind speed of various locations in Cyprus by district (The area "Athalassa" is situated in the Nicosia District) (Koroneos et al., 2005: p. 1895)

Figure 2.4 is a complementary map of mean annual wind speed distribution measured at a height of **10 m**. The dots represent the major cities of the island and their names are shown next to their location on the map. As it can be observed, the most preferred areas for constructing wind farms are located in the south, southeast and southwest of the island, near the cities of Larnaca, Limassol and Paphos. As a result the five wind farms operating in Cyprus are situated in these regions, as indicated by the white rhombus markers; also their locations are marked in red on Figure 2.6 (TSO, 2012 & Google Maps, 2015).

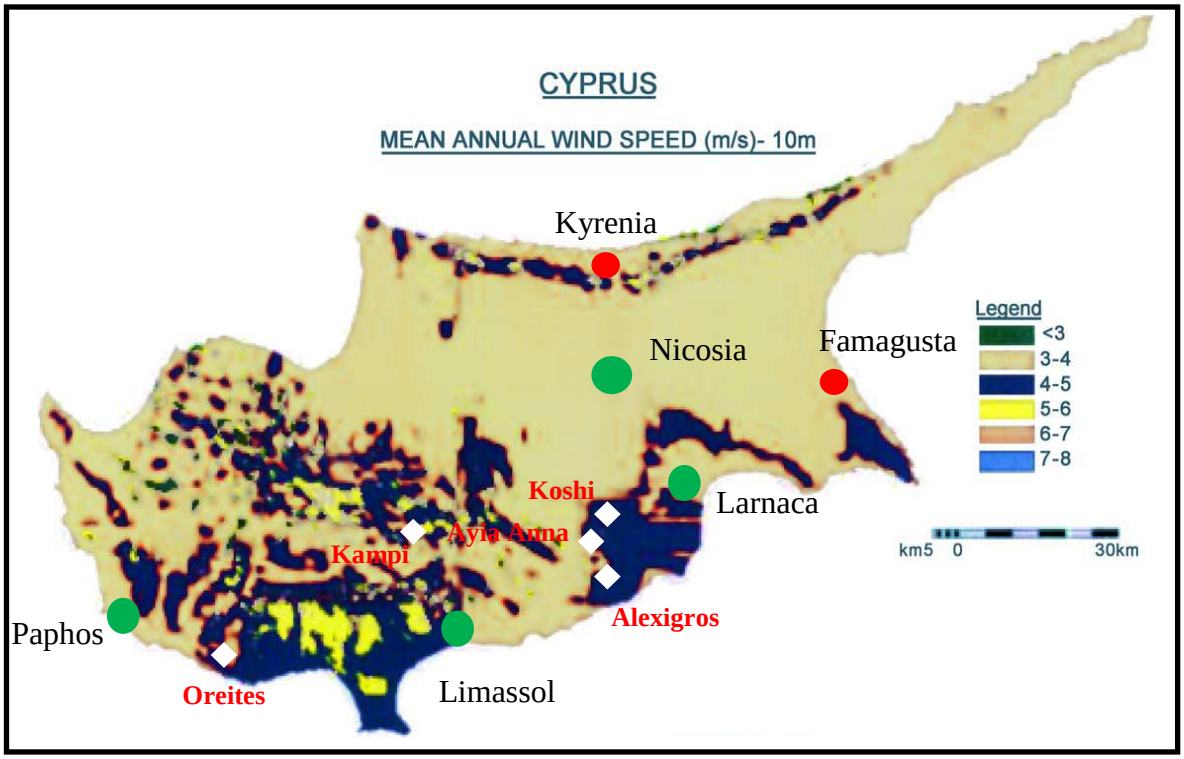

Figure 2.4: Annual mean wind speed geographical distribution in Cyprus at 10 m (Koroneos et al., 2005: p. 1895)

As the previous two figures presented data for wind energy, Figure 2.5 (Koroneos et al., 2005: p. 1896) indicates the daily solar availability throughout the year in four regions around the island. These regions are Nicosia (Athalassa and Prodromos), Larnaca and Limassol (Saitas). Athalassa region is situated near the Nicosia city centre while Prodromos is the village located on the highest altitude in the country. The exact locations of the Athalassa, Saitas, Larnaca and Prodromos regions are marked in green in Figure 2.6 (Google Maps, 2015a). As observed, the solar radiation is available the longest during July, with an average of **11.5 hour**s per day and the shortest during December and January with **5.5 hours** per day. This means that even during winter, Cyprus encounters significant solar insolation and this enabled the country to become the first in the EU to have the largest capacity in solar collector area and solar thermal power produced per capita, regarding solar water heating systems in 2010 (EurObserv'ER, 2011: p. 89).

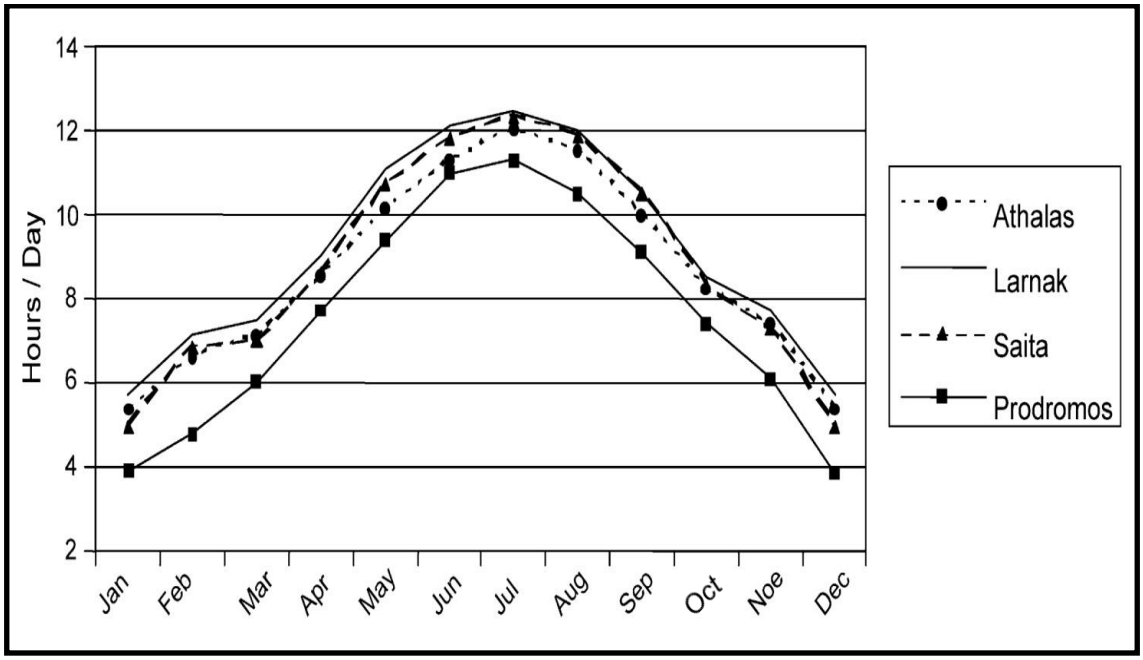

Figure 2.5: Daily solar availability per month (Areas "Athalassa" and "Prodromos" are situated in Nicosia District while "Saita" in Limassol District") (Koroneos et al., 2005: p. 1896)

In addition to Figure 2.6, Figure 2.7 (Koroneos et al., 2005: p. 1896) shows the mean daily direct solar radiation per hour of every month. The figure has been re-created into MS Excel, as the "Hours" axis on the paper's original graph is erroneous. The radiation is measured in $Wh/m^2/h$ (which can be simplified into W/m^2) and as it appears from the graph, the month with the largest amount of radiation, more than **700 $Wh/m^2/h$** is July between the 1100 and 1200 hours. The data shown in Figures 2.5 and 2.7 explain the tendency of Cypriots to rely on solar energy to cover their needs and also proves that the solar potential of Cyprus is greater that the wind one. It should be noted, however, that Koroneos et al. do not mention which region the data of Figure 2.7 represent. Moreover, Cyprus's national Meteorological Service and World Bank database do not contain data neither wind nor solar energy; they rather contain historical air temperature and rainfall data (MARE, 2015 & World Bank, 2015). So, the only source for this kind of data is the paper by Koroneos et al.

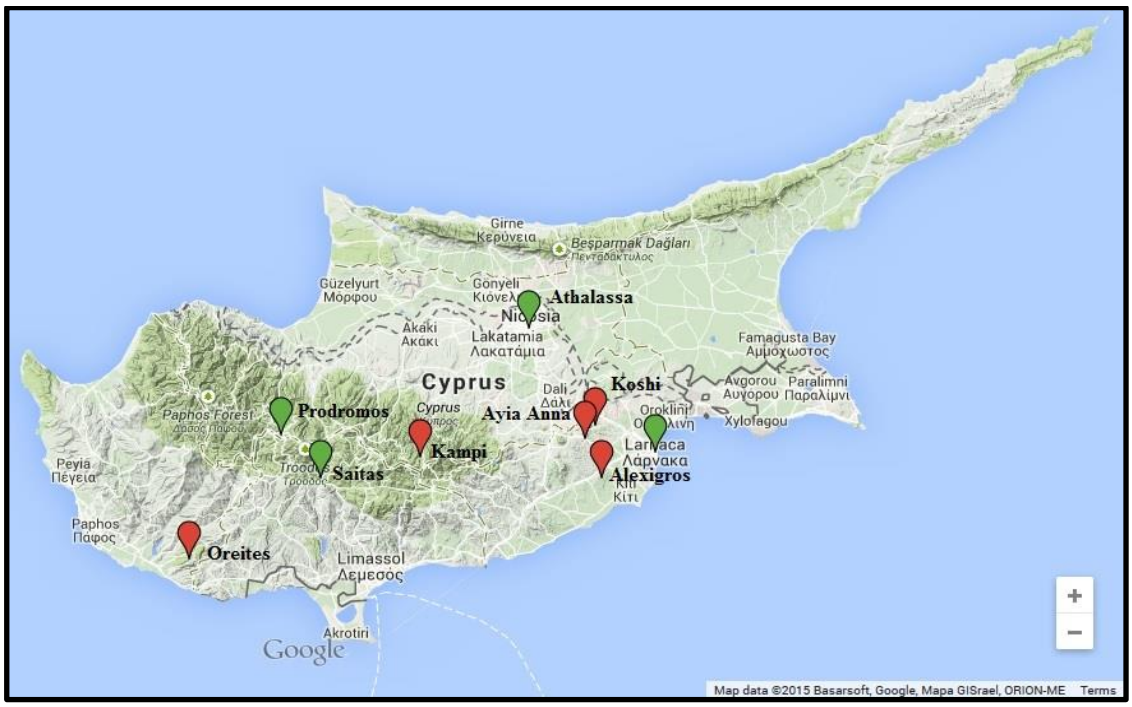

Figure 2.6: Location of the five wind farms (red) and the four minor regions (green) mentioned in Figures 2.4 and 2.5 (Google Maps, 2015a)

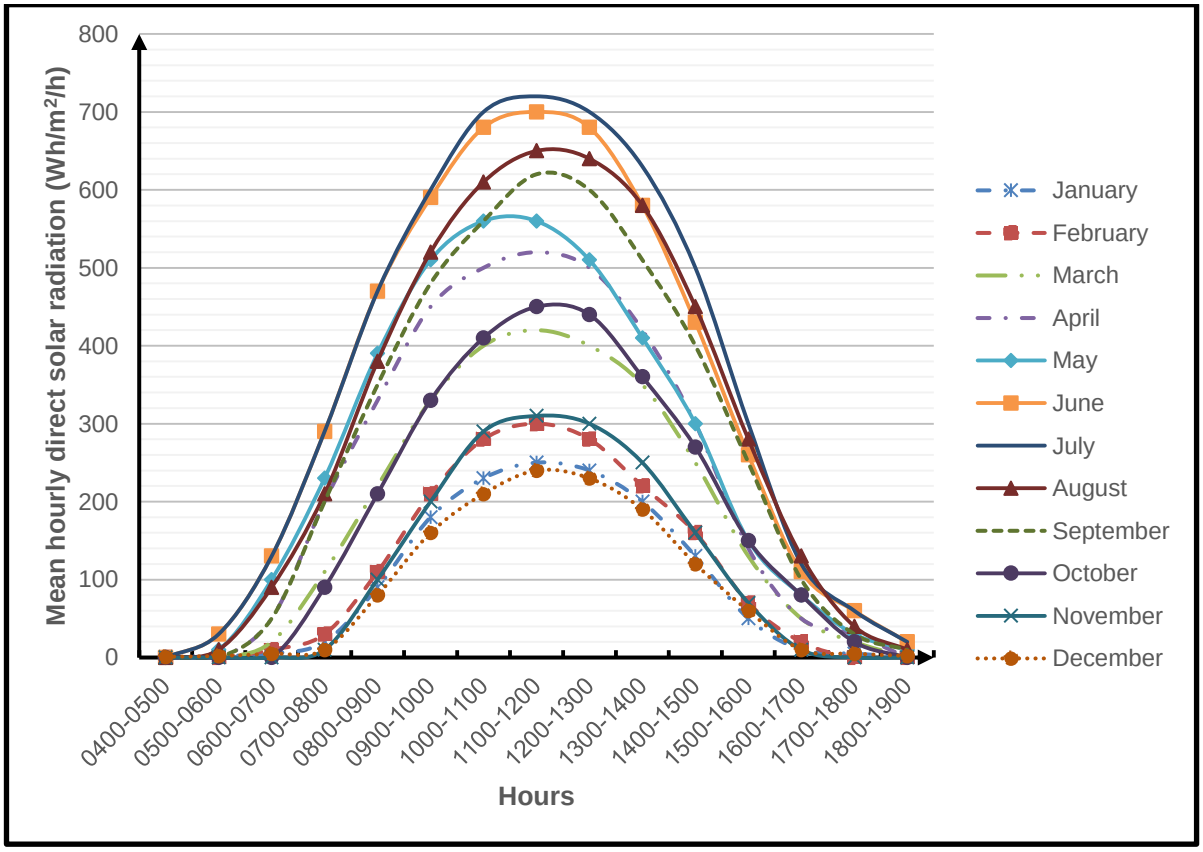

Figure 2.7: Mean hourly direct solar radiation (Koroneos et al., 2005: p. 1896)

Section 2.3: Demand and Consumption

Section 2.3.1: Electricity consumption by sector

Electricity is the main source of energy supply in Cyprus. The most recent data regarding overall energy and power consumption can be retrieved from the latest Annual Reports of the Electricity Authority of Cyprus (EAC). This is the government's electricity service and for the time being it is the only national scale power company in Cyprus. The files of Annual Reports are available to the public free of charge and they contain technical and quantitative information about the amount of electrical energy being produced per annum, how much electricity has been sold to the public, the cost of electricity in those years, the maximum power demand met and the maximum output capacity of the company's generation system. Historical data from 1995 and from 2000 until 2013 can also be found in the Statistical Service's website (MF, 2008a). The quantities of these statistics are almost in full correlation with those found in the Annual Reports of the EAC. So, the required electricity consumption data for this section are retrieved from the EAC's Annual Reports. The reason is that this is a primary source that organizes the data in a tabulated and graphical manner and secondly, the data from the Statistical Service confirm those of the EAC's Annual Reports, classifying them as highly representative. The mentioned data are presented in the chart of Figure 2.8 (EAC, 2006, 2007a, 2008, 2009, 2010, 2013).

One can observe the increasing rate of consumption, especially in the commercial and domestic sectors until 2010, while in contrast from 2011 until 2013 there was a decreasing consumption rate. The main reason for this tread is most probably that Cypriots were living in prosperity until 2011 when the global financial crisis and several erroneous government decisions lead to the increase of the unemployment rates of people between the ages 15-24 and 25-64 from **16.6%** and **5.3%** in 2010 respectively (MF, 2012d) to **38.9%** and **13.7%** in 2013 correspondingly (MF, 2015a). In combination with the austerity measures enforced on Cyprus's economy during that period, the population reduced their overall expenses including their domestic electrical consumption and also their shopping expenses forcing commercial business to do the same.

The financial crisis also affected the industrial and agricultural sectors, as seen in Figure 2.8. In the Industrial sector, the increase in consumption is not as sharp as in the previous two sectors and also from 2004 until 2007 there was a slight decrease from 2008

until 2010, that usage increased again, reaching over **800 GWh**. After remaining relatively in the same value in 2011, there was a sharp decrease from 2012 to 2013, finally reaching less than **600 GWh** in 2013. In the last two sectors, agricultural and public lighting, consumption has increased over this period but at a slower pace compared to the other sectors. In fact the Agricultural usage increased from about **75 GWh**, in 1997 to just over **150 GWh** in 2010; it also experienced a slight decrease from 2011 to 2013, reaching a bit over **100 GWh** in 2013. Lastly, the Public Lighting sector is the only one that still increases, as it is a necessary expense for ensuring the safety of highway users. More specifically the consumption has nearly doubled from 1997 until 2013, from about **50** to **100 GWh** respectively.

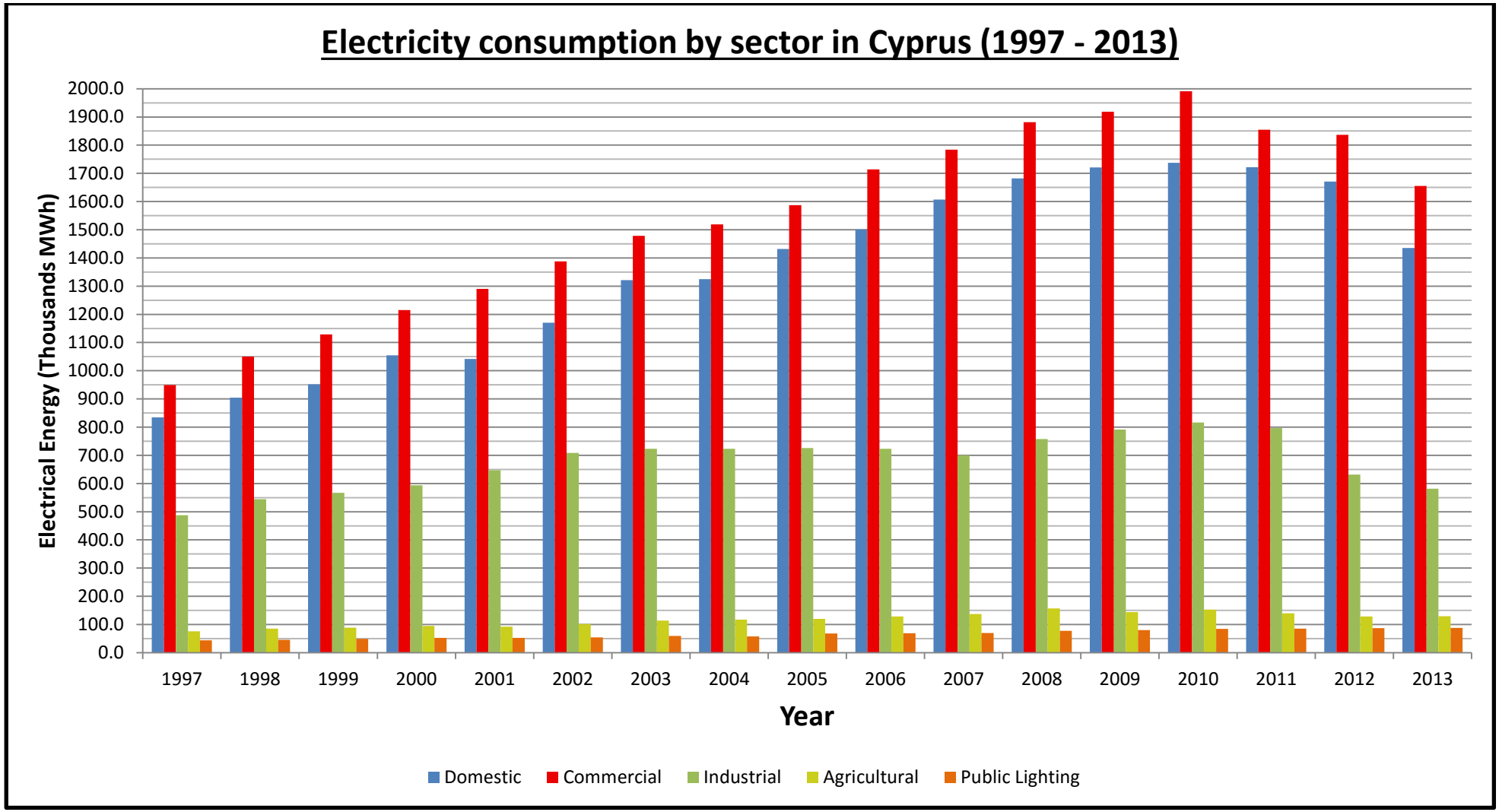

Figure 2.8: Electricity consumption by sector (1997 – 2013) (EAC, 2006, 2007a, 2008, 2009, 2010, 2013)

Section 2.3.2: Statistical data about housing stock in Cyprus

Two additional statistical files (MF, 2011a & 2012a) contain the figures of electricity and oil products respectively. Additionally the former file contains details, for 2009, about the operation time of various household appliances, the percentage of households fitted with specific types of appliances and proper insulation. This file also shows the household energy consumption in 2009 by sector (space heating and cooling, cooking and lighting) and also the end-use energy for that year by fuel category.

A number of charts can be extracted from this file. Firstly, the percentage of households by surface area in Figure 2.9 (MF, 2011a) is important information, as larger houses impose a greater demand for space heating/cooling and lighting. The figure shows that the vast majority of house stock has a surface area range from **51** to **200 m^2**, which includes medium size households. Additionally, Figure 2.9 shows that houses are typically larger than **100 m^2** of surface area.

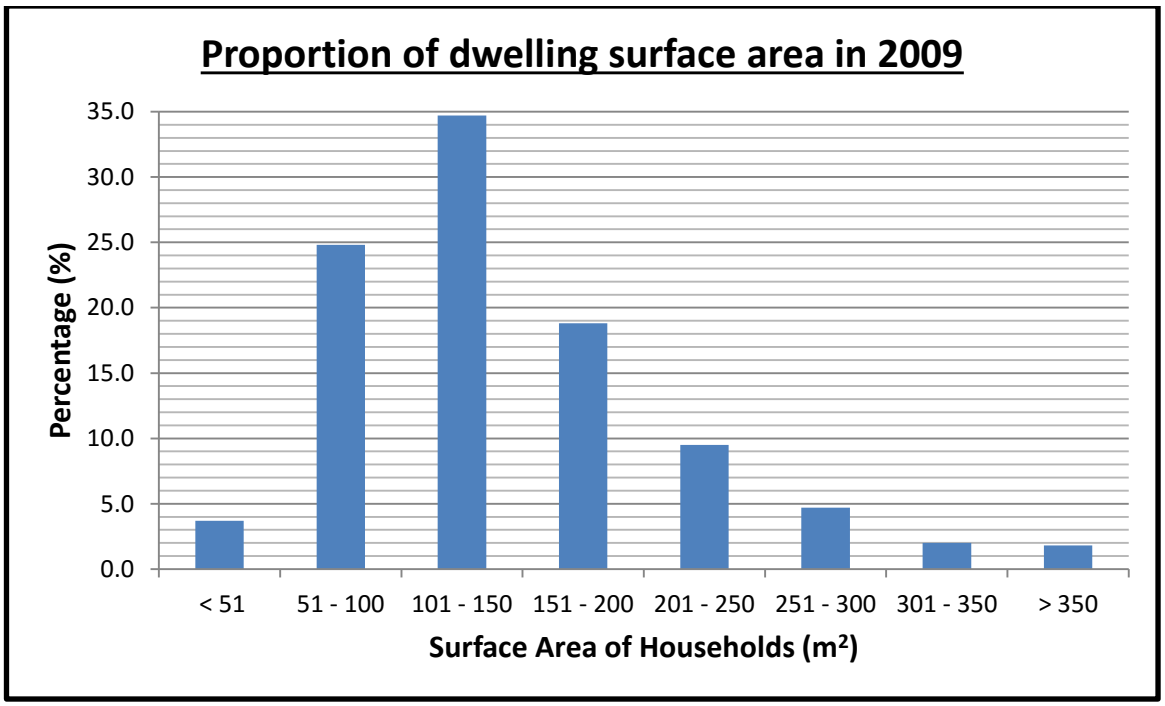

Figure 2.9: Proportion of surface area of households in Cyprus in 2009 (MF, 2011a)

In addition to Figure 2.9, Figure 2.10 (MF, 2011a) presents the share of households by construction period. This enables any observer to see that about **87%** of existing households in 2009 were built before 2004, the year of Cyprus's accession to the EU. Consequently, these households are most likely not to be fitted with proper

insulation, since there were no energy legislation or government regulations in effect prior to this year, especially in the domestic sector (CIE, 2012a: p. 58).

The share of households by type is another important aspect at this point, as it shows the Cypriots' preference to a particular kind of housing. Figure 2.11 (MF, 2011a) indicates that only about **22%** of households in Cyprus in 2009 were apartments. Cyprus residents prefer to live in houses instead of apartments, most probably due to their more traditional mentality relative to other European's. Most members of the Cypriots' paternal generation today were born and raised in villages, rather than the urban and suburban areas. Furthermore, the concept of living in cities and not in villages is relatively recent and that it is also likely to be caused by the Turkish invasion in 1974, when a large proportion of the Greek – Cypriot population were forced to vacate their houses and be transported to the unoccupied zone of the country.

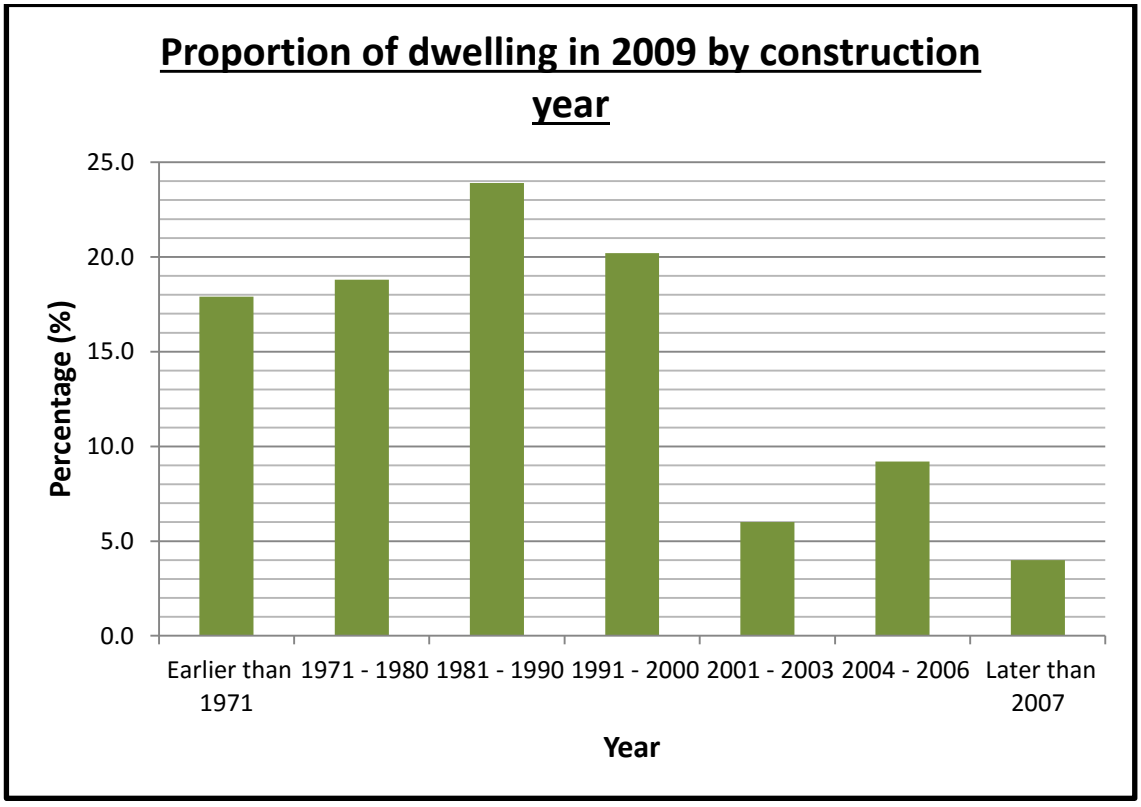

Figure 2.10: Proportion of households in 2009 by construction year (MF, 2011a)

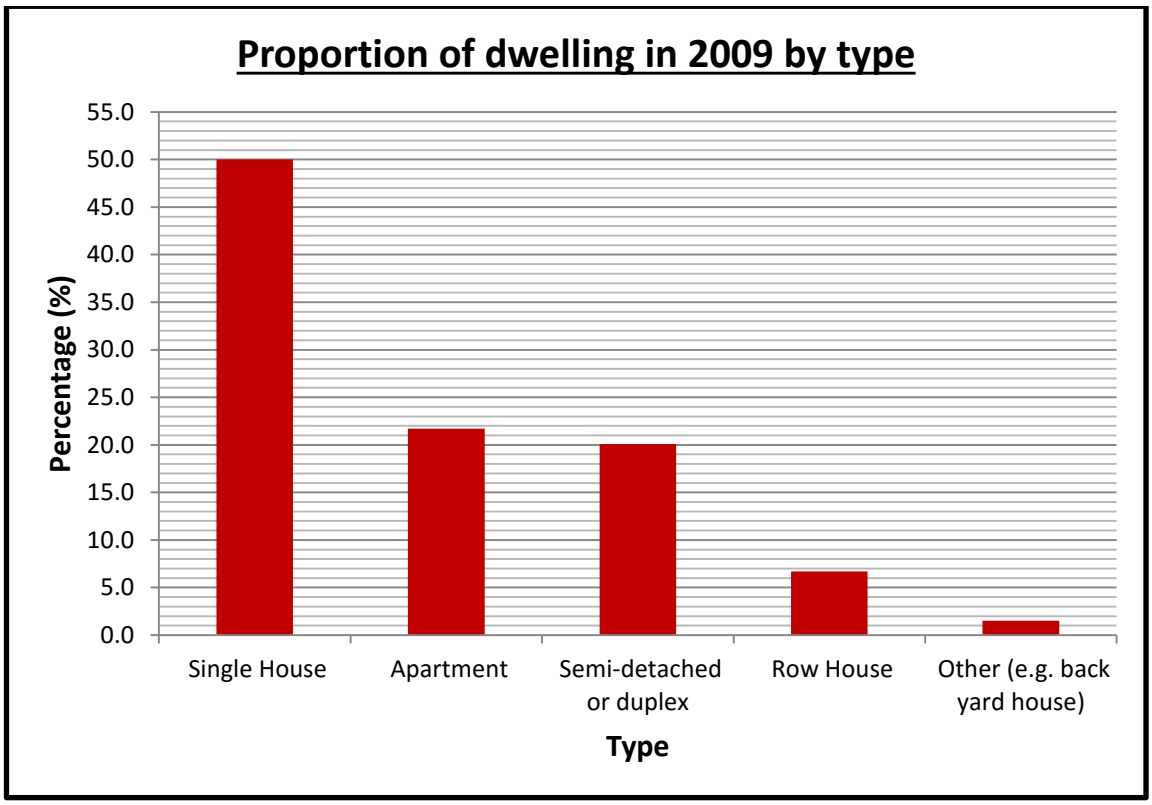

Figure 2.11: Proportion of households in 2009 by Type (MF, 2011a)

Figure 2.12 (MF, 2011a) presents the proportion of households in Cyprus fitted with different types of insulation in 2009. It can be seen that the share of all dwellings that did not have any type of insulation was over **54%**, that year. This means that over half of residential buildings in 2009 had great thermal losses during the winter and great thermal gains during the summer and that could have led to unnecessary expenditure of electrical energy for compensating with these losses. Therefore, it can be considered that households in Cyprus are more likely to have greater needs for space heating and cooling compared to households in other EU countries, for example the UK.

The different types, ownership proportion and daily operation time of electrical appliances and devices is another domain that could explain the increased demand of electrical energy in Cyprus. Figure 2.13 (MF, 2011a) presents the amount of time that some of those appliances were used on a weekly basis in 2009. The most popular appliances, according to Figure 2.13, are televisions and refrigerators with freezer with uptake of about **99%**. A refrigerator is a necessary appliance for a household and that is the reason why it operates throughout the day. This also becomes apparent in section 6.4 of Chapter 6, which analyses the electrical load of a typical household in Cyprus. The television, on the other hand is an appliance of entertainment and almost every residence possesses at least one. Additionally it can be observed that about **91%** of households were

fitted with incandescent light bulbs, a piece of electrical equipment that requires large amounts of electricity. A standard incandescent light bulb of this type consumes **60 W** of electricity to produce **830 lm** of light, while a compact fluorescent (CFL) light bulb consumes much less power, **13 W** for about the same amount of luminance. Even better, a Light Emitting Diode (LED) light bulb consumes only **8.3 W** to produce **830 lm**. (Eleek Inc., 2011). So, this shows that Cypriots in 2009, at least, didn't have significant knowledge about energy saving, which is another factor that could explain the increasing electricity demand during the previous years.

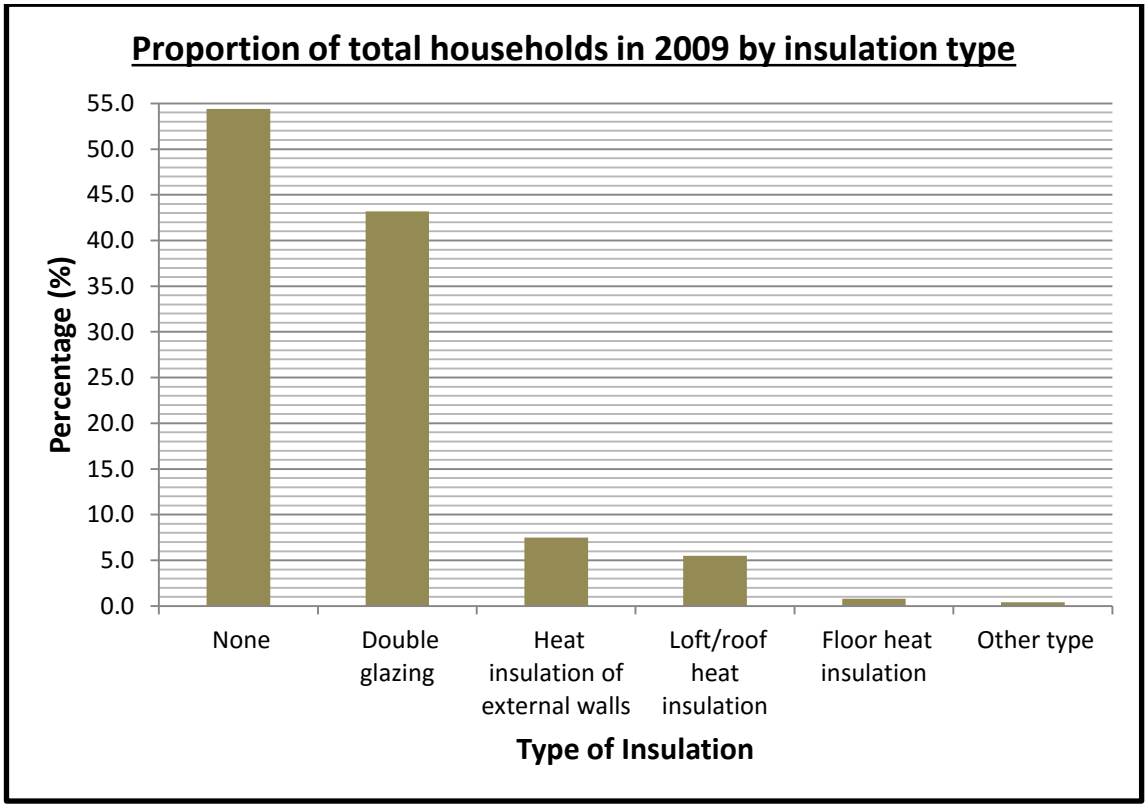

Figure 2.12: Proportion of total households by type of insulation in 2009 (MF, 2011a)

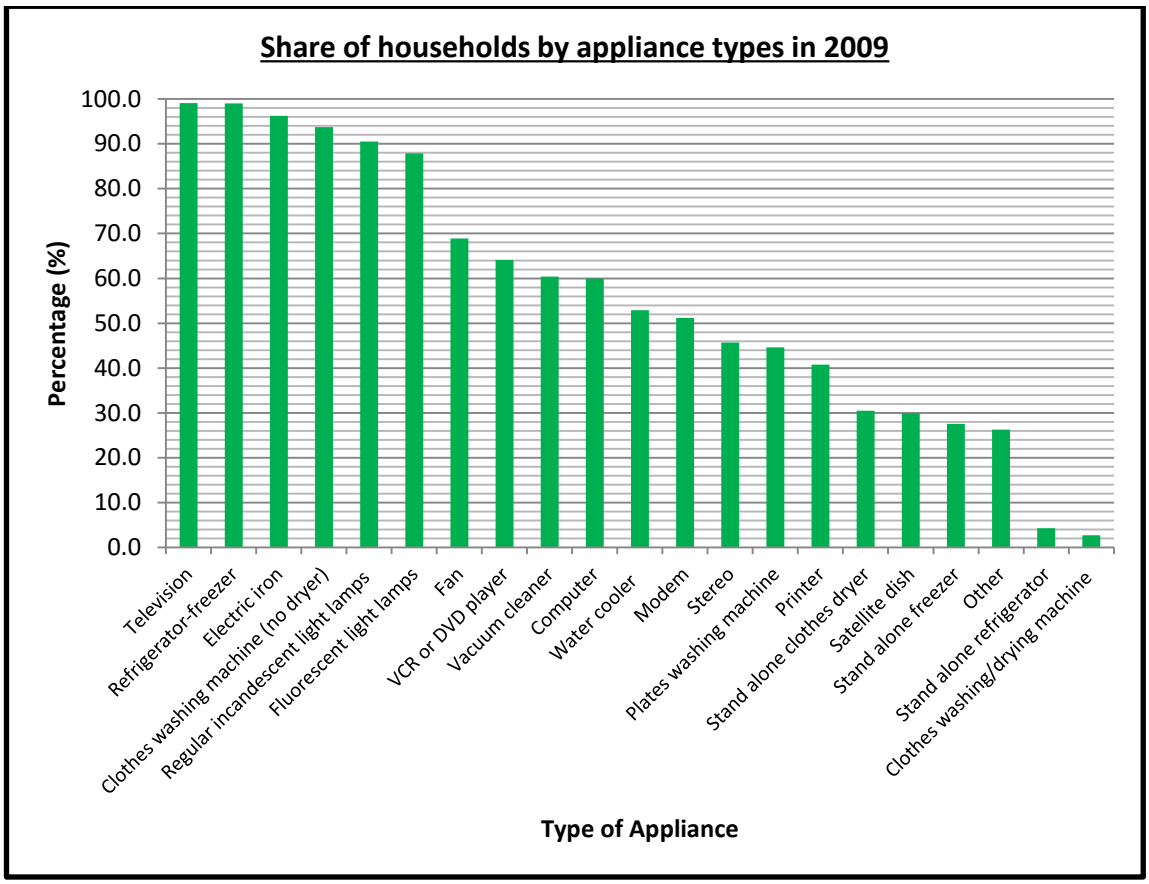

Figure 2.13: Percentage of Cypriot residences containing specific kinds of electrical appliances (MF, 2011a)

As mentioned, the complementary chart in Figure 2.14 (MF, 2011a) contains the usage profile of several of the above types of appliances on a weekly basis. The most recent data is from 2009. By combining that knowledge with the consumption rate of each appliance, the overall increasing domestic energy demand can be explained. The figure shows that the television was the most commonly used appliance in Cypriot households in 2009, reaching almost **46 hours per week**. A computer is a tool for both work and leisure; however it is not used for such a long period of time each week as a television. An LCD television consumes on average **226 W**, while a desktop and a laptop computer consume **112.5 W** and **70 W**, respectively (Borg and Kelly, 2011). This means, according to these statistics, that maybe television was one of the factors responsible for the largest amount of energy consumed in households in 2009. However, Figure 2.14 does not contain the mean weekly operation periods for electric cookers or incandescent light bulbs, which overall may consume more energy than televisions, nor any details about stand by consumption for televisions or other devices.

The last remark for the Statistical Service at this point is that it has not prepared a similar series of files containing data for each year as other categories since 2011. Even though the large volume of information acquired from this file is not recent, it cannot be

considered as outdated as the technological and domestic needs Cypriots have not changed significantly since then. The financial crisis and increase of the unemployment rates after 2010 may have shifted the preference of young couples towards living in apartments instead of applying for mortgages; however the already existing house stock is a factor that changes over longer periods than just 5 or 6 years.

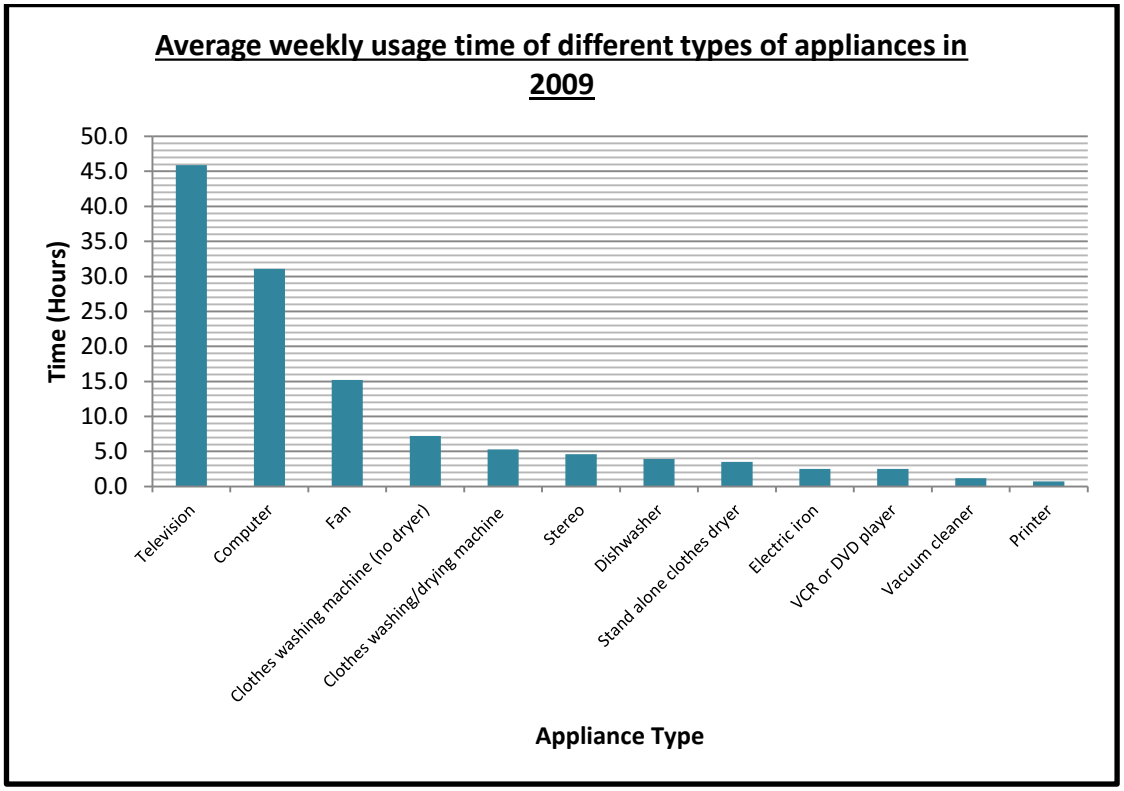

Figure 2.14: Weekly average use of some household electrical appliances (MF, 2011a)

Section 2.3.3: Petroleum products imports and consumption

Continuing with the issue of energy demand, there are several archived files in the Statistical Service's website that compare the monthly and annual imports and market absorption of oil derivative products, by type of fuel until 2014. By combining the data from these files, two charts can be extracted. Firstly, the imports of petroleum products for the operating purposes of EAC, and cement Industry are presented in Figure 2.15 (MF, 2011c, 2012b, 2014, 2015b). The figure shows a decrease in the acquisition of heavy fuel oil, which is mainly used for electricity production in the Power Stations. Gasoil imports increased from 2008 until 2013; however in 2011 and 2014 those imports decreased to about the levels of 2009. Additionally, both petroleum coke and bituminous coal imports decreased during these years; the remaining stock at the end of each year may explain this fact. This is fact is confirmed in Figure 2.16; it presents the cumulative commercial annual

sales and stocks of petroleum derivatives, for example unleaded motor gasoline 95 RON, Gasoil with low sulphur and asphalt. The chart shows that the total sales remained about the same at around **1640 thousand tonnes** during the period 2007 – 2008 and then they had a slight decrease in 2009 at about **1550 thousand tonnes**, remaining relatively steady until 2011. The following years, however, those sales experienced a sharper decrease reaching just under **1200 thousand tonnes** in 2013 and finally settling at about **1260 thousand tonnes** in 2014. On the other hand, the total stock at the end of each year remained relatively steady between **80** and **100 thousand tonnes**. These two charts confirm that Cyprus's economy is heavily dependent on fossil fuel and even though imports and sales have reduced during the last three years most probably due to the effects of the financial crisis, the necessity of investing into renewable energy based technologies should be considered seriously.

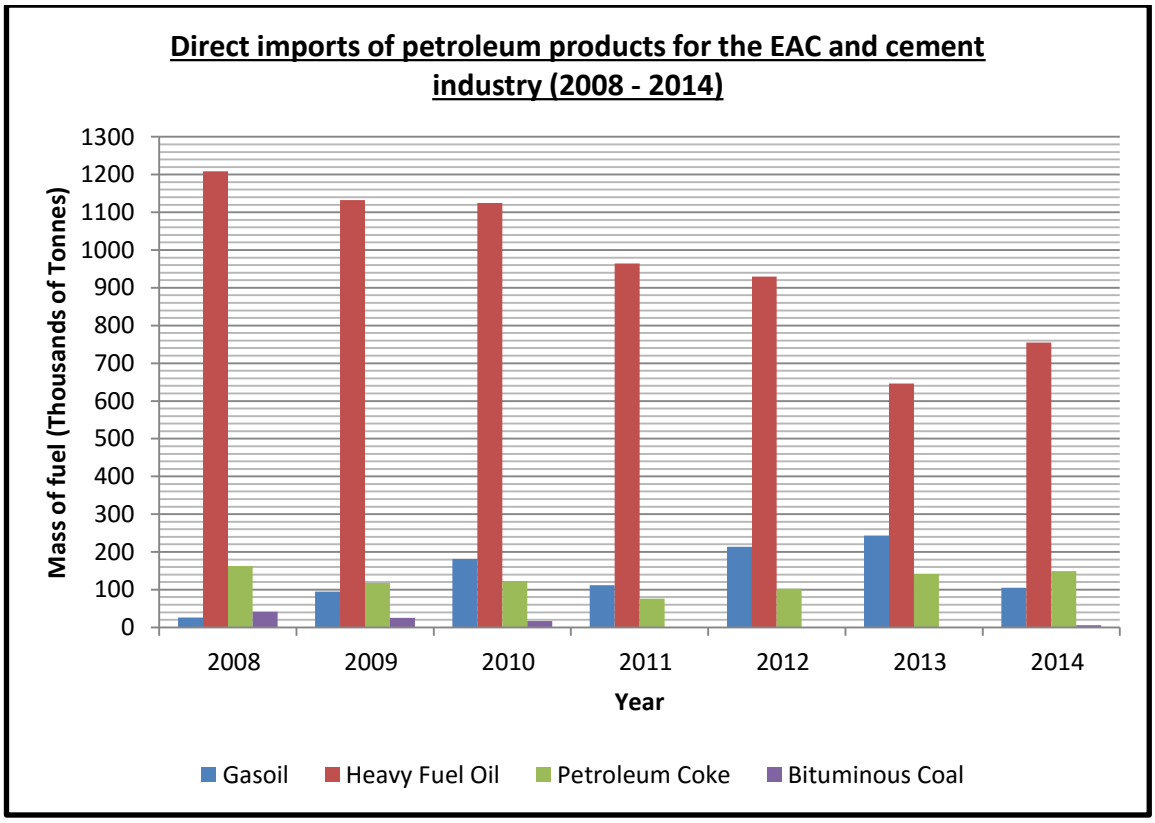

Figure 2.15: Petroleum products for electricity and cement production between 2008 and 2014 (MF, 2011c, 2012b, 2014, 2015b)

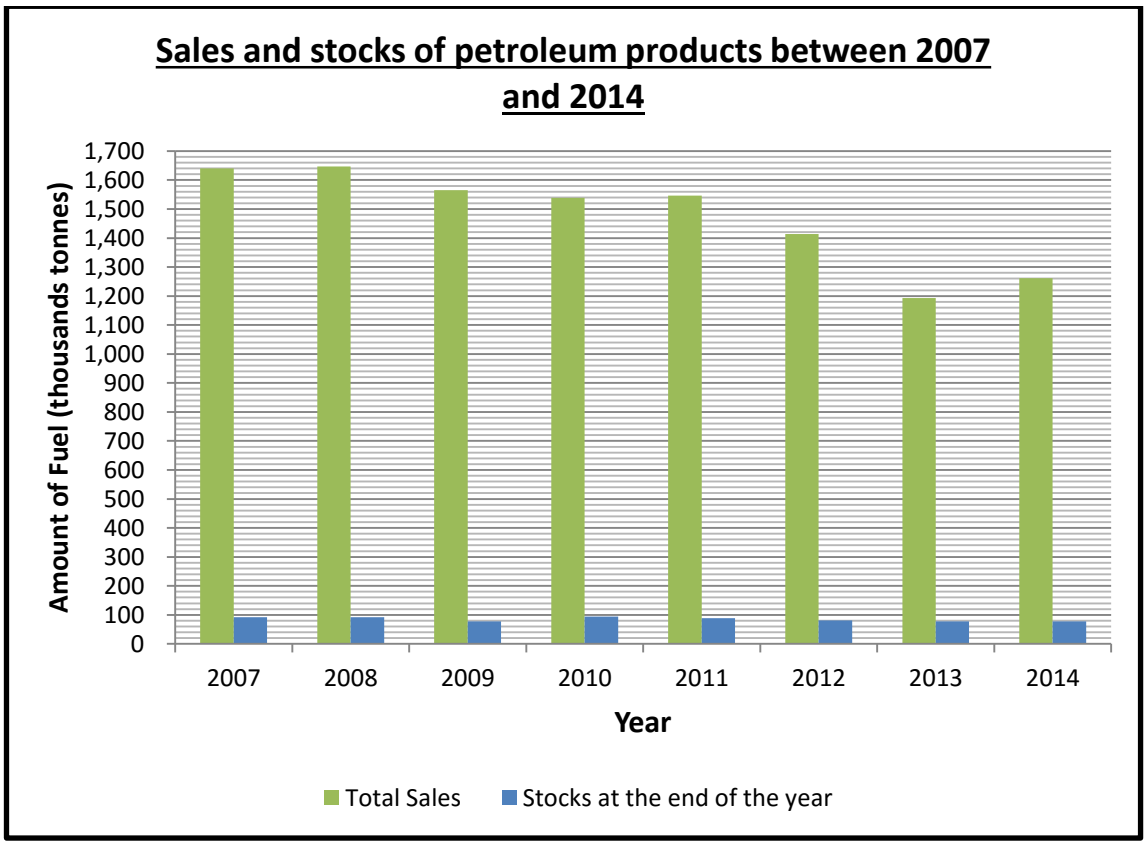

Figure 2.16: Petroleum product supply and stocks from 2007 until 2014 (MF, 2008b, 2009, 2011c, 2012c, 2014, 2015c)

Section 2.3.4: Transport in Cyprus

Finally, files on transport (MF, 2011b, 2014b) contain statistical details about the amount of registered vehicles by type at the end of each year. The data indicate that privately owned passenger vehicles have been increasing in numbers compared to other types, as shown in Figure 2.17 (MF, 2011b, 2014b). In addition, they support the increasing demand in light fossil fuels mentioned fuel above and it is probably due to the lack of public transportation, also suggested by Figure 2.17. Another reason is probably the more traditional mentality of Cypriots compared to other Europeans in preferring to own a vehicle rather than using public transport. Figure 2.17 also projects a linear prediction for each type of vehicle until 2025. It suggests that passenger cars would continue to increase in relation to the other types and probably reach about **0.7 million** in number by 2025. The number of passenger cars in 2009 was about **460 500** (MF, 2011b) and the population in the unoccupied areas, that year, was about **803 200** (MF, 2010), giving a ratio of people per passenger car of **1.74** in 2009. Additionally, Figure 2.18 (MF, 2011b, 2014b) further classifies the amount of passenger vehicles by type. The scale of the amount axis of the chart is logarithmic as the sheer number of the privately owned family cars would not allow the other two types to be visible on the chart. More

specifically, private cars have been increasing since 1990, while rental cars had a major increase between 2001 and 2004, while the amount of taxis has remained relatively unchanged throughout the whole period. Lastly, a chart containing the percentage of rental passenger cars relative to the total number of passenger cars is seen in Figure 2.19 (MF, 2011b, 2014b). This percentage decreased from 1995 to 1999, remained almost the same in 2000 and then in 2001 it increased steeply and continued until 2003. From that point on a steady decrease occurred, until started increasing once more from 2010. It is noted that the proportions in question are relatively small compared to the proportions of the privately owned cars and so the impact of the latter category to the environment is greater. Lastly, all other types of vehicles did not show any significant increase during that period, as shown in Figure 2.17. As a result, the category of vehicles that probably had the most significant impact on the demand for fossil fuel is the passenger vehicle type.

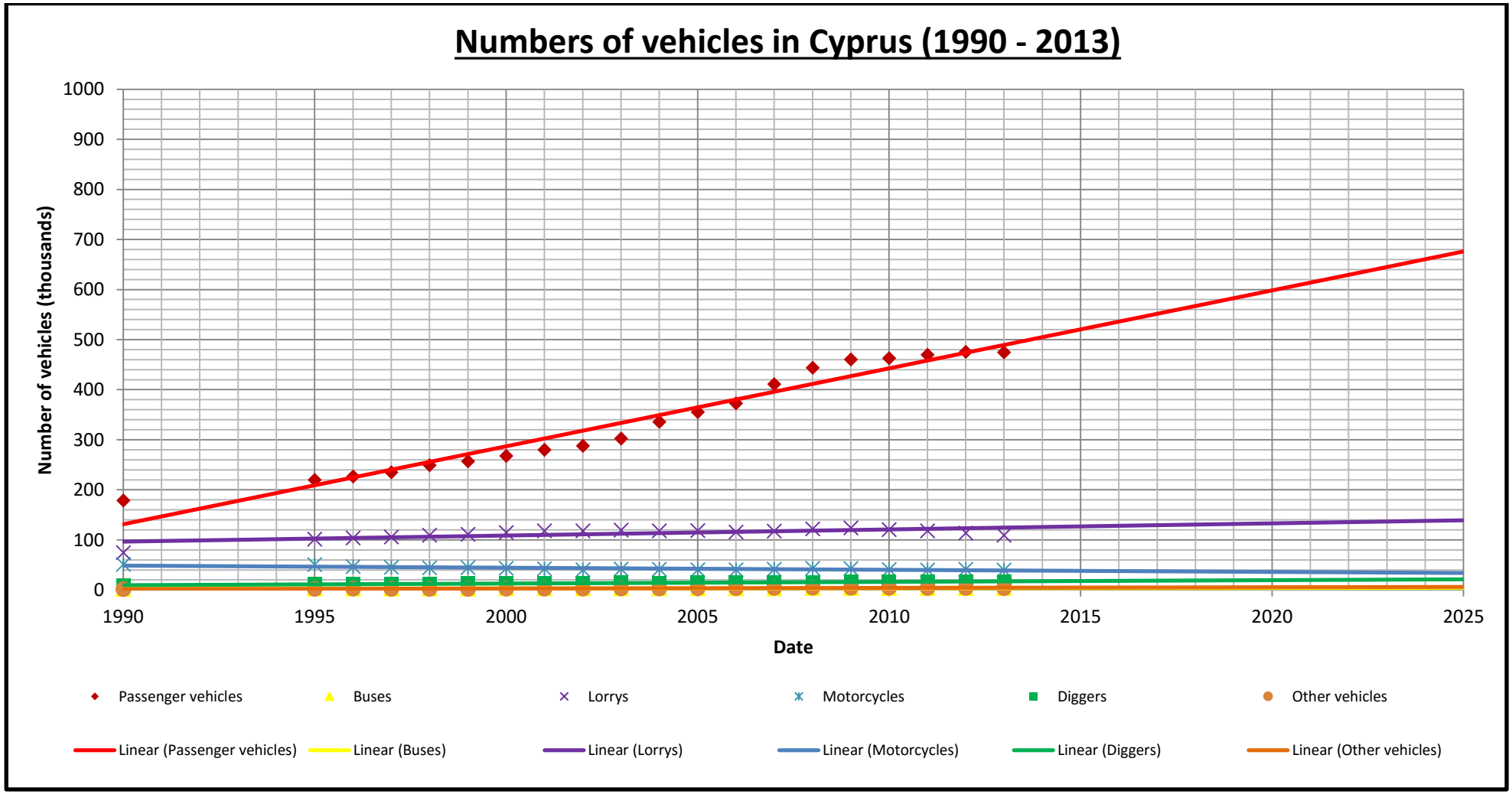

Figure 2.17: Amounts of vehicles by type in Cyprus from 1990 until 2013 with forecast until 2025 (MF, 2011b, 2014b)

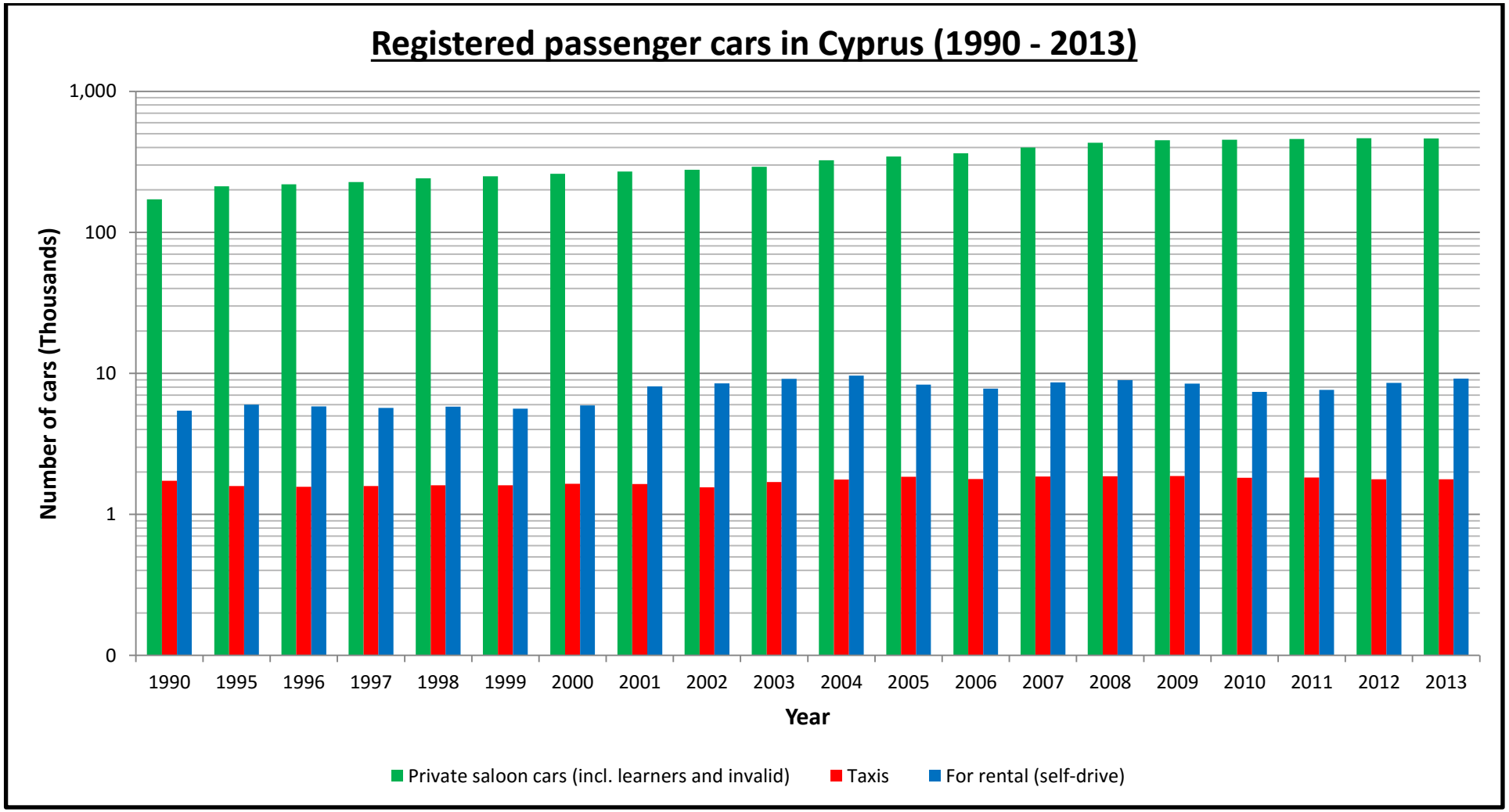

Figure 2.18: Analysis of passenger cars by type in 1990 and between the years 1995 and 2013 (MF, 2011b, 2014b)

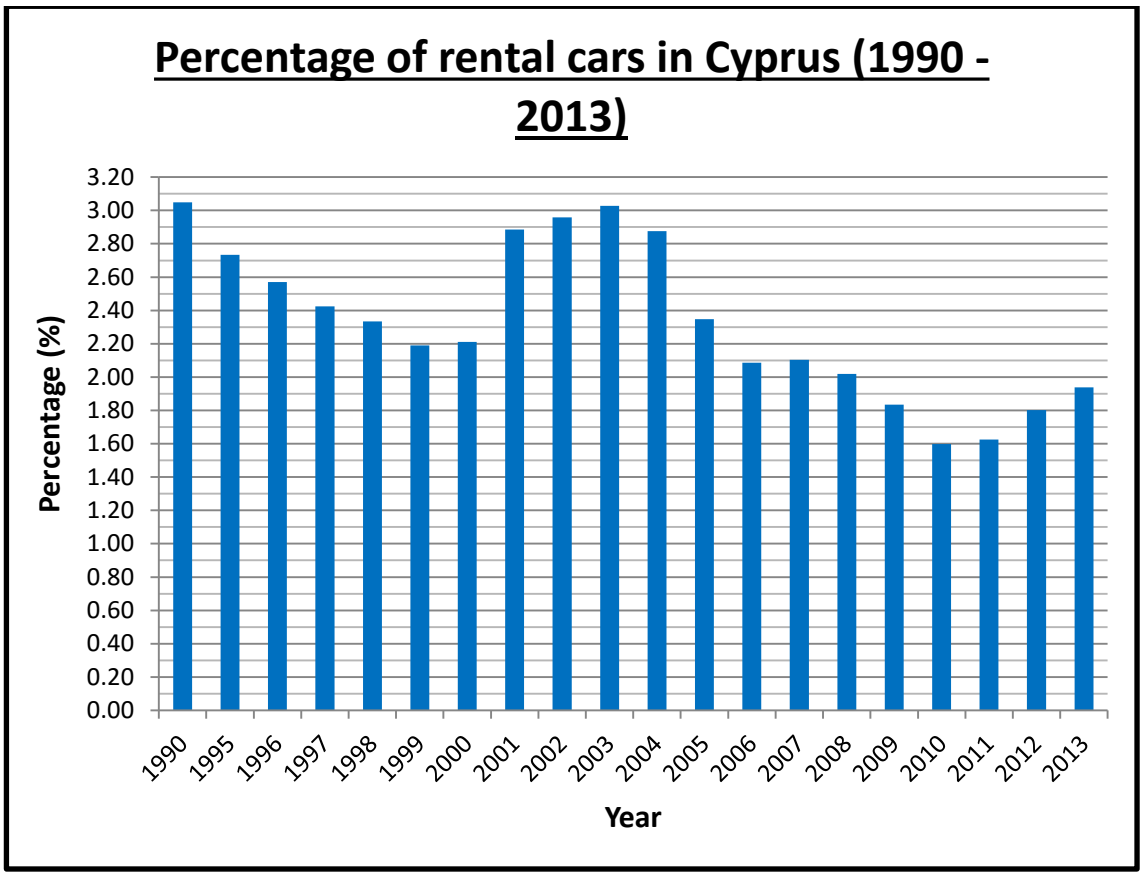

Figure 2.19: Share of rental cars relative to the total number of passenger cars in 1990 and between 1995 and 2013 (MF, 2011b, 2014b)

Section 2.4: Power Production, Transmission and Distribution

Section 2.4.1: Electrical infrastructure

Section 2.4.1.1: Historical background information on the existing electrical system

The Cyprus population has been using electrical power for over 100 years, since 1903. At that time the island was a British colony, since 1878 when it was assigned to the British Empire by the Ottoman Empire. The colonial government generated electricity with two power generators installed in the Commission building and the then General Hospital in Nicosia for covering those facilities' demand. In 1912, electricity became available to a small proportion of the general population due to the creation of "The Limassol (Lemesos) Electric Light Company" by several local businessmen, such as the Stamatiou brothers and George Giannopoulos. A year later, the "Nicosia Electricity Company" was established by the then economic giant George Pierides, while during 1922 the "Municipal Electricity Authorities" of Larnaka, Famagusta and Paphos were

formed followed by Kerynia's electric company in 1927. Even though these companies appeared during the 1920s, electrical power did not accommodate the countryside and small villages until 1952, when the "Electricity Authority of Cyprus (EAC)" was established. By that time, Cyprus contained 28 electricity companies that supplied the 6 cities plus 22 townships and villages with electricity during night time only. However, apart from the benefits that electricity provided Cypriots were reluctant to embrace the newly established power source in the country; this was mainly due to the long and frequent power interruptions along with the scarcity of electrical appliances. After the independence of Cyprus from the British colonial territories in 1960, the electrification of the country improved drastically, as between that year and 1972 the company managed to make the power source available to all the towns and villages around the island (EAC, 2014b).

Section 2.4.1.2: Dhekeleia "A" Power Station

In the early years of their operation, the mentioned small electricity companies had many problems to solve. Firstly, as their power plants were built in town and village centres they caused noise and discomfort to the residents living in the surrounding area. In addition, the weather conditions (especially during the summer months) caused damage to those plants' operational components. Thirdly, their early distribution networks were not in a good condition and the price of electricity was extremely high relative to today's prices. To solve these problems, the colonial government considered to build either one or two central power stations to cover the needs of the entire country. In 1950 the construction of the first Dhekeleia began and when it was completed, it had a capacity of **84 MW** and its location is indicated by the blue marker in Figure 2.20 (Google Maps, 2015b). Meanwhile with the establishment of the EAC in 1952, under the "Electricity Development Law" the company assume control of the other electric companies and gradually the entire electrical supply in Cyprus was produced by a government owned company (EAC, 2014b).

Apart from the absorption of the smaller companies, the EAC started constructing transmission lines linking Dhekeleia with Nicosia and Limassol with Larnaca. After the gradual decommission of the old generators, the EAC began to grow at a fast pace after the independence of Cyprus was granted in 1960, as mentioned in (EAC, 2014b).

Section 2.4.1.3: Moni Power Station

While the demand for electricity was growing at a rapid rate, the need for a second power station was presented and the government decided to construct it in Moni village, on the southern part of Cyprus in Limassol District. The red marker in Figure 2.20 indicates the station's location, **20 km** east of the city of Limassol (EAC, 2015b). The station became operational in 1966, when the first phase of construction was completed and it was finalized in 1976 with an output capacity of **180 MW**. The first two steam generators were installed in 1966 and the sixth in 1976, while the remaining four gas turbines were installed in two phases. In the first phase the first two were commissioned in 1992 and the other two in the second phase, in 1995. The station was eventually upgraded, consisting of 6 steam turbine units of **30 MW** each and 4 gas turbines of **37.5 MW** each, having an overall capacity of **330 MW**, until 2012 (EAC, 2012: p. 20; 2015b). From 2012 until 2013, all capacity from the steam turbine units was reduced, as the EAC decommissioned all the steam turbine units (EAC, 2012: p. 20; 2013: p. 18). Currently, the power station consists of the 4 gas turbine units, yielding a total capacity for the station at **150 MW** with a thermal efficiency of **10.7%** (EAC, 2013: p. 18).

Section 2.4.1.4: Dhekeleia "B" Power Station

In the summer of 1974, Turkey invaded Cyprus in two phases: the first in July and the second in August. The invasion caused massive damages and economic loss in all aspects of the Cypriot community, including the electricity supply (EAC, 2015b). Along with nearly **40%** of Cyprus soil being under Turkish occupation until today, the EAC is still supplying the occupied areas with electrical power for free (unbilled consumption), reaching the amount of **6.5 GWh** or about **0.17%** of total sales in 2013 (EAC, 2013: p. 9). From 1974 and until 1980, the EAC faced numerous difficulties caused by the invasion; however it managed to overcome them with dedication and hard work, making it one of the main factors of the country's economic development in the post invasion era. With that mentioned the Authority decided to replace the old and decaying Dhekeleia power station, as it was becoming uneconomical to run. The Dhekeleia "B" power station is situated on the same site as "A", with construction beginning in 1980 and the first **60 MW** unit was commissioned after two years. The final phase of this station was completed in 1993 and its total capacity reached **360 MW** (EAC, 2015b) and it currently contains 6 steam turbine units of **60 MW** and **28%** efficiency each along with 2 internal combustion units of **50 MW** and efficiency of **40.6%** each, raising the stations overall

capacity to **460 MW** (EAC, 2013: p. 17). The Dhekeleia "A" power station was decommissioned in 2002, having served the Cyprus public more than 30 years (EAC, 2015b).

Section 2.4.1.5: Vasilikos Power Station

Lastly, the third and final power station of Cyprus was commissioned in 2000, **25 km** east of Limassol; the green marker in Figure 2.20 shows the station's location. Initially, the station was commissioned in two phases: in the first phase two steam units of **130 MW** each and a gas turbine of **38 MW** were installed, while in the second phase, another steam unit of **130 MW** was added. Eventually, the station possessed three additional combined cycle units, capable of operating on both natural gas as well as diesel (EAC, 2015b). However, on the 11th of July 2011, the Vasilikos power station was severely damaged after an explosion occurred at the nearby Lieutenant General Evaggelos Florakis naval base. Less than two week after the accident, the Israeli government offered spare generators with a total output capacity of **15 MW**, while on the 16th of July the Cyprus government and a Turkish power company operating in the occupied areas signed an agreement for additional supply of **120 MW**, until the 29th of February 2012. Furthermore, the Greek government dispatched temporary generators with total capacity of **71.6 MW** and the station's gas turbine unit was repaired and became again operational on the 17th of August (EAC, 2011: p. 21). Today, the EAC fully completed the restoration programme of the power station, which currently possesses a total installed capacity of **868 MW**, possessing 3 steam units of **130 MW** and **35.1%** efficiency, 2 combined cycle units of **220 MW** of **46.1%** and **46.9%** efficiency and a gas turbine unit of **38 MW** (EAC, 2013: p. 17).

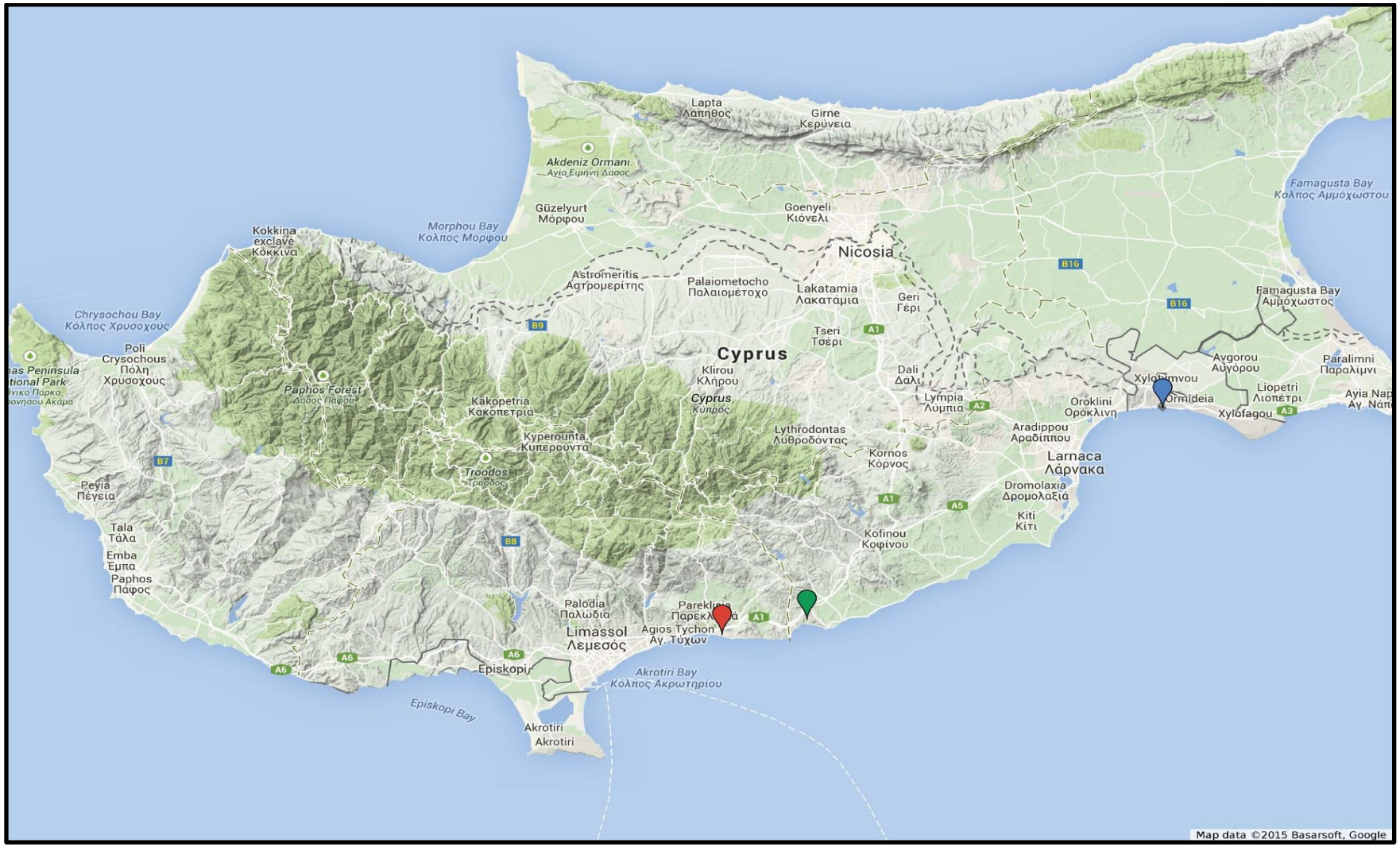

Figure 2.20: Location of the Dhekeleia (blue), Moni (red) and Vasilikos (green) power stations (Google Maps, 2015b)

Section 2.4.2: Electricity supply and demand

Electricity in Cyprus is produced by three power stations. Accurate details about them can be retrieved either from the EAC's Annual Reports, found in the authority's website. The most recent is for 2013 and it contains information regarding the electrical equipment of the power stations as well as the transmission/distribution network. It also contains the most recent plans about the building of new transmission substations, the upgrading of the existing power lines and the integration of electricity power generators based on renewable energy sources. Another important aspect of power production in Cyprus is the total output capacity of the three power stations and their ability to cover the overall country's demand. Statistics regarding the growth rate of that capacity as well as the maximum demand met between the years 2005 and 2013 are shown in Figure 2.21 (EAC, 2006: p. 13; 2007a: p. 13; 2008: p. 11; 2009: p. 11; 2010: p. 11; 2011: p. 9; 2012a: p. 9 & 2013: p. 9).

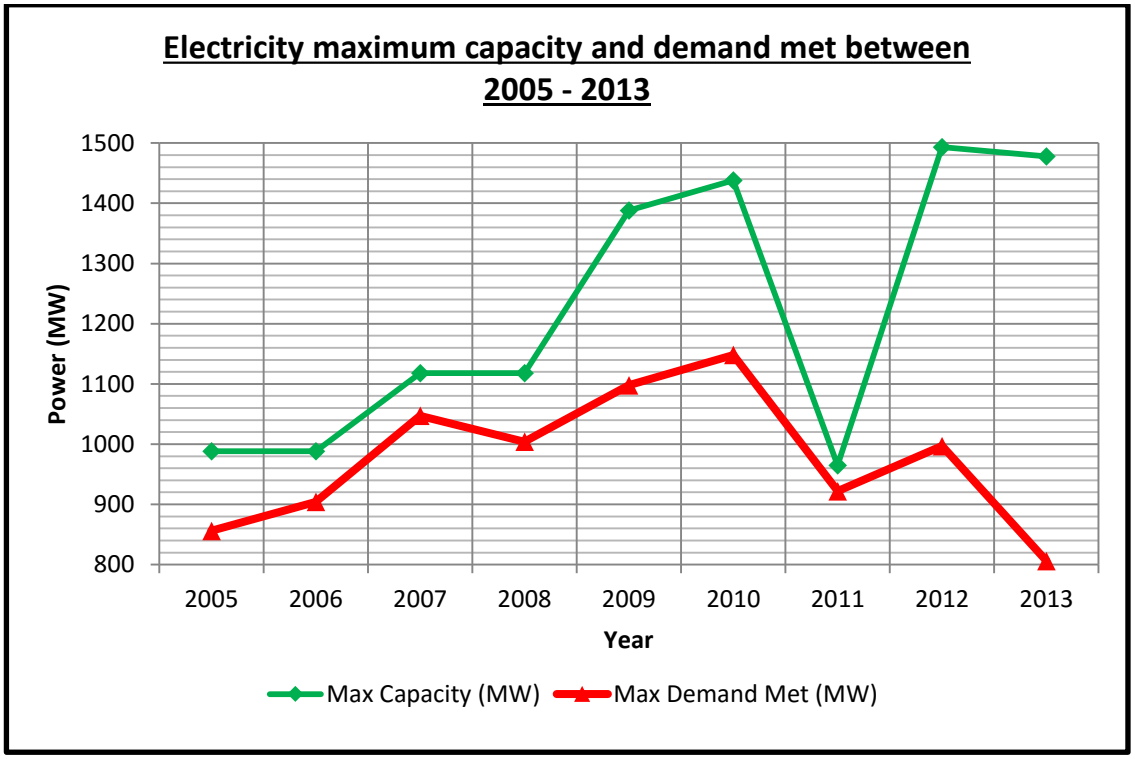

Figure 2.21: Total output capacity and maximum demand met in Cyprus between 2005 and 2013 (EAC, 2006: p. 13; 2007a: p. 13; 2008: p. 11; 2009: p. 11; 2010: p. 11; 2011: p. 9; 2012a: p. 9 & 2013: p. 9)

The electricity production capacity has been greater than the maximum electricity demand throughout the period. The reason is that if the capacity is less that the demand, then the system collapses, either partially or totally and either a "brownout" or a "blackout" occurs, respectively. The electrical generators in the power stations are

desynchronized and recovery from such events is time consuming. The most notable feature of the graph is the pinch point of the two lines in 2011, during the year in which the large explosion nearly destroyed Vasilikos power station (EAC, 2014b). As the graph suggests, the EAC's overall capacity dropped sharply from about **1420 MW** to less than **980 MW**. For this reason the demand had to be reduced to about **920 MW** as well with a series of planned switch offs for the system not to collapse, as explained above. Nevertheless, due to EAC personnel's efforts, the power station has been fully restored as indicated by the increased capacity during 2012 and 2013. The demand levels remained reduced since 2011, most probably due the global financial crisis affecting the country.

Figure 2.22 and 2.23 present each year's demand percentage compared to the network's capacity and the annual average electricity price per kWh, respectively (EAC, 2006: p. 13; 2007a: p. 13; 2008: p. 11; 2009: p. 11; 2010: p. 11; 2011: p. 9; 2012a: p. 9 & 2013: p. 9).

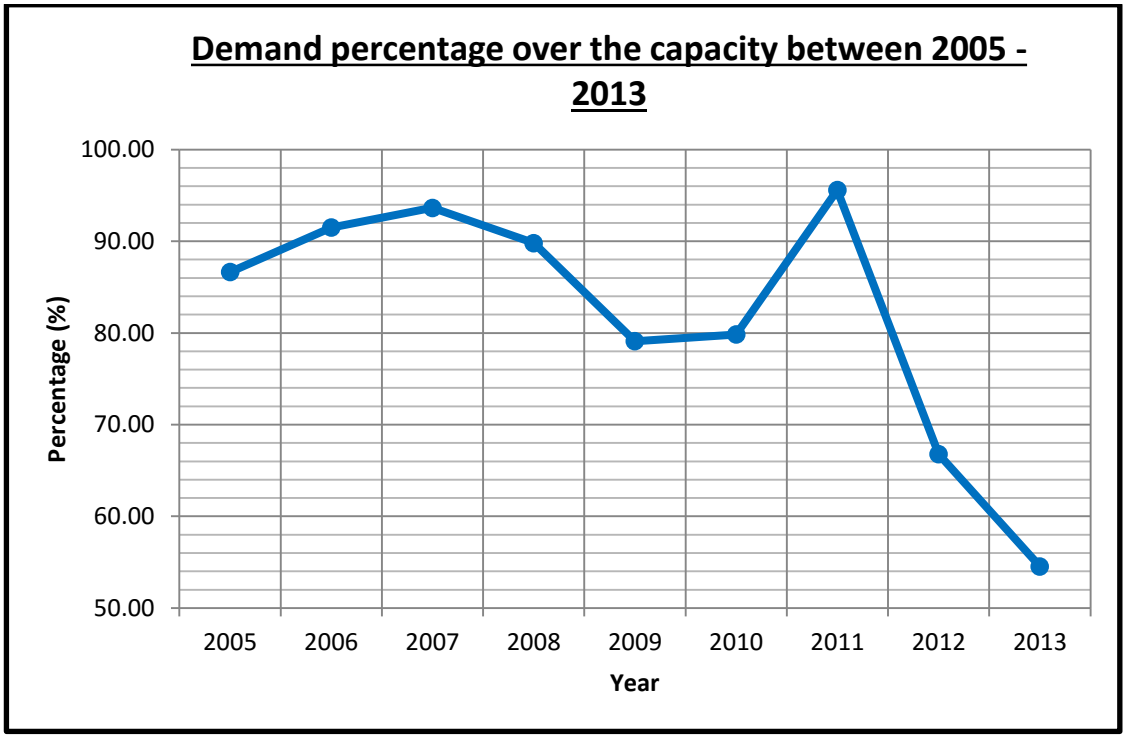

Figure 2.22: Companion graph to Figure 2.21 that shows the percentage of demand over the capacity between 2005 and 2013 (EAC, 2006: p. 13; 2007a: p. 13; 2008: p. 11; 2009: p. 11; 2010: p. 11; 2011: p. 9; 2012a: p. 9 & 2013: p. 9)

The graph shows that from 2005 to 2007, the demand was increasing compared to how much the network was capable of covering, marginally reaching the limit of that capacity at about **92%** in 2007. For that point until 2010 the capacity was improving each year, as the demand became less than **80%** of the capacity in 2009, while in 2011 the mentioned

explosion at the Vasilikos Power Station reduced the capacity to almost the levels of demand during that year. This is the reason why the EAC enforced the also mentioned power cut schedule for a few months. Finally, the graph shows an overall improvement since 2012, with the demand falling below **60%** of the capacity in 2013, as the demand decreased while simultaneously the capacity improved during that period.

In contrast to the overall improvement of the electrical network's capacity for accommodating the citizens' demand, the average price of electrical energy in the country during the same period as Figures 2.21 and 2.22 indicates an overall increasing trend as shown in Figure 2.23. As it becomes clear, since the EAC produces electricity using exclusively imported petroleum based fossil fuels, the average price of electricity would follow the trend of those fuels' price. This fact constituted Cyprus in 2013 as the EU country with the most expensive domestic electricity (excluding taxes), according to Eurostat (2015). This is an issue that the government officials as well as the citizens need to understand and start changing their mentality towards investing into renewable energy, especially during this recent financial crisis period.

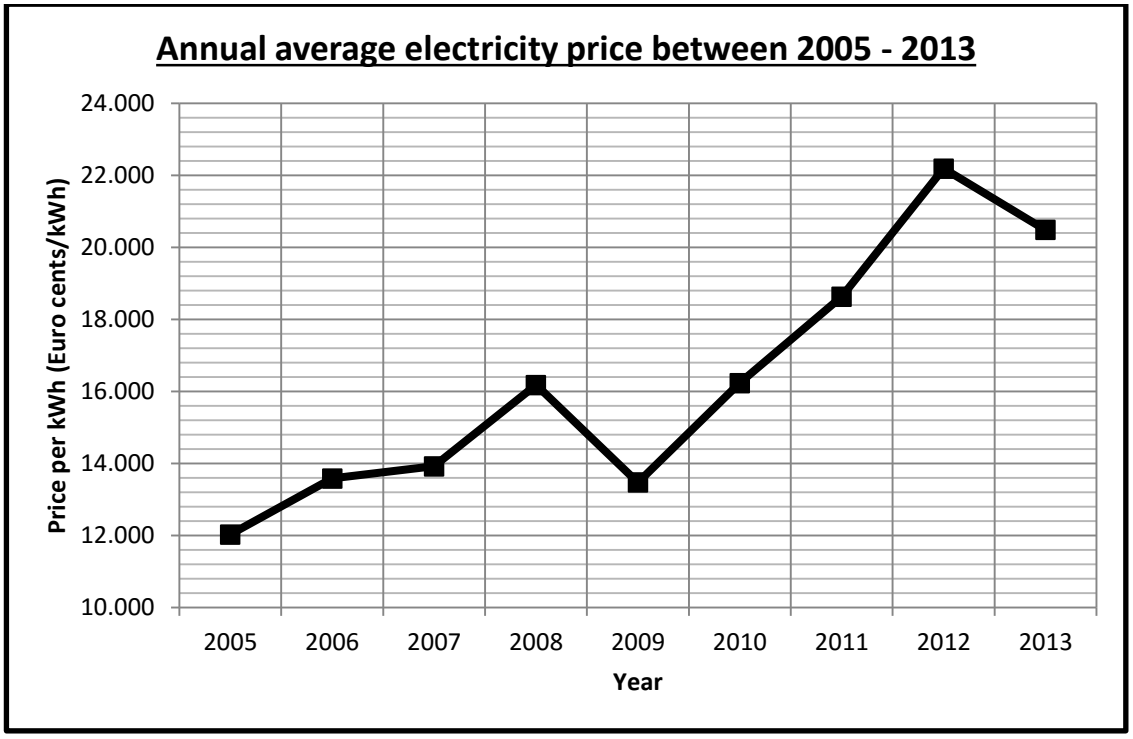

Figure 2.23: Average annual electricity price per kWh between 2005 and 2013 (EAC, 2006: p. 13; 2007a: p. 13; 2008: p. 11; 2009: p. 11; 2010: p. 11; 2011: p. 9; 2012a: p. 9 & 2013: p. 9)

Section 2.4.3: Electricity production/distribution equipment and transmission network

This section classifies (for informative purposes) the equipment for producing, transmitting and distributing electrical power throughout the country, which belongs to the EAC and thus, the public sector. Tables 2.1 and 2.2 contain the amounts of each EAC's equipment piece, as they were catalogued on the 31st of December 2013 (EAC, 2013: p. 131). These data are also in comparison with each previous year; in this case the data of 2013 are compared with those of 2012.

The deployment of the Transmission Network is also presented in the Annual Report of 2013 and it is shown in the map of Figure 2.24 (EAC, 2013: p. 19). In this latest available map all the transmission lines are shown and are colour coded according with their voltage level and depending on them being overhead or underground. Specifically the overhead lines are shown by the solid lines, while the underground ones are represented by dashed lines with the same colour as their overhead counterparts. The power stations and the transmission substations, by type, are also shown on the map. One can clearly see that the numbered locations of the power stations are on the south and southeast of the island; the reason is for tanker ships to supply them directly with fuel, thus eliminating road transportation costs. In the near future it will be possible to use Liquefied Natural Gas (LNG) for the operation of the number 4, 5 and 6 Combined Cycle Turbine units of the Vasilikos Power Station, which are designed to operate on both distillate fuel oil and LNG (EAC, 2007b).

Additional information regarding the proper operation of the country's entire electrical system can be found in the website of the Transmission System Operator (TSO) (TSO, 2015a). The website contains information and operating rules regarding the consumer's connection conditions on the network, maintenance, communication and electricity demand forecast, especially what involves the RES producers and the rules under which they can connect to the national network. Moreover, one can retrieve daily data about the country's overall electrical production, the network's total available capacity and the production from wind energy. Figure 2.25 presents the weekly data between the 6th and 13th of April 2015 (TSO, 2015b). It should be noted that the wind farms in Cyprus are directly connected onto the national network, while any form of storage for their power does not exist. This issue is further addressed in section 2.7.3.

Electricity Production & Transmission equipment					
Description	**Unit**	**In Commission by 31/12/2012**	**Commissioned in 2013**	**Taken out of Commission in 2013**	**In Commission by 31/12/2013**
Power Stations					
Dhekeleia Power Station:					
Steam Turbines	No.	6	---	---	6
Total Capacity	MW	360	---	---	360
Internal Combustion Engines	No.	6	---	---	6
Total Capacity	MW	100	---	---	100
Moni Power Station:					
Steam Turbines	No.	4	---	4	---
Total Capacity	MW	120	---	120	---
Gas Turbines	No.	4	---	---	4
Total Capacity	MW	150	---	---	150
Vasilikos Power Station:					
Steam Turbines	No.	---	3	---	3
Total Capacity	MW	---	390	---	390
Gas Turbines	No.	1	---	---	1
Total Capacity	MW	38	---	---	38
Combined Cycle Turbines	No.	2	---	---	2
Total Capacity	MW	440	---	---	440
Transmission Equipment					
220 kV Transmission Lines operated at 132 kV:					
Route Length	km	43.885	---	---	43.885
Circuit Length	km	87.77	---	---	87.77
132 kV Transmission Lines:					
Route Length	km	430.532	10.574	---	441.106
Circuit Length	km	861.064	21.148	---	882.212
132 kV Transmission Underground Lines:					
Route Length	km	206.763	0.779	---	207.542
Circuit Length	km	206.763	0.779	---	207.542
132 kV Transmission Lines operated at 66 kV:					
Route Length	km	56.66	---	3.048	53.612
Circuit Length	km	113.32	---	6.096	107.224
132 kV Underground Lines operated at 66 kV:					
Route Length	km	7.471	---	3.75	3.721
Circuit Length	km	7.471	---	3.75	3.721
66 kV Transmission Lines:					
Route Length	km	117.686	---	35.428	82.258
Circuit Length	km	117.686	---	35.428	82.258
66 kV Underground Lines:					
Route Length	km	2.185	---	1.43	0.655
Circuit Length	km	2.185	---	1.43	0.655

Table 2.1: Power Production and Transmission equipment on the 31st of December 2013 (EAC, 2013: p. 131)

Electricity Transmission & Distribution equipment					
Description	**Unit**	**In Commission by 31/12/2012**	**Commissioned in 2013**	**Taken out of Commission in 2013**	**In Commission by 31/12/2013**
132/66 kV Interbus Transformers:					
Quantity	No.	13	---	---	13
Transformer Power	MVA	648	---	---	648
132/11 kV Step Down Transformers:					
Quantity	No.	94	8	1	101
Transformer Power	MVA	3152	272	31.5	3392.5
132/6.6 kV Step Down Transformers:					
Quantity	No.	2	---	---	2
Transformer Power	MVA	58	---	---	58
132/3.3 kV Step Down Transformers:					
Quantity	No.	2	---	---	2
Transformer Power	MVA	20	---	---	20
66/11 kV Step Down Transformers:					
Quantity	No.	56	1	2	55
Transformer Power	MVA	588	15	26	577
66/3.3 kV Step Down Transformers:					
Quantity	No.	2	---	---	2
Transformer Power	MVA	5	---	---	5
15.75/132 kV Step Up Transformers:					
Quantity	No.	3	---	---	3
Transformer Power	MVA	495	---	---	495
11/132 kV Step Up Transformers:					
Quantity	No.	20	---	---	20
Transformer Power	MVA	1304	---	---	1304
11/66 kV Step Up Transformers:					
Quantity	No.	4	---	---	4
Transformer Power	MVA	150	---	---	150
Transmission Substations:					
Quantity	No.	64	---	---	64
Distribution Equipment					
MV Overhead Lines	km	5696.21	101.605	20.57	5777.28
MV Underground Lines	km	3608.98	101.28	13.75	3696.6
LV Overhead Lines	km	9558.19	146.108	34.57	9669.73
LV Underground Lines	km	5366.61	325.33	5.295	5686.65
22000 – 11000/433/250 V:					
P.M. Transformers	No.	9754	253	74	9933
	kVA	910756	21548	8815	923489
22000 – 11000/433 V:					
G.M. Transformers	No.	6023	136	10	6149
	kVA	3377800	83508885	28440	3432868.89

Table 2.2: Power Transmission and Distribution equipment on the 31st of December 2013 (EAC, 2013: p. 132)

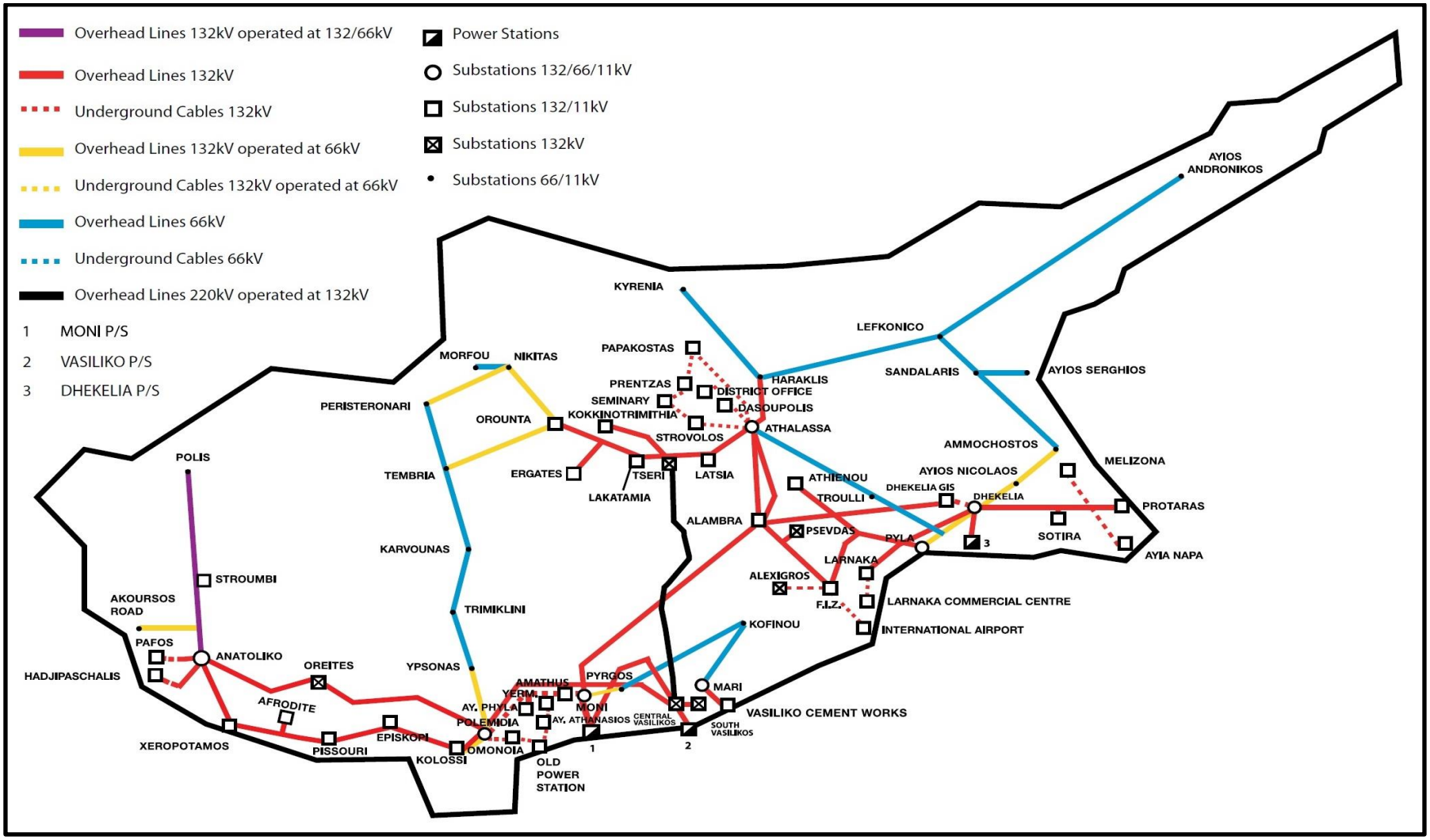

Figure 2.24: Map of the Transmission network of Cyprus at the end of 2013 (EAC, 2013: p. 19)

Section 2.5: Emissions

Section 2.5.1: Introduction

Using fossil fuels to cover the demand for electricity production transport and building heating releases dangerous gases into the atmosphere that worsens the Greenhouse effect and causes health and other environmental problems. These include more frequent flood and heat wave events, increase of air pollutants, easier spread of infectious diseases, such as **malaria**, **tick borne encephalitis**, **Lyme disease** and **West Nile fever**, **heat wave related deaths** and **allergic reactions** (Confalonieri et al., 2007: p. 395). Since those fuels consist mainly of large hydrocarbon molecules, their combustion products are mainly carbon dioxide (**CO_2**) and water vapours (**H_2O**). Moreover, in the cases that combustion is incomplete a proportion of the fuel converts into carbon monoxide (**CO**), which is also toxic as well as a greenhouse gas. The European Union is seriously conserved about this issue and it has already considered measures for reducing the effects of greenhouse gases and for promoting the exploitation of RES.

Section 2.5.2: European Union Emissions Trading Scheme (EUETS)

To protect the health of its residents, the European Union created the European Union Emissions Trading Scheme (EUETS), which gives economic motives to the Member States for reducing their greenhouse emissions in a financially effective manner. It is based on the principals of the Kyoto Protocol, the Joint Implementation (JI) and the Clean Development Mechanism (CDM) systems, even though it is completely independent from them. EUETS is the first company level programme incorporating a system of allowances per tonne of carbon dioxide equivalent (tCO_2e) worldwide. In other words it assigns a financial price on each tCO_2e that each Member State emits so that they further promote green and low carbon technologies and for attracting investments (European Commission, 2009: p. 5).

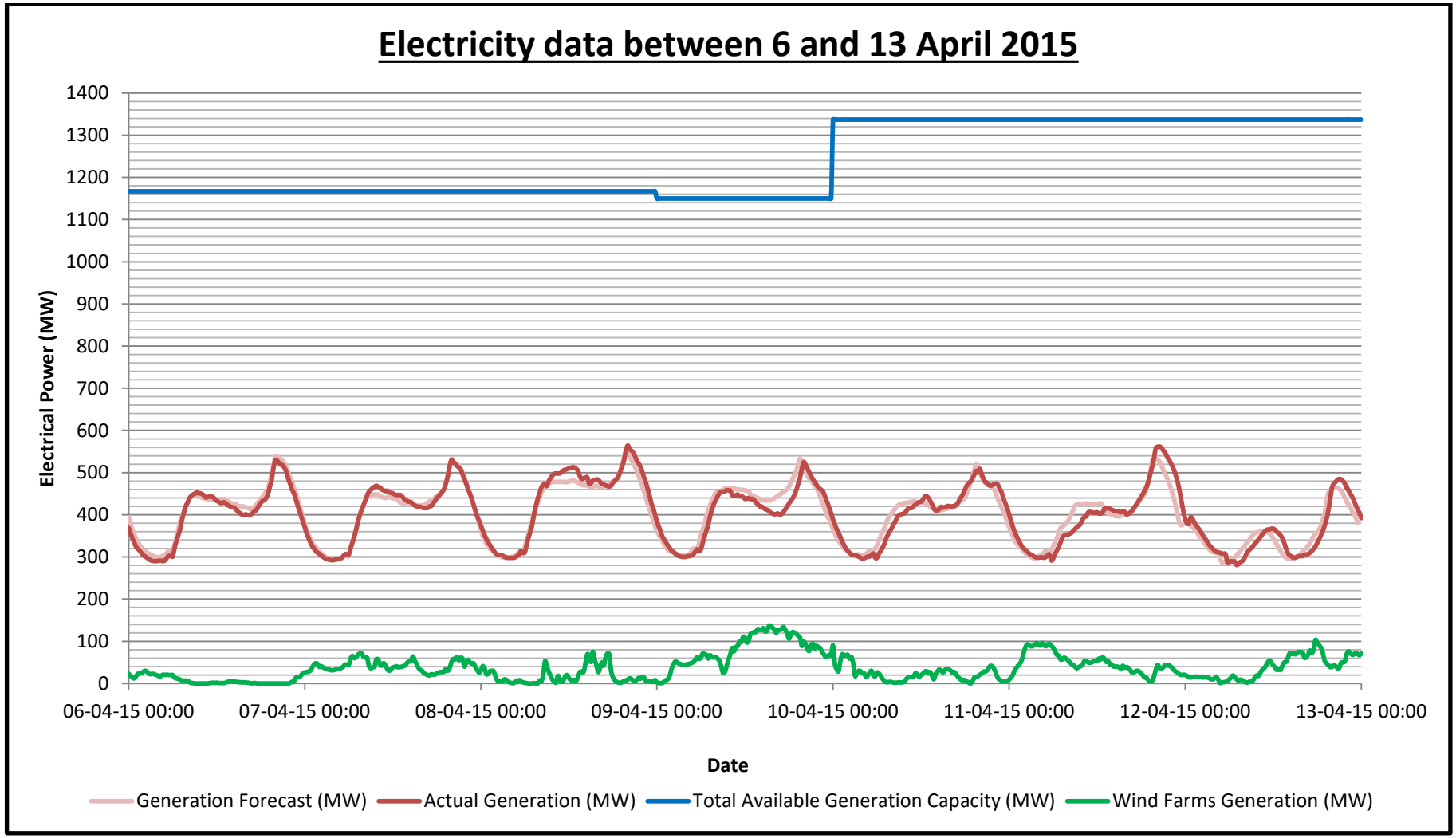

Figure 2.25: Electrical power data for the week between 6 and 13 of April 2015 (TSO, 2015b)

As already mentioned, the core of this system is the emission allowance, which serves as a universal currency of measuring how many tCO_2e a Member State is allowed to emit. More specifically, one allowance permits its owner to emit one tCO_2e. All the nations will have to forecast their emissions level for each trading period and by submitting these forecasts to the European Commission, the appropriate amount of allowance would be allocated to each one. As it is a company level programme, if an industrial unit emits less tCO_2e than the amount of its allowance permit, that unit could sell the excess. On the other hand, if a unit exceeds the amount of tCO_2e allowed to emit, it can either purchase allowance, incorporate green technologies or both; this scheme can be integrated to a national level as well. One can understand that buying allowance acts as a penalty to the organization which does not operate in an environmentally friendly manner. With that mentioned all organizations within the EU are motivated to reduce their carbon footprint, hence reducing the effects of climate change (European Commission, 2009: p. 9). Aside from this, the EU has set three targets through this scheme planned to be achieved by **2020** to further motivate the Member States into embracing the concept of emission reduction and the promotion of Renewable Energy Sources (RES). These targets are (European Commission, 2009: p. 11):

a) Reduction of CO_2 emissions by at least **20%** of the levels of 1990 (base year),
b) Reduction of energy consumption by at least **20%** of the levels of the base year and
c) Production of at least **20%** of overall energy from RES

European Commission (2009) explains the aims of this scheme, its targets and foundations; hence it is an important part of this project. It can be used as a guide for comparisons between Cyprus and the rest of the Union in terms of emission handling and energy production.

Since Cyprus is one of the EU's 28 (for the time being) Member States, it is obliged by law to follow its Directives. Evidence of the greenhouse gas levels in the Cypriot atmosphere can be found in the Statistical Service of the government (MF, 2014c). This file contains data from 1990 until 2012 and these data were used to construct two charts seen in Figures 2.26 and 2.27 (MF, 2014c). The former figure presents the actual quantities of greenhouse gases, in $MtCO_2e$ that had been emitted in the years between 1990 and 2012, keeping in mind that 1990 is the base year according to the EUETS. It can be observed clearly that the overall levels of those gases increased as the

time progresses, except in the case of 1995, 2002 and from 2009 until 2012. Given that Cyprus's accession to the EU was in 2004 and the EUETS was implemented in 2005, it can be seen from Figure 2.26 that no significant effort has been made to reduce greenhouse gases being emitted in Cyprus, until 2009. Figure 2.27 presents a complementary chart, in which the total gas emission quantities are represented as their percentage, relative to the levels of the base year. The highest percentage was recorded in 2008 with about **175%** the amount of greenhouse gases emitted of 1990. That is almost double the amount emitted during the base year, which is unacceptable since the island is being obliged by the EUETS. Therefore it is necessary for the government to take immediate action for reducing the emissions to the levels set by the EUETS otherwise Cyprus will face financial consequences. This concept can be further analysed by presenting data concerning emissions of the major greenhouse gases by sector in the next section.

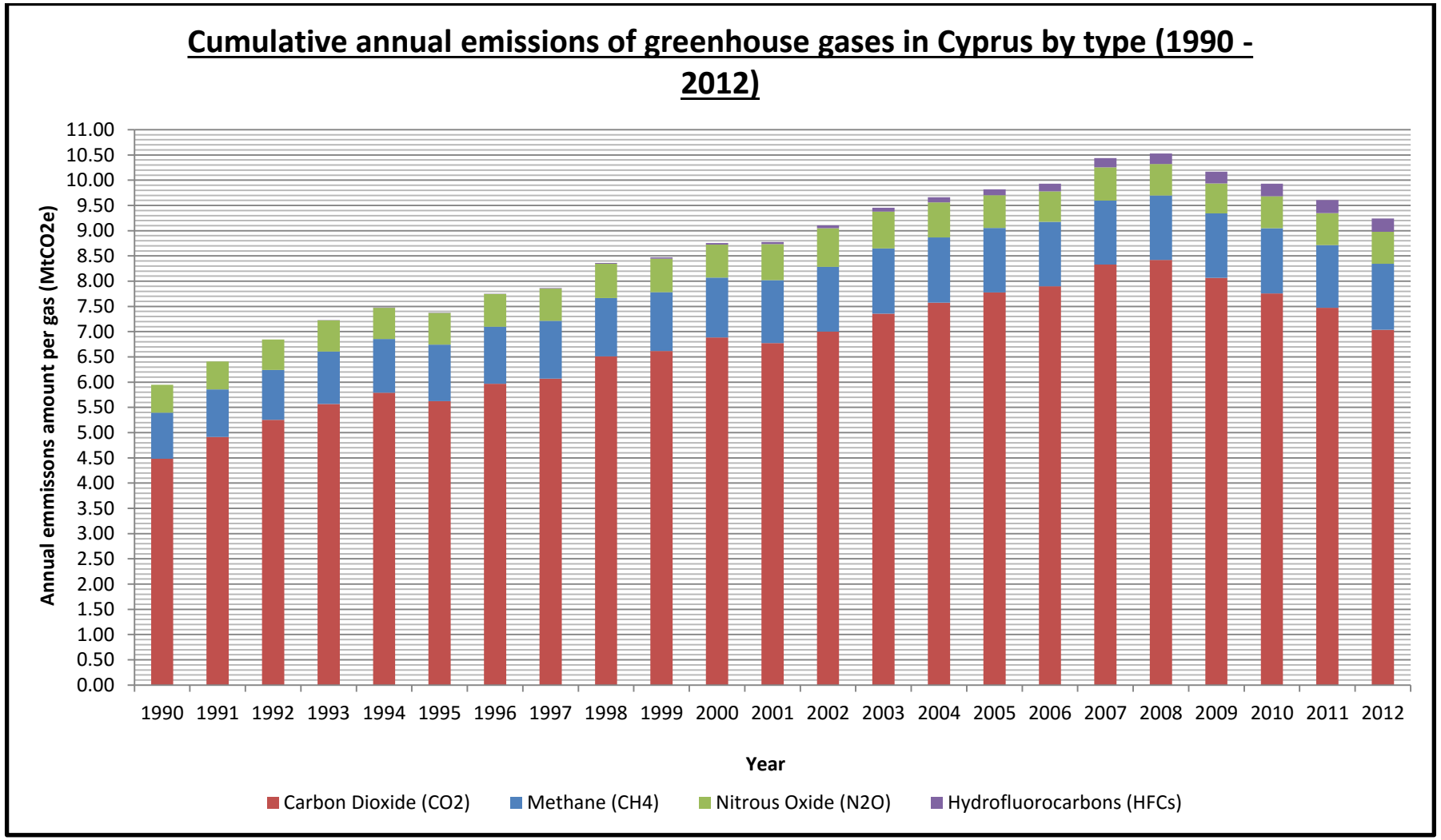

Figure 2.26: Quantity of greenhouse gases in Cyprus between 1900 and 2012 (MF, 2014c)

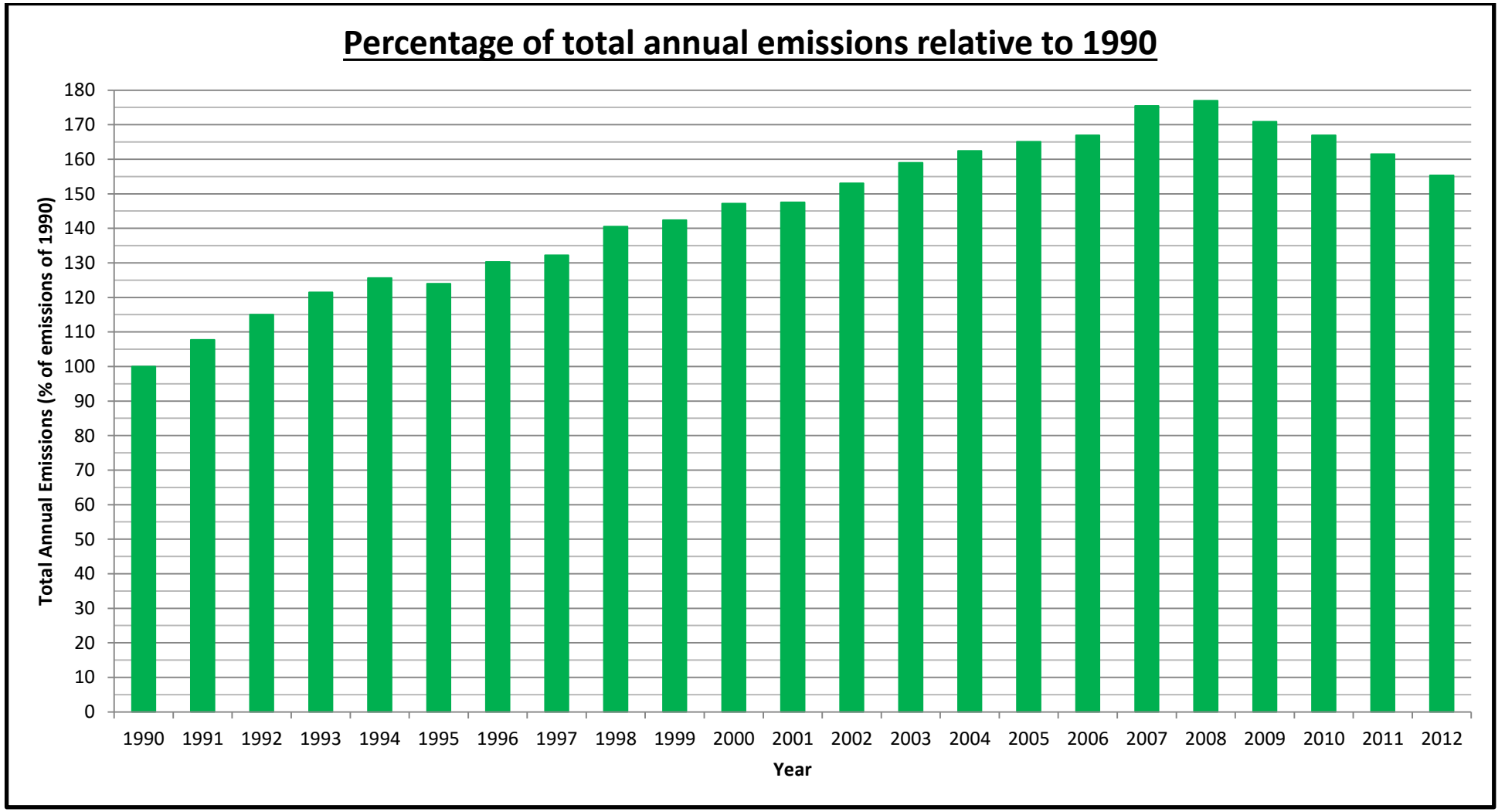

Figure 2.27: Percentage of greenhouse gases produced every year between 1990 and 2012 relative to the level of 1990 (MF, 2014c)

Section 2.5.3: Important greenhouse gas emissions by sector

The most important greenhouse gases are carbon dioxide (CO_2), methane (CH_4), nitrous oxide (N_2O), ozone (O_3) and chlorofluorocarbons (CFCs). The former three are abundant in the atmosphere, as they occur from both natural processes and human activity; Figure 2.26 confirms this. For this reason, the levels of these gases are annually measured and it is very important to be kept as low as possible. Researches created the unit of tCO_2e, so that the strengthening of the greenhouse effect by each greenhouse gas is compared to that of the CO_2. The reason is that the lifespan of this particular gas in the atmosphere is relatively infinite, since there are neither chemical nor photochemical sinks for CO_2 in the atmosphere (Harvey, 1993: p. 24, 33). The conversion to tCO_2e occurs when the mass of a greenhouse gas in tonnes is multiplied by its Global Warming Potential (GWP). The GWP of a number of the most important greenhouse gases, according to the Second Assessment Report (SAR), are shown in Table 2.3 (IPCC, 2012).

Greenhouse Gas	Chemical Formula	Global Warming Potential Factor
Carbon Dioxide	CO_2	1
Methane	CH_4	21
Nitrous Oxide	N_2O	310
Trifluoromethane	CHF_3	11700
Bifluoromethane	CH_2F_2	650
Tetrafluoromethane	CF_4	6500
Hexafluoroethane	C_2F_6	9200

Table 2.3: Global Warming Potential Factors of some greenhouse gases (IPCC, 2012)

For example, CH_4 has a GWP of 21, which means the 1 tonne of methane has the same effect on the environment as 21 tonnes of CO_2. The most dangerous gas in this table is CHF_3; its GWP is 11700 meaning that even small amounts emitted is capable of causing massive greenhouse pollution. More specifically, **1 kg** of the gas has the equivalent effect on global warming as almost **12 tonnes** of CO_2.

Three additional figures (2.28, 2.29 and 2.30) present the emissions of the three primary greenhouse gases by sector (MF, 2014c). The charts indicate that the sector with the most significant contribution to global warming is energy that had an overall increasing trend until 2008, being responsible for over **7.5 $MtCO_2e$** emitted during that year. On the other hand, land use change and forestry had a decreasing contribution throughout the period, even though it was negligible. This means that the preservation

and increase of forests is imperative for this sector to have a more significant impact on the reduction of CO_2 levels. The waste and agriculture sectors were responsible for releasing the greatest proportion of CH_4, even though its levels are not comparable to those of CO_2 during the whole period. This particular gas can be collected from the mentioned sectors and be used as fuel at a district level, instead of being left to pollute the atmosphere. Finally, Figure 2.30 shows that the most impactful sector for emitting N_2O during the whole period was agriculture, while the contribution of the other two was not significant. The most significant causes of the N_2O emissions are the usage of fertilizers containing nitrogen compounds and manure management (MF, 2014c). The solution for reducing the emissions of this gas is the substitution of those fertilizers by farmers with organic fertilizers, such as dried livestock manure and composted farming plant waste.

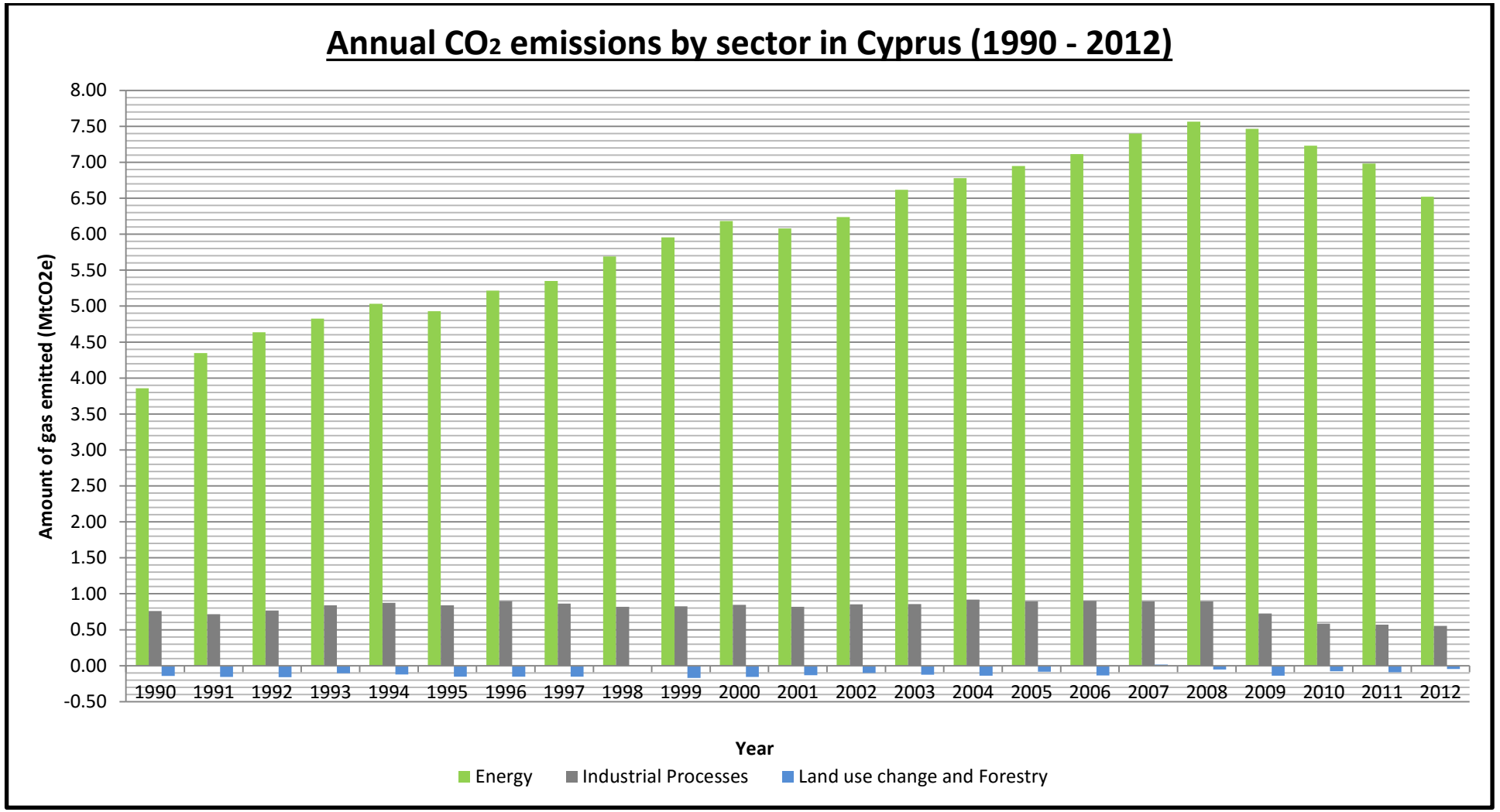

Figure 2.28: Amount of carbon dioxide (CO_2) emitted by sector between 1990 and 2012 (MF, 2014c)

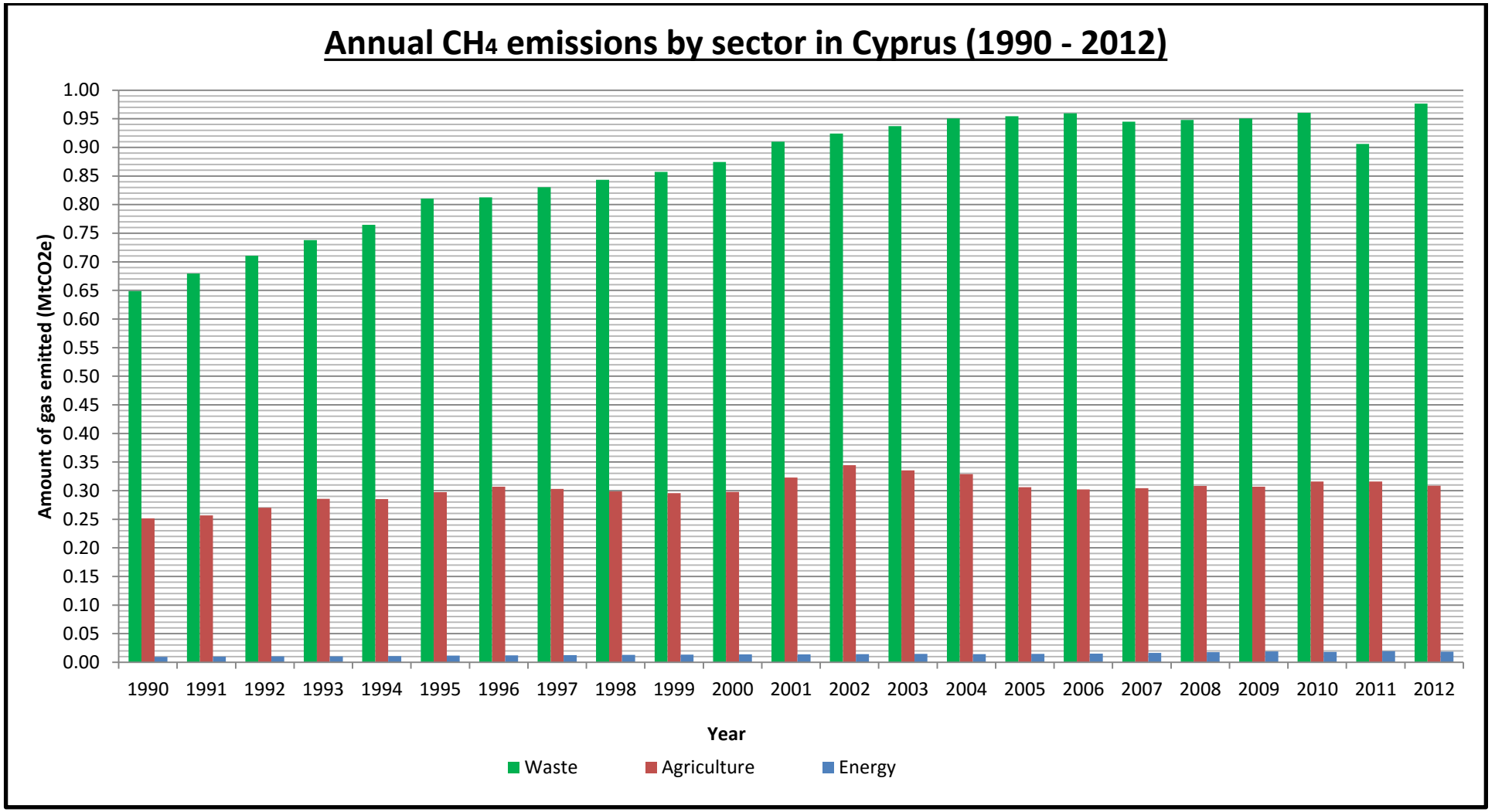

Figure 2.29: Amount of methane (CH_4) emitted by sector between 1990 and 2012 (MF, 2014c)

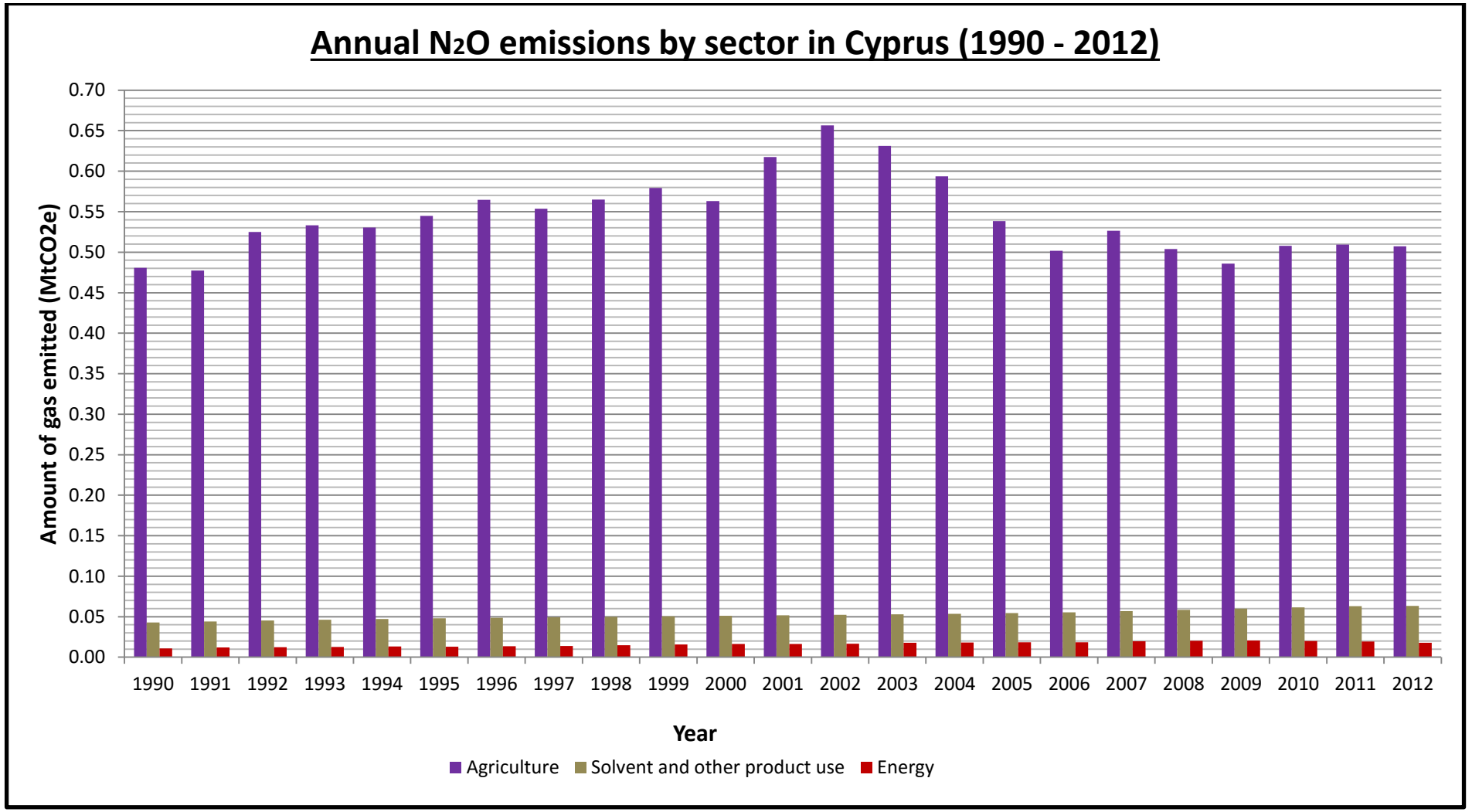

Figure 2.30: Amount of nitrous oxide (N_2O) emitted by sector between 1990 and 2012 (MF, 2014c)

As expected, the largest proportion of air pollutant emissions are due to the energy industry, as seen in Figure 2.28 and more specifically, the greenhouse gas emitted in this case is CO_2. This is strongly correlated to the fact that, during the sample period, Cyprus' energy sector was dependant entirely on fossil fuel. Furthermore the annual registered passenger car number has been increasing exponentially, as seen in Figure 2.17 (MF, 2011b, 2014b). Lastly, the EUETS has been into effect since 2005, so any emissions control mechanisms set by the EU to its members did not exist until then and as a result air pollution was uncontrolled. By observing Figure 2.26 the CO_2 emissions had 3 periods of increase, between 1990 and 1994, from 1995 until 2000 and from 2001 until 2008. Even worse the EU had allocated to Cyprus for the period between 2008 and 2012 annual allowance worth of **5.48 $MtCO_2e$** (EUROPA, 2007) and from the statistics in Table 2.4 (MF, 2014c), the total annual levels during that period were almost double of the annual amount of allowances allocated from the EUETS programme.

Greenhouse gas	**Annual amount of CO_2e in millions of tonnes ($MtCO_2e$)**				
	2008	**2009**	**2010**	**2011**	**2012**
CO_2	8.42	8.06	7.75	7.47	7.04
CH_4	1.28	1.28	1.30	1.24	1.31
N_2O	0.63	0.60	0.63	0.63	0.63
HFCs	0.21	0.23	0.25	0.26	0.26
Total Annual Emissions Level	**10.54**	**10.17**	**9.93**	**9.60**	**9.24**
Total Annual Emissions Level if CO_2 emissions from Energy sector were halved	**6.33**	**6.14**	**6.06**	**5.87**	**5.72**

Table 2.4: Total annual emission levels from 2008 until 2012 (MF, 2014c)

As Table 2.4 also suggests, if the proportion of the total annual emission levels of CO_2 sector during the mentioned period was half of what was actually measured, then the total annual levels of all gases in 2012 would have been only **0.24 $MtCO_2e$** greater than the amount of the annual EUETS allowance.

Section 2.6: Energy saving measures

Section 2.6.1: Introduction

Solving the increasing demand problem will be a difficult task that requires the collaborative effort of all people around the world. However, this goal is rather achievable and its initiative is the reduction of energy demand per capita followed by the invention of new and more efficient clean energy producing technologies. Chapter 5 of this thesis describes these issues in more detail.

Section 2.6.2: EAC's energy saving advisory instructions

As mentioned, the first and most important step towards energy demand reduction is to for each individual person to decrease his personal energy consumption, especially in the cases where energy is wasted. This is achieved when every resident of a country follows a simple set of advisory instructions in order to save precious energy and when the government takes measures to enforce those instructions, by penalising those who do not collaborate with them. In the case of Cyprus, the EAC in its website is the one to provide those energy saving rules. These instructions are divided into six categories, covering thermal insulation, space heating and cooling, water heating, lighting and appliances. Additionally, Table 2.5 summarizes the mentioned rules (EAC, 2014c).

These instructions are not mandatory and it is left up to each individual resident to apply them in his own household. However, it is in each government's best interest to enforce them, accompanied by informative seminars and television programmes in order to intrigue the public's genuine interest.

Category	Rules
Thermal Insulation	1. Application of proper insulation in every building
	2. Application of heat loss reducing measures
Space Heating and Cooling	1. Allowance of sunlight to enter building spaces
	2. Adjustment of central heating thermostats to 20 ºC and below
	3. Heating panels and radiators must not be covered
	4. Central heating systems have to be maintained once a year
	5. Air conditioning units must be used in minimum
	6. Application of appropriate household shading
	7. Plantation of broadleaf trees for shading and cooling
	8. The wall and rooftop colour has to be bright, preferably white
	9. Reduction of excess heat by not using specific appliances and by changing the incandescent lighting with fluorescent
	10. It is better for building to be ventilated only during night time in summer
	11. Strategic openings and fans can ventilate buildings more effectively
Lighting	1. Natural lighting should be allowed in building spaces
	2. Internal walls and ceilings should be painted with bright colours
	3. Artificial lighting should only be used when needed
	4. The usage of economical fluorescent light bulbs is recommended
	5. Light bulbs and fittings should be cleaned on a regular basis
Electric Water Heaters	1. Installation of a solar water heating system is highly recommended, rather than an electric one
	2. Residents should use of an electric water heater only when needed and have a shower, rather than a bath.
	3. Washing machines should be connected with the solar heating system for hot water
Appliances	1. All appliances should be labelled with energy class C and above

Table 2.5: Major energy saving advice given by the EAC (Reproduced: EAC, 2014c)

Section 2.7: Renewable Energy Sources' exploitation potential in Cyprus

Section 2.7.1: Introduction

Another solution to the problem of greenhouse gas emissions is to use alternative means of producing energy for all of human activities. Additionally, people need to preserve as much energy as possible and not waste it. Furthermore, Section 2.5 mentions that one of the EUETS goals is by 2020 at least **20%** of overall energy should be produced by Renewable Energy Sources (RES) (European Commission, 2009: p. 11). In recent years, important steps have been made towards this goal and large scale RES power plans have been commissioned. This section analyses the current RES infrastructure in Cyprus along with the future plans regarding this sector and it is not a discussion about individual technologies. Finally, Figure 2.31 analyses the annual electricity production in Cyprus for 2013, by energy type (EAC, 2013: p. 9, 46).

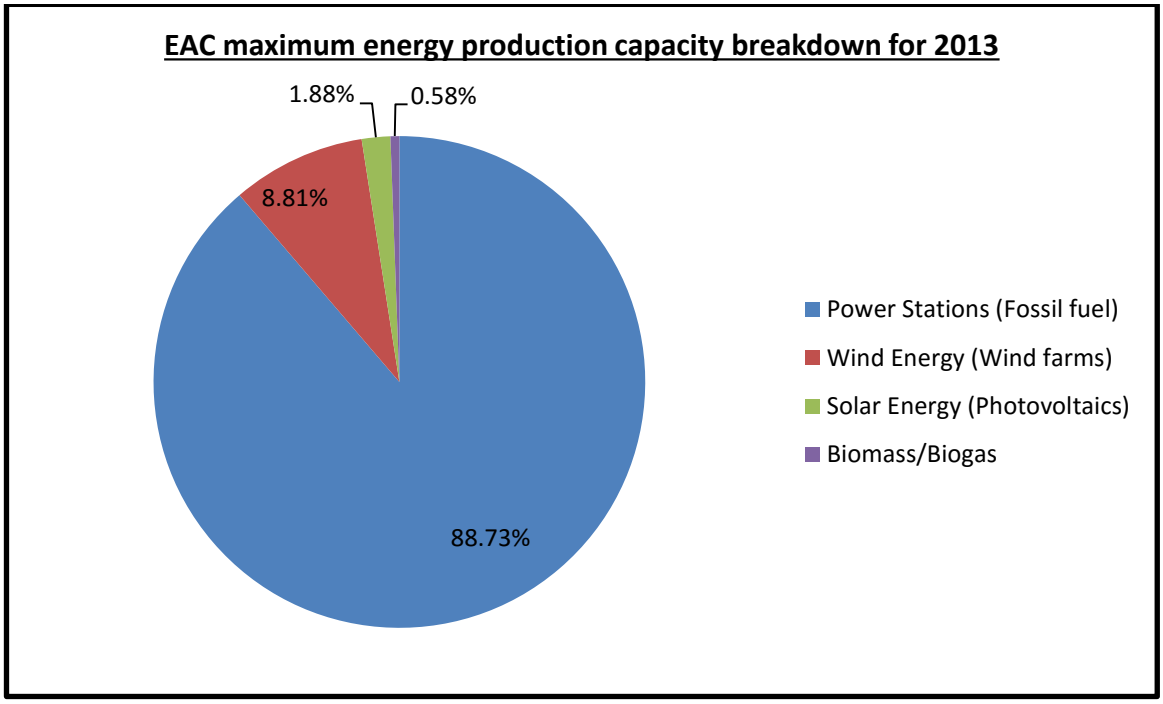

Figure 2.31: Annual electricity production capacity percentage in Cyprus for 2013 by energy type (EAC, 2013: p. 9, 46)

Figure 2.31 shows that in 2013 nearly **89%** of the overall installed electricity production capacity was due to the three power station using fossil fuel. So, only about **11%** of the overall electricity production is due to renewable sources, which is less than the EUETS **20%** target for 2020 (see Section 2.5.2). Fortunately, the EAC is constantly moving towards increasing this percentage.

Section 2.7.2: Solar energy

Renewable energy is not a newly established concept into the minds of Cypriots. Cyprus was the leading EU country in 2010 in solar energy exploitation, since it had the largest proportion of solar collector surface area relative to the other Member States, with **0.873 m^2** per capita (EurObserv'ER, 2011: p. 89). This article also includes the already installed concentrated solar power plants in operation in 2010, the annual installed solar thermal collector surface area by type and the total EU solar thermal collector capacity in 2009 and 2010. These pieces of information are useful in this thesis, as the government of Cyprus can make comparisons with the other EU Member States and take into consideration the measures that countries with similar climate take regarding solar energy exploitation. In contrast, Photovoltaic (PV) Systems are not as popular as solar water heaters are in Cyprus because of their small efficiency. According to the Australian company SunPower Corporation, they provide PV collectors with the highest efficiency of all silicon based panels, with a maximum efficiency of **21%** (X-Series) (SunPower, 2014). Additionally, Sharp distributes its own solar products; **NU–R250(J5)** (monocrystalline) and **ND–R250A5** (polycrystalline) both of which having efficiencies of **15.2%** (Sharp Electronics (UK) Ltd., 2015a; 2015b). Furthermore, Panasonic has developed its own, HIT (Heterojunction with Intrinsic Thin layer) solar modules, **VBHN240SJ25** and **VBHN245SJ25** with **19.4%** efficiency (Panasonic Corporation, 2015). So, for the time being the Photovoltaic technology is not efficient enough to convert the large quantities of the Mediterranean sunlight into useful electricity and so such an investment today is costly.

As PV is a relatively new technology, Solar Thermal (STh) is a well-established and cost effective technology that is been utilized for hundreds of years and includes a number of applications. These involve: space and water heating, cooling and dehumidifying ambient air and process heating; in the case of Cyprus, it may be possible to be used for the purposes of sea water desalination. Several countries, such as Germany, are amongst the world's leading solar thermal industries with high expertise in producing and utilizing solar thermal systems, regardless of its Central European latitude range (DENA, 2014: p. 47).

For domestic applications, STh technology offers a variety of options, depending on the type of application. A common type is heating water for washing purposes or Domestic Hot Water (DHW), in which all the needed water is heated to the desired

temperature during day time, especially during the summer period. During the winter period, however, solar thermal systems support other systems based on fossil fuel for producing DHW, instead. Nevertheless, the STh system is capable of covering about **60%** of the DHW demand per annum, a significant contribution to the reduction of fossil fuel dependency in this sector (DENA, 2014: p. 47).

An extension of the solar heating system is the so called "Combi-system" that has the additional function of space heating of its host – building. These systems have larger collectors than the regular water heating systems and they are capable of covering between **20** and **30%** of the building's space heating demand, depending on how well insulated the building is and its required level of heat. In addition to space heating, STh systems can be utilised for space cooling and refrigeration processes as well. Components, such as absorption chillers, are capable of harnessing thermal energy and through several evaporation and condensation stages, provide space cooling as air conditioning systems and refrigeration for industrial purposes (DENA, 2014: p. 48).

The capability of a STh system to cover the demand of its host building is of great importance, as this is an indication of the system's performance. Dongellini et al. (2015) simulated the operation of a DHW system with various solar collectors, storage tank capacities and hourly consumption profiles in order to evaluate its solar thermal energy absorption capability by measuring the dependency of the system's Solar Coverage Factor (SCF) (an indicator of efficiency and therefore performance of the system) on the three mentioned factors. Using a dynamic model, they proved that the SCF of the system is strongly influenced by the consumption profile of the building. The type and number of collectors were not as important, as the experiment indicated that by using three evacuated (EC) collectors provide would give the best SCF annual results, but with small differences compared to the other two types (pp. 633-634).

An innovative polygeneration system has been simulated and optimized by the team of Mohan et al. (2015), for space cooling, distilled fresh water and DHW in the UAE. Even though this system is not of a residential scale, its novelty is very significant as it exploits solar thermal energy to a great extent by providing a precious distilled water and cooling in a country situated in the Arabian Desert. The second remarkable issue of this system, is that DHW is a by-product of its operation, meaning that waste of heat is minimized. The system throughout the year has a combined efficiency between **31** and **38%**, producing on a daily basis between **70** to **94 kg** of distilled water, between **114** and

370 kWh of chiller productivity and between **171** and **302 kWh** of DHW productivity per annum. Moreover, the researchers calculated that under optimal settings, the system's payback period would be **6.75 years** with a net cumulative saving of about $**0.5m**. Further improvements of these last two figures are achieved through the prevention of **109 tons** (or about **98.9 tonnes**) of **CO_2** being emitted into the atmosphere, leading to a reduction by **8%** of the payback period and increase by **14%** of the net cumulative saving.

Section 2.7.3: Wind energy and hydro pumped storage

Wind energy is also embraced in Cyprus on a commercial scale. The country already has an electricity capacity of **146.7 MW** (EAC, 2013: p. 46) derived from Wind Farms and this fact is responsible for the **9.9%** of electricity being produced by wind energy. As mentioned in section 2.2.3, the most common wind speed range in the country is the one between **2** and **4 m/s** and also that most wind generators have their wind speed threshold for electricity production at **4 m/s**. This means that Cyprus is not the most suitable area for the establishment of wind farms; however investments have been made and several wind farms have been commissioned. Another important issue that should be taken into consideration when constructing a wind farm is the Hydro Pumped Storage System. The Canary Islands utilized this system, which increases the reliability of a wind farm by omitting the amplitude and frequency fluctuations of the voltage produced from wind energy. This is done by combining the wind farm's operation with naturally occurring or fabricated water reservoirs for storing the electrical energy produced by the farm into potential energy. Water from the lower altitude reservoirs is pumped into the higher altitude ones using the electricity the Wind Farm produces during periods of low demand. When the demand increases, the water from the higher altitude reservoirs flows into a hydroelectric power station that has high efficiency and the voltage generated is more stable than the voltage produced directly from a wind generator (Bueno et. al, 2006: p. 316 – 317). The necessity of the storage should be stressed since Figure 2.25 (TSO, 2015b) suggests that there is a correlation between the amount of wind produced electricity injected into the network and the stability of the power generated from the power stations. More specifically, the figure shows that when there is increased production from the wind farms, the actual generated power presents various fluctuations and does not follow exactly the forecasted generation pattern. This is most probably due to the fluctuations of the wind produce voltage causing it not to fully parallelize with the network's more stable energy from fossil fuels.

A similar system exists in the UK, at Ffestiniog in Wales. The hydroelectric power station in the area operates by driving water from an upper reservoir (Llyn Stwlan) to a lower reservoir (Tan-y-Grisiau) through its turbines, during periods of high demand. The difference with the Canary Islands' system is that the upper reservoir is refilled by utilizing electricity from the national network of the UK and not from renewable wind energy during night time, when demand is low (FHC, 2015).

Section 2.7.4: Electricity from Renewable Energy selling prices

Apart from the two previous RES, the Government of Cyprus wishes to promote the development of other RES. It reports that the national goal for the share of RES in the overall energy production by 2020 is to reach **13%** (MCIT, 2012: p. 9), which is low compared to the **20%** goal set by the EUETS (European Commission, 2009: p. 11). Specifically, by 2020 the electrical power produced by RES will be divided according to the following: a) Wind Farms (**300 MW**), b) Photovoltaic (PV) system (**192 MW**), c) Biomass systems (**17 MW**) and d) Solar Thermal (STh) systems (**75 MW**) (MCIT, 2012: pp. 104-105). In order to gradually achieve this target, the EAC planned to sponsor the following RES systems in 2013: a) Wind Farms up to **165 MW**, b) Photovoltaic systems up to **2 MW** each year and c) Solar Thermal systems up to **25 MW** (Anastasiades, 2011). The sponsorships or subsidies are calculated by subtracting the Total Selling Price to the network, as displayed in Table 2.6 (CIE, 2012b, p. 8) and the electricity purchase price of EAC or other suppliers (CIE, 2012b, p. 3). Furthermore, the term "commercial" refers to the non-domestic type of RES system used in the production process. Here there is no special reference regarding the selling price of domestic photovoltaic systems, which they are part of the NMP2 category. Additionally, a subsidy premium of **1.71 €c/kWh** is awarded to the RES producer during the period who produces electricity by means of cogeneration (CHP) or utilization of land fill gas (CIE, 2012b, p. 9).

The respective prices of the UK market for 2012 and 2013 are shown in Table 2.7 (HMG, 2012a: p. 4; 2012b: p. 17). As the prices are in British pence per kWh, they are converted into Euro cents per kWh for comparison reasons with the conversion rate of the 26th of April 2015. That day's conversion rate was: **1 GBP = 1.39647 Euros**, at 19:43 local time (XE.com, 2015). By comparing the PV categories for both the UK (**0 – 10 kW**) and Cyprus (**< 20 kW**), the subsidy offered by the government of Cyprus was greater than that of the UK's, by an average of **3.75 €c/kWh**. The Cyprus subsidy was also greater for the large and commercially used PV systems. On the other hand, the Biomass and Biogas

category (NBH) in Cyprus offered smaller subsidies than the Anaerobic Digestion (AD) category in UK, by at least **1.05 €c/kWh** for Biogas and **6.6 €c/kWh** for Biomass, even though the biomass subsidy in Cyprus was greater than the **AD 500 – 5000 kW** category in the UK.

Further comparisons cannot be made as the Cyprus government did not offer subsidies for the wind energy category, hydroelectric stations do not exist and the UK did not offer any subsidies for Concentrated Solar Thermal systems.

Category	Investment	Subsidy Duration	Year	Total Selling Price
NMW	**NMW1:** Large commercial wind systems	20 Years	2012	**---**
NMP	**NMP1:** Large commercial photovoltaic systems, 21 – 150 kW, connected to producer's network	20 Years	2012	**€0.25/kWh**
	NMP2: Large commercial photovoltaic systems, < 20 kW, connected to producer's network	20 Years		**€0.25/kWh**
NMS	**NMS1:** Small commercial solar thermal systems connected to producer's network	20 Years	2012	**€0.21/kWh (max)**
NBH	**BH1:** Electricity production from using biomass	20 Years	2012	**€0.135/kWh** (Subsidy = 0.1179 + 0.0171 premium – purchase price of EAC)
	BH2: Electricity production from biogas emitted from Waste Burial Sites (WBS)	20 Years		**€0.1145/kWh** (Subsidy = 0.0974 + 0.0171 premium – purchase price of EAC)

Table 2.6: Total selling prices of electrical power produced by RES given by the EAC to the producers (CIE, 2012b, p. 8)

Section 2.7.5: Electrical network technologies

The last issue addressed in this review is the one regarding electrical networks in terms of stability, reliability and readiness to accept energy produced by RES. Before he allows any RES producer to connect to the network, the network's manager should take into consideration the total number of those producers, their generating capacities and locations as well as the network's maintenance and upgrade schedule and the conditions of synchronization. Additionally, he should gather the technical specification of each RES generator type regarding their voltage and frequency fluctuations from the producers so

that the network's engineering personnel is able to take measures for that the existing equipment of the country's electrical system does not get damaged and to avoid problems such as blackouts or brownouts.

The existing electrical network technology across the world can be characterized as passive, since it is only responsible for transmitting and distributing electricity in bulk from the centralized power stations to the consumer. It does not regulate nor take any action when a problem occurs; in contrast it is susceptible to malfunction due to its nature of large scale deployment. Additionally, it presents problems as well as inability in managing itself and controlling the end use electricity demand. The reasons for this situation are the primitive electromechanical metering devices installed inside the consumers' properties and also the communication limitations between the producer and the consumer. This leads to flat price rates for the customers or even worse, the use of consumption estimations in order to calculate the charges (Sioshansi, 2012: p. xxxii). Another controversy that derives from the network's limitations is that the power utilities, in order to reduce their supply costs and thus their prices, are encouraging customers to increase their electricity consumption (Sioshansi, 2012: p. xxxix). Furthermore, system overloads made their appearance in 1980s when air conditioning was introduced. In the USA, these overloads are called "loads from hell", as they appear during the hottest summer periods and it was due to the vast usage of air conditioning devices in combination with the decreasing flat prices (Sioshansi, 2012: p. xl).

Lastly, the most important weakness of passive networks is their incapability of adapting to energy injections from renewable sources, as they are intermittent and fluctuating in nature. Prime examples are solar and wind sources, which are the most mature and popular RES types make transmission operators reluctant to embrace them, as the existing networks do have the capability of either controlling nor regulating the supply from them (Sioshansi, 2012: p. xl). As the EU promotes the increase of a more localized and distributed RES power production, this increasing number of individual producers would certainly challenge the network managers responsible for the maintenance of the network and energy balance (Sioshansi, 2012: p. xli).

A revolutionary network concept is currently being developed for surpassing the previous problematic issues and rendering the existing power transmission/distribution networks more reliable, manageable, secure and cost effective. This concept is called "Smart Grid" and it integrates a country's already established electrical system with a

data communication network and a computerized control system (Gao et al., 2012: p. 391 – 392). This would upgrade the passive network technology via monitoring, control, remote sensing and communication (Kabalci et al., 2012: p. 19) into an interactive and intelligent electrical system. With these properties, a Smart Grid implements real time pricing feedback to the consumer with the energy consumption status and most importantly the near real time response to energy demand fluctuation as well as the capability of serving the network's load more effectively by means of control and storage applications.

Category	Selling Price from 2012/13
Wind Systems (≤100 kW)	**€0.293/kWh**
Wind Systems (100 – 500 kW)	**€0.244/kWh**
Wind Systems (500 – 1500 kW)	**€0.133/kWh**
Wind Systems (2000 – 5000 kW)	**€0.063/kWh**
Photovoltaic (PV) Systems (≤ 4 kW)	**€0.223/kWh**
Photovoltaic (PV) Systems (4 – 10 kW)	**€0.202/kWh**
Photovoltaic (PV) Systems (10 – 50 kW)	**€0.189/kWh**
Photovoltaic (PV) Systems (50 – 100 kW)	**€0.161/kWh**
Photovoltaic (PV) Systems (100 – 150 kW)	**€0.161/kWh**
Photovoltaic (PV) Systems (150 – 250 kW)	**€0.153/kWh**
Photovoltaic (PV) Systems (250 – 5000 kW)	**€0.099/kWh**
Stand Alone Photovoltaic (PV) Systems	**€0.099/kWh**
Anaerobic Digestion (AD) Systems (≤ 250 kW)	**€0.205/kWh**
Anaerobic Digestion (AD) Systems (250 – 500 kW)	**€0.191/kWh**
Anaerobic Digestion (AD) Systems (500 – 5000 kW)	**€0.126/kWh**
Hydroelectric (Hydro) Systems (≤ 15 kW)	**€0.293/kWh**
Hydroelectric (Hydro) Systems (15 – 100 kW)	**€0.275/kWh**
Hydroelectric (Hydro) Systems (100 – 500 kW)	**€0.216/kWh**
Hydroelectric (Hydro) Systems (500 – 2000 kW)	**€0.169/kWh**
Hydroelectric (Hydro) Systems (2000 – 5000 kW)	**€0.063/kWh**

Table 2.7: UK's standard generation prices for new RES installations since August 2012 (HMG, 2012a: p. 4; 2012b: p. 17)

Immediate response to energy demand peaks and load management strategies are the key for mainly preventing the danger of blackouts and overloads, thus making the system more reliable and flexible, especially during high demand periods. Furthermore, the capability of providing the consumer with information about his energy consumption levels is also an important issue; this allows him to calculate his daily usage and willingly reduce it to the absolute necessary amount (Gao et al., 2012: p. 391 – 392). This article presents the structure of the Smart Grid and analyses it in detail. However, there is no reference regarding the interconnection of RES to the Smart Grid, which is one of the most important concerns of this thesis. Moreover, the EAC announced, in July 2012, the completion of a technical evaluation by the Dutch company KEMA for implementing an

Automatic Meter Management (AMM) system. This will provide the national network with data gathering and analysis capabilities, automatic connection/disconnection functions, better energy transfer management and the capability of upgrading the network into a Smart Grid (EAC, 2013). However, there are no further updates about this topic.

An article by Kabalci et al. (2012) describes a Smart Grid application that involves a photovoltaic energy system, connected to an electrical network and its power rate observation through a power line communication (PLC) feature. For this concept, a power line of **220 V** at **50 – 60 Hz** can be used as a part of the power system as well as a communications line, capable of transmitting and receiving data with rates up to 200 Mbps. According to them, the most economical solution for PV systems is stand-alone applications, connected directly to the electrical network, as this eliminates the costs for extra power conversion stages and storage equipment. In addition, the costs of extra communication lines for the observation of the PV system are also omitted and as a result a single power line can be used for both data and power transmission (Kabalci et al., 2012: p. 19). Their main goal was to simulate the accuracy and reliability of such a system in terms of monitoring, metering and data analysis. Their simulation showed more accurate results from the previously developed BPSK model and also the PLC model is most likely to be utilized by the industry, due to its provision of reliable and real time results (Kabalci et al., 2012: p. 27).

Another article, from Bliek et al. (2011) takes the example of PowerMatching City in Groningen in the Netherlands, presented in a previous article of the authors, to show how the integration of local electricity production with immediate demand response along with the integration of gas and electricity installations can assist the reliable incorporation of RES to a Smart Grid electrical system. As mentioned, RES are characterized as fluctuating and intermittent and so the more their electricity production share increases, as the EU dictates, the more flexible the backup electrical production system should be in order to compensate the power demand. Nowadays, backup or base load maintaining electrical systems can be utilized by the existing large scale power stations, which operate on fossil fuel. However, these systems are not capable of responding immediately to the sudden changes of the power balance, thus the reliability of the electrical system decreases. The Smart Grid technology utilizes the feasibility needed for the electricity network to have a near real time response regarding power balance using various methods. Firstly, the interconnection of the local electricity systems (domestic or

metropolitan) with each other, which implements the growth of electricity capacity and also the way of balancing supply and demand fluctuations with low cost. A second method refers to the usage of large hydroelectric and gas fuelled power plants that provide stable energy for as long as needed. Hydroelectric power plants, as mentioned in section 2.7.3, implement the reliable Hydro Pumped Storage systems and due to their large scale production, their energy can be transmitted over large distance to its local destination. Combined cycle production and Combined Heat and Power (CHP) can be incorporated into individual households, producing the base loads locally. Additionally, the use of energy storage equipment is another significant factor for covering energy shortage from the primary renewable production; it also eliminates the intermittent character of these sources for direct electricity introduction into the transmission/distribution system. Several ways of storing energy are referred in the article and also in the UK Parliamentary Office of Science and Technology post note number 306 (2008). These storage ways include, heat (hot water storage tanks), electrochemical (batteries), electrical (supercapacitors) and geological (compressed air energy storage) (Bliek et al., 2011: p. 609, 610).

Apart from the above theoretical approach of Smart Grids, Stimoniaris et al. (2011) presented two experimental smart grid topologies and compared their disadvantages. The first topology represented a centralized distribution micro network, controlled by a Smart Integration Module (SIM) with the addition of a DC bus to the existing AC one, DC generators and storage arrays (Stimoniaris, 2011: p. 1). It consisted of a cluster of 4 PV panels and a small **1 kW** wind generator that were connected onto the DC bus, while the system's loads, 2 PV clusters of 6 panels each with their inverters were connected onto the AC bus. A second AC bus connected the SIM (Sunny Island 3324) with the large national network (Stimoniaris, 2011: p. 2). The second topology consisted of only the AC bus and each of its components were connected onto it via a Special Control Unit (SCU). All DC components were connected to their corresponding SCU via their respective inverters. A dedicated personal computer provided the decision commands for this system (Stimoniaris, 2011: p. 3). Moreover, all the experimental hardware pieces are installed in Kozani, Greece. Due to timing problems, they gathered measurements only for the first topology; however this fact was enough to show its disadvantages, one of which is an advantage for the other topology. These disadvantages were the high investment costs due to the extra DC bus and the installation of the expensive SIM, the PV systems were connected to the AC bus through inverters, which

is an advantage for the second topology and thirdly the system was centralized, meaning that is not reliable. The fourth and final disadvantage is that none of its components had an autonomous mode, meaning that load forecasting could not be possible and as a result, the stability of this topology was bounded by that of the national network. The only possible disadvantage of the second topology is that all storage elements required their own inverter, thus increasing its investment costs (Stimoniaris, 2011: p. 5). The experiment not only confirmed the disadvantages of the first topology, it also showed that renewable energy could not be fully exploited (Stimoniaris, 2011: pp. 7 – 8). The problem is that the authors could not experimentally see if the second topology had any additional disadvantages and therefore propose improvements, since it had not as many as the first one did.

Interconnection between alternating current (AC) systems is also achievable through a High Voltage Direct Current (HVDC) transmission network. As mentioned by Kundur (1994), such a system transmits electrical energy in bulk where AC transmission is impractical. Specifically it is used for overhead lines of over **600 km** in length and underground or submarine lines of over **30 km** in length. Additionally, it provides an asynchronous connection between systems of different nominal frequency or when their AC interconnection would present stability problems. Lastly, they are capable of controlling their transmitted energy with no significant delay, rendering them a vital component for their system's stability (Kundur, 1994: pp. 463 – 464). Unfortunately however, HVDC networks cannot be utilized in Cyprus as the power line distances are short compared to the **600 km** length that makes them feasibly attractive. Nevertheless, since March 2012 Cyprus is playing a crucial role in the "EuroAsia Interconnector" project, assumed by the Greek Public Power Company (PPC) and the Quantum Energy Company. An illustration of the interconnection between the three countries is shown in Figure 2.32 (Askja Energy, 2015). This project is set to interconnect Israel with Cyprus and then Cyprus with Greece through Crete, connecting Cyprus' electrical system with the Asian and European networks and thus cease to be an isolated one. The overall cost of the project will be **€1.5bn**, while its expected total income over its lifespan is **€17.5bn** (EAI, 2012b). For this case, it is feasible to use an HVDC system, as the cables will be of submarine type and their length will be greater than **65 nautical miles** of about **120 km**. The connection will have capacity of **2 GW** (EAI, 2012b), while the capacity of Cyprus could increase by **1.2 GW** with the collaboration of the EAC, as the president of PPC – Quantum Energy, Nasos Ktorides stated (EAI, 2012a). A third benefit is that the stability

of Cyprus' electrical system will be greater, as it will a part of a much larger system and serious problems, similar to the one occurred in 2011 in Mari village, would be negligent in the future.

Another important issue is how efficient is the electrical network's deployment; more specifically, if it is more feasible to have a centralized and large scale power production and transmission system or smaller and more localized Distributed Generation (DG) systems. Fazeli et al. (2011) describe the benefits of transitioning from centralized to distributed production within smart energy communities combined with the usage of RES. Furthermore, the authors examine which is the appropriate size of such communities for effective demand management and lastly, they built a model for the discovery of additional benefits from the application of this technique. At the time their concern was that the UK government was planning on upgrading the railway system and promoting the introduction of electrical vehicles (EV). However, the current centralized power systems are operating on fossil fuel, their efficiency is low (around **35%** in average in the UK), their equipment is aged and their capacity is challenged each year due to the annual growth of electricity demand, especially with the addition of the new EV and railway loads. The most important of these characteristics is that no active load demand management existed then, which lowered the reliability of the power systems, making them more susceptible to faults including brownouts and blackouts (Fazeli et al., 2011: p. 1). On the other hand, decentralized local production combines electricity producing RES with the micro Combined Heat and Power (μCHP) systems and promises more than double efficiency relative to a current fossil fuel system and also the introduction of the mentioned active management and balance control (Fazeli et al., 2011: p. 2). Additionally, this process could localize the effects of a damaged unit to its community and events such as the 2011 destruction of the Vasilikos Power Station would not impact the consumers at a national level in the UK.

A Smart Energy Community (SEC) will be composed of several hundred households fitted with energy storage devices and dynamically controlled household appliances. Each community will have a central control system that will regulate the energy demand and supply, while being able to operate autonomously in islanded mode; in other words, operate autonomously without being connected onto the national transmission/distribution network. It is important to mention that the various SECs will be interconnected via regional divisions of the national electrical network and this will

optimize the traditional power stations' operation (Fazeli et al., 2011: p. 2). The regulation of energy production will be done by a Demand Side Management (DSM) system within each community and this technology will be based mostly on a bi-directional communication network connecting the distributed production with the consumers and the central control unit of the community's smart grid. The benefits of the DSM system mentioned in the paper are: supply security, allowance of intermittent renewable energy introduction to the network, increase of the systems' efficiency and the desirable balance of energy production and consumption (Fazeli et al., 2011: p. 3). DSM algorithms are already being developed in order to closely match a forecasted load curve with the real load curve of an SEC. The authors simulated the effects of such an algorithm and presented their benefits. The results showed that the optimal number of households of an SEC, in which a DSM algorithm operates, is **1000** (Fazeli et al., 2011: p. 6). Additionally, a Loading Shifting DSM is capable of rendering systems with spinning reserves of the power stations obsolete, since it has a faster frequency response and so it can be combined efficiently with wind energy supply. Lastly, a Load Curtailment DSM is only suitable when the system is operating in islanded mode, as it reduces the imported power from the national network and thus decreasing the electricity expenses of the consumers (Fazeli et al., 2011: p. 5).

However, the SEC plan would only be able to operate in islanded mode and regulate the supply and demand balance through the DSM scheme, if they are fitted with the key element of storage. Electricity is for the time being a form of energy that cannot be stored easily and efficiently. Various electricity storage technologies have risen so far, with battery technology being the most popular.

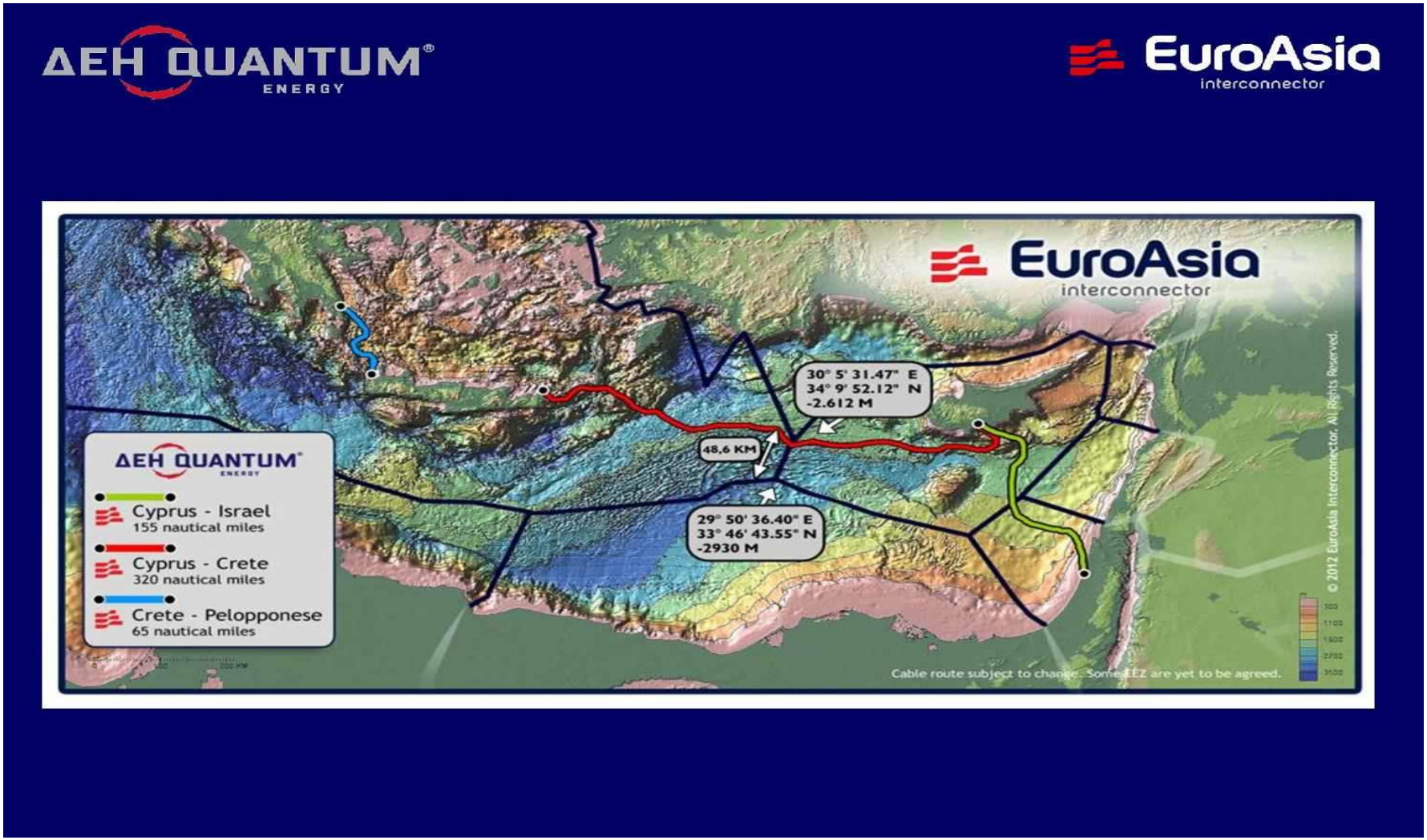

Figure 2.32: Map of eastern Mediterranean region where the EuroAsia Interconnector is scheduled to be implemented (Askja Energy, 2015)

Researchers are attempting to develop new, more efficient and more environmentally friendly types of network scale electricity storage technologies, to assist the upcoming concept of distributed generation based on RES. The paper of Blarke et al. (2012) presents such a concept storage technology, the Thermal Battery (TB) with a carbon dioxide (CO_2) compression heat pump. From an economic point of view, investing in thermal energy storage technology is better that investing in electrochemical one; specifically, in terms of specific energy cost, lifetime, effect of usage on capacity and charging – discharging efficiency. Another advantage of a TB is that it is a suitable means for using in combination with intermittent RES, therefore allowing their efficient incorporation on Smart Grid system applications, buildings and industrial units (Blarke et al., 2012: p. 129). The TB diagram is available in this paper, shown in Figure 2.33 (Blarke et al., 2012: p. 130).

The TB converts electricity from intermittent sources into heat through the CO_2 high compression heat. This operation is responsible for the simultaneous heat exchange between the evaporator and gas cooler with the cold and hot thermal tanks respectively, therefore providing heating and cooling at the same time. It can be used for space heating and cooling or as a part of a μCHP system's cycle for further electricity production, with lower cost and greenhouse gas emissions (Blarke et al., 2012: p. 129). CO_2 is more preferred as a compression gas than hydrofluorocarbons (HFCs) and hydrocarbons (HCs), as they have greater GWP that CO_2 and so the risk of severe air pollution in case of a leakage is eliminated. Additionally, as HCs are flammable the risk of fire and explosion is also eliminated. On the other hand, CO_2 allows the achievement of higher temperatures, thus increasing the thermal efficiency of the TB. The authors simulated an optimized model of the Thermal Battery in a case study presented in the paper, for a specific location in San Jose, California. This was done to confirm the proper operation of the battery and also for studying the cost its technology's effectiveness, by replacing the hot water electrical heater and air conditioning unit of a typical, 4 member single family household (Blarke et al., 2012: p. 130, 135).

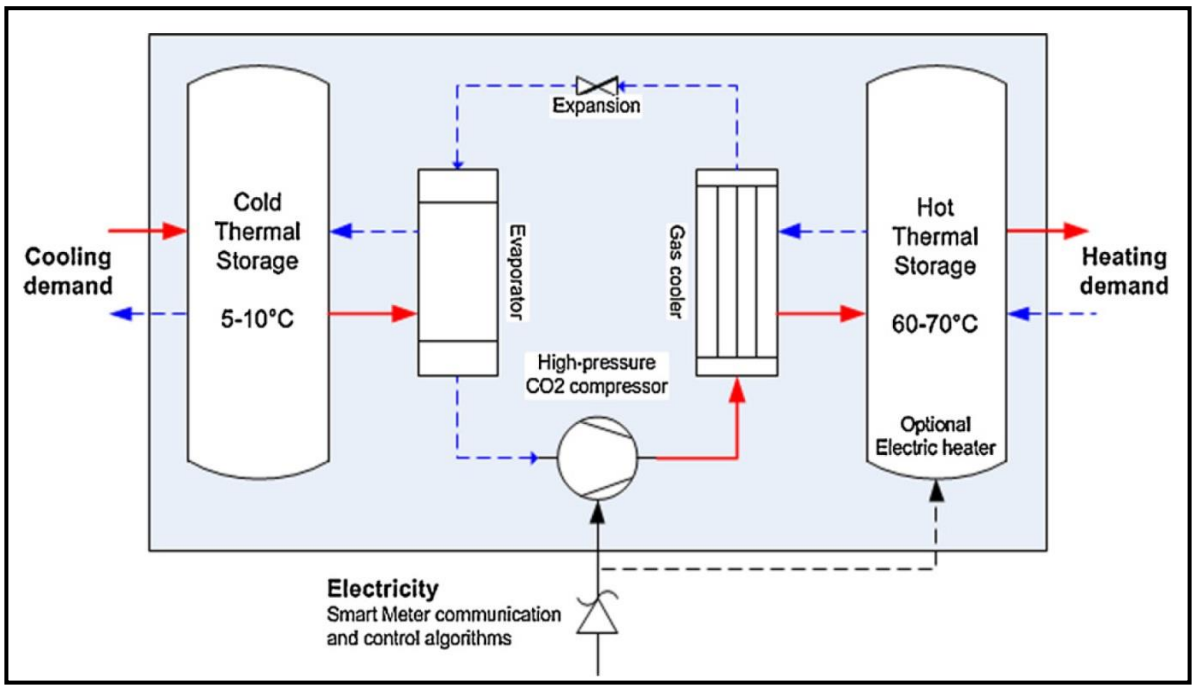

Figure 2.33: The TB concept diagram (Blarke et al., 2012: p. 130)

They also compared reference residential energy consumption measurements collected in 2003, with their simulation measurements with the usage of the TB system (Blarke et al., 2012: p. 134). In the heat pump case, they also simulated two compressors, from Sanyo and Danfoss, with the Coolpack/EES software package (Blarke et al., 2012: p. 137). Their characteristics rendered the Sanyo heat pump the better of the two, as it had lower electricity consumption, **0.49 kW** and also it had higher total COP, with its COP for heating was about **3.71** and its COP for cooling was **3.07**; the Danfoss one had **0.61 kW** of consumption and the two COPs were **3.54** and **2.49** respectively (Blarke et al., 2012: p. 134). Finally, the simulation results showed that this technology does not produce any CO_2 emissions and also the operation cost of the battery fitted building was **0.36 US Dollars per day** (USD/d) on average, relative to **1.09 USD/d** of the reference model, without the TB systems. Furthermore, the reference building's electricity consumption was **9.15 kWh per day** (kWh/d), while the simulated building's with the TB system was **3.38 kWh per day** on average that corresponds to about **64%** decrease (Blarke et al., 2012: p. 135). Finally, they calculated several average values, as the simulation results were collected under 2 tariff schemes. The experiment showed that using electricity from intermittent energy sources combined with the usage of the TB system is more cost efficient for Smart Grid technology than using electrochemical or mechanical storage (Blarke et al., 2012: p. 138). However,

researchers need to execute real experiments on this topic, since the results in this paper were the product of simulation and so, it is questionable how reliable these results are.

The concept of the Smart Grid is new and the technology to support it is at an early stage of modelling and development. Nevertheless, the Smart Grid a promising technology that could assist private RES producers to supply their country's existing electrical network with clean energy in a safer and cost effective manner, while increasing its reliability and remote controllability.

Section 2.7.6: Micro Combined Heat and Power (μCHP) systems

Combined Heat and Power (CHP) or Cogeneration is an attractive technology that utilizes fossil fuel for the production of electrical and thermal energy, either simultaneously or sequentially, as usually the heat is the product of the electricity production process. The technology exists in various scales, ranging from under **100 kW** to **100 MW** with various applications, one of which is building sector (commercial and domestic) (Kreith & Goswami, 2007: p. 17-2). For these building applications, small-scale or micro-CHP systems are being used, exploiting waste heat for space heating, cooling and humidity control as well as for, at least partially, covering the electricity demand of the host building, thus yielding an overall efficiency of between **85%** and **90%** (Kreith & Goswami, 2007: p. 17-34). This means that the amount of fuel used for such devices is being exploited almost completely, making the technology high efficient.

There are several types of μCHP devices in existence today, based primarily on the type of prime mover they are fitted regarding the electricity production. The first type of μCHP is the one possessing a reciprocating internal combustion engine and they are divided into two categories: the spark-ignition one and compression-ignition one. The former operates on natural gas, propane or gasoil; while the latter operates on diesel oil or it can be configured to operate on dual-fuel mode, primarily using natural gas and using smaller amounts of diesel. Units of this type of μCHP are capable of producing between **10** and **200 kW**, with a relatively high thermal-to-electrical efficiency between **24%** and **45%** and they are relatively cheap to acquire. However, they need frequent maintenance, they are noisy and they have high emissions, thus rendering them unsuitable for domestic usage (Kreith & Goswami, 2007: p. 17-35).

Along with internal combustion engines, microturbines are used as the prime mover of a μCHP device, for applications between **25** and **250 kW**. The disadvantage of this type is that shaft rotating speeds reach **10000 rpm**, much greater than the **3000 rpm** (50 Hz) that the electrical network provides, meaning that the voltage needs to be rectified and then inverted to a **50** or **60 Hz** voltage. This would cause the electrical efficiency (between **25%** and **30%**) of the device to be reduced even further as the mentioned extra components would be added and thus increasing its acquisition cost. Even so, microturbine-based devices are quiet, they do not need frequent maintenance and as they can operate on alcohol in addition to natural gas and biogas, they have reduced carbon and NO_x emissions (Kreith & Goswami, 2007: p. 17-35).

Stirling engines are another type of prime mover for μCHP units and they are suitable for small-scale applications between **2** and **50 kW**. Unlike the internal combustion engines, Stirling engines are external combustion ones, meaning they are capable of utilizing low grade or waste heat as their thermal source in addition to heat from renewable and fossil fuel sources. The advantages of this type is quiet operation, little but frequent maintenance and low emission levels, especially when using a renewable heat source. A major disadvantage is that their electrical efficiency is lower than the other types (**15%** to **35%**) since the Stirling engine is a closed-loop system itself and thus its efficiency is bound by its low Carnot efficiency due to the low temperatures of its heat source; additionally they it is expensive to acquire and its frequent maintenance increases its cost even more (Kreith & Goswami, 2007: pp. 17-35, 36). The former three types of prime mover are mentioned again in Section 3.3.3.

The final type of μCHP devices is the one using hydrogen fuel cells. They produce electricity via the oxidation-reduction reaction of the fuel and oxygen from the atmosphere. The thermal energy extracted from the reaction is used for space heating or air conditioning, by driving heat exchangers and absorption chillers within the host building. This type is more efficient than the other types in producing electricity (**40%** to **55%**) and its emissions are very low, especially if the fuel is exclusively hydrogen. Moreover, they can be used in a wider range of applications, from **2** to **200 kW**; however they are the most expensive to acquire and their maintenance costs are about the same as Stirling engine based units (Kreith & Goswami, 2007: pp. 17-35, 36).

Section 2.8: Chapter Summary

All the above subtopics described in this chapter are important background information about the current state of energy production, demand and supply, the annual greenhouse gas emission and the extent of renewable energy exploitation in Cyprus. They serve as the reason that this project is executed and explains why immediate action is imperative. The following paragraphs summarize this chapter.

After a brief introduction, the data presented in section 2.2 show that the population of Cyprus is steadily increasing and also that the country's climate and terrain renders solar the ideal source for electricity production and water heating.

Section 2.3 analyses the increasing electricity consumption by sector for identifying which ones present the greatest demand proportion and the possible reasons for this phenomenon. These may be the large number of citizens living in single households, the large proportion of those households lacking proper insulation and the energy waste due to the overuse of certain household appliances. Further analysis of petroleum sales data reveal that there is also increased demand for fossil fuels, primarily for electricity production and transport. Lastly, the scarcity of public transport in Cyprus makes the privately owned automobiles a necessity for the entire population, thus their numbers increase rapidly.

The next section presents historical information about the national electrical infrastructure, showing that the EAC makes significant efforts to keep the system at an astonishingly good condition. Recent data on capacity and accommodated demand, electricity pricing and the current state of the national electrical system of the EAC is not the most important factor in the increasing demand, even though it presented a slight decrease in the last 3 years, most probably due to the global financial crisis. Even so, the EAC could replace the generators of Dhekeleia power station models of higher efficiency, similar to those of Vasilikos power station.

The rapidly increasing greenhouse gas emission levels, is another important issue that the general public and the government in Cyprus should be aware about. Section 2.5 presents the data of **CO_2**, **CH_4** and **N_2O** annual levels emitted in the country, since 1990. After a brief description of the EUETS, which dictates that all Member States need to reduce their annual

emission levels to **80%** of the 1990 levels, the section graphically presents the mentioned data and thus identifying that the energy sector is responsible for the largest proportion of emissions in the country. For this reason, RES should be incorporated for producing electricity at a national level as soon as possible; in any other case, the EU would impose severe financial penalties to Cyprus, even during the recession period.

Finally, after a small section about energy saving measures, section 2.7 explains the possible RES exploitation routes for Cyprus today. Solar energy is already an established source for heating domestic hot water; however its exploitation should include the production of electricity also due to the satisfactory availability of sunlight throughout the year. Secondly, the also established wind farms should utilized along with storage technologies for ensuring that they supply the electrical network without causing issues related with stability. Storage units can also be incorporated by each individual household and in combination with smart metering devices and real time consumption updates, the electrical network can become active and "smart". This will allow the government and the consumer to monitor and control the demand as well as reduce waste and gain the capability of quick response in emergence cases.

Following the accumulation of the useful, energy related background data for Cyprus, Chapter 3 presents several basic topics on Thermodynamics in order to lay the foundations for the main body of the project, presented in Chapters 4 and 5. Chapter 3 also presents the specifications of a typical household regarding the electricity and Domestic Hot Water demand, while analyses the parameters and components of a basic concept system design that would accommodate that household's needs.

Reference List

Anastasiades, E (EAC, Studies Department). [Interview] (23 December 2011).

Askja Energy (2015) ***Upcoming New World Record Subsea Electric Cables,*** Available at: https://askjaenergydotcom.files.wordpress.com/2013/12/hvdc-euroasia-interconnector-map-2.jpg [Accessed: 28 April 2015]

Blarke, M. B.; Yazawa, K.; Shakouri, A. & Carmo, C. (2012) 'Thermal battery with CO_2 compression heat pump: Techno – economic optimization of a high – efficiency Smart Grid option for buildings'. ***Energy and Buildings*****, 50, pp. 128 – 138**.

Bliek, F. W.; van den Noort, A.; Roosien, B.; Kamphuis, R.; de Wit, J.; van der Veide, J. & Eijgelaar, M. (2011) 'The role of natural gas in Smart Grids'. ***Journal of natural gas Science and Engineering*****, 3, pp. 608 – 616**.

Borg, S. P.; Kelly, N. J. (2011) 'The effect of appliance energy efficiency improvements on domestic electric loads in European households'. ***Energy and Buildings*****, 43, pp. 2240 – 2250**.

Bueno, C.; Carta, J. A. (2006) 'Wind powered pumped hydro storage systems, a means of increasing the penetration of renewable energy in the Canary Islands', ***Renewable and Sustainable Energy Reviews*****, 4 (10), pp. 312 – 340.**

Confalonieri, U., B. Menne, R. Akhtar, K.L. Ebi, M. Hauengue, R.S. Kovats, B. Revich and A. Woodward (2007) 'Human health', in ***Climate Change 2007: Impacts, Adaptation and Vulnerability. Contribution of Working Group II to the Fourth Assessment Report of the Intergovernmental Panel on Climate Change.*** **Cambridge: Cambridge University Press, pp. 391-431.** [Online]. Available at: https://www.ipcc.ch/pdf/assessment-report/ar4/wg2/ar4_wg2_full_report.pdf [Accessed: 03 May 2015].

Cyprus Institute of Energy (CIE) (2012a). ***Energy efficiency policies and measures in Cyprus*****.** [Online]. Available at: http://www.odyssee-indicators.org/publications/PDF/cyprus_nr.pdf [Accessed: 19 March 2015].

Cyprus Institute of Energy (CIE) (2012b) ***Grant scheme for the promotion of electricity generation using Wind, Solar Thermal, Photovoltaic systems and the utilization of Biomass (2012 – No. 3).*** [Online]. Available at: http://www.cie.org.cy/menuEn/pdf/grant-schemes/ELECTRICITY_GENERATION_SCHEME-FINAL.pdf [Accessed: 08 May 2012].

Deutsche Energie-Agentur GmbH (DENA) (2014) ***Energy Supply with Renewables – Made in Germany.*** [Online]. Available at: http://www.renewables-made-in-germany.com/fileadmin/EMP_2014/renewables_Made_in_Germany_2015_EN.pdf [Accessed: 08 January 2016].

Dongellini, M.; Falcioni, S. & Morini, G. L. (2015) 'Dynamic simulation of solar thermal collectors for domestic hot water production', ***Energy Procedia,*** **82, pp. 630 – 636.**

Electricity Authority of Cyprus (EAC) (2006) ***Annual Report 2006*****.** [Online]. Available at: https://www.eac.com.cy/EN/EAC/FinancialInformation/Documents/2006%20-eng.pdf [Accessed: 25 March 2015].

Electricity Authority of Cyprus (EAC) (2007a) ***Annual Report 2007*****.** [Online]. Available at: https://www.eac.com.cy/EN/EAC/FinancialInformation/Documents/2007%20-eng.pdf [Accessed: 25 March 2015].

Electricity Authority of Cyprus (EAC), Customer Service, Informative Publications. (2007b) ***Vasilikos Power Station*****.** [Online]. Available at: https://www.eac.com.cy/EN/EAC/NewsAndAnnouncements/Informative%20Leaflets/VASILIKOS%20POWER%20STAT-ENG.pdf [Accessed: 19 April 2015].

Electricity Authority of Cyprus (EAC) ***Annual Report 2008*****.** [Online]. Available at: https://www.eac.com.cy/EN/EAC/FinancialInformation/Documents/2008%20-eng.pdf [Accessed: 25 March 2015].

Electricity Authority of Cyprus (EAC) (2009) ***Annual Report 2009*****.** [Online]. Available at: https://www.eac.com.cy/EN/EAC/FinancialInformation/Documents/2009%20-%20eng.pdf [Accessed: 25 March 2015].

Electricity Authority of Cyprus (EAC) (2010) ***Annual Report 2010*****.** [Online]. Available at: https://www.eac.com.cy/EN/EAC/FinancialInformation/Documents/2010%20-%20eng.pdf [Accessed: 25 March 2015].

Electricity Authority of Cyprus (EAC) (2011) ***Annual Report 2011*****.** [Online]. Available at: https://www.eac.com.cy/EN/EAC/FinancialInformation/Documents/2011-%20eng.pdf [Accessed: 06 April 2015].

Electricity Authority of Cyprus (EAC) (2012a) ***Annual Report 2012*****.** [Online]. Available at: https://www.eac.com.cy/EN/EAC/FinancialInformation/Documents/2012%20-eng.pdf [Accessed: 06 April 2015].

Electricity Authority of Cyprus (EAC) (2013) ***Annual Report 2013*****.** [Online]. Available at: https://www.eac.com.cy/EN/EAC/FinancialInformation/Documents/AHK%202013%20ENGLISH.pdf [Accessed: 25 March 2015].

Electricity Authority of Cyprus (EAC), Operations (2014a) ***History*****.** [Online] Available at: https://www.eac.com.cy/EN/EAC/AboutEAC/Pages/History.aspx [Accessed: 05 May 2015].

Electricity Authority of Cyprus (EAC), Operations (2014b) ***Generation*****.** [Online] Available at: https://www.eac.com.cy/EN/EAC/Operations/Pages/Generation.aspx [Accessed: 06 April 2015].

Electricity Authority of Cyprus (EAC), Save Energy (2014c) ***Saving Energy Advice.*** [Online] Available at: https://www.eac.com.cy/EN/CustomerService/SavingEnergy/Pages/SavingEnergy.aspx [Accessed: 01 September 2015].

Eleek Incorporated, Home, Eleek Lamping Guide. (2011). ***Eleek Lamping Comparison Chart.*** [Online]. Available at: http://www.eleekinc.com/eleekchart.pdf [Accessed: 24 March 2012].

EuroAsia Interconnector (EAI) (2012a) ***Momentous contribution of EAC.*** [Online]. Available at: http://www.euroasia-interconnector.com/News-Momentous_contribution_of_EAC,3?Section=None&WebContentCode [Accessed: 28 April 2015].

EuroAsia Interconnector (EAI) (2012b) ***Our Quest.*** [Online]. Available at: http://www.euroasia-interconnector.com/Index.aspx [Accessed: 28 April 2015].

Eurostat (2015) ***Electricity prices for domestic consumers - bi-annual data (from 2007 onwards).*** Available at: http://appsso.eurostat.ec.europa.eu/nui/show.do [Accessed: 01 September 2015]

European Commission (2009) ***EU Action Against Climate Change: The EU Emissions Trading Scheme.*** [Online]. Available at: http://www.ab.gov.tr/files/ardb/evt/1_avrupa_birligi/1_6_raporlar/1_3_diger/environment/eu_emmissions_trading_scheme.pdf [Accessed: 19 April 2015].

EurObserv'ER (2011) 'Solar Thermal and Concentrated Solar Power Barometer'. ***Le Journal d' Énergies Renouvelable*****, (203), pp. 66 – 93**. [Online]. Available at: http://www.eurobserv-er.org/pdf/solar_thermal_barometer_2011.pdf [Accessed: 15 March 2012].

EUROPA, Press Room, Press Releases (2007) ***Emissions trading: Commission adopts decision on Cyprus' national allocation plan for 2008 – 2012.*** [Online]. Available at: http://europa.eu/rapid/pressReleasesAction.do?reference=IP/07/1131&format=HTML&aged=1&language=EN&guiLanguage=en [Accessed: 03 May 2012].

European Wind Energy Association (EWEA) (2012) ***Wind in Power: 2011 European Statistics*****.** [Online]. Available at: http://www.ewea.org/fileadmin/ewea_documents/documents/publications/statistics/Stats_2011.pdf [Accessed: 28 April 2015].

Fazeli, A.; Christopher, E.; Johnson, C. M.; Gillot, M. and Sumner, M. (2011) 'Investigating the Effects of Dynamic Demand Side Management within Intelligent Smart Energy Communities of Future Decentralized Power System', ***2nd IEEE PES International Conference and Exhibition on Innovative Smart Grid Technologies (ISGT Europe)*****. Manchester, 5 – 7 December 2011.**

First Hydro Company (FHC) (2015) ***Ffestiniog Power Station,*** Available at: http://www.fhc.co.uk/ffestiniog.htm [Accessed: 29 May 2015]

Gao, J.; Xiao, Y.; Liu, J.; Liang, L. & Chen, C. L. P. (2012) 'A survey on communication/networking in Smart Grids', ***Future Generation Computer Systems,*** **28, pp. 391 – 404.**

Google Maps (2015a) ***Location of Athalassa, Larnaca Airport, Prodromos and Saita along with the wind farms in Alexigros, Ayia Anna, Kampi, Koshi and Oreites*****.**

Google Maps (2015b) ***Location of the Dhekeleia, Moni & Vasilikos power stations*****.**
Harvey, L. D. D. (1993) 'A Guide to Global Warming Potentials (GWPs)'. ***Energy Policy*****, 21(1), pp. 24 – 34.**

Her Majesty's Government (HMG), Department of Energy and Climate Change, Meeting Energy Demand, Renewable Energy Policy, Feed in Tariffs. (2012a). ***Feed in Tariffs Scheme, Government response to Consultation on Comprehensive Review Phase 2A: Solar PV cost control*****.** [Online]. Available at: https://www.gov.uk/government/uploads/system/uploads/attachment_data/file/43085/5386-government-response-to-consultation-on-comprehensi.pdf [Accessed: 24 April 2015].

Her Majesty's Government (HMG), Department of Energy and Climate Change, Meeting Energy Demand, Renewable Energy Policy, Feed in Tariffs. (2012b). ***Feed in Tariffs Scheme, Government response to Consultation on Comprehensive Review Phase 2B: Tariffs for non – PV technologies and scheme administration issues.*** [Online]. Available at: https://www.gov.uk/government/uploads/system/uploads/attachment_data/file/42917/5905-government-response-to-consultation-on-comprehensi.pdf [Accessed: 24 April 2015].

Intergovernmental Panel on Climate Change (IPCC) (2012) ***Direct Global Warming Potentials.*** [Online]. Available at: https://www.ipcc.ch/publications_and_data/ar4/wg1/en/ch2s2-10-2.html [Accessed: 21 April 2015].

Kabalci, E.; Kabalci, Y. & Develi, I. (2012) 'Modelling and analysis of a power line communication system with QPSK modem for renewable Smart Grids'. ***Electrical Power and Energy Systems*****, 34, pp. 19 – 28**.

Koroneos, C.; Fokaidis, P. & Moussiopoulos, N. (2005) 'Cyprus energy system and the use of renewable energy sources'. ***Energy*****, 30(10), pp. 1889 – 1901**.

Kreith, F. & Goswami, D. Y. (2007) ***Handbook of Energy Efficiency and Renewable Energy*****, CRC Press: Taylor & Francis Group.**

Kundur, P. S. (1994) ***Power Systems Stability and Control*****. New York; London: McGraw – Hill.**

Mohan, G.; Kumar, U.; Pokhrel, M. K. & Martin, A. (2015) 'A novel solar thermal polygeneration system for sustainable production of cooling, clean water and domestic hot water in United Arab Emirates: Dynamic simulation and economic evaluation', ***Applied Energy*****.**

New York State Energy Research & Development Authority (2005) ***Wind Energy Technology: Overview*****.**

Panasonic Corporation (2015) ***Photovoltaic module HIT® VBHN245SJ25 / VBHN240SJ25*****.** Available at: http://eu-solar.panasonic.net/fileadmin/user_upload/downloads/technical_documents/NEW_VBHN240SJ25_PEWEU_EN.pdf [Accessed: 01 September 2015].

Republic of Cyprus, Ministry of Agriculture, Rural Development and Environment (MARE), Department of Meteorology (2015) ***Climatological Information.*** [Online]. Available at: http://www.moa.gov.cy/moa/ms/ms.nsf/DMLclimatological_en/DMLclimatological_en?OpenDocument [Accessed: 26 March 2015]

Republic of Cyprus, Ministry of Commerce, Industry and Tourism (MCIT), Energy Service, Renewable Energy Sources, National Action Plan 2010 – 2020. (2010). ***National Action Plan for Renewable Energy, based on the Directive 2009/28/EC*** **(in Greek).** [Online]. Available at: http://www.mcit.gov.cy/mcit/mcit.nsf/All/789553C60B9DF658C225777D0033353D/$file/National%20Action%20Plan_Final.pdf [Accessed: 26 April 2015].

Republic of Cyprus, Ministry of Finance (MF), Statistical Service, Energy & Environment, Energy, Key Features. (2008a). ***Energy*****.** [Online]. Available at: http://www.mof.gov.cy/mof/cystat/statistics.nsf/energy_environment_81main_en/energy_environment_81main_en?OpenForm&sub=1&sel=2 [Accessed: 12 March 2012].

Republic of Cyprus, Ministry of Finance (MF), Statistical Service, Energy & Environment, Energy, Key Features, Archived Key Figures: 2007. (2008b). ***Sales and Stocks of Petroleum Products, 12/07*****.** [Online]. Available at: http://www.mof.gov.cy/mof/cystat/statistics.nsf/energy_environment_81main_keyfarchive_en/energy_environment_81main_keyfarchive_en?OpenForm&yr=20071F9610ADDAE8786CDA1213D449944EB0&n=2007 [Accessed: 29 March 2012].

Republic of Cyprus, Ministry of Finance (MF), Statistical Service, Energy & Environment, Energy, Key Features, Archived Key Figures: 2008. (2009). ***Sales and Stocks of Petroleum Products, 12/08*****.** [Online]. Available at: http://www.mof.gov.cy/mof/cystat/statistics.nsf/energy_environment_81main_keyfarchive_en/energy_environment_81main_keyfarchive_en?OpenForm&yr=20087C1B9FBE871920BC782A442BEB0DE9A1&n=2008 [Accessed: 29 March 2012].

Republic of Cyprus, Ministry of Finance (MF), Statistical Service, Population and Social Conditions, Population, Key Features. (2010). ***Population Summary Data 1995 – 2009*****.** [Online]. Available at: http://www.mof.gov.cy/mof/cystat/statistics.nsf/populationcondition_21main_en/populationcondition_21main_en?OpenForm&sub=1&sel=2 [Accessed: 12 March 2012].

Republic of Cyprus, Ministry of Finance (MF), Statistical Service, Energy & Environment, Energy, Key Features. (2011a). ***Final Energy Consumption in Households 2009*****.** [Online]. Available at: http://www.mof.gov.cy/mof/cystat/statistics.nsf/energy_environment_81main_en/energy_environment_81main_en?OpenForm&sub=1&sel=2 [Accessed: 12 March 2012].

Republic of Cyprus, Ministry of Finance (MF), Statistical Service, Services, Transport & Communications, Key Features (2011b) ***Transport 1990 – 2010*****.** [Online]. Available at: http://www.mof.gov.cy/mof/cystat/statistics.nsf/services_72main_en/services_72main_en?OpenForm&sub=2&sel=2 [Accessed: 12 March 2012].

Republic of Cyprus, Ministry of Finance (MF), Statistical Service, Energy & Environment, Energy, Key Features, Archived Key Figures. (2011c). ***Imports, Sales and Stocks of Petroleum Products, Dec 2010*****.** [Online]. Available at: http://www.mof.gov.cy/mof/cystat/statistics.nsf/energy_environment_81main_keyfarchive_en/energy_environment_81main_keyfarchive_en?OpenForm&yr=201051476A018082487420F3C6D00BB89796&n=2010 [Accessed: 28 March 2012].

Republic of Cyprus, Ministry of Finance (MF), Statistical Service, Population and Social Conditions, Population Census, Key Features. (2012a). ***Population by District and Urban – Rural Area, 2011*****.** [Online]. Available at: http://www.mof.gov.cy/mof/cystat/statistics.nsf/populationcondition_22main_en/populationcondition_22main_en?OpenForm&sub=2&sel=2 [Accessed: 12 March 2012].

Republic of Cyprus, Ministry of Finance (MF), Statistical Service, Energy & Environment, Energy, Key Features. (2012b). ***Imports, Sales and Stocks of Petroleum Products, Feb 2012*****.** [Online]. Available at: http://www.mof.gov.cy/mof/cystat/statistics.nsf/energy_environment_81main_en/energy_environment_81main_en?OpenForm&sub=1&sel=2 [Accessed: 28 March 2012].

Republic of Cyprus, Ministry of Finance (MF), Statistical Service, Energy & Environment, Energy, Key Features, Archived Key Figures. (2012c). ***Imports, Sales and Stocks of Petroleum Products, Dec 2011*****.** [Online]. Available at: http://www.mof.gov.cy/mof/cystat/statistics.nsf/energy_environment_81main_keyfarchive_en/energy_environment_81main_keyfarchive_en?OpenForm&yr=20111C6726A0846089035578A9ECCE6F6064&n=2011 [Accessed: 28 March 2012].

Republic of Cyprus, Ministry of Finance (MF), Statistical Service, Labour, Unemployment, Key Features, Archived Key Figures. (2012d). ***Labour Force Survey – Main Results, 2011*****.** [Online]. Available at: http://www.mof.gov.cy/mof/cystat/statistics.nsf/labour_32main_keyfarchive_en/labour_32main_keyfarchive_en?OpenForm&yr=20111C6726A0846089035578A9ECCE6F6064&n=2011 [Accessed: 27 March 2015].

Republic of Cyprus, Ministry of Finance (MF), Statistical Service, Energy & Environment, Energy, Key Features. (2014a). ***Imports, Sales and Stocks of Petroleum Products, Dec 2013.*** [Online]. Available at: http://www.mof.gov.cy/mof/cystat/statistics.nsf/energy_environment_81main_keyfarchive_en/energy_environment_81main_keyfarchive_en?OpenForm&yr=201378B6314716D85BF7A15A85C7C5DE280F&n=2013 [Accessed: 28 March 2015].

Republic of Cyprus, Ministry of Finance (MF), Statistical Service, Services, Transport & Communications, Key Features. (2014b). ***Transport 1990 – 2013.*** [Online]. Available at: http://www.mof.gov.cy/mof/cystat/statistics.nsf/services_72main_en/services_72main_en?OpenForm&sub=2&sel=2 [Accessed: 28 March 2015].

Republic of Cyprus, Ministry of Finance (MF), Statistical Service, Energy & Environment, Environment, Key Features, Archived Key Figures. (2014c). ***Emissions of Greenhouse Gases, 1990-2012.*** [Online]. Available at: http://www.mof.gov.cy/mof/cystat/statistics.nsf/energy_environment_82main_en/energy_environment_82main_en?OpenForm&sub=2&sel=2 [Accessed: 20 April 2015].

Republic of Cyprus, Ministry of Finance (MF), Statistical Service, Labour, Unemployment, Key Features. (2015a). ***Labour Force Survey – Main Results, 4th Quarter 2014.*** [Online]. Available at: http://www.mof.gov.cy/mof/cystat/statistics.nsf/labour_32main_en/labour_32main_en?OpenForm&sub=2&sel=2 [Accessed: 27 March 2015].

Republic of Cyprus, Ministry of Finance (MF), Statistical Service, Energy & Environment, Energy, Key Features. (2015b). ***Imports, Sales and Stocks of Petroleum Products, Feb 2015.*** [Online]. Available at: http://www.mof.gov.cy/mof/cystat/statistics.nsf/energy_environment_81main_keyfarchive_en/energy_environment_81main_keyfarchive_en?OpenForm&yr=201579A8BB536616B7880786B84672CDF8C1&n=2015 [Accessed: 28 March 2015].

Republic of Cyprus, Ministry of Finance (MF), Statistical Service, Energy & Environment, Energy, Key Features. (2015c). ***Imports, Sales and Stocks of Petroleum Products, Dec 2014.*** [Online]. Available at: http://www.mof.gov.cy/mof/cystat/statistics.nsf/energy_environment_81main_keyfarchive_en/energy_environment_81main_keyfarchive_en?OpenForm&yr=2014380DDB90F3C58213004E0A12E623A895&n=2014 [Accessed: 28 March 2015].

Ruegamer, T.; Kamp, H.; Kuckelkorn, T.; Schiel, W.; Weinrebe, G.; Nava, P.; Riffelmann, K. & Richert, T. (2014) 'Molten salt for parabolic trough applications: system simulation and scale effects', ***Energy Procedia,*** **49, pp. 1523 – 1532.**

Sharp Electronics (UK) Ltd, Sharp United Kingdom, Products, Solar, Solar Products, Monocrystalline. (2015a) ***NU-R250(J5).*** Available at: http://www.sharp-electronics.ie/cps/rde/xchg/ie/hs.xsl/-/html/product-details.htm?product=NUR250J5&cat=46000 [Accessed: 26 April 2015].

Sharp Electronics (UK) Ltd, Sharp United Kingdom, Products, Solar, Solar Products, Polycrystalline. (2015b) ***NA-R250A5*****.** Available at: http://www.sharp.co.uk/cps/rde/xbcr/documents/documents/Marketing/Datasheet/NDR250A5_NDR245A5_Flyer_0414_en.pdf [Accessed: 26 April 2015].

Sioshansi, F. P. (2012). 'Introduction' in *Smart Grid: Integrating Renewable, Distributed & Efficient Energy*. Oxford: Elsevier Inc., pp. xxix – lvi.

Stimoniaris, D.; Tsiamitros, D.; Poulakis, N.; Kottas, V.; Kikis, T. and Dialynas E. (2011) 'Investigation of Smart Grid Topologies Using Pilot Installations Experimental Results', *2nd IEEE PES International Conference and Exhibition on Innovative Smart Grid Technologies (ISGT Europe)*. Manchester, 5 – 7 December 2011. [Online]. Available at: http://ieeexplore.ieee.org/stamp/stamp.jsp?tp=&arnumber=6162612 [Accessed: 22 June 2012].

SunPower (2014) ***Facts about Solar Technology from SunPower***. [Online] Available at: http://us.sunpower.com/solar-panels-technology/facts [Accessed: 03 December 2014]

Transmission System Operator (TSO) (2012) ***Wind Energy Development in Cyprus*****.** [Online]. Available at: http://www.dsm.org.cy/nqcontent.cfm?a_id=3570&tt=graphic&lang=l2 [Accessed: 25 March 2015].

Transmission System Operator (TSO) (2015a) ***Transmission System Operator (TSO) Cyprus*****.** [Online]. Available at: http://www.dsm.org.cy/nqcontent.cfm?a_id=1&lang=l2 [Accessed: 04 May 2015].

Transmission System Operator (TSO) (2015b) ***Total Daily System Generation (MW).*** [Online]. Available at: http://www.dsm.org.cy/nqcontent.cfm?a_id=2741&tt=graphic&startdt=06%2F04%2F2015&type=7&submit=Go [Accessed: 04 May 2015].

United Kingdom Parliament, Office of Science and Technology (2008) ***Postnote 306*****.** [Online]. Available at: http://www.parliament.uk/documents/post/postpn306.pdf [Accessed: 27 April 2015].

The World Bank Group (2015) ***Climate Change Knowledge Portal,*** Available at: http://sdwebx.worldbank.org/climateportal/index.cfm?page=country_historical_climate&ThisRegion=Asia&ThisCCode=CYP [Accessed: 26 March 2015]

XE.com, Universal Currency Converter (2015) ***British Pound to Euro Rate.*** Available at: http://www.xe.com/currencyconverter/convert/?Amount=1&From=GBP&To=EUR [Accessed: 26 April 2015].

Chapter 3: Fundamental topics and system component selection

Section 3.1: Introduction

Chapter 2 has established that solar energy in Cyprus is the most potent renewable source for exploitation. Consequently, this project proposes a Solar Thermal (STh) system design solution for electricity and Domestic Hot Water (DHW) production, at a residential level in Cyprus. In order to converge on an optimal solution for this task, Chapter 4 studies three similar concept system scenarios based on the models of the large scale power station in operation today.

Chapter 3 begins by presenting the reasons why the project leans towards a STh solution instead of a PV one and then presents several fundamental topics of Thermodynamics, as they are the basis of the simulation procedures for the three systems in Chapter 4. Furthermore, Chapter 3 describes the process of selecting the components for constructing the three systems' models and finally, it presents the template on which the systems are based on.

This chapter is essential for this thesis, as the author's main field of study is Electrical & Computer Engineering and not Mechanical Engineering. As a result, his undergraduate academic experience did not provide him with the necessary in-depth knowledge for completely understanding the field of Thermodynamics. For this reason, he explains the relevant topics to this project in Chapter 3, before proceeding to the actual calculations for the three systems.

Section 3.1.1: Reasons for not using PV technology

There are several reasons for avoiding the usage of Photovoltaic (PV) components when designing a solar based electrical system, not only for the purpose of this project but for any system for the time being. Photovoltaics are a very useful technology, as it converts light into DC electricity directly, without the usage of any other device. PV systems also operate with any kind of light, so it is not be limited to just sunlight. These are the reasons why it is popular among the renewable electricity producing technologies and also in the minds of most Cypriots. However, there are several important disadvantages that render PV technology not the most favourable amongst the engineering community, at least in this stage of development. These disadvantages are the following:

1. A major disadvantage of the PV technology is the low efficiency of its components. SunPower is an Australian company that manufactures PV panels and claims that those panels have the highest efficiency in the market. Specifically, the **X21 series** has a maximum efficiency of about **21%** (SunPower, 2013 & 2015) and this is confirmed by the Energy Informative website (2015). Solar thermal collectors, such as parabolic trough ones, have more than 3 times higher efficiency than PV, a feature that will be analysed in Chapter 4. This feature assists the overall increase of the thermal-to-electrical efficiency of a STh system and is seen when the settings the project's optimal system solution are presented in Chapter 4.

2. Solar energy, as mentioned, is an intermittent source. This means that the electricity supply produced by a PV solar panel would be unstable and unsuitable for household usage and direct network feed. The energy produced by a PV system needs to be stored first in order to be rendered stable according to the standards of the EAC. These additional electrical energy storage components are expensive and they have a small lifespan ranging from 2 to 3 years up to 5 to 10 years, which is probably shorter than the payback period of the system due of the low overall efficiency of their system (Solar Direct, 2015).

3. Another issue is that a PV based system would also need a **DC to AC converter** or **inverter** to render its output electricity suitable for the majority of household appliances and also for the ability of selling the excess energy produced safely into the EAC low voltage network. Taking into account that the efficiency of the PV panels would drop the overall efficiency of the system to less than **21%**, adding the extra inverter could reduce that overall efficiency even more, while increasing the investment and maintenance costs to higher values. In addition, since the inverter consists of power electronic elements it would introduce parasitic harmonics into the output voltage, making it unreliable for injecting into the national network.

4. The output power rating of a PV panel can be further reduced with temperature. The datasheet of the X-series PV collectors from SunPower (2013: p. 2) indicates a reduction of the output power by **0.30% per ºC**, with **25 ºC** as its nominal operation temperature. Summer temperatures in Cyprus may reach **45 ºC** and thus the collector's temperature would increase even more, as it is enclosed in glass. So, the collector's output power along with its

efficiency would reduce by at least **6%** during a typical summer heat wave, reaching a rate of about **324 W** per panel instead of **345 W**. The collector efficiency in this case would become **20.2%** from the **21.5%** (SunPower, 2013: p. 2).

5. The manufacturing processes of PV systems have a dangerous impact on the environment as well. Fthenakis (2012: p. 1085) mentions the potential risks of these processes, which include fires/explosions, acid burns, carcinogenesis and heavy metal poisoning. More specifically, the Silicon Valley Toxics Coalition White Paper of 2009 states that PV manufacturing is intensely energy demanding and wasteful and also enumerates several dangerous substances capable of causing the above problems (SVTC, 2009: p. 9):

a) **Silane (SiH_4).** An extremely explosive gas, which is shown to spontaneously explode after accidentally released into the atmosphere, endangering the lives of those manufacturing PV systems as well as the proximate properties to the manufacturing plant (SVTC, 2009: p. 10).

b) **Silicon Tetrachloride ($SiCl_4$).** This toxic chemical reacts violently with water, it is capable of causing respiratory, skin and eye problems and it can also cause serious environmental issues (SVTC, 2009: p. 10).

c) **Cadmium (Cd).** A carcinogen and a toxic metal, capable of causing internal organ damage and lung cancer, cadmium is mainly used to produce cadmium telluride (**CdTe**), a compound used in the manufacturing process of thin film PV cells (SVTC, 2009: p. 13) and on which very little is known about its potential hazards. Additionally, CdTe's production process requires the addition of other dangerous materials, such as tin (**Sn**), nickel (**Ni**), sulphur (**S**) and molybdenum (**Mo**) (SVTC, 2009: pp. 14 – 15).

d) **Gallium Arsenide (GaAs).** This compound semiconductor's production involves the element arsenic (**As**), which can cause cancer and it widely known to be extremely toxic. Moreover, the synthesis of GaAs involves the toxic gases phosphine (**PH_3**) and arsine (**AsH_3**), used for doping the GaAs and also the carcinogen trichloroethene (**CCl_2=CHCl**), which is used as a solvent and cleaning fluid (SVTC, 2009: pp. 17 – 18).

6. Finally, an additional problem regarding the PV manufacturing processes' environmental impact is their degree of recyclability. Solar PV panels also have a relatively short lifespan of **20** to **30** years (Fthenakis, 2012: p. 1094). So, end-of-life decommissioning is a serious consideration for such devices, especially for those that contain cadmium (**Cd**) and lead (**Pb**). Fthenakis (2012: p. 1094) explains that if these devices are destroyed by means of incineration, those heavy metal would be released into the atmosphere, unless the incineration facilities are fitted with electrostatic precipitator equipment. Additionally, the resultant ash from this procedure must not be handled lightly as the danger of leakage of the metals into the soil is high. As a result, special landfills are created for disposing the ash, raising their overall cost even higher. However, recent studies have shown various recycling methods, such as reclaiming metals from used devices and hydro-metallurgical separation, have been developed and are incorporated into the PV industry (Fthenakis, 2012: p. 1095). Additionally, scientists have found that magnesium chloride (**$MgCl_2$**) is a benign and much cheaper replacement for the hazardous cadmium chloride (**$CdCl_2$**) in the thin film solar cells industry (IEEE Spectrum, 2014).

Section 3.1.2: Reasons for using Solar Thermal technology

In contrast to Photovoltaic based systems, Solar Thermal (STh) based systems appear to be more promising in terms of controllability, efficiency, lifespan and pricing. These features may allow consumers to make more reliable and versatile investments for their properties. The advantages that Solar Thermal systems offer over PV systems are listed below:

1. Cyprus is situated within the so called "Solar Belt", between **- 40º** to **40º** latitude. This zone, according to Fernández – García et al. (2010: p. 1703), is characterized by its annual direct solar irradiation potential of around **2000 Wh/m^2** per year, a value that allows Concentrated Solar Power (CSP) commercial scale plants to produce electricity with an acceptable range of operation costs.

2. Another advantage of STh systems is the issue of storage. These systems are capable to store hot water or hot oil in order to be used 24 hours per day for steam production or water heating by using Phase Changing Heat Exchangers (PCHE) and regular ones,

respectively. In contrast, PV systems use electrical batteries for storing energy; as mentioned, a battery's lifespan could be up to 10 years, while a storage tank's lifespan is virtually unlimited, as heat carrying fluids can be stored more easily than electricity.

3. Electricity in a STh system is produced by a synchronous three phase electrical generator. This provides the consumer with a direct feed of AC electrical power, while the generator itself has its own mechanism of sustaining the frequency of that electricity stable. Additionally, the working fluid flow that acts as the prime mover of the generator's turbine can be controlled more easily than the direct solar irradiation that PV cells need for electricity production.

4. STh collectors have a much higher efficiency rate than that of PV panels. As mentioned above, the highest PV panel efficiency achieved so far is **21%**, while the thermal efficiency of the SkyTrough collectors by SkyFuel could reach **73%** and the indicative net thermal to electric efficiency is **37.5%** (SkyFuel, 2010: p. 4). The UltimateTrough® by Flabeg and EuroTrough collectors possess similar thermal characteristics with SkyTrough; Ruegamer et al. (2014: p. 1526) simulated the operation of several power plants based on these two collectors, using the weather data of Daggett, CA, which incidentally has a very similar latitude as Cyprus. The optical efficiency of UltimateTrough® and EuroTrough are **80.1%** and **77.7%** at **393℃** respectively, offering a thermal to electric efficiency of **38.5%**, almost identical to SkyTrough's. This means that a STh based electricity producing system could have more than 1.5 times the efficiency of PV based system.

5. The final advantage of STh technology is that it is easier to design and implement closed loop systems. This will enable the maximum possible exploitation of solar energy for purposes other than just electricity production, such as using the exhaust steam of a turbine for the coverage of the hot water demand of the building. In addition, energy is being lost only through thermal loses, which is unavoidable; however, the rest of the energy collected by the solar collectors could be used again and not being wasted into the atmosphere. This could enable a possible increase in the system's overall fluid capacity, without the installation of extra storage components. This is further analysed in Section 4.3.2 of Chapter 4.

Section 3.2: Fundamental Thermodynamics

Section 3.2.1: Basic topics and terminology

Thermodynamics is the science that studies all topics involving energy transfer and energy conversions in various systems. It is based on the fundamental law of energy conservation, which states that energy cannot be created nor destroyed; it is simply converted from one form to another (Çengel and Boles, 2015: p. 2). Throughout this project the word "produce" suggests the extraction of useful work or power from a thermodynamic system the word "consume" indicates the absorption of work or power by that system in order to operate. They do not imply, in any case, the actual production of energy from nothing or its destruction, respectively.

Section 3.2.1.1: Thermodynamic state

Before explaining the various topics of thermodynamic processes, a description of terminology used should be mentioned. A **thermodynamic state** of a system or even a material is the set of macroscopic properties (including mass, volume and temperature) that completely describe the condition that the system or material is in. Therefore, these properties or state variables must have unique values for each individual state of the thermodynamic system. Furthermore, Thermodynamics studies not only the transitions between individual states in a process, but also the initial and final states of that process in which the system is at equilibrium or balance; this means that the system in those two states has constant state variables and for this reason they are called **equilibrium states**. This is illustrated in Figure 3.1 (Çengel and Boles, 2015: p. 14), where a certain amount of a gas is contained within a thermally isolated cylinder and at the initial state 1 its volume is **1.5 m^3** and at the final state 2, its volume is **2.5 m^3**. The two states are being described by the mentioned variables and these do not change after all the transition effects have resolved. Additionally, the values of the initial and final states of a system are independent of that process's path. This means that in the case of a cyclic process or **thermodynamic cycle**, where the initial and final states of a system are the one and the same, that system's state would not change at all. However, there are other variables, such as heat **Q** and work **W** that are not state variables of the system; hence they do not remain unchanged after a cyclic process has been completed. More

specifically, heat can be absorbed or extracted and work can be produced or consumed by the system. This is the reason why humans use various thermodynamic engines for producing useful energy for their everyday lives.

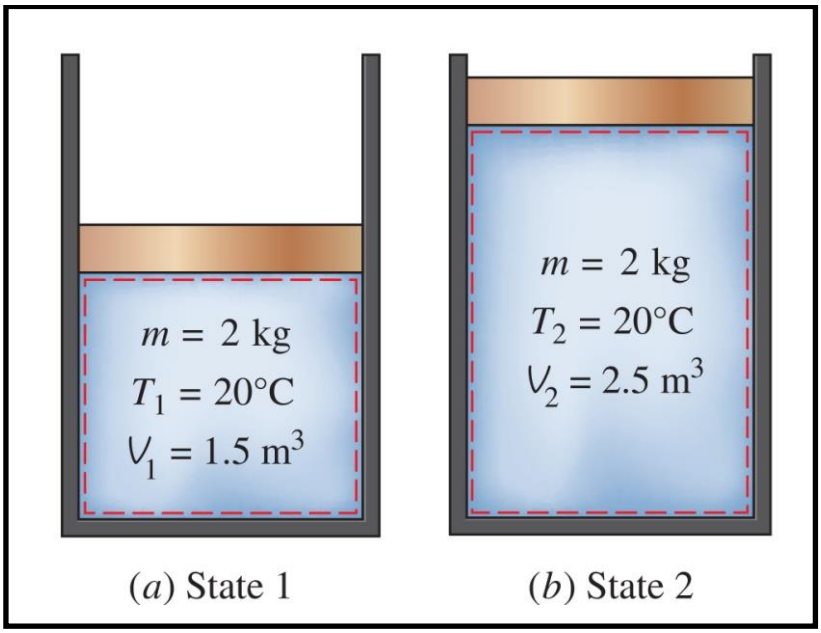

Figure 3.1: A gas contained in a thermally isolated cylinder in shown in two different states (Çengel and Boles, 2015: p. 14)

Section 3.2.1.2: First Law of Thermodynamics

Thermodynamics has four laws that govern all thermodynamic systems and processes (Zeroth, First, Second and Third); for the purposes of this project, only the First and Second laws are needed. The First Law of Thermodynamics is simply a quantitative form of the energy conservation law. As mentioned above, the heat and work differences (**ΔQ** and **ΔW**) in a cyclic process are not equal to zero, in contrast to the difference in temperature for example. More specifically, the First Law states that: "In every thermodynamic process the change or difference of the system's internal energy **ΔU** is equal to the sum of **ΔW** and **ΔQ** associated with that process". In its mathematical form, this last sentence is summarized in Equation 3.1 as such:

$$\boldsymbol{\Delta U = \Delta Q + \Delta W}$$

Equation 3.1: Mathematical form of the First Law of Thermodynamics

Since the internal energy **U** of a system is a state variable, its overall change **ΔU** in a cyclic process is equal to zero, hence **ΔQ** and **ΔW** are equal in magnitude, as seen in Equation 3.2. The notation used in this case is that if an amount of energy or power is being imported into or consumed by a system is assigned a positive sign, while energy or power extracted from or produced by that system is assigned a negative sign.

$$\boldsymbol{\Delta Q = -\Delta W}$$

Equation 3.2: Mathematical form of the First Law of Thermodynamics in a cyclic process

This is the notion that energy is conserved, by being converted from one form into another and it also shows that heat and work are not state variables, as they are not independent of the process's path. One can also observe the negative sign of the **ΔW** in the above equation, which means that work in a power system is needed to be **produced** by the cyclic process and then be exploited. On the other hand, in a refrigeration system, work is positive as it is needed to be **consumed** by the system to extract heat from some place in order to become colder. In this case, **ΔW** is positive and **ΔQ** is negative.

Section 3.2.1.3: *Second Law of Thermodynamics*

The Second Law of Thermodynamics is responsible for restricting the possible outcomes of the First Law. According to the German physicist Rudolf Clausius the Second Law states that: "It is impossible to create a thermal engine whose sole function is the heat transfer from a cold body to a hot body" (Serway, 1990: p. 186). This means that without actually "spending" work, a body cannot become hotter spontaneously, rather than the exact opposite. This implies the existence of a notion which shows the most probable path a process could take, thus showing in a sense the path of time. This notion is a state variable of every thermodynamic system and it is called **Entropy** and it summarizes the Second Law in Equation 3.3 below:

$$\Delta S = \frac{\Delta Q}{T} = \frac{Q_h}{T_h} - \frac{Q_c}{T_c} \geq 0$$

Equation 3.3: Mathematical form of the Second Law of Thermodynamics

In other words, the Second Law states that the most probable path of any process is the one that increases or does not affect the entropy **S** of its system; decreasing the entropy of the system is impossible. Quantitatively, the entropy difference **ΔS** is derived by the difference of the absorbed heat from a hot reservoir $\mathbf{Q_h}$, divided by the temperature of that reservoir $\mathbf{T_h}$ minus the extracted heat to a cold reservoir $\mathbf{Q_c}$, over the temperature of that reservoir $\mathbf{T_c}$. The fraction $\frac{\mathbf{Q_h}}{\mathbf{T_h}}$ is equal to the $\frac{\mathbf{Q_c}}{\mathbf{T_c}}$ only in the case of a **reversible** process, thus **ΔS** is equal to zero. In such a process the system follows a thermodynamic path from state 1 to state 2 in the example of Figure 3.3 (Moran et al., 2011: p. 48) and if the reverse path is followed, the net amount of heat involved would be equal to zero and therefore the system would reach state 1 again. To characterize a process as **irreversible**, the reverse transition of the thermodynamic path would end at state 1, one of less entropy than state 1. A state 1 of greater entropy cannot be achieved at all, as this would imply that heat and therefore energy was created out of nothing and this statement contradicts the First Law of Thermodynamics.

This is the theoretical basis that governs the operation of a thermal system. The next section briefly describes the various thermodynamic cycle, eventually leading to the preferred one for this project.

Section 3.2.2: Thermodynamic cycle

Section 3.2.2.1: Ideal Gas Law and work calculation

The study of Thermodynamics was significantly improved by the invention and development of Thermal Engines, devices that convert thermal energy into more useful mechanical or electrical energy. Such engines contain a medium, which they manipulate and subject it into a **thermodynamic cycle** or a cyclic set of processes as the means of the energy conversion. This medium is always a fluid and it is called the **working fluid** of the engine.

A characteristic example of a vastly used thermal engine is the locomotive, in which the working fluid is water. The working fluid is heated to become steam inside a boiler, then the steam is expanded in order to push the wheel pistons of the engine and lastly it is liquefied and re-enters the boiler again (Serway, 1990: p. 164).

As mentioned, the working fluid of a Thermal Engine is subjected to a series of thermodynamic processes in order produce useful energy from heat. Additionally, every thermodynamic process is completely represented by the values of its state variables at a given moment. However, keeping track of only the most important ones every time has the same results as keeping track of all of them. Due to the fact that a Thermal Engine's working fluid is in the gas state most of the time, the simplest way of knowing all the most useful information about it, at a given moment, is by studying its pressure (**P**), volume (**V**) and absolute temperature (**T**), through the Ideal Gas Law, summarized in Equation 3.4:

$$\mathbf{PV = nRT}$$

Equation 3.4: Ideal Gas Law State Equation

where **n** is the number of moles of the gas involved in the process and **R** is the universal gas constant, equal to **8.314 J/mol-K** (Çengel and Boles, 2015: p. 135). The behaviour of the gas phase working fluid could be studied simply by a series of calculations in a spreadsheet software package; however the most common method for this behaviour study is the observation of the gas's **Pressure – Volume** (P-V) diagram, shown in Figure 3.2 (Moran et al., 2010: p. 48). The specific example illustrates a gas compression process, where the initial and final volume and pressure values represent the gas's states 1 and 2 respectively. The value pairs of pressure and volume or each dot on the diagram is enough to describe the condition of the gas, since the Ideal Gas Law is universal. It should be noted that the transition from one state to another does not occur in a single and sudden move; in the example of Figure 3.2 is the nation of the piston moving from position 1 to position 2 immediately. If this happens, the thermodynamic system cannot be studied, as these sudden changes in the properties of the gas would not have uniform characteristics. For example, the gas's pressure inside the confined space would not be uniform inside the cylinder, thus causing irreversibilities and also renders the system unpredictable and impossible to be calculated. So, every transition takes place near equilibrium in relatively small steps, called **quasi –**

static, ensuring the uniformity and hence reversibility of the process (Çengel and Boles, 2015: p. 16).

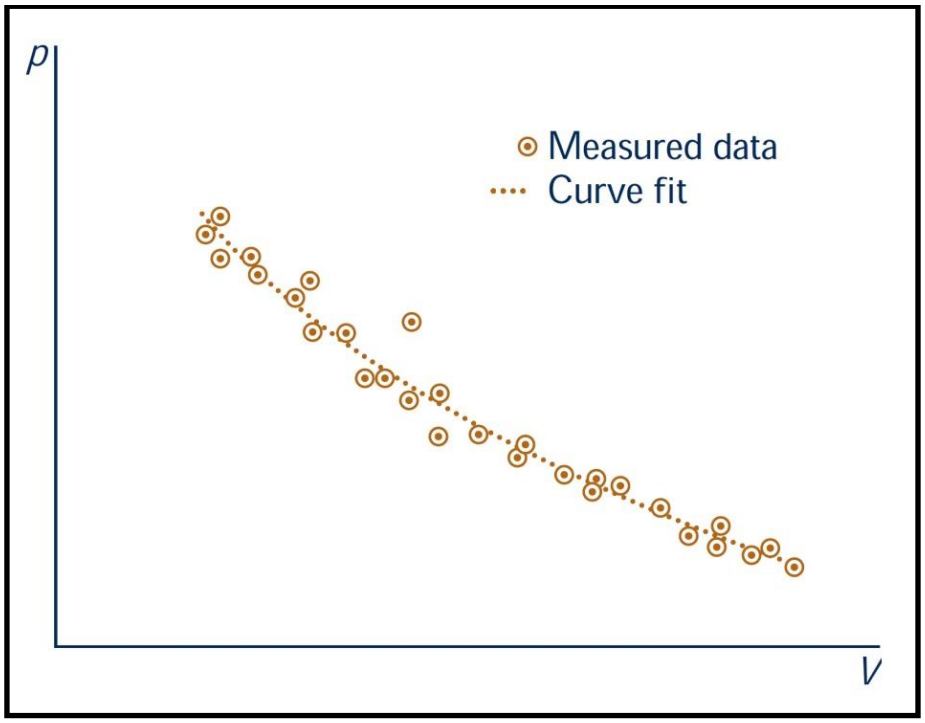

Figure 3.2: P-V diagram of a gas compression process including the quasi-static steps (Moran et al., 2011: p. 46)

For every process represented on a P-V diagram, the area under the process's curve represents the work involved during that process. This statement is proven below in Equation 3.5:

$$\mathbf{W = -\int Fdx = -\int PBdx}$$

$$\mathbf{\Rightarrow W = -\int P(Bdx)}$$

$$\mathbf{\Rightarrow \boxed{W = -\int PdV}}$$

Equation 3.5: Proof of work calculation on the P-V diagram

where **F** is the compressive force on the piston of Figure 3.2 and **dx** is the infinitesimal compression displacement the piston covered. **F** is equal to the pressure **P** of the gas under

the piston and inside the cylinder by **B**, which is the piston's surface area. The product **B** by **dx** is isolated and since **B** is constant, it represents the infinitesimal change of the gas's volume **dV** in only one dimension. So the integral, which represents the area under the process's curve on the P-V diagram, is actually the work involved in the process. Additionally, the default negative sign of the integral implies that the work is being produced or extracted from the gas. The direction of the process's path determines the overall sign of the integral after all the operations end; if the overall sign remains negative the gas then produces work, while if it changes then the gas absorbs or consumes work. All those described are summarized in Figure 3.3 (Moran et al., 2011: p. 48).

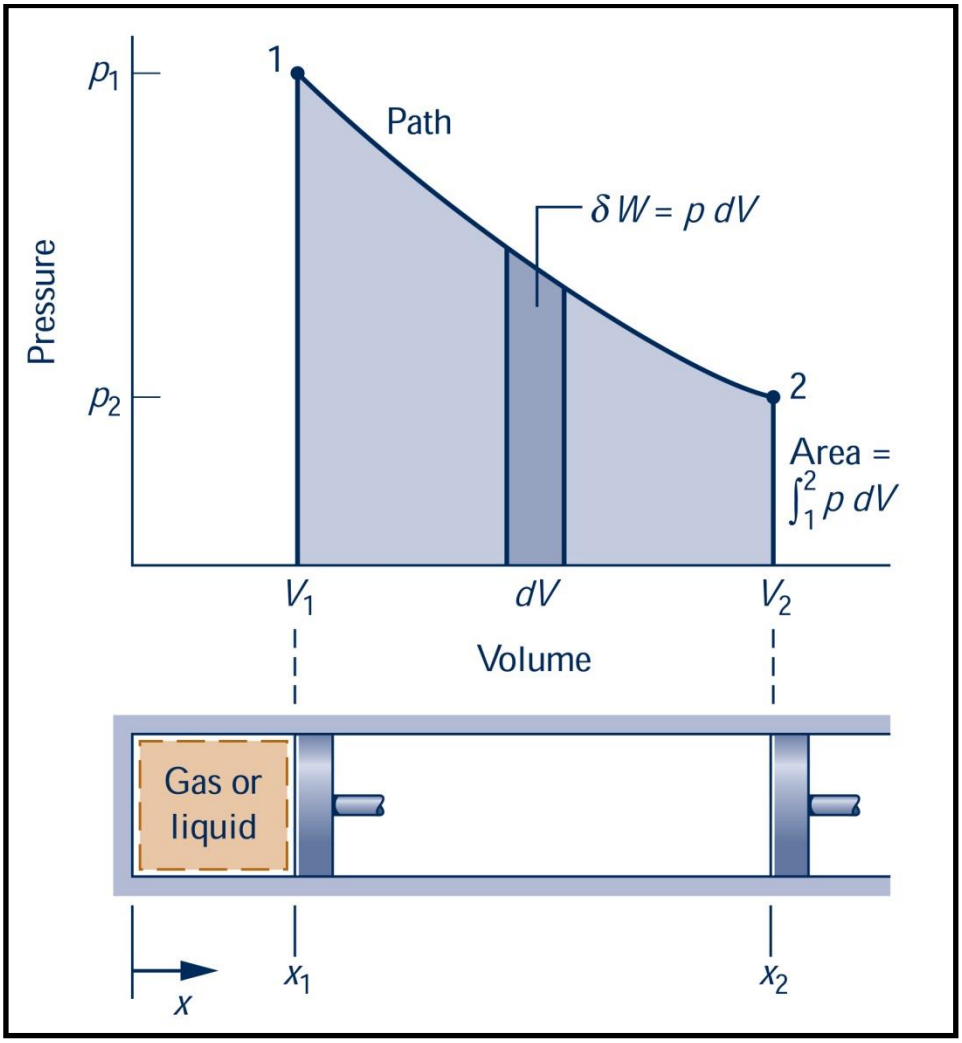

Figure 3.3: Geometric proof of work production on the P-V diagram (Moran et al., 2011: p. 48)

The execution of a thermodynamic process produces useful work; however the single transition from just one state to another would produce an amount of work only once. Human activities require undisrupted and continuous production of work around the year and this requires that thermodynamic process to be executed continuously. So, to produce work the working fluid of a thermodynamic system needs to be subjected to a series of processes in order to return eventually to its initial state and repeat this series of processes again and again in exact same order, hence the name thermodynamic cycle. This can be seen in the simple example in Figure 3.4 (Çengel and Boles, 2015: p. 165).

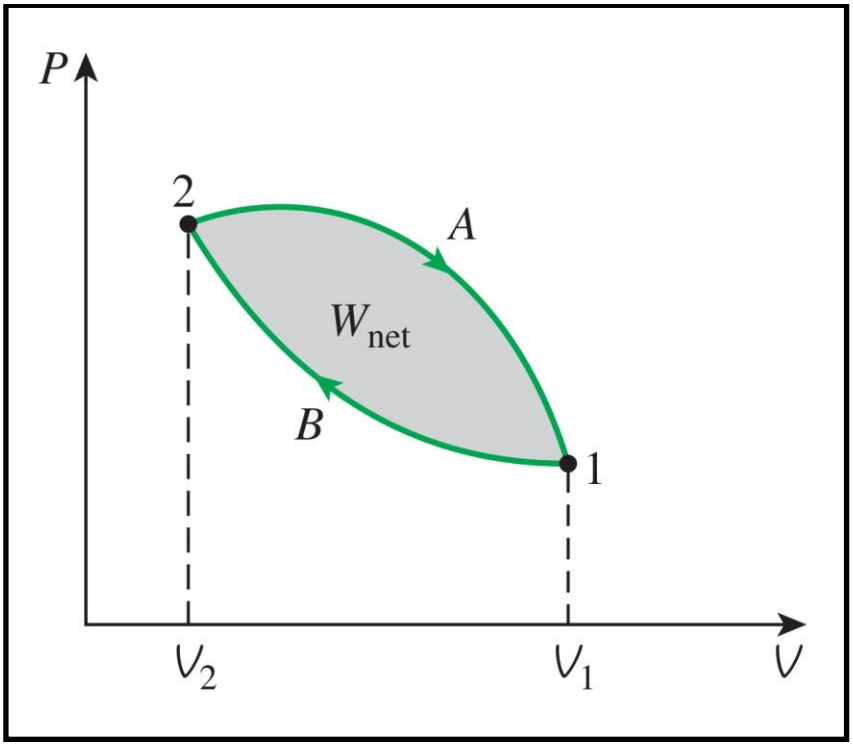

Figure 3.4: Geometric representation of a simple thermodynamic cycle (Çengel and Boles, 2015: p. 165)

Section 3.2.2.2: Temperature – Entropy (T-s) diagram

Before entering into the analysis of the various thermodynamic cycles, there are several more basic issues that need to be mentioned in this section regarding the methods of studying these cycles. Firstly, according to the definition of the state variable of entropy, the total involved thermal energy or heat **Q** during a process or a cycle can be calculated as such:

$$dS = \frac{\delta Q}{T} \Rightarrow \delta Q = T dS$$

$$\Rightarrow \boxed{Q = \int T dS}$$

Equation 3.6: Relationship between heat and entropy

As with the P-V diagram, in which the involved work can be calculated by taking the final integral of Equation 3.5, by using the **Temperature – Entropy** (T-s) diagram of a process, one can calculate the involved heat under the respective curve of that process, as shown in Equation 3.6. According to Müller and Müller (2009: p. 110), using the T-s diagram of a process has several advantages such as:

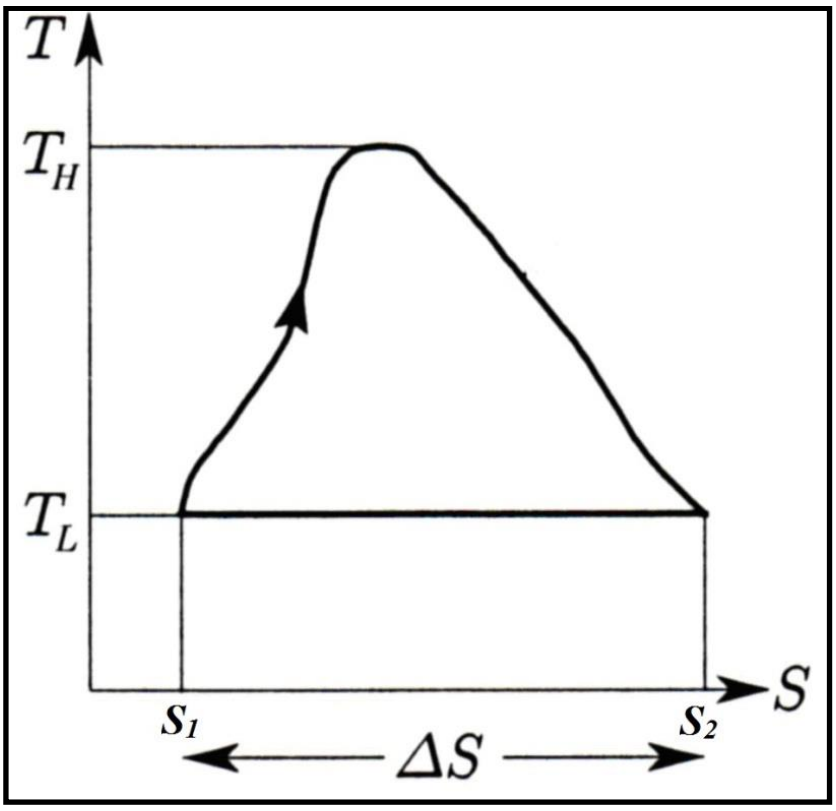

Figure 3.5: Example of a thermodynamic cycle represented on a T-s diagram (Müller and Müller, 2009: p. 110)

a) In a cyclic process, as shown in Figure 3.5, by integrating the upper portion of the curve using the limits for the integral from S_1 to S_2 (on the increasing entropy path following

the arrow) the integral has a positive value, which means that the calculated heat is absorbed by the working fluid.

b) In contrast, by integrating the lower portion of the curve from $\mathbf{S_2}$ to $\mathbf{S_1}$ (on the decreasing entropy path), the integral has a negative value that represents the amount of heat that was dissipated from the working fluid in order to bring it to its original state (S_1, T_L) and repeat the cycle.

c) If these two heat values were to be added, the sum therefore would be equal to the net work involved in the cyclic process, according to the First Law of Thermodynamics. So, as with the P-V diagram, the area in the T-s diagram within the closed loop of the cycle's curve represents the net work involved.

d) Lastly, adiabatic processes are represented on the T-s diagram by vertical lines (there is no involvement of heat) and not as steep hyperbolic lines, as in the P-V diagram, which makes the studying of the cycle much easier. Additionally, isothermal processes are represented by horizontal lines on this diagram, rather than first order hyperbolic lines as in the P-V diagram. This advantage can be seen by comparing the representation of the Carnot cycle in both the P-V and T-s diagrams, shown in Figures 3.6 (Moran et al., 2011: p. 264) and 3.7 (Moran et al., 2011: p. 293):

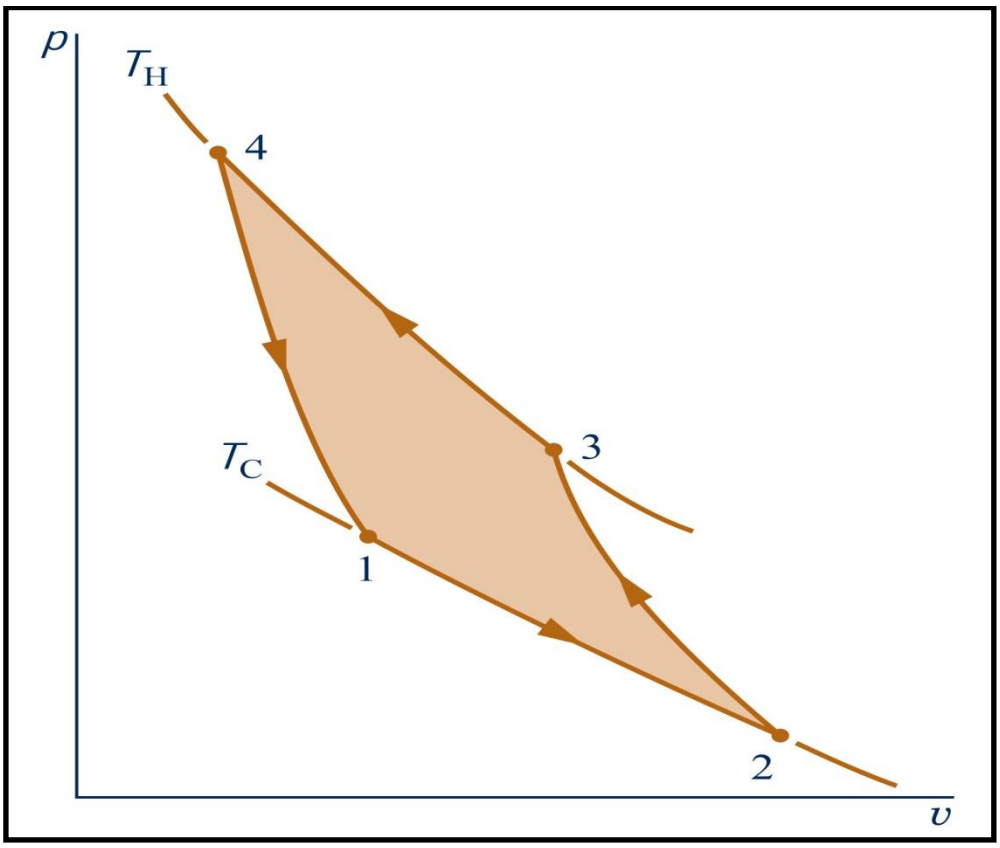

Figure 3.6: The Carnot cycle represented on a P-V diagram (Moran et al., 2011: p. 264)

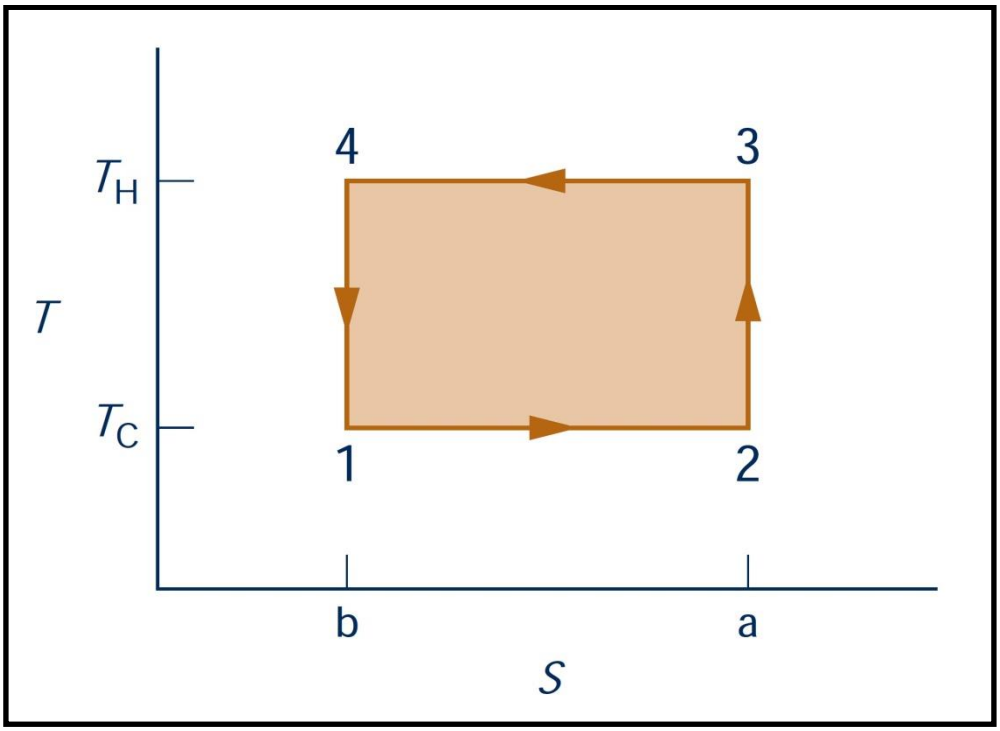

Figure 3.7: The Carnot cycle represented on a T-s diagram (Moran et al., 2011: p. 293)

It should be noted that the usage of "**δ**" for symbolizing the infinitesimal amount or differential of heat or work involved in a process (instead of the traditional "**d**") means that the corresponding differential is not exact or it does depend on the path of the process; whereas the "**d**" symbol is used for exact or independent of the process's path differentials of any state variable, including entropy.

For designing a power system using a thermodynamic cycle, engineers simply utilize the T-s diagram of a pure substance that they will be using as the Thermal Engine's working fluid. An example of the T-s diagram for water/steam is shown in Figure 3.8 (Moran et al., 2011: p. 286):

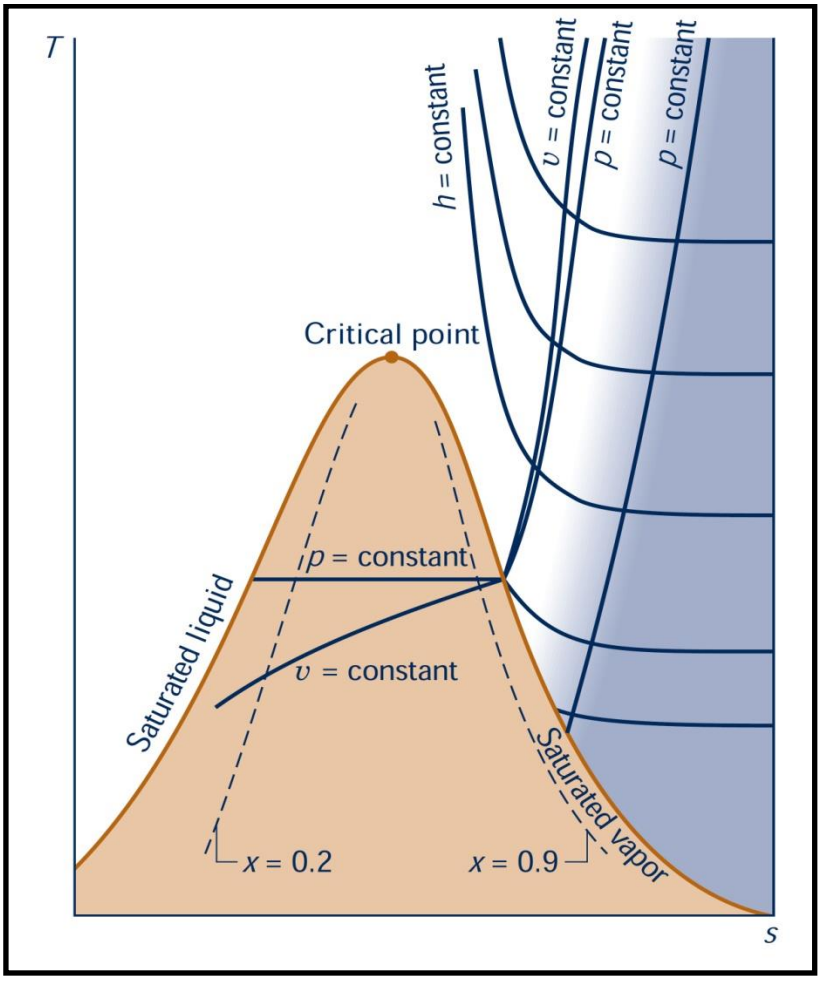

Figure 3.8: The T-s diagram of a pure substance (Moran et al., 2011: p. 286)

For every substance, its T-s diagram has a bell shaped curve that peaks at the substance's **critical point** or state, which is the state of specific pressure and temperature values that the

liquid and gas phases coexist. The curve's portion left of the critical point is the **Saturated Liquid Line** that contains all the states that exist at the boiling point of water for various pressure values. The space on left of the curve contains the states that water has at various temperatures below the boiling point and it called **Sub-saturated Liquid Region**. The curve's right hand portion is the **Saturated Vapour Line**, where the substance has already absorbed all the latent heat needed to be converted entirely from liquid to vapour at the boiling point and not above, while the space on the right of the curve contains the states that the vapour has temperatures beyond the boiling point and it called **Superheated Vapour Region**. Lastly, the area under the curve is the **Liquid-Vapour Mixture Region**, where the liquid is absorbing latent heat and gradually changes phase. In addition, these diagrams contain some more information including constant pressure and specific volume lines (Çengel and Boles, 2015: p. 338 – 339). It is noted that the diagram is calibrated on the specific entropy **s** of the substance and not the actual entropy **S**, as each application has different amounts of working fluid involved and so, the diagram presents the values of temperature against the values of entropy of a single kg of substance. The designer takes the diagram, extracts the best cycle for his application and then calculates the total mass of the working fluid his design needs.

Section 3.2.2.3: Enthalpy

One final state property that is needed for the design of a Thermal Engine is a measure of the total thermal energy of each of the working fluid's state. This property is called enthalpy (**H**) and renders the study of Thermal Engines very easy, as it allows the designer to ignore all the restriction about the absorption and emission of heat from the working fluid. Mainly the designer does not have to worry if the working fluid is changing phase or if it is absorbing sensible heat. For example, in order to determine the total amount of heat absorbed by **1 kg** of water for transitioning from liquid of **60 ºC** to vapour of **125 ºC** at **1 bar** of pressure (about 1 atm) all it needs to be done is find the difference of the specific enthalpy **h** of these two states, usually from a steam table. Enthalpy is defined as the sum of internal energy **U** with the product **PV**, as shown in Equations 3.7. For the same reason mentioned previously, the calculations done in this project use the specific enthalpy values of the working fluid, as shown in Equation 3.7.2 (Çengel and Boles, 2015: p. 124 – 125).

$$\mathbf{H = U + PV} \quad (1)$$

$$\mathbf{h = u + Pv} \quad (2)$$

Equations 3.7: The mathematical definition of enthalpy and specific enthalpy (Çengel and Boles, 2015: p. 124)

Section 3.2.2.4: Types of thermodynamic cycles

There are several thermodynamic cycle that have been developed by various scientists and engineers, all with the same goal: produce the highest possible amount of work per unit of absorbed thermal energy, or in other words convert as efficiently as possible heat into useful work. The Second Law of Thermodynamics restricts the complete conversion of the absorbed heat in a thermodynamic cycle into work, so each cycle has an efficiency factor called thermal efficiency ($\boldsymbol{\eta_{th}}$) and this is equal to the percentage of net work the cycle extracts divided by the amount of heat injected into the working fluid during the cycle's operation (Çengel and Boles, 2015: p. 486). Actual or real thermodynamic cycles never achieve their full potential thermal efficiency as they possess irreversibilities, including: friction, thermal losses from the boundaries of the engines and that the expansion and compression of the fluid do not occur in a purely isentropic (adiabatic) manner (Çengel and Boles, 2015: p. 487).

The best possible thermodynamic cycle that has been studied is the **Carnot** cycle and it is proven that its efficiency is the greatest achievable, compared to any other cycle. This is why engineers calculate the Carnot efficiency of any power cycle they design so they could find the highest possible potential efficiency they can achieve with their design. The Carnot efficiency is presented in Equation 3.8 (Çengel and Boles, 2015: p. 488):

$$\boldsymbol{\eta_{th,Carnot} = 1 - \frac{T_c}{T_h}}$$

Equation 3.8: The Carnot thermal efficiency (Çengel and Boles, 2015: p. 488)

where, $\mathbf{T_c}$ and $\mathbf{T_h}$ are the lowest and highest temperatures of the cycle in **K**, respectively. Other cycles include the **Otto** and **Diesel** cycles that are the ones used in petrol and diesel oil internal combustion reciprocating engines, respectively (Çengel and Boles, 2015: p. 491) and the **Stirling** and **Ericson** cycles, which differ from the basic Carnot cycle by utilizing a regenerator to store the rejected heat from the cycle and reuse it in the main cycle (Çengel and Boles, 2015: pp. 502 – 503).

Finally, there is the **Brayton** cycle that was originally used in the oil extraction industry and today it is used exclusively in gas turbines. There are two types of this cycle, the open type and the closed type. The open type collects fresh air at its inlet, then the air is being compressed isentropically by a compressor, the compressed air is then heated in a combustion chamber and then expanded again isentropically by a steam turbine. Lastly, the spent air and flue gases are extracted from the exhaust of the turbine. The schematic of the open Brayton cycle is shown in Figure 3.9 (Çengel and Boles, 2015: p. 506). On the other hand, the closed type has a specific amount of working fluid to operate and it can be greener that the open type, as it can operate with any kind of heat source, not necessarily by the combustion of fossil fuel. The operation of the closed type involves the isentropic compression and then expansion of the working fluid; however, the fluid is heated by a heat exchanger and not necessarily in a combustion chamber, which means that even a renewable heat source can be used for this process. Eventually, the gas needs to be cooled by another heat exchanger in order to be able to be recompressed. The closed type or closed loop Brayton cycle appears in Figure 3.10 (Çengel and Boles, 2015: p. 507).

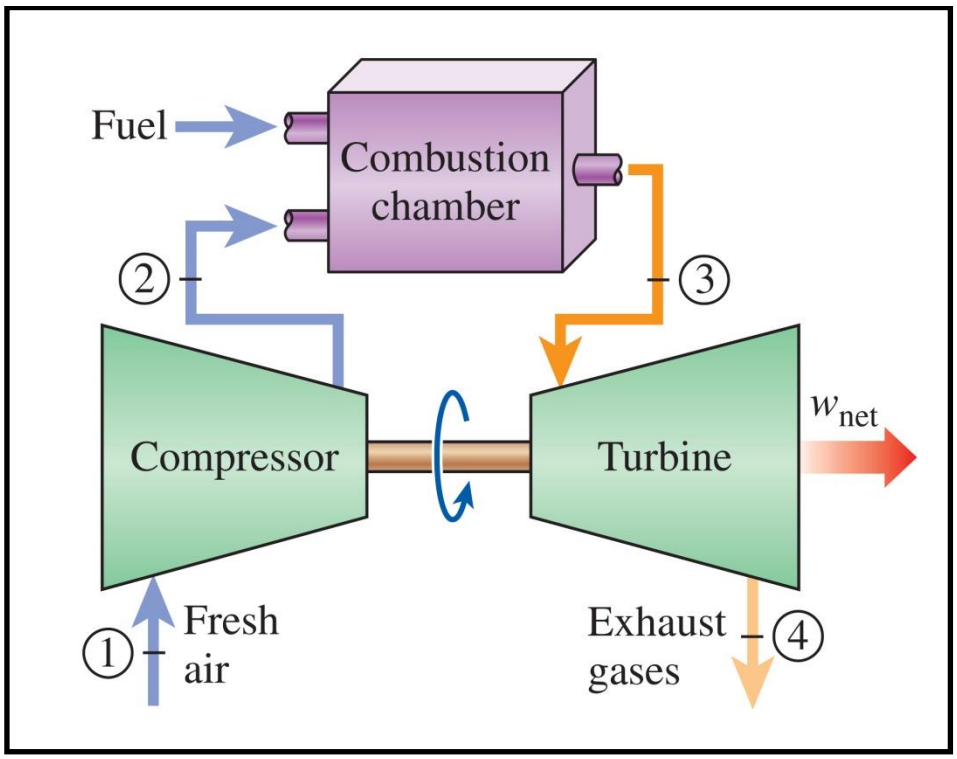

Figure 3.9: The open type Brayton cycle (Çengel and Boles, 2015: p. 506)

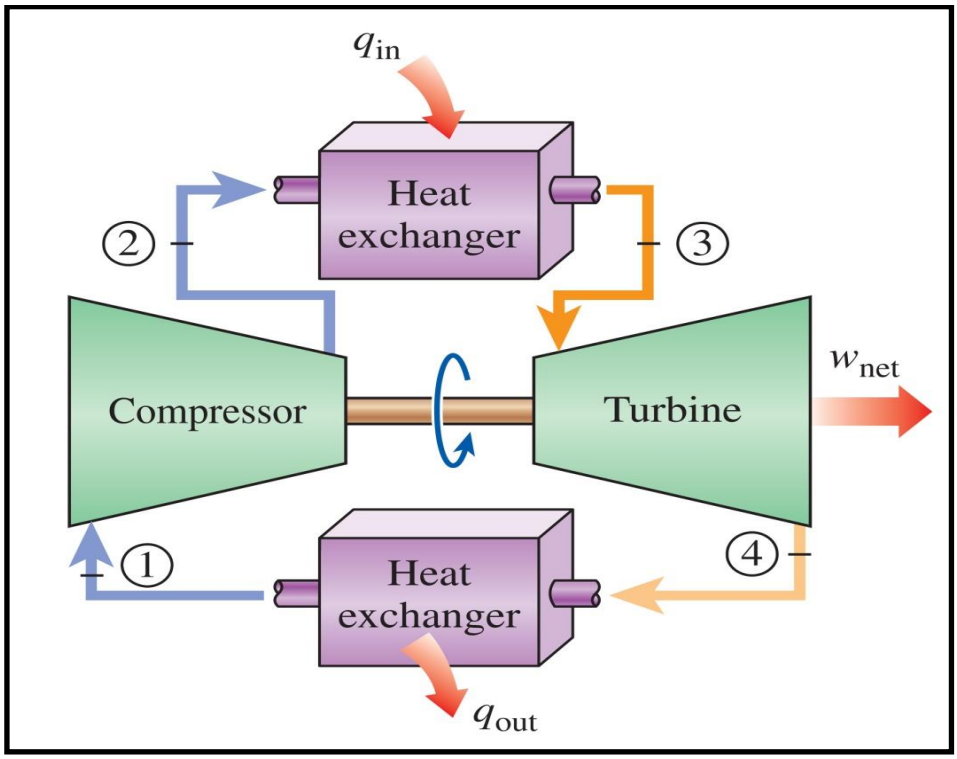

Figure 3.10: The closed type Brayton cycle (Çengel and Boles, 2015: p. 507)

Section 3.2.3: Rankine cycle

The previous section explains the various types of thermodynamic cycles in existence. This section analyses the Rankine cycle, as it is the one utilized in the national scale power stations today.

Apart from the previous gas power cycles where their working fluid is exclusively in the gas phase, there are also liquid – vapour power cycles in which their working fluid changes phase from liquid to gas and vice-versa. The thesis focuses on the Rankine cycle, which is very similar with the previously mentioned closed loop Brayton cycle; the difference between them is that the Rankine cycle uses water as its working fluid that is converted into steam instead of air. The schematic and T-s diagram of the cycle is shown in Figure 3.11(Çengel and Boles, 2015: p. 555):

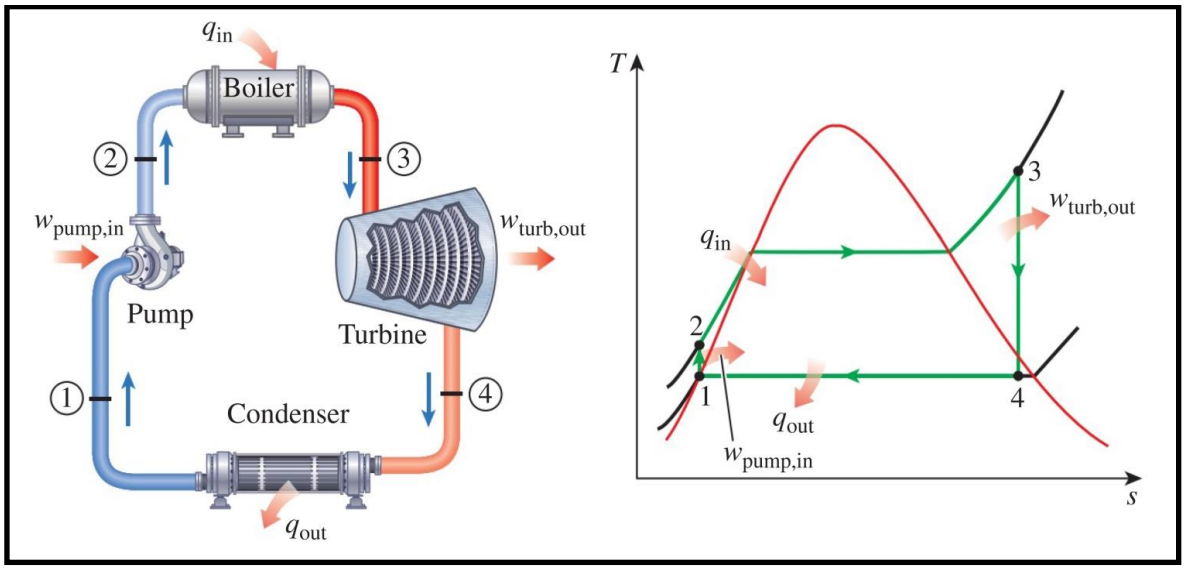

Figure 3.11: The basic Rankine cycle (Çengel and Boles, 2015: p. 555)

The reason why the Rankine cycle converts the working fluid back into its liquid form before compressing, it is that a conventional compressor consumes large amounts of energy to compress a gaseous fluid. Instead, the working fluid is fully condensed into saturated liquid to be re-pressurised by a feed pump. As changes in the specific volume of a liquid are minimal, the pump consumes a negligible amount of power to compress it and so the heat engine's output power is almost unaffected by the usage of the pump (Hoyle & Clarke, 1973: p. 237).

For each stage of the cycle, the mathematical equations for determining each one's energy (heat and/or work) involvement in relation to the working fluid's properties is the first step before the actual calculations can start. There are four stages in the Rankine cycle and so four equations can be derived. It should be noted that as this cycle is to be used for a power plant design, the calculations are set to determine values of power, instead of total energy absorbed or extracted. This can be done very easily by calculating the rate of energy involved in each stage over time, in other words calculating the first derivative over time of the equations' energy components. As a result, from this point on the energy quantities are being symbolized with a dot over them (for example $\dot{\mathbf{Q}}$ instead of **Q**). Likewise, since the properties of the fluid are in their specific form (specific volume, specific entropy and specific enthalpy), they have to be multiplied by the mass flow rate $\dot{\mathbf{m}}$ as well, in order for the equations to be dimensionally homogeneous. The ideal cycle equations, based on Figure 3.11, are presented below:

Stage 1 – 2 (Pump Power Input)

$$\dot{W}_P = \dot{m}(h_2 - h_1) \qquad (1)$$

Stage 2 – 3 (Boiler Heat Input)

$$\dot{Q}_B = \dot{m}(h_3 - h_2) \qquad (2)$$

Stage 3 – 4 (Turbine Power Output)

$$\dot{W}_T = -\dot{m}(h_4 - h_3) \qquad (3)$$

Stage 4 – 1 (Condenser Heat Output)

$$\dot{Q}_C = -\dot{m}(h_1 - h_4) \qquad (4)$$

Cycle Efficiency

$$\eta_{th} = \frac{|\dot{W}_T - \dot{W}_P|}{\dot{Q}_B} \qquad (5)$$

Equations 3.9: The Rankine Cycle formulae

Section 3.3: Component selection

After the analysis of theoretical Thermodynamics foundations, this section explains the selection procedure for the systems' components. This is necessary so that the systems can be feasible and realistic at a theoretical level, before the sizing and eventually the mathematical simulation phases can begin. Following the selection process, section 3.3 presents and analyses the block diagrams of the three systems.

Section 3.3.1: Solar collector

Firstly, since the goal of the project is solar energy exploitation, the most important component is consequently the solar collector. There are two categories of solar collectors: the non-concentrating type and the concentrating ones. **Non-concentrating** collectors include: the flat plate, evacuated tube, hybrid PV/T and the enriched hybrid – bifacial PV/T collectors. They can be used for heating domestic hot water or to drive absorption cooling systems. The PV/T collector combines a PV one, for direct electricity production and a Thermal one at the former's back side for absorbing waste heat and using it in other applications (Tian & Zhao, 2013: p. 539 – 541). The **concentrating** kind, on the other hand, uses reflecting surfaces along with concentrating plastic or glass Fresnel lenses to divert and concentrate the solar rays onto a small area, thus achieving higher temperatures than the non-concentrating ones that allow them to reach a higher thermodynamic efficiency. There are three types of concentrating collectors: the solar tower or heliostat field collector, the parabolic dish and the parabolic trough ones (Tian & Zhao, 2013: p. 542 – 543). The task of this project's collectors is transferring large amounts of solar energy efficiently into the heat absorbing medium, either organic oil or water. In the case of water, this collector must be capable of vaporizing it with relative ease, especially when the water is being pressurised to

the desired level by a feed pump. Additionally, since the collector is to be installed on the roof of a domestic building, it must occupy the least surface area possible. The **solar tower** type requires a large land area for its mirror field to be set and also the lower limit of the minimum collector area is directly dependent on the operating temperatures. The **parabolic dish** collector consists of dish shaped mirrors that concentrate solar irradiation into a common focal point for electricity production of **7** to **25 kW** and they can be scaled up to accommodate out of reach areas in large countries (Tian & Zhao, 2013: p. 542). Finally, the **parabolic trough** collector consists of mirrors with a parabolic cross-section to make solar rays to converge onto a metallic channel inside its geometry. They can cause the temperature of the channel to increase up to **400 ºC**; they also have advantages over the other two types, such as scalability and that their solar tracking is done only in two dimensions. The scalability aspect allows these collectors to be scaled down and fit easily on a small surface area, such as the roof of a household and the fact that they only require two dimension tracking makes their application less complex that the other two types (Tian & Zhao, 2013: p. 543). Keeping these in mind, the **parabolic trough collector** is the most suitable for this project. This project also provides several reasons why it offers a STh solution instead of a PV one, which are listed next.

Section 3.3.2: Solar Thermal heat storage

For a solar system, some form of storage is imperative due to the lack of solar energy during the night time or heavily cloudy days and that intermittently solar produced electricity needs to be stored before it becomes usable. In contrast to electrical energy, heat can be stored much more easily as the technology is simpler than that of electrochemical batteries. That stored heat can be then used for producing electricity of stable amplitude and frequency.

The rechargeable battery technology is complex, as it stores electricity by causing a chemical reaction to their salt – electrolyte solution flowing between several metal plate arrays, when on those plates there is a potential difference. The life expectancy of such batteries is relatively small, from **1** up to **24 years** and they also need to operate within a specific temperature band (from **40** to **80 ºF** or about **4.5** to **26.7 ºC**). An additional feature of this storage type is the amount of cycles to **80% Depth of Discharge** (**DoD**), which is the number of times the battery can be almost completely discharged (over 80%) before it loses

its charging capacity and needs to be replaced (Solarray, 2014). In comparison, the optimal solar thermal system could be fitted with a storage tank containing a certain amount of heat absorbing material that would store purely thermal energy, giving it a very long lifespan.

Thermal energy storage is classified into three categories: sensible heat, latent heat and chemical heat storage. Section 4.5.2 further explains these types and also provides the mathematical relationships that govern each one.

Sensible heat storage is the most popular type; however it has the smallest storage capacity amongst the three, since it is based on increasing its heat absorbing material's temperature within a narrow range. Nevertheless, the operating temperatures of this type ranges from **200** to **1200 ºC** and the materials used have excellent thermal conductivities, especially when they are metal based. They have also the lowest cost per kg compared to the other two categories.

In contrast, the **latent heat** type has higher storage capacity than the sensible heat one, since it is capable of absorbing larger amounts of energy without the restriction of temperature changes. In this case, the heat absorbing material has constant temperature since it changes phase usually from solid to liquid, hence they are called Phase Changing Materials (PCM) (Tian & Zhao, 2013: p. 543 – 544). More specifically, Tian and Zhao (2013: p. 545) present an extensive list of PCMs, with the majority of them being salts (ionic compounds) with high melting points and condensation latent heat capacities. The disadvantage with PCMs is that they have small thermal conductivities. However, this problem can be overcome by enriching them with heat transfer enhancement agents. Further details about thermal enhancement of latent heat storage are described in Section 4.5.2.

Lastly, the **chemical heat storage** category includes those materials that absorb or release thermal energy when they are involved in chemical reactions; essentially, they convert heat into chemical bond energy. They have the highest heat storage capacity of the three categories; however they have serious disadvantages. These are: low long-term reversibility issues, chemical stability and also several of the mentioned reactions are complicated (Tian & Zhao, 2013: p. 544 – 545). Chemical heat storage is therefore not considered in this thesis.

Section 3.3.3: Heat engines

The next important component of a power plant is a heat engine. This is a device that operates in a thermodynamic cycle, which moves thermal energy from a heat source or hot reservoir into a heat sink or cold reservoir in order to produce useful mechanical work (Sonntag, et al., 2003: p. 215). The two major categories of heat engines are the **internal** and **external** combustion heat engines; the term "combustion" refers to the process of heat production and collection and it is not restricted to burning fuel per se. In this sense, "combustion" can refer to solar, nuclear, geothermal energy or any other process that produces thermal energy.

As its name suggests, an **internal combustion engine** produces heat in a special chamber inside its body. A characteristic example is the automobile motor, which combusts fossil fuel inside each of its piston cylinders, forcing the pistons to move reciprocally and thus producing rotational mechanical work. On the other hand, in an **external combustion engine** heat production occurs externally and not inside the engine. For example, in electricity power plants thermal energy is produced either by burning fossil fuel in a furnace or by utilising renewable sources in order to raise the temperature and eventually changing the phase of the Rankine cycle's working fluid. A turbine then expands the compressed fluid, producing mechanical work.

As mentioned in Section 3.1.5, there are two types of power plants: the vapour power plant and the gas power plant. The former is the one used in steam power plants, where the working fluid is being vaporized by a heat source, it gets expanded in a turbine, then it gets liquefied again through a condenser and lastly it gets pressurised by a feed pump to repeat the cycle (Hoyle & Clarke, 1973: p. 99). In a gas power plant, on the other hand, the working fluid remains in its gaseous phase throughout the whole cycle. Another difference is that the feed pump is replaced by a gas compressor (Hoyle & Clarke, 1973: p. 100). In both cases, the **turbine** is the expander of the working fluid and the device responsible of producing mechanical power that the electrical generator needs for electricity production. According to Wu & Wang (2006: p. 464) such components can have extensive lifespan and they are very reliable, even though they have long start up time and poor partial load performance. They

also mention that turbines (especially steam turbines) are suitable for large scale power plants and industrial units, rather than smaller scale systems.

In contrast to steam turbines, **internal combustion reciprocating engines** are the most suitable component for applications under **1 MW**. As a mature technology, they are available in a vast range of sizes, they can handle partial loads very well and they have quick start up along with good operating conditions. However, they have a large number of moving parts (pistons, crank and cam shafts, valves) and so they frequently require maintenance, hence they have increased maintenance costs. Moreover, they produce high frequency vibrations that may cause problems and most importantly, since they require fossil fuels, they release greenhouse gases into the environment, mainly CO_2 and NO_x (Wu & Wang, 2006: p. 464).

Turbines today are designed for large scale applications and not for needs of individual households, so **micro turbines** are a promising alternative solution to this issue. They are the extension of a larger group of components called combustion turbines that use natural gas, diesel or gasoline as their primary fuel. Another advantage of micro turbines is that they have only one moving part and so they do not need frequent maintenance. Moreover, they have low greenhouse gas emissions and they are less noisy than other, similar sized engines. They are also very versatile and they could easily be used for the purposes of this project. The problem is that they have large rotational speeds, around **120000 rpm**, whereas the frequency of AC power is **50 Hz** or **3000 rpm**, the highest speed a synchronous generator can receive on its shaft. So, the turbine that drives the synchronous generator should have low and easily controllable rotational speeds. Additionally, since they are a newly developed technology they are difficult to acquire they have high acquisition costs (Wu & Wang, 2006: p. 465).

The last engine type described here is **Stirling engines**. In contrast to the previously described engines in this section, Stirling engines are closed loop external combustion ones with either hydrogen (**H_2**) or helium (**He**) as their working fluid. They can receive thermal energy from virtually any source, either from fossil fuel or renewable sources; specifically, they can be coupled with a Parabolic Dish collector that was mentioned in Section 3.3.1. Because of this, Stirling engines do not require a combustion based source to operate and

thus allowing the reduction or even the elimination of greenhouse gas emissions, they have lower noise levels and vibrations and they do not need frequent maintenance, as they have fewer moving parts compared to conventional engines. Even though the technology is relatively unknown and the acquisition of such units is very expensive at this point, they can easily attract the attention of researchers for further development. Nevertheless, they can very easily be used for domestic applications, since they are small in size and quiet, while the compatibility with renewable harnessing equipment makes them a good candidate for the optimal system of this project (Wu & Wang, 2006: p. 465).

As there are several candidates of heat engines regarding the concept systems' expander, a selection process is needed for determining the most suitable for this project. Table 3.1 is a Pugh selection matrix, presenting the weighted selection criteria for the project's expander along with the previously mentioned types of heat engines; the weight of each criterion is a number from **1** to **5**, depending on the importance of that criterion to this project; **1** being the least important and **5** the most. In addition, the following symbols are used to indicate the degree of advantage or disadvantage of each heat engine at a particular criterion. The advantages and disadvantages are the ones mentioned in the previous paragraphs. Any criteria that are not mentioned above for a particular engine would receive a "Neutral" symbol.

++	Very good
+	Good
N	Neutral
-	Bad
--	Very Bad

			Expander Candidates			
	Pugh Selection Matrix	**Weight**	Steam Turbine	Internal Combustion Reciprocating	Micro Turbine	Stirling Engine
Selection Criteria	Open-loop expander – Efficiency	5	**++**	**-**	**N**	**--**
	Lifespan	2	**++**	**N**	**+**	**N**
	Reliability	3	**++**	**++**	**++**	**N**
	Thermal source versatility	4	**++**	**--**	**+**	**++**
	Small scale application suitability	4	**+**	**++**	**++**	**++**
	Cost	2	**--**	**--**	**-**	**--**
	Greenhouse emissions reduction	5	**++**	**--**	**-**	**++**
	Shaft speed suitability	5	**++**	**++**	**--**	**++**
	Weighted Total +		**52+**	**24+**	**20+**	**36+**
	Weighted Total -		**4-**	**27-**	**17-**	**14-**
	Weighted Final Score		**48+**	**3-**	**3+**	**22+**

Table 3.1: Pugh Matrix for selecting the project's expander

From this Pugh matrix it has become clear that the **steam turbine** is the most suitable heat engine for this project. A Stirling engine is also a good candidate; however the mechanical work is produced by utilizing a working fluid undergoing a closed-loop Stirling thermodynamic cycle that is bound by its Carnot efficiency, whereas a steam turbine is an open-loop expander and it does not have an issue with Carnot efficiency.

Section 3.3.4: Underground condenser

The condenser is responsible for liquefying the working fluid into saturated liquid of the same temperature and pressure by extracting only the latent heat from its vapour. In large scale power plants, this process either utilizes the water flow of a nearby river or by using cooling towers. However, these condensation methods cannot be used in individual households, especially those built away from seaside and river areas. Additionally, cooling towers are large and expensive constructions, thus being not suitable for domestic level usage. A Ground Heat Exchanger (GHE) can solve the problem of heat rejection by utilizing the ground as a heat sink. This type of heat exchanger was studied by a group of Cypriot researchers, who recorded ground temperature measurements in various depths at numerous location of the unoccupied Cypriot region. Specifically, they drilled six borehole sites at six

separate locations around the country, making sure that they covered mountainous, semi – mountainous, seaside and inland areas. These locations are shown in Figure 3.12 (Florides et al., 2013b: p. 86). The researchers measured ground temperatures in these locations in three depth sections for each one: the **surface zone** (from **0** to **0.5 m**), the **shallow zone** (from **0.5** to **8 m**) and **deep zone** (from **8 m** onward) (Florides et al., 2013b: p. 87). They discovered that the deep zone temperatures are constant throughout the year with an average value of **21 ºC** while the other two zones' temperatures are susceptible to ambient temperature fluctuations and also that the lithology of the ground is the main factor affecting that temperature (Florides et al., 2013b: p. 87, 88).

In addition to this task, Florides et al. (2013b) simulated the thermal capacity of a series and a parallel flow double vertical loop, U – tube borehole heat exchangers against a single U – tube one. There are two main categories of GHE, open and closed loop type: The **open loop** type uses the ground water as the heat carrying fluid and consequently it is circulated inside the GHE. The **closed loop** GHE uses the ground as its heat source or heat sink, as the ground temperature is constant in deeper layers throughout the year; that temperature is also greater than the ambient one during the winter, while being less than the ambient during the summer. Additionally, the GHEs are divided into two further categories, based on the installation configuration: vertical (borehole) and horizontal types.

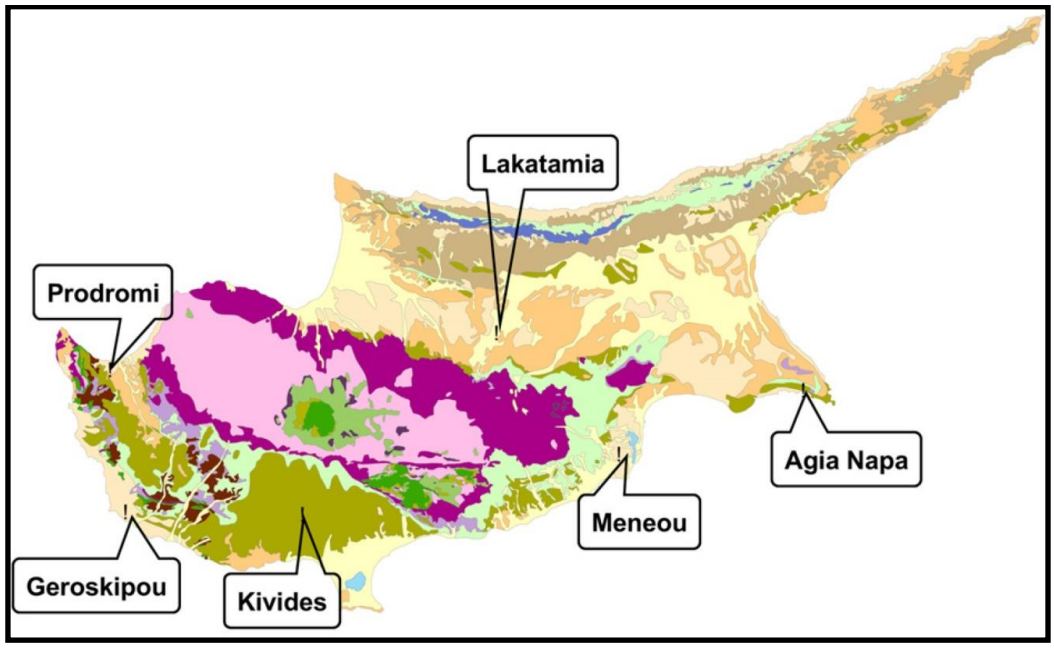

Figure 3.12: Ground Heat Exchanger borehole drill sites (Florides et al., 2013b: p. 86)

A horizontal GHE (**HGHE**) is a ground heat exchanger, placed at a specific depth and its length is parallel to the ground's surface. It does not require the drilling of deep boreholes for installing it; however, it might be more feasible to install it before the construction of the host building. Its disadvantage is that it is susceptible to seasonal temperature fluctuations, if it is installed at a shallow depth. This fact could renders this type of GHE unsuitable for this project's systems, as they demand a specific and constant temperature difference for the condensation process of the working fluid. On the other hand, it could eventually be a feasible solution if the tubing of the exchanger is placed in the deep zone.

In contrast, the vertical GHE's (**VGHE**) tubing is placed in boreholes of **20** to **300 m** deep, which is within the range of depth that ground temperature is constant. The area around the vertical tubing is usually filled with a thermal conductivity enhancing agent (such as grout) for improved thermal coupling of the GHE with the ground. This means that the heat transfer mechanism of such a GHE could be deterministic and more reliable than that of a horizontal one (Florides et al., 2013a: pp. 364 – 365). The cross sectional configuration of single and double U – tube vertical GHE (VGHE) is shown in Figure 3.13 (Florides et al., 2013a: pp. 368 – 369).

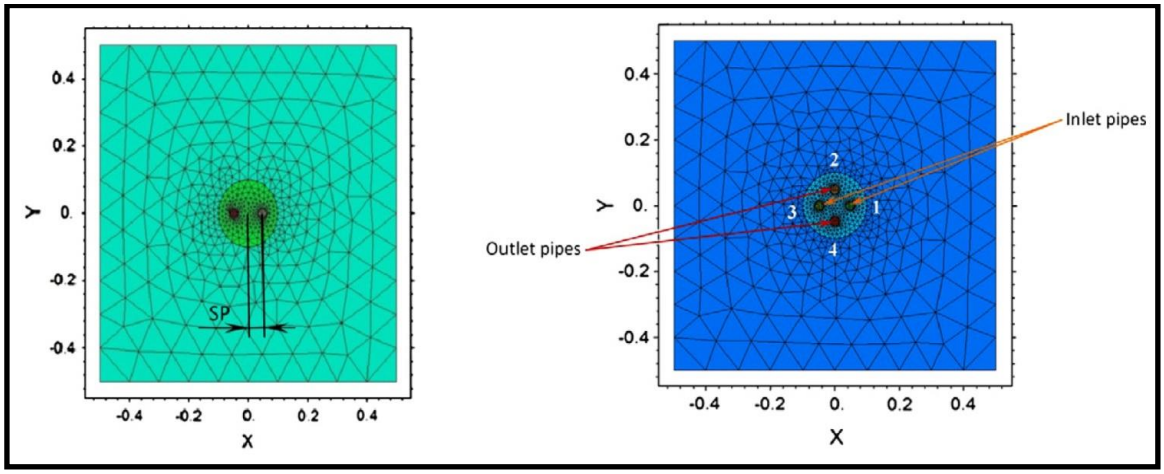

Figure 3.13: Cross sectional model top view of the single (left) and double (right) vertical U – Tube GHE (Florides, Christodoulides & Pouloupatis, 2013: pp. 368, 369)

As mentioned, the researchers compared the performance of a single U – tube VGHE with a double series-flow and double parallel-flow ones, by using a mathematical model (Florides et al., 2013a: p. 366) and the simulation software **FlexPDE** (Florides et al., 2013a:

p. 367). Their model showed that a series-flow double VGHE is the most efficient configuration with heat absorption/rejection capability of **4390 W**, with temperature difference of **3.4 ºC** and fluid velocity of **0.5 m/s**, which is **22** to **29%** more efficient than a parallel-flow double U – tube VGHE and **42** to **59%** more efficient than the single U – tube VGHE (Florides et al., 2013a: pp. 372 – 373). Additionally, the cost of constructing a double U – tube VGHE is **26** to **29%** more than the single one; however, the enhanced efficiency of a series-flow double U – tube VGHE would probably render this type to be a better investment than the single one, especially in the case of multiple VGHE in a single project (Florides et al., 2013a: p. 371).

The horizontal type is used when **1** to **2** metre deep trenches are easy to be dug and if there is sufficient area inside the building's land space and sometimes they are bent into a curled shape, called **slinky loop GHE** (Florides et al., 2013a: p. 364). Mohamed Reda Othman Ali (2013) executed his Ph.D. Thesis on modelling the performance of a Horizontal GHE (HGHE) using ground data collected from various locations in his home country, Egypt. Even though his findings apply specifically to Egypt, his conclusions on the ground conditions that have a significant effect on an HGHE could be also applicable to countries of proximate latitude to Egypt's, such as Cyprus. His simulation analysis showed that moisture content of both surface and underground soil layers plays a significant role in the propagation of thermal energy from both ambient and geothermal sources. Specifically, the smaller the percentage of soil moisture, the more difficult it is for thermal energy to be conducted through the various ground layers. He also simulated the ground thermal behaviour of three major cities in Egypt under different surface dryness and underground moisture conditions of two types of soil at various ground depths. His simulation results show that in all cases, using **5 m** deep trenches for a HGHE is enough to eliminate any ambient temperature fluctuations and also by using the average ground temperature, any calculations regarding GHEs would be performed with accuracy (Ali, 2013: p. 181).

Additionally, Ali examined the thermal behaviour of a HGHE, which had the cross sectional configuration shown in Figure 3.14 (Ali, 2013: p. 85). Simulation input data included the vertical position of the pipelines **d** and the horizontal distance between two pipeline branches **HSD**, while its boundary conditions are thermal convection from the air to the ground through the latter's surface and a constant temperature at **5 m** deep. The

simulation was executed for several operating conditions: **type of soil** (clay or loamy sand), **ground surface dryness**, **soil moisture percentage** (0%, 20% and saturated) and lastly **climate and location** (Cairo, Alexandria and Al – Minia) (Ali, 2013: p. 163). His conclusions were that the separation distance HSD of the GHE's pipes is optimum at **40 cm** for heat exchanging without interaction between the pipe branches, for wet surface, loamy sand soil and 20% to saturated moisture soil content (Ali, 2013: p. 202). Finally, the soil itself must not be poorly moist, in order to conduct heat more easily and also in the case of clay soil ground conditions, the backfill of the GHE's trench needs to consist of thermal conductivity enhancing sand grout (Ali, 2013: p. 227).

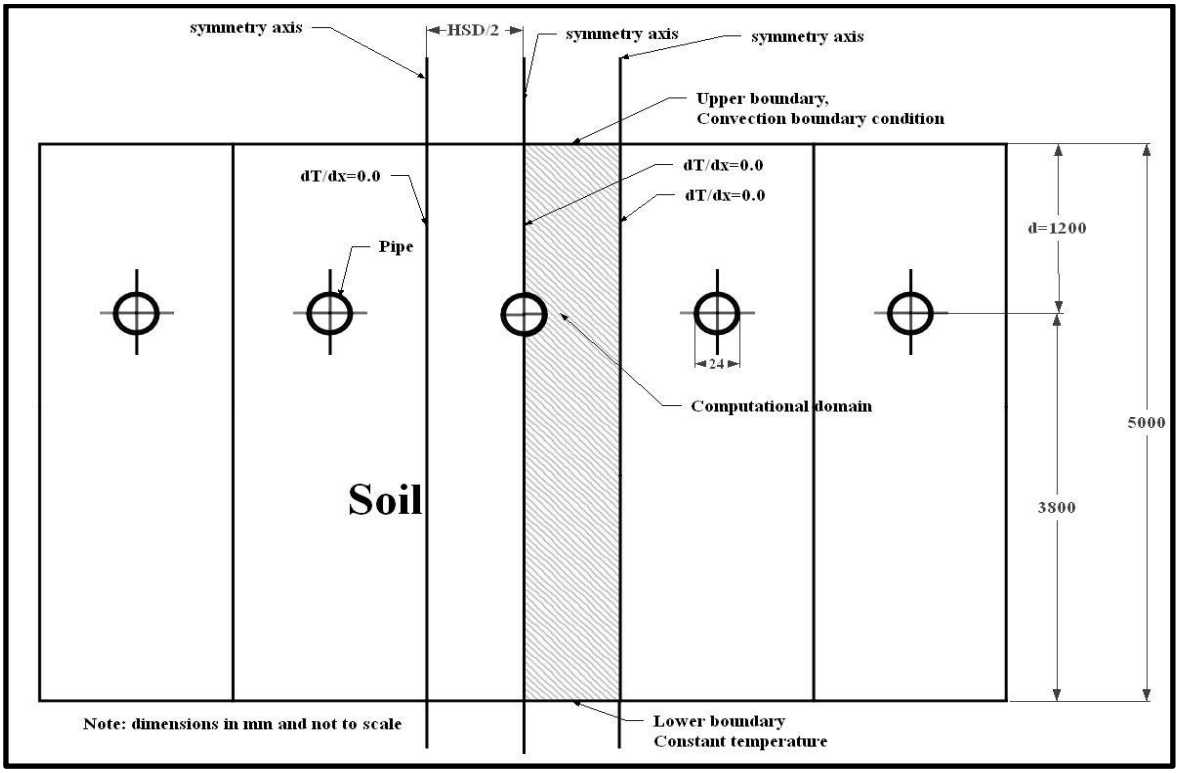

Figure 3.14: Cross sectional configuration of Ali's HGHE simulation design (Ali, 2013: p. 85)

For the purposes of this work a GHE has been implemented using basic heat exchanger engineering equations, information from Mohamed Ali's thesis and pipe material data from a specific manufacturer. Firstly, the GHE design is shown in the next diagram, in Figure 3.15. For more accurate and stable behaviour of the GHE, the ground depth in which its pipes would be placed into must have constant temperature for as long as possible and it must also be unaffected by the seasonal and weather conditions.

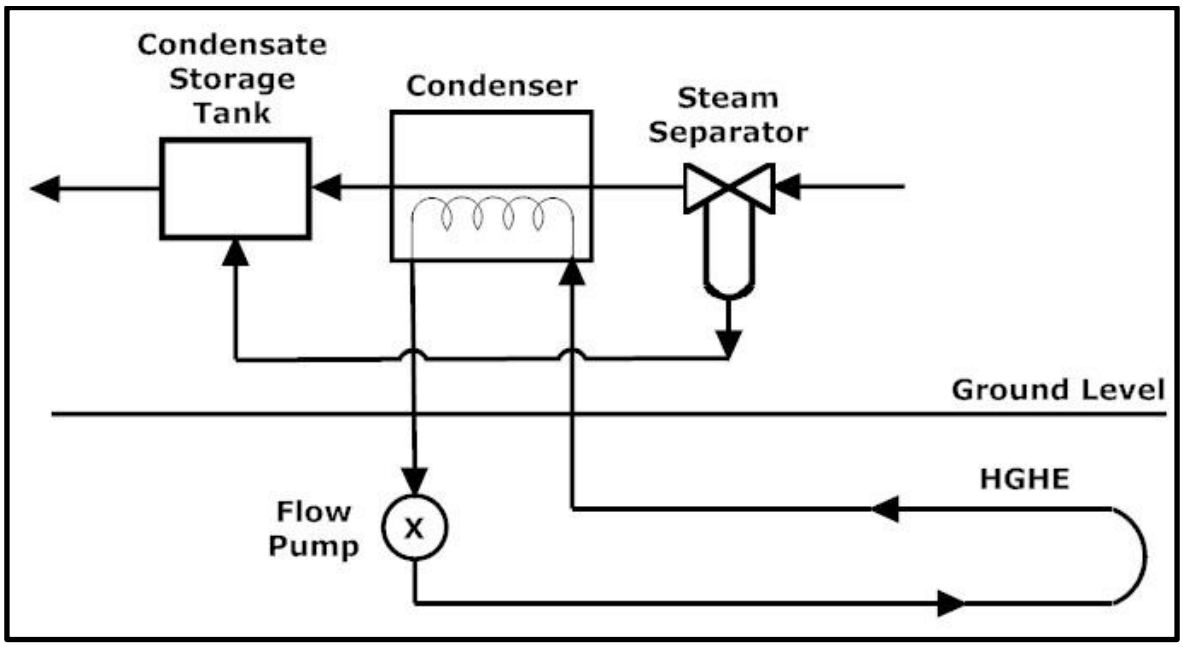

Figure 3.15: Working fluid condenser – HGHE block diagram

As already mentioned, in **5 m** of depth ground temperature is relatively constant and that any calculations under this conditions would be accurate enough (Ali, 2013: p. 181). For this reason there is no need to design a vertical GHE that will be reaching over **20 m** deep, as its digging, labour and material acquisition expenses would be greater than a horizontal one's. So, a Horizontal Ground Heat Exchanger is more preferable for the purpose of this project.

After this section described the selection criteria of the desired basic components, section 3.4 presents the template on which three concept system models for the project's purposes are based on and explains their functionality. The project presents the capabilities of each one and ultimately indicates the best of three as its optimal solution for using in the households of Cyprus.

Section 3.4: Concept systems' general design blueprint and specifications

Section 3.4.1: Block diagram template

The three concept systems of this project follow the generic template that Figure 3.16 presents. The block diagram of this system template consists of the core system dotted block, a parabolic trough collector array as its input and a steam turbine coupled with a synchronous electrical generator for the output. The core system is what differentiates the three concepts

from each other. As indicated, the turbine's exhaust is the system's feedback circuit, in which any residual heat in the working fluid can be further utilized by a calorifier or an absorption chiller before it reaches the condensing part of the Rankine cycle. Sections 4.2, 4.5 and 4.6 of Chapter 4 present and analyse the specific designs for this project based on this template, while their final illustrations appear in Figures 4.13, 4.18 and 4.23.

For each concept system, the capacity of each component could be larger than the one needed for cover the electricity demand of the building. This ensures that energy flows into the Low Voltage Distribution Network continuously during the system's operation period. It is essential for the government to keep the current central power stations operational, but on base load for four reasons:

a) Electrical energy produced by the power stations should always be available in case of emergency, as it takes several hours to start and calibrate their large furnaces and generators (Prieto – Fernández et al., 1999: p. 16)

b) In the case that a concept system solution does not possess storage components, the building would need energy during night time

c) The interconnection with the network could also provide a form of backup in case the installed system is damaged or needs maintenance and

d) Components, such regulators, pumps and the system's computerized control subsystem need an independent electrical source for their operation, which this eliminates the need for electrochemical storage.

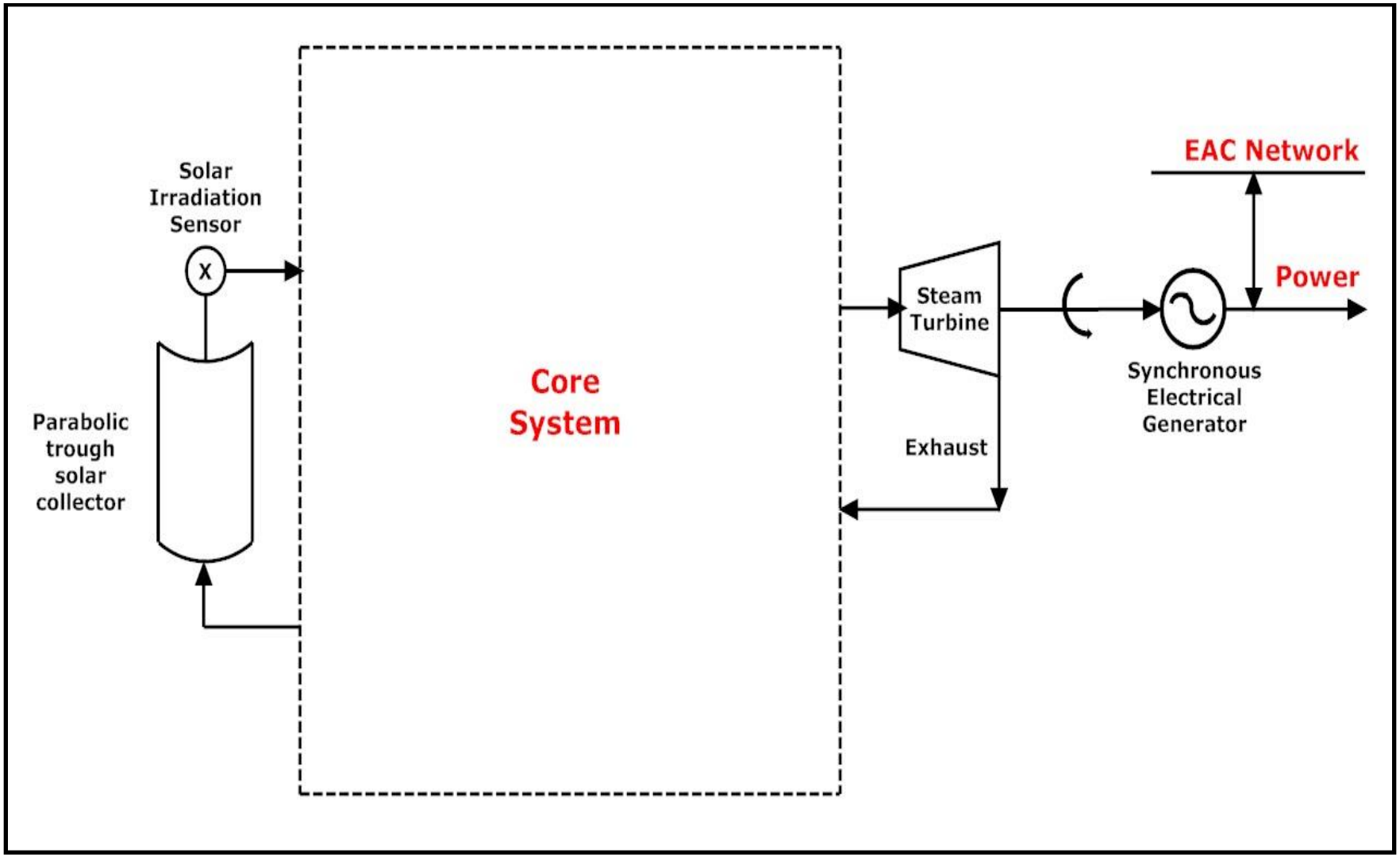

Figure 3.16: Concept system block diagram basic template

The ultimate goal is for the optimal system to render its host building as a net zero energy one, or even better, a building that produces more energy than it consumes. The extra energy would be injected directly into the local Distribution Network, so that that could be consumed by facilities that do not have the ability produce their own electricity and this would increase the capacity and stability of that network segment. An immediate consequence of this goal is the reduction or elimination of electricity bills of that building, which would shorten the investment's payback period even more. Additionally, the second and third systems would have the capability of operating in islanded mode as they are going to possess storage and a natural gas boiler, respectively, for covering the operation demand of their computerized control subsystem and other essential parts, such as pumps, regulators and sensors.

Section 3.4.2: System specifications

Before concluding this chapter, the next sections mention the host building's demand in electricity and amount of DHW for understanding the systems' constraints explained in Section 4.2.2 of Chapter 4. The systems should be capable of fully accommodating their building's electricity and hot water daily demand. At a theoretical level, the systems' component capacities are calculated in order to exactly cover that demand. However, real components that would implement the optimal system should have greater capacities than the design ones, for ensuring that the system would always be capable of feeding the electrical network with electricity. The following specifications are those which the sizing of the systems' various components is based on.

Section 3.4.2.1: Electrical power demand of the building

Beginning with the project's main function for covering the electricity demand of an individual household or apartment, the maximum specifications of the synchronous generator are shown next:

a) **20.7 kVA (about 16.6 kW)** for three-phase installations, with line voltage of **400 $V_{L\text{-}rms}$** (and phase voltage of **230 $V_{P\text{-}rms}$**) and maximum current safety fuse of **30 A_{rms}** at **50 Hz**, per individual household or per flat in the case of an apartment block and

b) **9.2 kVA (9.2 kW)** for single-phase installations, with voltage of **230 $V_{P\text{-}rms}$** and maximum current safety fuse of **40 A_{rms}** at **50 Hz** per individual household or per flat in case of retrofitting existing buildings

These features are the normal supply of electricity from the EAC for new installations. This means that if the systems are set to supply the network as well, their electrical characteristics must exactly match those of the national network (EAC, 2014). Further analysis on how to derive these feature appear in Section 4.2.2 of Chapter 4.

Section 3.4.2.2: Domestic Hot Water demand of the building:

Secondarily, the systems are designed to act as a solar water heater in addition to electricity power plants. The reason for making this adaptation is to preserve the solar water heater tradition that almost all Cypriot citizens have embraced until now. According to the EU's solar thermal and concentrated solar power barometer, Cyprus had the largest percentage of solar collector surface area per capita relative to all the other Member States of the Union in 2010 and 2013, with **0.873 m^2** and **0.837 m^2** per capita respectively (EurObserv'ER, 2011: p. 89 & 2013: p. 67). The overall and hot water demand as well as a description of hot water temperatures for various functions around the building are noted below:

a) The national average of water consumption in existing UK homes is **150 litres/person/day** (NHBC, 2011: p. 1). The British Government aims to make that consumption per person per day under **125 litres**, according to regulation 17K of The Building Regulations: Part G (HM Government, 2010: p. 15).

b) The percentage of hot water relative to the total water consumption is **32%**, which is equal to **40 – 48 litres/person/day** (NHBC, 2011: p. 2). Whittle and Warren concluded from a series of surveys in 1978 that then the average hot water consumption was **45 litres/person/day** (Whittle & Warren, 1978: p. 1). As a result, this consistency between the data in 1978 and 2011 implies that throughout the years the hot water demand in UK homes has remained relatively constant.

c) Whittle and Warren (1978: p. 1) also mention that the ideal water temperature for clothing washing machines is **80 ºC** and Oughton & Hodkinson (2008: p. 619) mentioned that dish washers require an even higher **85 ºC**, while a satisfactory temperature for bathing and hand washing is **40 ºC** (Whittle & Warren, 1978: p. 1). The main issue regarding hot water is its storage temperature, as there are concerns about the growth of the hazardous Legionella pneumophilia bacterium; it is discovered that it can rapidly multiply in domestic warm water tanks and especially in power plant cooling towers, causing the Legionnaires' Disease when steam from a hot bath, shower or a cooling tower is inhaled or by drinking water infested with the bacteria (ASSE, 2012: p. 7). Oughton and Hodkinson (2008: p. 619) mention in that at temperatures under **20 ºC** the bacteria is dormant, at temperatures between **25 ºC** and **45 ºC** the bacteria rapidly multiply, while they are instantly killed at **70 ºC** and above. These temperatures ranges are confirmed by the American Society of Sanitation Engineering (ASSE, 2012: p. 12). So, the ideal temperature for storing hot water is over **70 ºC**, as in this range the Legionella bacteria are killed and also this temperature is proximate to the operation temperature of dishwashers and clothing washing machines. However, there are also safety measures regarding hot water scalding injury that should be considered, so that the building's residents do not receive thermal burns when washing their hands or having a bath. Since the maximum shower temperature is **43 ºC** and at **68 ºC** a permanent second degree burn occurs in just one second of contact (ASSE, 2012: p. 11), the safest temperature range for storing hot water is between **55 – 65 ºC** and no less than **55 ºC**. If lower temperatures are needed, there can be mixing of hot water with cold to achieve the desired temperature (Oughton & Hodkinson, 2008: p. 619).

d) The hot water demand for appliances, such as dishwashers and clothing washing machines is included in the average daily allowance of **45 litres per person**. So, a storage calorifier or modular calorifiers that would be fitted onto the three systems should be capable of storing the amount of hot water for dish and clothing washing as well as for person washing purposes (NHBC, 2011: p. 2). The specific capacity of that calorifier is specifically calculated in Section 4.4.10 of Chapter 4.

In conclusion, this chapter covered the Thermodynamics fundamentals about the operation of a typical power plant and explained the reasons for selecting specific components to include into the modelling of the three concept systems. With this information,

the theoretical sizing and mathematical simulation of these system scenarios can begin in Chapter 4.

Reference List

Ali, Mohamed Reda Othman (2013) ***Modelling the performance of Horizontal Ground Heat Exchangers of Ground – Coupled Heat Pump Systems in Egypt*****. Ph.D. Thesis. The University of Manchester. United Kingdom.**

American Society of Sanitary Engineering (ASSE) (2012) ***Understanding Potential Water Heater Scald Hazards*****.** [Online]. Available at: http://www.asse-plumbing.org/WaterHeaterScaldHazards.pdf [Accessed: 04 February 2013].

Çengel, Y. A. & Boles, M. A. (2015) ***Thermodynamics: An Engineering Approach*****, 8th edition. New York: McGraw-Hill.**

Electricity Authority of Cyprus (EAC) (2014) ***New Supplies*** [Online]. Available at: https://www.eac.com.cy/EN/customerservice/electricitysupplyinformation/Pages/NewSupply.aspx [Accessed: 16 May 2015].

Energy Informative (2015) ***What Are the Most Efficient Solar Panels? Comparison of Mono-, Polycrystalline and Thin Film*****.** Available at: http://energyinformative.org/best-solar-panel-monocrystalline-polycrystalline-thin-film/ [Accessed: 16 May 2015]

EurObserv'ER (2011) 'Solar Thermal and Concentrated Solar Power Barometer', ***Le Journal d' Énergies Renouvelable,*** **(203), pp. 66 – 93**. [Online]. Available at: http://www.eurobserv-er.org/pdf/solar_thermal_barometer_2011.pdf [Accessed: 04 February 2013].

EurObserv'ER (2013) 'Solar Thermal and Concentrated Solar Power Barometer', ***Le Journal d' Énergies Renouvelable,*** **(215), pp. 46 – 72**. [Online]. Available at: http://www.energies-renouvelables.org/observ-er/stat_baro/observ/baro215.pdf [Accessed: 03 October 2013].

Fernández-García, A.; Zarza, E.; Valenzuela, L. & Pérez, M. (2010) 'Parabolic-trough solar collectors and their applications', ***Renewable and Sustainable Energy Reviews,*** **14, pp. 1695 – 1721**

Florides, G.; Christodoulides, P. & Pouloupatis, P. (2013a) 'Single and double U-tube ground heat exchangers in multiple – layer substrates', ***Applied Energy,*** **pp. 364 – 373**

Florides, G.; Pouloupatis, P. D.; Kalogirou, S.; Messaritis, V.; Panayides, I.; Zomeni, Z.; Partasides, G.; Lizides, A.; Sophocleous, E. & Koutsoumpas. K. (2013b) 'Geothermal properties of the ground in Cyprus and their effect on the efficiency of ground coupled heat pumps', ***Renewable Energy,*** **pp. 85 – 89.**

Fthenakis, V. M. (2012) 'Overview of Potential Dangers', in Markvart, T. & Castaner, L. (2nd ed.) ***Practical Handbook of Photovoltaics: Fundamentals and Applications*****. Elsevier, pp. 1083 - 1096.**

HM Government (2010) ***The Building Regulations, Part G (Sanitation, hot water safety and water efficiency)*****.** [Online]. Available at: http://www.planningportal.gov.uk/uploads/br/100312_app_doc_G_2010.pdf [Accessed: 02 February 2013].

Hoyle, R. & Clarke, P. H. (1973) ***Thermodynamic Cycles and Processes,*** **London: Longman Group Ltd.**

IEEE Spectrum (2014) ***Thin-film Solar Cells Freed From Toxic Processing*****.** Available at: http://spectrum.ieee.org/energywise/green-tech/solar/thin-film-solar-cell-freed-from-toxic-processing [Accessed: 03 November 2014]

Moran, M. J.; Shapiro, H. N; Boettner, D. D. & Bailey, M. B. (2011) ***Fundamentals of Engineering Thermodynamics*****, 7th edition. New Jersey: John Wiley & Sons, Inc.**

Müller, I. & Müller, W. H. (2009) ***Fundamentals of Thermodynamics and Applications*****, Berlin: Springer.**

NHBC Foundation (2011) ***Water consumption in sustainable new homes*****.** [Online]. Available at: http://products.ihs.com/cis/Doc.aspx?AuthCode=&DocNum=296746 [Accessed: 21 February 2013].

Oughton, D. R. & Hodkinson, S. L. (2008) ***Faber & Kell's Heating and Air Conditioning of Buildings*****. 10th edn.**

Prieto – Fernández, I.; Luengo – García, J. C. & Ponte – Gutiérrez, D. (1999) 'Improvements in light oil combustion by adding small quantities of alcohol. Possible application in cold starts up, in thermal power stations', ***Fuel Processing Technology*****, 60, pp. 15 – 27.**

Serway, R. A. (1990) ***Physics: For Scientists and Engineers, Volume III*****, 3rd (Greek) edition., Athens: A. Chondrorizos & Sia O.E..**

Silicon Valley Toxics Coalition (SVTC) (2009) ***Toward a Just and Sustainable Solar Energy Industry: A Silicon Valley Toxics Coalition White Paper.*** [Online]. Available at: http://svtc.org/wp-content/uploads/Silicon_Valley_Toxics_Coalition_-_Toward_a_Just_and_Sust.pdf [Accessed: 16 May 2015]

SkyFuel Inc. (2009) ***SkyTrough: Next-Generation Solar Parabolic Trough Technology*** [Online]. Available at: http://www.skyfuel.com/downloads/brochure/SkyTroughBrochure.pdf [Accessed: 16 May 2015]

Solar Direct (2015) ***Solar PV Electric: PV Battery,*** Available at: http://www.solardirect.com/pv/batteries/batteries.htm [Accessed: 16 May 2015]

Solarray Inc. (2014) ***Batteries,*** Available at: http://www.solarray.com/TechGuides/Batteries_T.php [Accessed: 02 November 2014]

SunPower (2013) ***SunPower X-Series Solar Panel Datasheet.*** [Online]. Available at: http://us.sunpower.com/sites/sunpower/files/media-library/data-sheets/ds-x21-series-335-345-residential-solar-panels-datasheet.pdf [Accessed: 05 June 2015]

SunPower (2015) ***Facts about Solar Technology from SunPower***. [Online] Available at: http://us.sunpower.com/solar-panels-technology/facts [Accessed: 16 May 2015]

Tian, Y. & Zhao, C. Y. (2013) 'A review of solar collectors and thermal energy storage in solar thermal applications', ***Applied Energy,*** **104, pp. 538 – 553.**

Whittle, G. E. & Warren, P. R. (1978) ***The efficiency of domestic hot water production out of the heating season*****. Watford: Building Research Establishment.**

Wu, D. W. & Wang, R. Z. (2006) 'Combined cooling, heating and power: A review', ***Progress in Energy and Combustion Science,*** **32, pp. 459 – 495.**

Chapter 4: Concept systems' calculations and simulation

Section 4.1: Introduction

This chapter presents and analyses the sizing calculations for the three concept systems according to the typical household's electricity and DHW demand. These results are incorporated in Chapter 5 so that the environmental impact of each one is also calculated and improvements can be proposed. It should be noted that the design and calculations of the three systems occur at theoretical level, as the creation of new technology is not the purpose of this project.

This chapter instead calculates the desired capacity of each component at a theoretical level, as several of them either do not exist in the marketplace today or their prices are not visible in the manufacturers' brochures and websites. The components include: a Steam Turbine (**ST**), Steam Accumulators (**SA**), a Parabolic Trough Solar Collectors (**PTSC**), a Calorifier and a Synchronous Electrical Generator (**SEG**).

As already mentioned, companies do not manufacture several of the needed components at the desired size. One particular example of a mass produced steam turbine coupled with an asynchronous generator, produces **75** to **300 kW_e** and costs around **215** to **260** thousand Pounds Sterling (2012 prices) for acquisition only, excluding the delivery and maintenance costs. The project needs a steam turbine capable of delivering about **20 kW_m** so it can be coupled with a synchronous generator of **20 kW_e**. Even the smallest available steam turbines, even from reliable manufacturers, exceed the specifications of the project and also they have very high prices to acquire for a single household investment. In another example of a **50 kW_m** steam turbine unit, the manufacturer does not display its price in the company's website nor in its brochures. For these reasons it was decided that the systems could be designed according to the demands of the single Cypriot household and the project would make a proposition in the discussion section of Chapter 5 for the development of new technology, so that the design of the optimal system can be realized.

Section 4.2: Concept System 1 (Direct Working Fluid Vapour Generation)

After presenting all the needed theoretical background for designing a power system in Chapter 3 the first step is the sizing of Concept System 1, which is the most generic of the three and acts as a basis for the other two. Figure 4.1 shows the schematic of this concept system and the next section describes its operation protocol. The default selection for its working fluid is water/steam as this the working fluid of the classic Rankine cycle.

Section 4.2.1: Operation protocol

This system is characterized by the fact that it produces steam by directly utilizing solar energy, otherwise known Direct Steam Generation (**DSG**). The operation protocol of this concept, which is stored and executed by a Computerised Control Subsystem (**CCS**) (not shown in any of the designs), is the following: When the Solar Irradiation Sensor (**SIS**) gets a reading that the Parabolic Trough Solar Collector (**PTSC**) is receiving sufficient solar energy (or turns on), it sends a signal to the CCS to activates the Condensate Pump (**CP**). It starts sending liquid water from the Condensate Storage Tank (**CStT**) through the PTSC, while simultaneously pressurising it to the desired pressure level. The water is then vaporized into pressurized saturated steam and it is stored inside the Steam Accumulator (**SA**), acting both as a steam storage tank and a buffer, until the Steam Flow Regulator (**SFR**) turns on, informing the CCS that there is sufficient quantity of steam for feeding the Steam Turbine (**ST**). Then the CCS commands the SFR for allowing steam to enter the ST's inlet at the designated flow rate and thus turning the shaft of the ST to drive the Synchronous Electrical Generator (**SEG**) for producing the needed electrical power output, calculated in Section 4.2.2. The depressurized steam exits the ST's outlet and reaches the three way Bypass Valve (**BV**); in this stage the CCS monitors the temperature of the water stored in the Storage Tank (**StT**) and if that is lower than the storage temperature mentioned in Section 4.2.2, the CCS commands the BV to allow steam to pass through the heating coil of the DHW StT until the stored water reaches the desired temperature. When that happens or if the water is already at the correct storage temperature the CCS commands the BV to resume its default position, diverting steam into the Steam Separator (**SS**) through the **T-connector**. Here, the steam is separated from any condensate derived from the water heating cycle and it reaches the **Condenser** where it is completely liquefied back into saturated condensate and stored inside

the CStT, while the separated condensate bypasses the condenser and arrives to the CStT to be stored as well. This protocol is schematically presented in the flowchart in Figure 4.2.

Section 4.2.2: Household electricity and DHW demand profile

The sizing procedure begins with design decisions about the purpose and functionality of Concept System 1. Firstly, the designing steps of a steam power plant based on the Rankine cycle that were used in this particular project are listed and analysed below:

1. **Determine the desired power output of the system**: In order to determine the desired electrical power output of Concept System 1, crucial information from the Electricity Authority of Cyprus (EAC) needs to be examined. The system is designed to produce three-phase electrical power and the way to calculate the desired electrical power output of the SEG is by using the following equation and the information from EAC regarding this issue (EAC, 2014):

$$\dot{W}_{el} = \sqrt{3} U_{Lrms} I_{Lrms} \cos\varphi$$

Equation 4.1: Electrical power demand per household in Cyprus

Property name	Property	Units	Value
Supply line voltage	U_{Lrms}	V_{rms}	400
Maximum allowed 3-phase current consumption	I_{Lrms}	A_{rms}	30
AC power factor	$\cos\varphi$	---	0.8
Maximum electricity demand	$\dot{W}_{el}$	**kW**	**16.6**

Table 4.1: Calculation of the electricity demand per household in Cyprus (EAC, 2014)

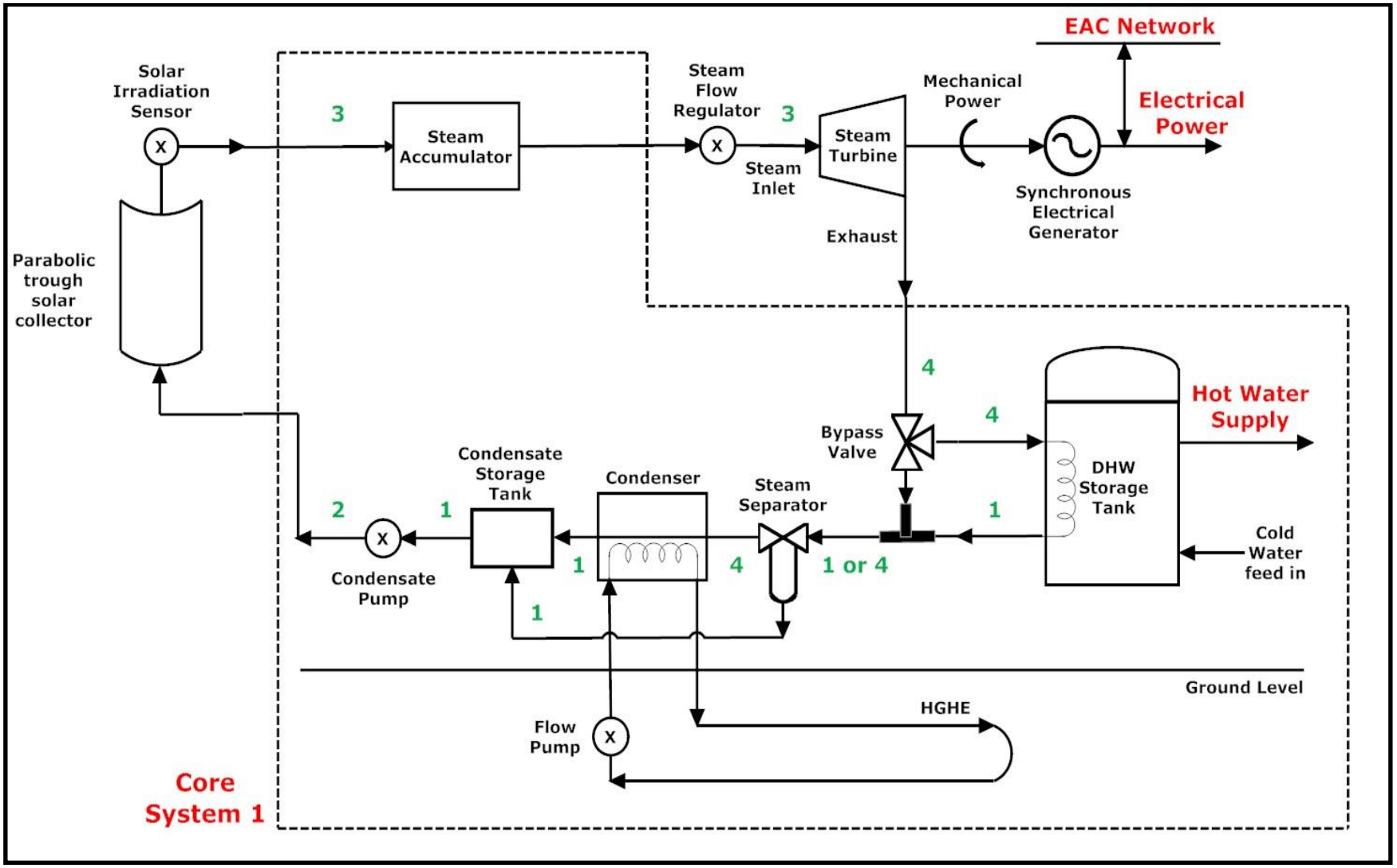

Figure 4.1: Concept System 1 (numbers in green indicate the state of the working fluid)

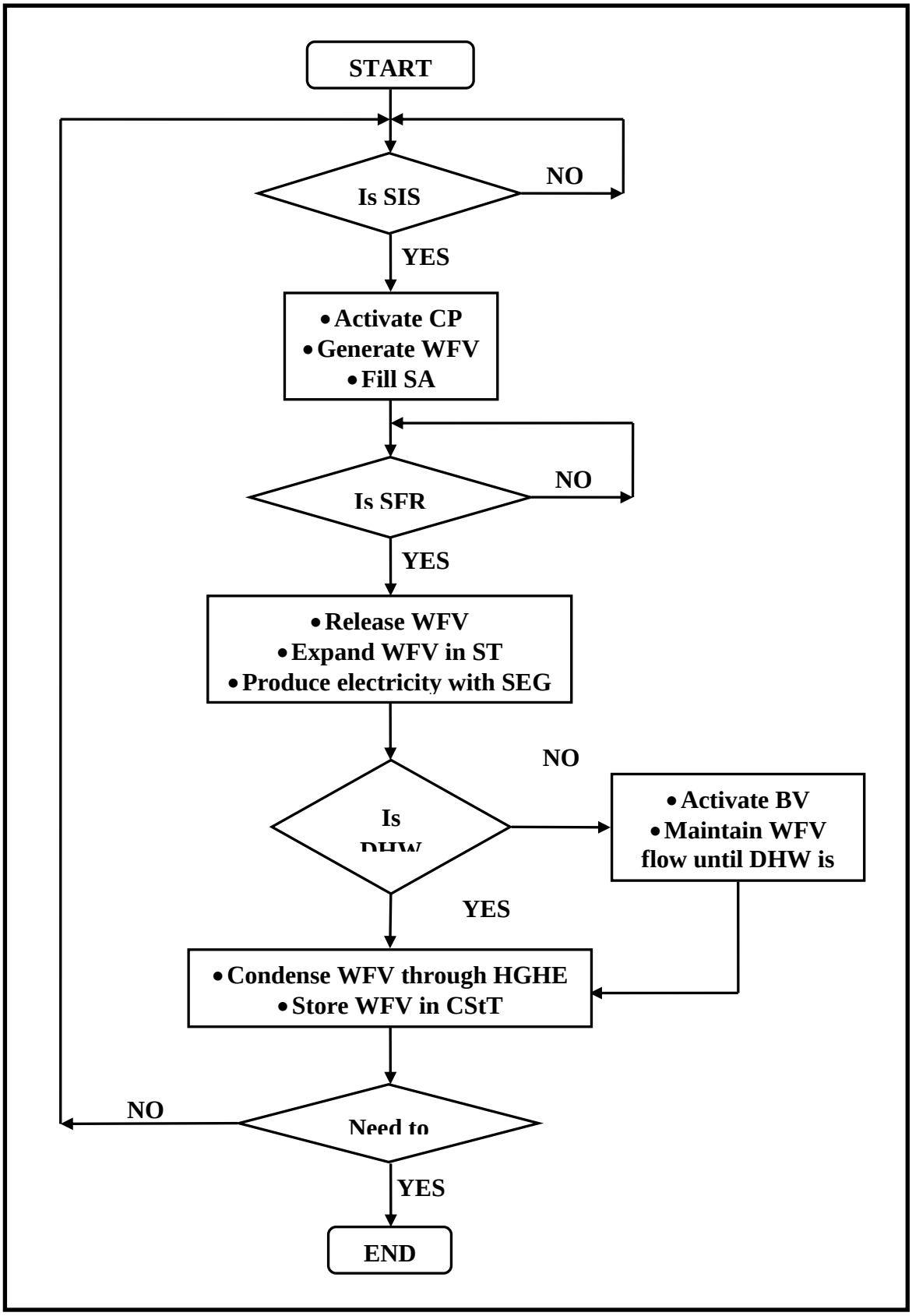

Figure 4.2: Flowchart of Concept System 1's operation protocol

For convenience reasons and also for rendering the system capable to continuously feed the national network, the desired power output of Concept System 1 is set to **20 kW**.

2. **Determine the higher and lower pressure levels of the working fluid**: As mentioned in Chapter 3, the net amount of work involved in the cycle is represented by the area under the cycle's curve on the T-s diagram, as seen in Figure 3.11. Additionally, the power input requirements of the condensate pump in the case of the Rankine cycle is negligible; this is also proven by the simulation results in Tables 4.2, 4.3 and 4.4. So the area enclose by the curve is with good approximation of the cycle's work output. Moreover, the work output is proportional to that area, in other words the larger the enclosed area the greater the work output of the cycle.

a) Firstly, the **lower pressure level** of states **1** and **4** in Figure 4.1 (**P_1 = P_4**) (the state of the working fluid at every point is indicated by the green number in Figure 4.1) needs to be set. This level has to be as low as possible, while the higher pressure level should be as high as possible in order to have a cyclic process with the greatest enclosed area on the T-s diagram. In addition, the working fluid at this pressure level should have a saturation temperature (boiling/condensation point) high enough for it to raise the DHW's temperature up to **60 ºC**. As an initial value for this project's calculations, P_1 is arbitrarily set as the atmospheric pressure [**P_1 = 1 bar (a)**].

b) The **higher pressure level** of states **2** and **3** as in Figure 4.1 (**P_2 = P_3**) is the one that must be defined next. In order to find the optimal level for this pressure, a trial simulation was executed by using the Engineering Equation Solver (EES) software package. The simulation used increasing pressure level intervals from **2** to **9 bar (a)**, keeping the lower pressure level constant and the results are shown in Table 4.2. To determine the optimal higher pressure level, since the work output of the cycle is constant at **20 kW**, the optimization criterion becomes the increase of efficiency, as the pressure increases. The first constraint for this value is that the specific entropy of the working fluid at state **3** needs to be equal with the one of state **4**, in other words at the saturation vapour temperature of the working fluid (**s_3 = s_4**). The second constraint is that the temperature at state **3** must be under **400 ºC**, as this the maximum capability of the PTSC.

3. **Acquire the specific enthalpies of states 3 & 4 and calculate the circuit's mass flow rate**: After browsing a steam table or the website of Spirax – Sarco Ltd. (2014), the specific enthalpy values of states **3** and **4** are acquired for each parametric value of the higher pressure level and then the system's mass flow rate $\dot{\mathbf{m}}$ is calculated, by using the Equation 3.9(3). The results are shown on the respective column of Table 4.2.

4. **Calculate the other three heat and work rates**: With the mass flow rate value available, the rest of the cycle's power values can very easily be calculated, as the specific enthalpy values of the other two states are acquired with the exact same way as the previous two. So, the values of heat absorption rate $\dot{\mathbf{Q}}_{\mathbf{B}}$, heat rejection rate $\dot{\mathbf{Q}}_{\mathbf{C}}$ and power consumption of the pump $\dot{\mathbf{W}}_{\mathbf{P}}$ are being determined.

5. **Determine the efficiency factor of the cycle**: Lastly, the cycle's efficiency is calculated by using the Equation 3.9(5). One can observe from the table that as the higher pressure level is increasing and since the turbine's power output is constant, the efficiency of the cycle also increases. Mathematically this means that the input of heat is decreasing, which can be proven by noticing the actual decreasing values of $\dot{\mathbf{Q}}_{\mathbf{B}}$. Additionally the input power requirement of the condensate pump is indeed very small compared to the work output of the cycle. More specifically, from the simulation data of Table 4.2 it can be observed that $\dot{\mathbf{W}}_{\mathbf{P}}$ is about **500** to **700** times smaller than $\dot{\mathbf{W}}_{\mathbf{T}}$, rendering it practically zero.

As the notion of increasing the higher pressure level confirms the increase of efficiency, the next step is the trial of reducing the lower pressure level below the atmospheric pressure. For this purpose Table 4.3 was constructed in a similar way as Table 4.2; however in this table the higher pressure level was kept constant at **9 bar (a)** and the simulation was made by decreasing the lower pressure level as the parameter of the table. The constraints are that the cycle's highest temperature again needs to be under **400 ºC** and that its lowest temperature (in this case the lower pressure level's saturation temperature) needs to be greater or equal to **60 ºC**, as the working fluid is set to be used to heat up the DHW supply. If the lowest temperature would have been under **60 ºC** then the system would not had been capable of heating the DHW up to that design temperature.

The progression of data in Table 4.3 also confirm that by reducing the lower pressure level while keeping the higher pressure level constant, the efficiency of the cycle increases. The table also indicates in red the optimal settings for this system's cycle; the optimal efficiency is about **20%**, the highest superheated steam temperature of state **3** is about **390 ºC** and the lowest steam saturation temperature of state **4** is **90 ºC**, at **0.7 bar (a)**. Another reason why these settings are the optimal ones within the constraints is that if the higher pressure level was to be increasing by **1 bar** and the lower pressure level by **0.1 bar** simultaneously, as shown in Table 4.4, the cycle's efficiency remains the constant, while the pump's power consumption increases and the superheated steam temperature of state **3** increases marginally towards the **400 ºC** limit.

Section 4.3: Optimizing the water based Rankine Cycle

Section 4.3.1: Increasing the higher pressure level to 20 bar (a)

As discussed in Section 3.1.4, the Rankine cycle is a very well understood power cycle and it is most commonly used in the electricity production industry. The main cycle has remained unchanged throughout the years and the various types of power stations differ from one another only on the type of fuel used to heat the working fluid to the desired temperature. Additionally, the most common working fluid used for this cycle is water, as it is abundant, cheap and thoroughly studied since the 1800s. Its thermodynamic properties are available in every textbook about Thermodynamics, along with other commonly used fluids such as ammonia (**NH_3**) and various refrigerants (**R-134a**, **R-22** & propane) so anyone interested in the topic can easily acquire those data. Examples of such steam tables in textbooks are found in (Çengel & Boles, 2015: pp. 904 – 915), (Moran et al., 2011: pp. 891 – 900) & (Avallone et al. 2007: pp. 4-45 – 4-50).

	T_1	P_1	h_1	s_1	T_2	P_2	h_2	s_2	T_3	P_3	h_3	s_3	T_4	P_4	h_4	s_4	$\dot{W}_T$	$\dot{m}$	$\dot{Q}_B$	$\dot{Q}_C$	$\dot{W}_P$	η
Run 1	100	1	417.55	1.303	100	2	417.73	1.303	167	2	2803	7.359	100	1	2675	7.359	20	1.56 $x10^{-1}$	372.7	352.7	2.81 $x10^{-2}$	5.4
Run 2	100	1	417.55	1.303	100	3	417.84	1.303	211	3	2888	7.359	100	1	2675	7.359	20	9.39 $x10^{-2}$	231.9	212.0	2.68 $x10^{-2}$	8.6
Run 3	100	1	417.55	1.303	100	4	417.94	1.303	245	4	2954	7.359	100	1	2675	7.359	20	7.17 $x10^{-2}$	181.8	161.8	2.79 $x10^{-2}$	11.0
Run 4	100	1	417.55	1.303	100	5	418.04	1.303	273	5	3008	7.359	100	1	2675	7.359	20	6.01 $x10^{-2}$	155.6	135.6	2.97 $x10^{-2}$	12.8
Run 5	100	1	417.55	1.303	100	6	418.15	1.303	297	6	3054	7.359	100	1	2675	7.359	20	5.28 $x10^{-2}$	139.1	119.1	3.16 $x10^{-2}$	14.4
Run 6	100	1	417.55	1.303	100	7	418.25	1.303	317	7	3095	7.359	100	1	2675	7.359	20	4.76 $x10^{-2}$	127.5	107.5	3.34 $x10^{-2}$	15.7
Run 7	100	1	417.55	1.303	100	8	418.36	1.303	336	8	3131	7.359	100	1	2675	7.359	20	4.39 $x10^{-2}$	119.0	99.0	3.54 $x10^{-2}$	16.8
Run 8	100	1	417.55	1.303	100	9	418.46	1.303	352	9	3164	7.359	100	1	2675	7.359	20	4.09 $x10^{-2}$	112.3	92.3	3.73 $x10^{-2}$	17.8

Table 4.2: Parametric Table for calculating the optimal higher pressure level with lower pressure level of 1 bar(a)

	T_1	P_1	h_1	s_1	T_2	P_2	h_2	s_2	T_3	P_3	h_3	s_3	T_4	P_4	h_4	s_4	$\dot{W}_T$	$\dot{m}$	$\dot{Q}_B$	$\dot{Q}_C$	$\dot{W}_P$	η
Run 1	100	1	417.55	1.303	100	9	418.46	1.303	352	9	3164	7.359	100	1	2675	7.359	20	4.09 $x10^{-2}$	112.3	92.3	3.74 $x10^{-2}$	17.8
Run 2	97	0.9	405.24	1.27	97	9	406.21	1.27	363	9	3186	7.394	97	0.9	2671	7.394	20	3.88 $x10^{-2}$	108.0	88.0	3.77 $x10^{-2}$	18.5
Run 3	94	0.8	391.74	1.233	94	9	392.58	1.233	374	9	3211	7.433	94	0.8	2665	7.433	20	3.66 $x10^{-2}$	103.2	83.3	3.05 $x10^{-2}$	19.4
Run 4	**90**	**0.7**	**376.78**	**1.192**	**90**	**9**	**377.61**	**1.192**	**389**	**9**	**3241**	**7.479**	**90**	**0.7**	**2660**	**7.479**	**20**	**3.44 $x10^{-2}$**	**98.6**	**78.6**	**2.86 $x10^{-2}$**	**20.3**
Run 5	86	0.6	359.94	1.145	86	9	360.64	1.145	405	9	3276	7.531	86	0.6	2653	7.531	20	3.21 $x10^{-2}$	93.6	73.6	2.25 $x10^{-2}$	21.4
Run 6	81	0.5	340.58	1.091	81	9	341.37	1.091	425	9	3319	7.593	81	0.5	2645	7.593	20	2.97 $x10^{-2}$	88.4	68.4	2.36 $x10^{-2}$	22.6

Table 4.3: Parametric Table for calculating the optimal lower pressure level with higher pressure level of 9 bar(a)

	T_1	P_1	h_1	s_1	T_2	P_2	h_2	s_2	T_3	P_3	h_3	s_3	T_4	P_4	h_4	s_4	$\dot{W}_T$	$\dot{m}$	$\dot{Q}_B$	$\dot{Q}_C$	$\dot{W}_P$	η
Run 1	**90**	**0.7**	**376.78**	**1.192**	**90**	**9**	**377.61**	**1.192**	**389**	**9**	**3241**	**7.479**	**90**	**0.7**	**2660**	**7.479**	**20**	**3.44 x10^{-2}**	**98.5**	**78.5**	**2.85 x10^{-2}**	**20.3**
Run 2	94	0.8	391.74	1.233	94	10	392.68	1.233	390	10	3243	7.434	94	0.8	2665	7.434	20	3.46 x10^{-2}	98.7	78.7	3.25 x10^{-2}	20.2
Run 3	98	0.9	405.24	1.270	98	11	406.41	1.270	392	11	3245	7.394	98	0.9	2671	7.394	20	3.48 x10^{-2}	98.8	78.8	4.07 x10^{-2}	20.2
Run 4	100	1.0	417.55	1.303	100	12	418.77	1.303	394	12	3248	7.359	100	1.0	2675	7.359	20	3.49 x10^{-2}	98.7	78.8	4.26 x10^{-2}	20.2
Run 5	102	1.1	428.89	1.333	102	13	430.10	1.333	396	13	3251	7.327	102	1.1	2679	7.327	20	3.50 x10^{-2}	98.7	78.7	4.23 x10^{-2}	20.2
Run 6	105	1.2	439.42	1.361	105	14	440.76	1.361	399	14	3254	7.298	105	1.2	2683	7.298	20	3.50 x10^{-2}	98.5	78.6	4.69 x10^{-2}	20.2
Run 7	107	1.3	449.25	1.387	107	15	450.72	1.387	400	15	3257	7.271	107	1.3	2687	7.271	20	3.51 x10^{-2}	98.4	78.5	5.16 x10^{-2}	20.3

Table 4.4: Parametric Table for calculating the optimal lower pressure level with higher pressure level of 9 bar(a)

Symbol	Quantity	Units
T	Temperature	ºC
P	Pressure	Pa
h	Specific Enthalpy	kJ/kg
s	Specific Entropy	kJ/kg-K
$\dot{W}_T$	Turbine Power Output	kW
$\dot{m}$	Working Fluid Mass Flow Rate	kg/s
$\dot{Q}_B$	Heat Power Input	kW
$\dot{Q}_C$	Heat Power Output	kW
$\dot{W}_P$	Pump Power Input	kW
η	Efficiency Factor	%

Table 4.5: Presentation of the variables used for the calculations and their measurement units

This is the reason why the first working fluid tested for this project's optimal system solution was water. Mentioning this and in addition to the already presented data, Table 4.6 presents a fourth set of simulation results in which the lower pressure level along with the maximum and minimum temperatures are kept constant while the higher pressure level is progressively increased from **9** to **20 bar(a).** This is done to test if any improvement upon the cycle's efficiency can be achieved. Moreover, since the two temperatures are constant the Carnot efficiency is also constant at about **45%**. As expected, the ideal Rankine cycle efficiency also improves as the pressure increases, reaching almost **25%** in the last run. This table also contains the dryness fraction or steam quality $\mathbf{x_4}$ of state **4** that indicates the steam's mass proportion that has been condensed back into saturated water during the turbine expansion. It is clear that as the maximum temperature of steam is kept constant, by increasing the pressure of water its entropy is slightly decreased. Nevertheless, the dryness fraction does not become less than **93%**, which is completely tolerable and above to the standard **90%** for protecting the turbine's blades (Moran et al., 2011: p. 447).

The system can be further improved by keeping the higher pressure level at the maximum **20 bar (a)** and lowering the lower pressure level progressively by **0.1 bar** decrements from **0.7** to **0.2 bar (a)**. These final results appear in Table 4.7 and the optimal set of data require the higher and lower pressure levels to be **20** to **0.4 bar(a)** respectively. Any lower values of the lower pressure level and the steam quality at state **4** ($\mathbf{x_4}$) drops to values less than or equal to the standard **90%** limit. With these conditions, the ideal efficiency of the cycle increased by just about **1%**, which is not a significant amount of improvement.

For large scale Rankine cycle applications, with high temperature (**530** – **585 ºC**) and pressure levels values (**130** – **165 bar**) (Siemens A.G., 2011: p. 8), water has been throughout time the dominant working fluid. However, researchers turned their attention to organic fluids for applications of smaller scale and specifications. Such applications include heat recovery or renewable energy power plants, which have temperature and pressure ranges well below the mentioned limits. As seen from Tables 4.6 and 4.7, this project's specifications dictate that the maximum temperature of the cycle should not be above **400 ºC**, as this is the maximum capability of PTSCs. Respectively, the minimum temperature should be above **60 ºC**, so that the fluid itself is capable of raising the temperature of DHW up to that specific level. As a consequence the lower pressure level cannot be below **0.2 bar (a)**, while the

higher pressure level cannot be over **20 bar (a)** for safety reasons. Within these parameters, a Rankine cycle with water as its working fluid could only achieve an efficiency of **25.6%** under ideal conditions. In other words assuming that all components have **100%** energy transfer/conversion efficiency, the highest achievable overall cycle efficiency (using water as the working fluid) for the size of Concept System 1 is about **26%**.

	T_1	P_1	h_1	s_1	T_2	P_2	h_2	s_2	T_3	P_3	h_3	s_3	T_4	P_4	h_4	s_4	x_4	$\dot{W}_T$	$\dot{m}$	$\dot{Q}_B$	$\dot{Q}_C$	$\dot{W}_P$	η
Run 1	90	0.7	377.0	1.193	90	9	378.0	1.193	390	9	3244	7.484	90	0.7	2661	7.484	1.000	20	3.43 x10^{-2}	98.2	78.3	3.45 x10^{-2}	20.3
Run 2	90	0.7	377.0	1.193	90	10	378.1	1.193	390	10	3243	7.433	90	0.7	2642	7.433	0.992	20	3.33 x10^{-2}	95.4	75.5	3.70 x10^{-2}	20.9
Run 3	90	0.7	377.0	1.193	90	12	378.3	1.193	390	12	3239	7.345	90	0.7	2611	7.345	0.978	20	3.18 x10^{-2}	91.0	71.0	4.19 x10^{-2}	21.9
Run 4	90	0.7	377.0	1.193	90	14	378.5	1.193	390	14	3236	7.270	90	0.7	2583	7.270	0.966	20	3.06 x10^{-2}	87.5	67.6	4.67 x10^{-2}	22.8
Run 5	90	0.7	377.0	1.193	90	16	378.7	1.193	390	16	3232	7.205	90	0.7	2559	7.205	0.956	20	2.97 x10^{-2}	84.8	64.9	5.15 x10^{-2}	23.5
Run 6	90	0.7	377.0	1.193	90	18	378.9	1.193	390	18	3229	7.146	90	0.7	2538	7.146	0.946	20	2.89 x10^{-2}	82.5	62.5	5.61 x10^{-2}	24.2
Run 7	90	0.7	377.0	1.193	90	20	379.1	1.193	390	20	3226	7.094	90	0.7	2519	7.094	0.938	20	2.83 x10^{-2}	80.6	60.6	6.08 x10^{-2}	24.7

Table 4.6: Parametric Table for calculating the ideal efficiency increase by increasing the higher pressure level from 9 to 20 bar (a)

	T_1	P_1	h_1	s_1	T_2	P_2	h_2	s_2	T_3	P_3	h_3	s_3	T_4	P_4	h_{4s}	s_{4s}	s_{4g}	x_4	$\dot{W}_T$	$\dot{m}$	$\dot{Q}_B$	$\dot{Q}_C$	$\dot{W}_P$	η
Run 1	90	0.7	376.97	1.193	90	20	379.12	1.193	390	20	3226	7.094	90	0.7	2519	7.094	7.484	0.938	20	2.83 $x10^{-2}$	80.6	60.6	6.08 $x10^{-2}$	24.7
Run 2	86	0.6	359.94	1.145	86	20	379.12	1.193	390	20	3226	7.094	86	0.6	2495	7.094	7.531	0.932	20	2.74 $x10^{-2}$	78.0	58.5	5.25 $x10^{-1}$	25.0
Run 3	81	0.5	340.58	1.091	81	20	379.12	1.193	390	20	3226	7.094	81	0.5	2468	7.094	7.593	0.923	20	2.64 $x10^{-2}$	75.1	56.1	1.02	25.3
Run 4	**76**	**0.4**	**317.67**	**1.026**	**76**	**20**	**379.12**	**1.193**	**390**	**20**	**3226**	**7.094**	**76**	**0.4**	**2435**	**7.094**	**7.669**	**0.913**	**20**	**2.53 $x10^{-2}$**	**72.0**	**53.5**	**1.55**	**25.6**
Run 5	69	0.3	289.33	0.944	69	20	379.12	1.193	390	20	3226	7.094	69	0.3	2393	7.094	7.767	0.901	20	2.40 $x10^{-2}$	68.4	50.6	2.16	26.1
Run 6	60	0.2	251.50	0.832	60	20	379.12	1.193	390	20	3226	7.094	60	0.2	2337	7.094	7.907	0.885	20	2.25 $x10^{-2}$	64.1	47.0	2.87	26.7

Table 4.7: Parametric Table for calculating the ideal efficiency increase by decreasing the lower pressure level from 0.7 to 0.2 bar (a)

Section 4.3.2: Usage of Internal Heat Exchangers (IHE)

Section 4.3.2.1: Introduction

The previous section presents the overall efficiency calculation of a small scale, water based Rankine cycle for domestic usage under ideal thermodynamic conditions. However, in reality the operation conditions are not ideal and energy is lost due to the components' irreversibilities. A great example is the ST that is expected to expand the working fluid isentropically for complete conversion of thermal energy into mechanical. Instead, the actual turbine expansion increases the entropy of the working fluid due to irreversibilities occurring during the expansion. This issue is graphically presented in Figure 4.3 (Moran et al., 2011: p. 322).

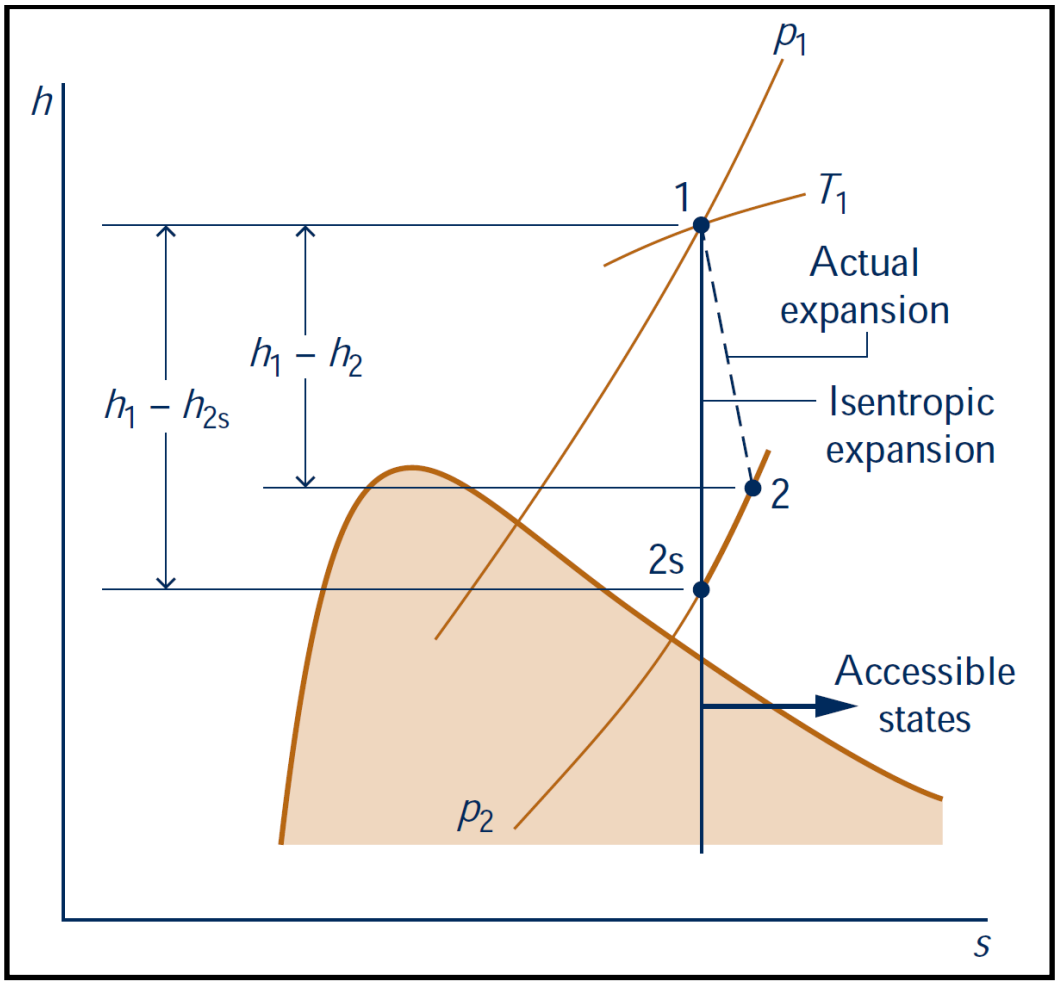

Figure 4.3: h-s diagram of isentropic vs. actual working fluid expansion of turbine (Moran et al., 2011: p. 322)

In this figure, the isentropic expansion is shown in the h-s diagram from state **1** to **2s** and the actual expansion from state **1** to **2**. It becomes clear that the isentropic expansion offers a greater efficiency factor than the actual expansion, as the energy difference $\mathbf{h_{2s} - h_1}$ extracted from the turbine is greater than the difference $\mathbf{h_2 - h_1}$, while the energy spent in raising the working fluid to state **1** is constant. However, this fact could become an advantage by adding only one more component, a simple HE. With this addition, the thermal energy difference between states **2** and **2s** that the condenser would extract from the fluid and essentially wasting it, would be injected back into the fluid.

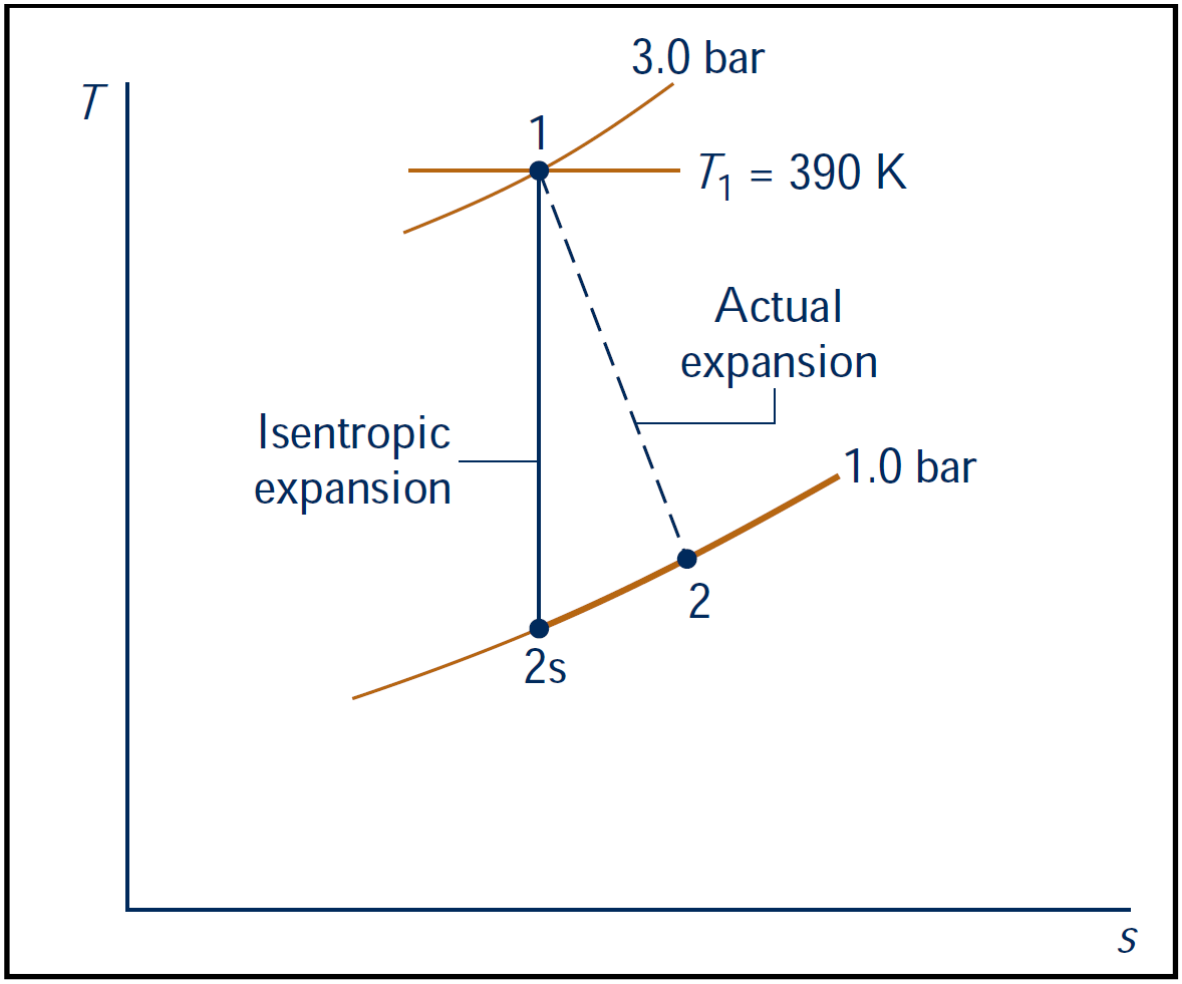

Figure 4.4: T-s diagram of isentropic vs. actual working fluid expansion example of turbine (Moran et al., 2011: p. 324)

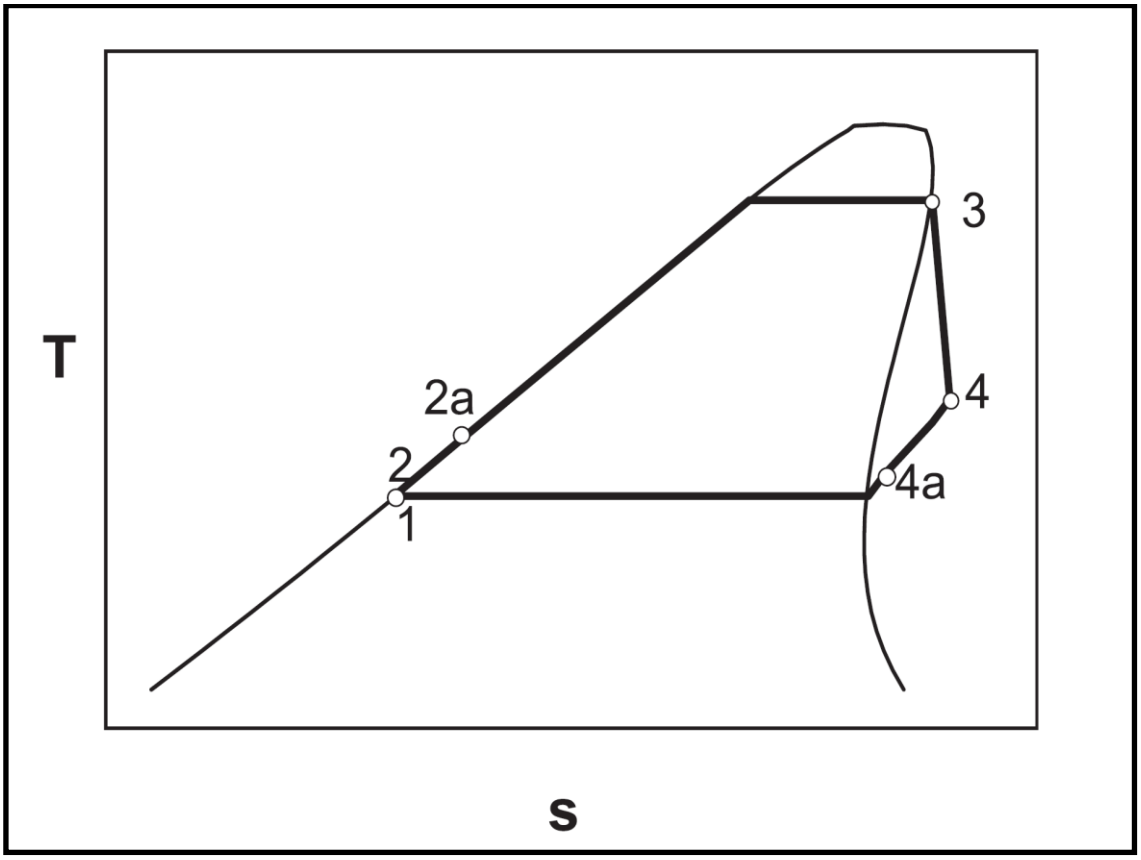

Figure 4.5: T-s diagram of an actual Rankine cycle using an IHE (Lai et al., 2011: p. 201)

In Figure 4.4 (Moran et al., 2011: p. 324) this issue is presented in a T-s diagram, which shows that state **2** also has a higher temperature as well relative to state **2s**, which means that the injected energy would raise the temperature of the working fluid at the level of that of state **2**. The complete illustration of the IHE operation can be seen in Figure 4.5 (Lai et al., 2011: p. 201). Here the actual turbine expansion is shown to occur from state **3** to state **4**, while the IHE transfers the energy difference between states **4** and **4a** to the portion of the curve between states **2** and **2a**. As a result, the fuel needed to be spent for raising the temperature of the cycle from state **2a** to **3** becomes less than the amount needed if boiling began from state **2**. Additionally in this project, point **4a** is actually on the saturation line while state **4** and **2a** are at about the same temperature. The basic hardware configuration of an IHE in a Rankine cycle, corresponding to Figure 4.5, is shown in Figure 4.6 (Lai et al., 2011: p. 201).

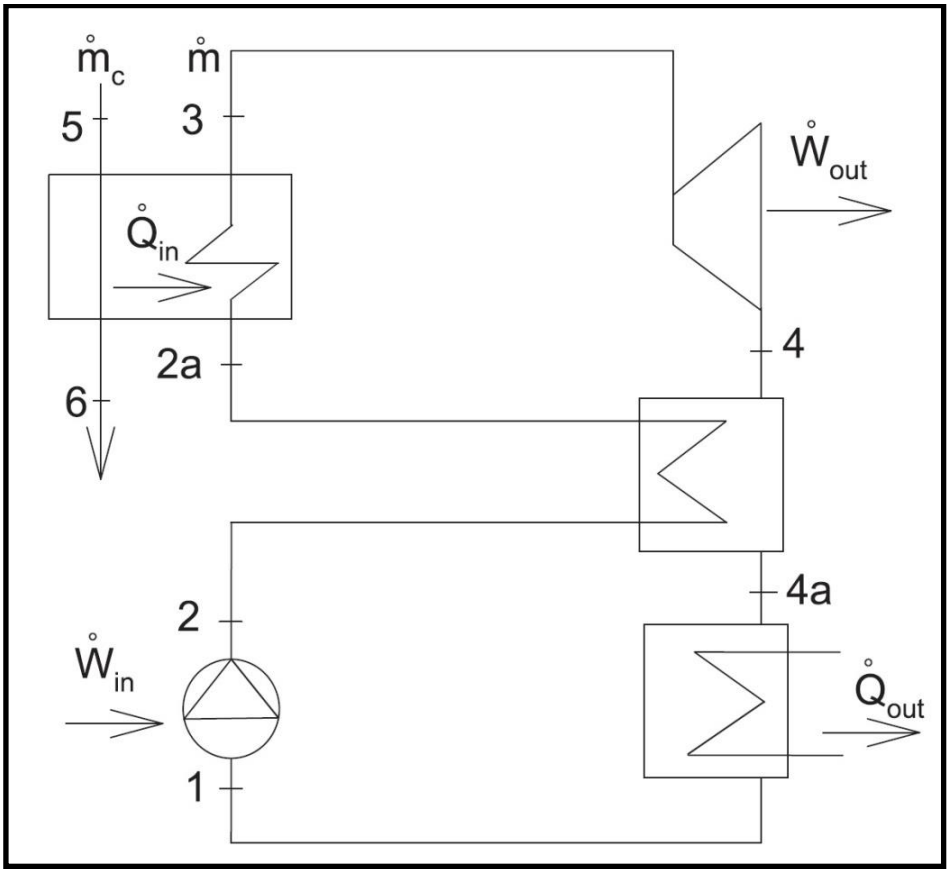

Figure 4.6: Configuration of a Rankine cycle plant with an IHE (Lai et al., 2011: p. 201)

In Figure 4.6, the already expanded working fluid at state **4** enters the primary circuit of the IHE and exits at state **4a** and after passing through the condenser and pump; it receives the extracted energy difference $\mathbf{h_4 - h_{4a}}$ by entering the secondary circuit of the IHE at state **2** and exits at the thermally higher **2a** state. The boiler then only needs to cover the smaller energy difference $\mathbf{h_3 - h_{2a}}$ instead of $\mathbf{h_3 - h_2}$ and therefore the needed amount of energy by the boiler is reduced by the amount $\mathbf{h_4 - h_{4a}}$ of waste heat. Such an analysis has been conducted for a regular water Rankine cycle based on the optimal data of Table 4.8 seen in red and it is presented in Section 4.3.2.4.

Section 4.3.2.2: Components' efficiency factors

Before Concept System 1's efficiency improvement analysis is explained, this section presents the typical values of each component's efficiency factor. This will assist the calculation of the non-ideal overall cycle efficiency both with and without the IHE. Moreover, these efficiency values are conservative for each component in order for the

resultant cycle efficiency that is calculated is a good representation of the minimum efficiency capability of the cycle.

1. Turbine Efficiency ($\boldsymbol{\eta_T}$)

Large scale steam turbines (ST), according to Moran et al. (2011: p. 323) and Çengel & Boles (2015: p. 367) have an isentropic efficiency of about **90%**, while smaller turbines have efficiency factors well below **70%**. The definition of an ST's efficiency factor is the one shown in Equation 4.2 (Çengel & Boles, 2015: p. 368):

$$\boldsymbol{\eta_T = \frac{h_3 - h_4}{h_3 - h_{4s}}}$$

Equation 4.2: Efficiency factor of steam turbines (Çengel & Boles, 2015: p. 368)

where $\mathbf{h_3}$ is the specific enthalpy of the fluid (in this case water) at the inlet of the turbine, $\mathbf{h_4}$ is the specific enthalpy of the fluid resulting after an actual (non-ideal) expansion as shown in Figures 4.2 and 4.3, while $\mathbf{h_{4s}}$ is the isentropic (ideal) expansion specific enthalpy of the working fluid at the turbine's outlet, all of them measured in **kJ/kg**.

The smallest turbines today have a capability of producing up to **110 kW** (Siemens A.G., 2013: p. 3), an energy production rate far greater than the specifications of this project. Therefore, a small size ST of around **20 kW** is yet to be available commercially; however it is confidently possible for such turbines to be designed in the future for the following reasons:

a) The (isentropic) efficiency factor of an ST is dependent on its irreversibilities, which cause the steam's entropy to increase during the expansion process, rather than remain constant. Firstly, the operation of the turbine should occur adiabatically, so that the energy difference between $\mathbf{h_3}$ and $\mathbf{h_{4s}}$ is converted completely into the useful power. In reality, there is thermal leakage from the turbine's expansion chamber through its casing into the ambient surroundings. As material engineering is constantly evolving, it would be no surprise if new and more effective insulating compounds are developed and placed on the turbine casing's envelope. In this way, less thermal energy would escape to the environment, thus improving the isentropic efficiency.

b) Another serious irreversibility is cause by friction between the turbine's moving parts and its stator and also between steam and the turbine's blades, causing the undesirable loss of thermal energy leading to an increase of state **4s**'s entropy. Material Science and Mechanical Engineering can also contribute in reducing these irreversibilities by developing almost frictionless rotor bearings containing special lubrication for this purpose. In addition, smaller turbines have lighter components and so since the rotor's weight would be smaller than today's models, friction between it and the stator would also be smaller. Lastly, turbine blade technology could also be improved for producing components with smoother surfaces, hence reducing the friction between steam and the blades.

Assuming that a **20 kW** ST is to be designed in the future, according to the above reasons it could be confidently stated that its efficiency factor could well be at **70%**.

2. PTSC Efficiency ($\boldsymbol{\eta_B}$)

A typical value for the efficiency of a Parabolic Trough Solar Collector (PTSC) can easily be found in existing product brochures. Specifically, a graph of the thermal efficiency of SkyTrough by SkyFuel® vs. temperature (2010) gives an approximate value of **71%** at **400 ºC** for direct normal incident radiation. These data are also supported by the National Renewable Energy Laboratory (NREL) report of Kutscher et al. (2010: p. 2), presenting the overall efficiency of the SkyTrough collector vs. the difference between operation and ambient temperatures under three direct normal radiation values: **1000**, **800** and **600** W/m^2. For the reasons above, the conservative value of **70%** is taken here as well.

3. Feed Pump Efficiency ($\boldsymbol{\eta_P}$)

For the issue of feed pump efficiency, Moran et al. (2011: p. 328) do not mention any typical values explicitly. At that page they only mention that a compressor's typical efficiency is around **75** to **100%** and also define that efficiency as seen in Equation 4.3:

$$\eta_{com} = \frac{h_{2s} - h_1}{h_2 - h_1}$$

Equation 4.3: Efficiency Factor of Compressors

where $\mathbf{h_1}$ is the specific enthalpy of the fluid at the compressor's inlet, $\mathbf{h_{2s}}$ is the isentropic (ideal) compression specific enthalpy of the fluid at the exiting the compressor while $\mathbf{h_2}$ is the specific enthalpy of the fluid after an actual compression, again measured in **kJ/kg**. However, they do mention that a pump's efficiency follows the same law. Additionally, Moran et al. (2011: p. 353, 415 – 416, 477 – 478, 581) and Çengel & Boles (2011: pp. 592 – 594) mention a range of pumps' efficiency to be between **75** and **100%** all over their textbooks in examples and exercises for the reader. So, the conservative value of feed pump efficiency can be taken as **75%**; however the contribution of the pump's energy requirement is not significant compared to the power output of the turbine, as seen in Tables 4.2 – 4.4 and 4.6 – 4.7. As a result, one can assume that even divided by its efficiency of **75%**, the actual value of the pump's efficiency factor does not affect the overall efficiency of the cycle and so it can be omitted from the overall efficiency of the cycle.

4. Condenser Efficiency ($\boldsymbol{\eta_C}$)

According to Holman (2010: p. 542), there is a specific law for calculating the efficiency of boilers and condensers (specifically called effectiveness for heat exchangers), appearing in Equation 4.4:

$$\boldsymbol{\eta_C = 1 - e^{-NTU_{max}}}$$

Equation 4.4: Efficiency Factor of Condensers

where $\mathbf{NTU_{max}}$ is the quotient of the overall heat transfer coefficient **U** of the HE (measured in **W/K-m²**) and its heat transfer surface area **A** in **m²**, over the heat capacity rate ($\mathbf{C_{min} = \dot{m}_c c_c}$) of the fluid that rejects energy measured in **W/K**. The mentioned **NTU** (**Number** of **Transfer Units**) relationship appears in Equation 4.5:

$$\boldsymbol{NTU_{max} = \frac{UA}{C_{min}}}$$

Equation 4.5: Condenser NTU factor

Holman also presents (2010: p. 543 – 545) a set of effectiveness vs. NTU_{max} number graphs for the different kinds of flow (parallel, counter and cross), each one containing the curves

of a HE's effectiveness (basically the efficiency factor) according to the quotient $\mathbf{C_{min}/C_{max}}$. As this quotient increases, the effectiveness of the HE is decreased. However, in the case of condensers or boilers this quotient is equal to zero, because the $\mathbf{C_{min}}$ has no meaning since the fluid changes phase and so it has a constant temperature. As a result, the fluid is rejects/absorbs heat according to its specific latent heat capacity and not the normal specific heat capacity. Additionally, both the parallel and counter flow configurations allow the assumption that the effectiveness factor is almost **100%** after an $\mathbf{NTU_{max}}$ number of **3.5**. So, the efficiency of the condenser and the DHW storage tank is assumed to be **100%**, with a counter flow configuration for this project.

Section 4.3.2.3: Calculation of the non-ideal Rankine cycle efficiency for water/steam

After mentioning the typical values of each component's efficiency, a so called "Realism factor" can be determined so that the actual Rankine cycle efficiency of the system can be estimated. This factor is nothing else than the product of the efficiency coefficients of the components with significant contribution to the efficiency of the cycle. So the factor is given by the following equation:

$$\boldsymbol{\eta_r = \eta_T * \eta_B}$$

Equation 4.6: Realism Factor

and by substituting the conservative efficiency values mentioned above, the realism factor is equal to **49%**. This means that the cycle loses about half of its efficiency due to the thermodynamic irreversibilities of its components, mainly its ST and PTSC. Therefore the non-ideal overall Rankine cycle efficiency of the system, without the usage of an IHE, is reduced from **25.6%** to **12.54%**, based on the optimal settings seen in red in Table 4.7. This means that only about **13%** of the solar energy input is converted into the useful electrical energy for the household. In the next section an attempt to improve the overall efficiency of the cycle by using an Internal Heat Exchanger (**IHE**) and to examine how much the overall efficiency can be improved.

Section 4.3.2.4: Improving the non-ideal Rankine cycle efficiency with an IHE

The determined actual overall efficiency of Concept System 1 calculated in the previous section is much less than that of a photovoltaic collector alone; the maximum acclaimed efficiency is about **21%** (SunPower, 2014; Energy Informative, 2014). This section analyses the operation of an IHE and also determines the actual cycle efficiency with an IHE.

As a heat exchanger, the IHE receives thermal energy from a fluid at its primary circuit and transmits it to the fluid at its secondary circuit via its internal transmission medium. Its efficiency $\boldsymbol{\eta_{IHE}}$ can be also calculated using the effectiveness vs. NTU_{max} number curves presented by Holman (2010: pp. 543 – 545). These curves for a counter-flow configuration appear in Figure 4.7 (Holman, 2010: p. 543). In order to choose a curve, the quotient $\boldsymbol{C_{min}/C_{max}}$ needs to be calculated. However, the mass flow rate of the two fluids is the same and so this quotient can become the quotient of the two fluids' specific heat capacities. This is shown by Equation 4.7, where $\boldsymbol{\dot{m}}$ is the system's mass flow rate, in **kg/s**, while $\boldsymbol{c_{ps}}$ and $\boldsymbol{c_{pw}}$ are the specific heat capacities of steam and water respectively, measured in **kJ/kg-K**. Since the effectiveness is by definition the efficiency of a heat exchanger, it means that the efficiency factor of the IHE is given by Equation 4.8, where the specific enthalpies are those of the fluid's corresponding state in Figure 4.6. In the case of water, state **4s** (same entropy as state **3**) is the same as **4a** (saturation point).

$$\frac{C_{min}}{C_{max}} = \frac{\dot{m}c_{ps}}{\dot{m}c_{pw}} = \frac{c_{ps}}{c_{pw}}$$

Equation 4.7: Effectiveness of IHE

$$\varepsilon = \frac{\dot{Q}_{in}}{\dot{Q}_{out}} = \frac{h_{2a} - h_2}{h_4 - h_{4a}}$$

Equation 4.8: Efficiency Factor of IHE

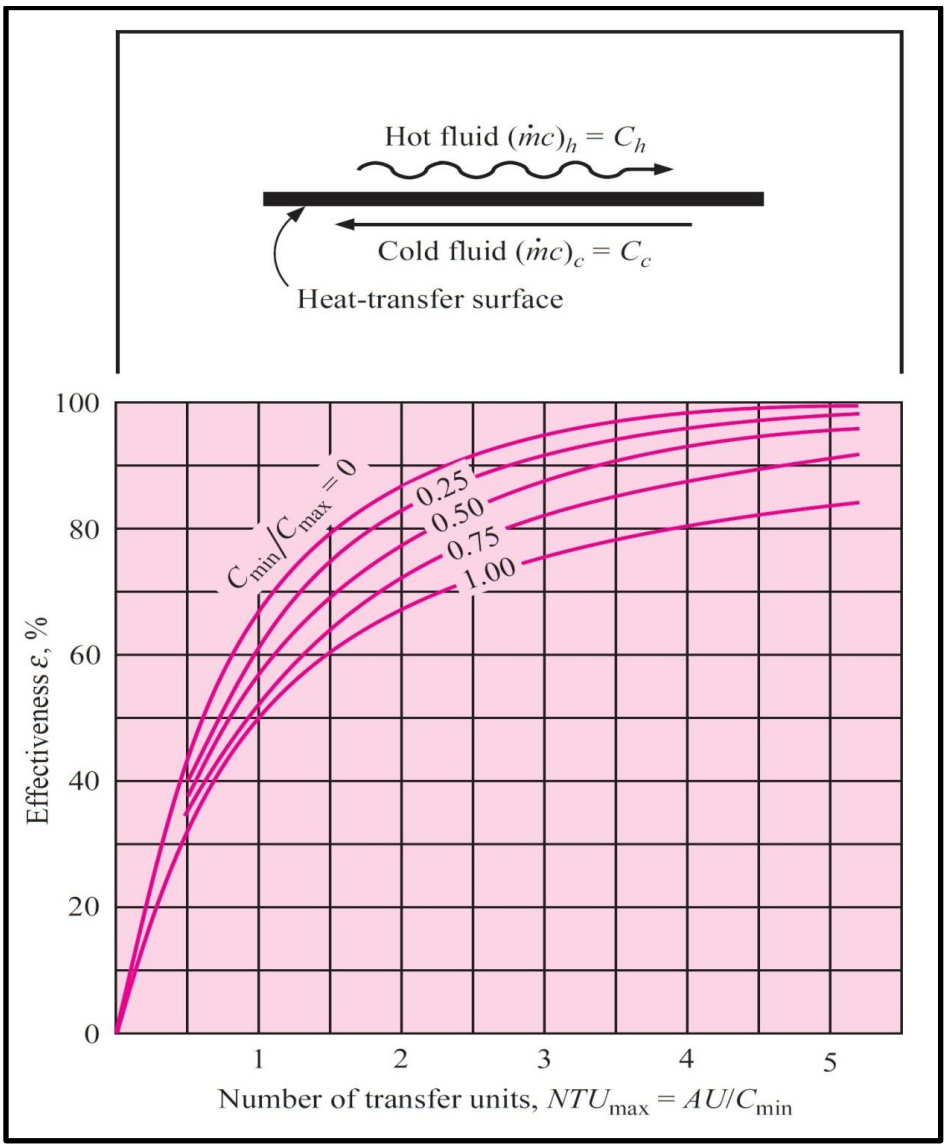

Figure 4.7: Configuration of a Rankine cycle plant with an IHE (Lai et al., 2011: p. 201)

Firstly the efficiency of the IHE needs to be determined. Considering that steam is rejecting heat at **0.4 bar(a)** of constant pressure, for small changes of it temperature $\mathbf{c_{ps}}$ does not change and so its value is the average of states **4** and **4s**, equal to **1.9619 kJ/kg-K**. Respectively, water is absorbing heat at constant pressure between states **2** and **2a** and so $\mathbf{c_{pw}}$ is also constant for small changes in temperature, so its value is **4.2166 kJ/kg-K** (20 bar(a) at 100 ºC) (Spirax – Sarco Ltd. 2014). With these values the quotient $\mathbf{C_{min}/C_{max}}$ equals to **0.456**, about **0.5**. By considering a counter flow configuration the efficiency of the IHE in this case is about **95%** for 5 NTU units (Holman, 2010: p. 543).

Using the optimal settings from Table 4.7 and the following equations along with those in Section 4.3.2.2, the overall efficiency of the system with the IHE can be calculated; the results are presented in Table 4.8.

$$q_B = \frac{h_3 - h_{2a}}{\eta_B}$$

Equation 4.9: Actual energy input of the PTSC per unit mass

$$w_T = (h_3 - h_4)$$

Equation 4.10: Actual work output of the Steam Turbine per unit mass

$$\eta_{R_{+IHE}} = \frac{w_T - w_P}{q_B} \simeq \frac{w_T}{q_B}$$

Equation 4.11: Overall actual efficiency of cycle with IHE

Property name	Property	Units	Value
PTSC efficiency factor	η_B	%	70
Steam Turbine efficiency factor	η_T		70
IHE efficiency factor	η_{IHE}		95
Specific enthalpy of state 3	h_3	kJ/kg	3226
Specific enthalpy of state 4s (and 4a)	h_{4s} (h_{4a})		2435
Specific enthalpy of state 4	h_4		**2672.30**
Specific enthalpy of state 2a	h_{2a}		**604.56**
Actual energy input per unit mass of PTSC	q_B		**3744.91**
Actual work output per unit mass of ST	w_T		**553.70**
Overall Cycle Efficiency (with the IHE)	$\eta_{R_{+IHE}}$	%	**14.79**

Table 4.8: Calculation of the SA charging component's minimum power output (data from Table 4.6 and Section 4.4.2.2)

The quantity w_P is the energy demand of the pump per unit mass ($h_2 - h_1$), which as mentioned is negligible. This efficiency shows that an IHE actually improves the overall efficiency of the cycle; however the improvement is only **2.3%**, an increase which is not very significant as **14.8%** is still less than the **21.5%** efficiency of a PV panel (SunPower, 2014; Energy Informative, 2014). Clearly water as a working fluid does not provide an alternative

to PV operation of this domestic scale system. Therefore, the actual overall efficiency could be improved if a different working fluid is used in the cycle. The next section examines different organic working fluids to find the best one that with an IHE gives a better overall efficiency from PV.

Section 4.4: Organic Rankine Cycle

Section 4.4.1: Introduction

As it is known, today's large scale power plants utilize successfully the regular water based Rankine cycle as it requires large temperature and pressure level differences in order to be efficient. This becomes apparent when one sees the two Siemens A.G. (2011 & 2013) product brochures; large scale power stations that use the company's STs are designed to accommodate the electricity demand of entire cities, even countries and they require temperature levels over **585 ºC** (about **855 K**), high pressure levels up to **165 bar** and low pressure levels of around **0.06 bar**. In order to achieve these large temperature and pressure scales, fossil fuel with high calorific value (including lignite, natural gas and crude oil) are used, alternatively called High Temperature Heat Sources.

Section 4.4.2: Other types of working fluids

In contrast to fossil fuels, thermal based RES (solar, geothermal, biomass and waste heat) do not achieve temperature as high as conventional fuels do. For this reason they are sources of a lower grade and they are called Moderate Temperature Heat Sources. Additionally, due to safety reasons the maximum pressure level of a Rankine cycle based domestic system cannot exceed **20 bar (a)**, which is another factor apart from temperature that affects the efficiency of the cycle, as seen from the trials listed in Tables from 4.2 to 4.7.

Tables 4.6 & 4.7 and the calculations in Section 4.3.2.4 of the cycle's actual efficiency contained in Table 4.8 prove that water cannot be used as the working fluid of a small scale Rankine cycle application, especially when operating with a moderate temperature source of thermal energy, such as solar radiation. Researchers have been studying the possibility of using alternative working fluids instead, for the so called **Organic Rankine Cycle** (**ORC**). These fluids are in their vast majority (though not necessarily) organic compounds with lower

boiling temperatures than water, so that they are capable of executing the cycle with the previously mentioned low grade temperature sources more easily. In addition, organic fluids are divided into three groups: wet, isentropic and dry. **Isentropic** and **dry** fluids do not require superheating; in contrast it is avoided in their case as it lowers the efficiency of the system. This fact gives the designer a large list of potential fluids, so it is much easier to choose those most suitable for each application. Lastly, ORC turbines are single-stage devices and as a result they are smaller, lower in price and more controllable (Chen et al., 2010: p. 3060).

Section 4.4.3: Categories of organic working fluids

As mentioned in the last paragraph, organic compounds are grouped into three categories depending on their thermodynamic properties. This section analyses this categorization and derives the possible effect it has on the efficiency of the ORC.

Chen et al. (2010: p. 3062) and Bao & Zhao (2013: p. 326) explain these three categories thoroughly. They study the three cases individually by examining the slope of the **vapour saturation line** on the T-s diagram examples Figures 4.8, 4.9 and 4.10 present (Bao & Zhao, 2013: p. 326). The basic knowledge of analytical geometry dictates that the slope of a graph is given by the limit of the value difference on the vertical axis's quantity divided by the value difference of the horizontal axis's quantity, as the latter approaches zero. In the case of a T-s diagram, since the vertical axis represents the Temperature values and the horizontal axis represents the Specific Entropy values of the fluid, the slope $\boldsymbol{\lambda}$ of the graph is given by Equation 4.12:

$$\boldsymbol{\lambda = \lim_{\Delta s \to 0} \frac{\Delta T}{\Delta s} = \frac{dT}{ds} = \tan(\theta)}$$

Equation 4.12: Slope of a T-s diagram

The slope is also equal to the trigonometric tangent of angle $\boldsymbol{\theta}$ that the geometric tangent line projection of the graph at a particular point creates with the horizontal axis. If the angle is acute ($\boldsymbol{< 90^o}$), the slope is positive thus the fluids is called "**Dry**". If it is obtuse ($\boldsymbol{90^o < \theta < 180^o}$), the slope is negative and the fluid is called "**Wet**" and finally if the angle is right ($\boldsymbol{90^o}$)

then the slope is infinite, where the fluid is given the name "**Isentropic**". To avoid the latter problem, both papers take the reciprocal of that slope $\boldsymbol{\xi} = \left(\frac{\mathbf{ds}}{\mathbf{dT}}\right)$ (Chen et al., 2010: p. 3062 & Bao & Zhao, 2013: p. 326) as shown on the above three graphs so **isentropic** fluids have a ξ index of approximately zero ($\boldsymbol{\xi \simeq 0}$), **dry** ones have a positive ξ ($\boldsymbol{\xi > 0}$) and finally **wet** fluids have a negative ξ ($\boldsymbol{\xi < 0}$).

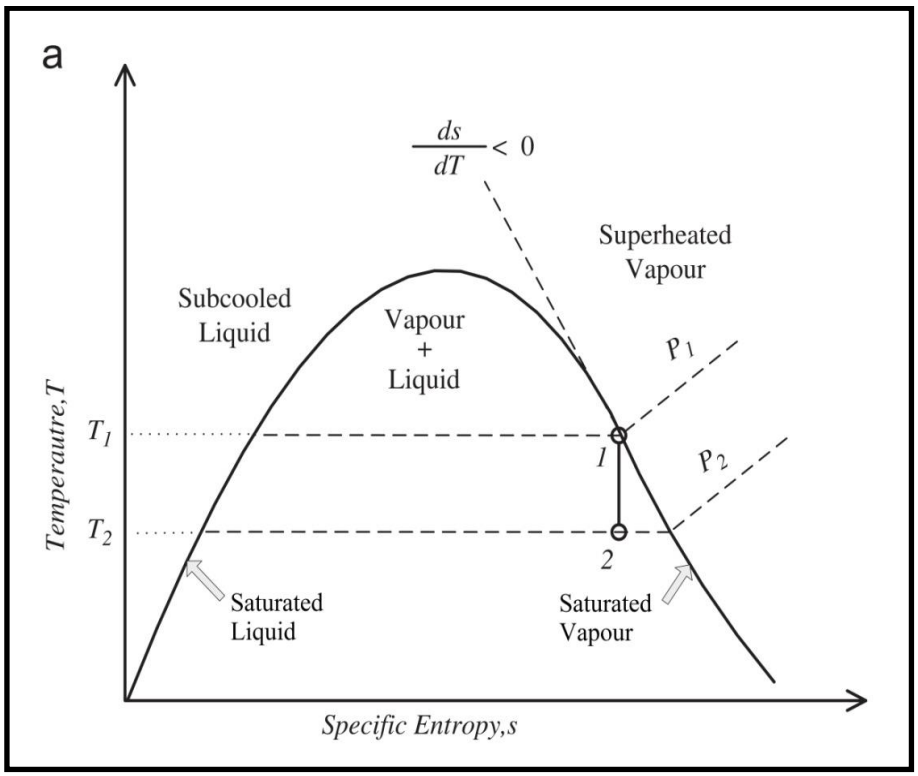

Figure 4.8: T-s diagram of a wet fluid (Bao & Zhao, 2013: p. 326)

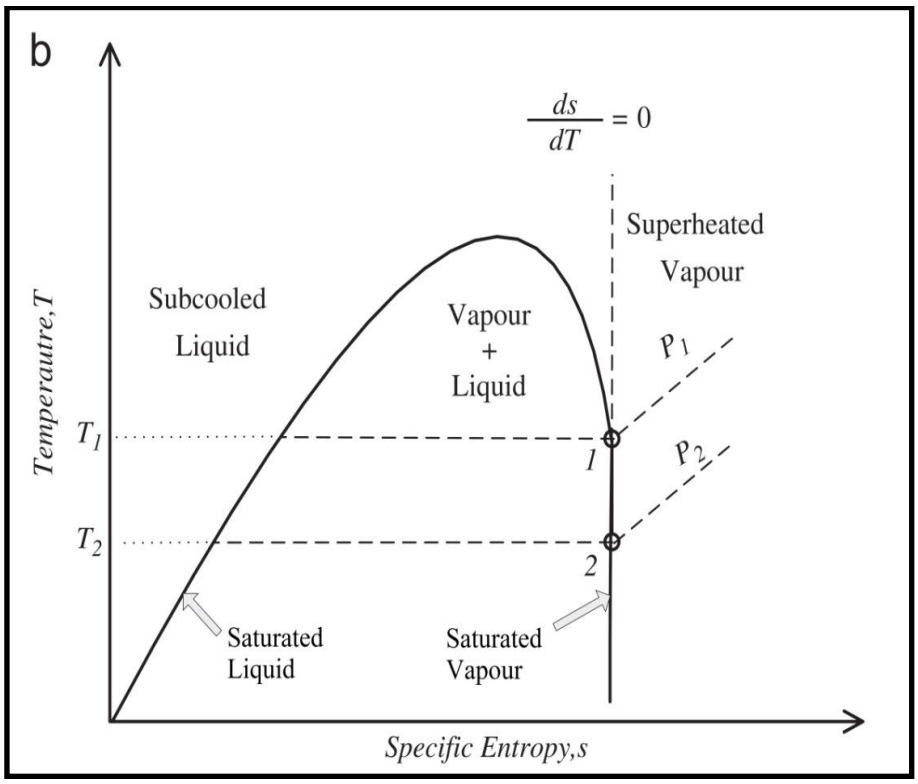

Figure 4.9: T-s diagram of an isentropic fluid (Bao & Zhao, 2013: p. 326)

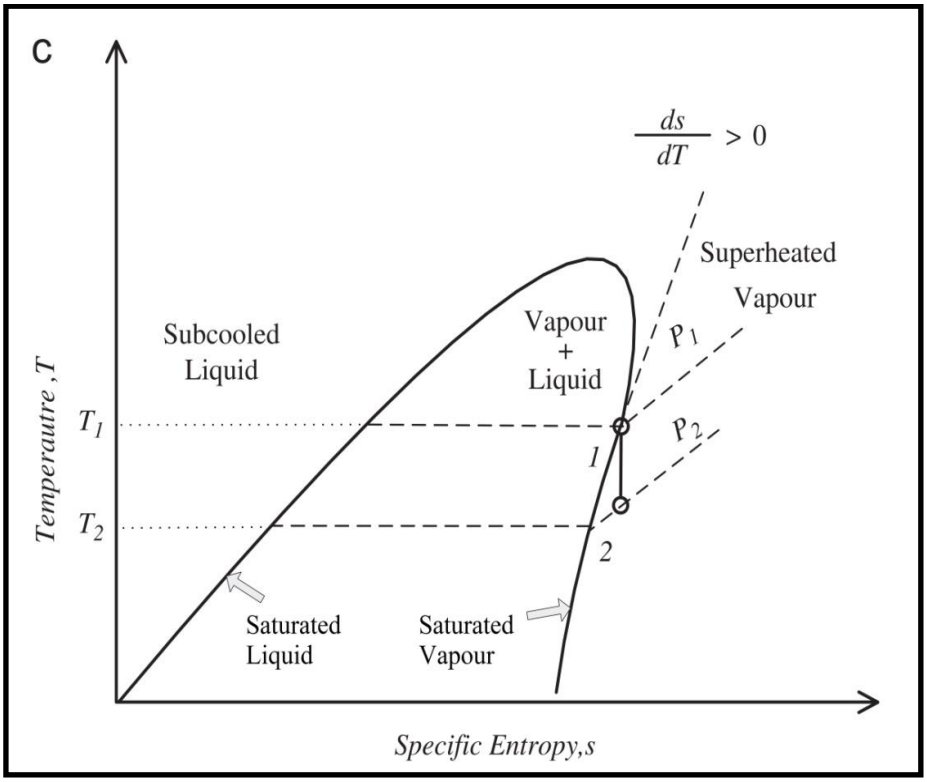

Figure 4.10: T-s diagram of a dry fluid (Bao & Zhao, 2013: p. 326)

Isentropic and **dry** fluids guarantee that their isentropic expansion would not create droplets of liquid during expansion, as they does not enter into the liquid – vapour mixture region of the T-s diagram. The case of pentane (dry) is presented in the paper of Chen et al. (2010: p. 3063) and featured in Figure 4.11 in a supercritical expansion. As seen in Figure 4.11, the broken line represents an actual (non ideal) expansion that only touches the vapour saturation line and then it does not enter into the mixture region as it expands. An isentropic fluid is just a critical case of a dry one. This means that an expansion from any point on the saturation line, even an ideal one, would not enter into the mixture region. This is the first reason why the fluids of these two categories do not need superheating. The second reason is that by superheating a dry fluid, the efficiency of the cycle is affected negatively, whereas this is very beneficial for wet fluids. Isentropic fluids are not affected by superheating almost at all (Chen et al., 2010: p. 3063 – 3064).

The next section describes several techniques of realising an organic Rankine cycle, based on the three categories of organic working fluids mentioned above.

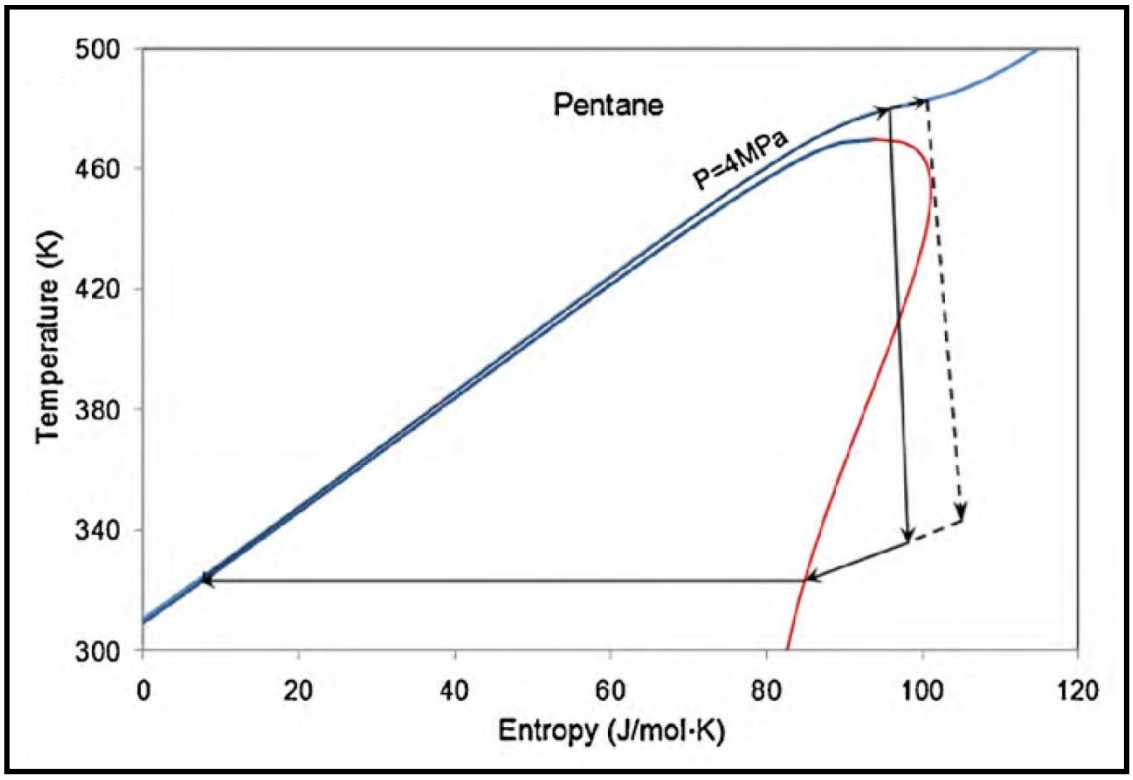

Figure 4.11: T-s diagram of Pentane (Dry) (Chen et al., 2010: p. 3063)

Section 4.4.4: Types of Organic Rankine Cycle

After mentioning the three categories of working fluids used for Rankine cycles and if they can be subjected to superheating or not, this section describes three techniques of configuring the cycle so that it offers the best possible efficiency factor.

Section 4.4.4.1: Organic Rankine Cycle with Superheat

The first operation setup of the ORC presented in this section is the one used already for water; it is called "Rankine cycle with Superheat" (**O_3**). This is presented in Figure 4.12 (Lai et al., 2011: p. 201). In this classic case, the higher pressure level of the working fluid is smaller than its critical pressure level at the top of the curve. In addition, the working fluid continues to receive thermal energy from the boiler after it reaches the vapour saturation point at the higher pressure level and its state **3** is situated within the superheated region of the T-s diagram, as shown in the above figure. Specifically, the working fluid passes through the turbine and reaches state **4**, still inside the superheated region and then the IHE receives the waste energy difference from state **4** to **4a** at the vapour saturation point of the lower pressure level and transfers it to the stage of the cycle after the feed pump. As seen in Figure 4.12, in the case of a dry fluid, state **4** has a significantly higher temperature than state **4a**, which means that at state **2a** the liquid working fluid has almost the same temperature as state **4**. So the boiler would need to spend less fuel to make the fluid reach state **3**, thus increasing the overall efficiency of the cycle more significantly that in the case of water, shown in the previous section. This is shown at the calculations section of the ORC next.

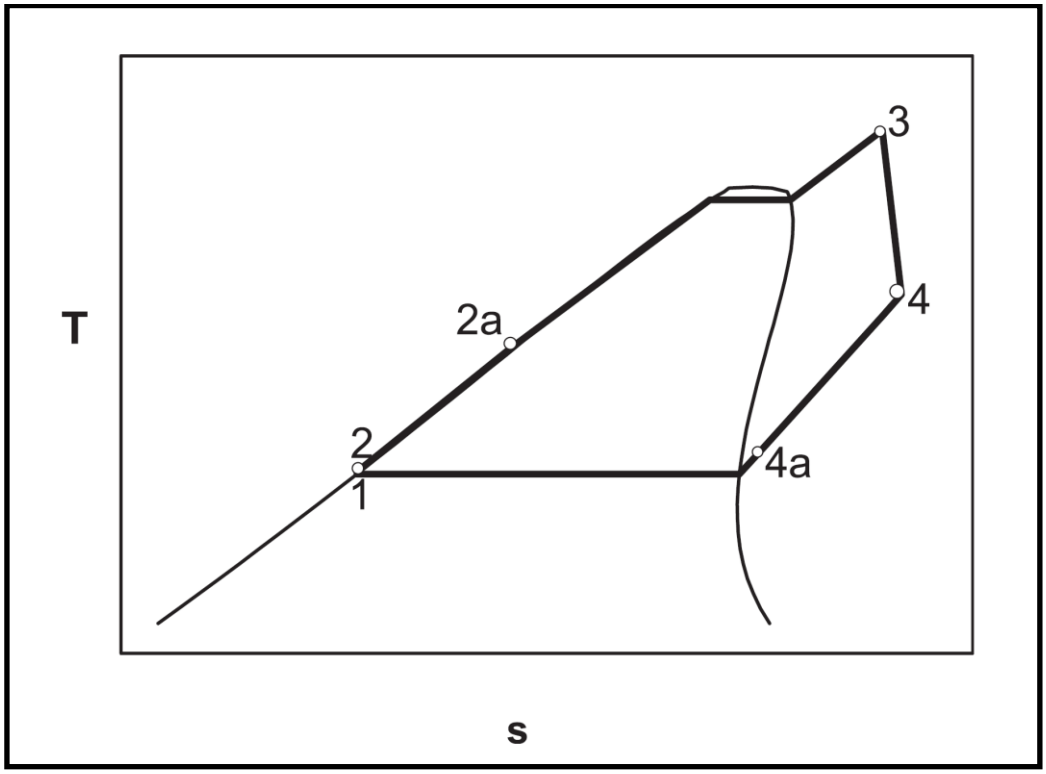

Figure 4.12: T-s diagram of an O_3 Rankine Cycle with an IHE (Lai et al., 2011: p. 201)

Section 4.4.4.2: Organic Rankine Cycle without Superheat

A similar cycle setting to **O_3** is the **O_2** ORC which is basically the same as previous one but without superheating, thus its state **3** is situated on the vapour saturation line at the higher pressure level. It is shown in Figure 4.13 (Lai et al., 2011: p. 201). As mentioned, this setting is used for dry fluids, while the **O_3** cycle suits wet fluids better. One can observe the difference in temperature of state **4** in this cycle compared to the **O_3** one; however this is a necessary trade off so that its efficiency does not decrease by superheating, as mention previously.

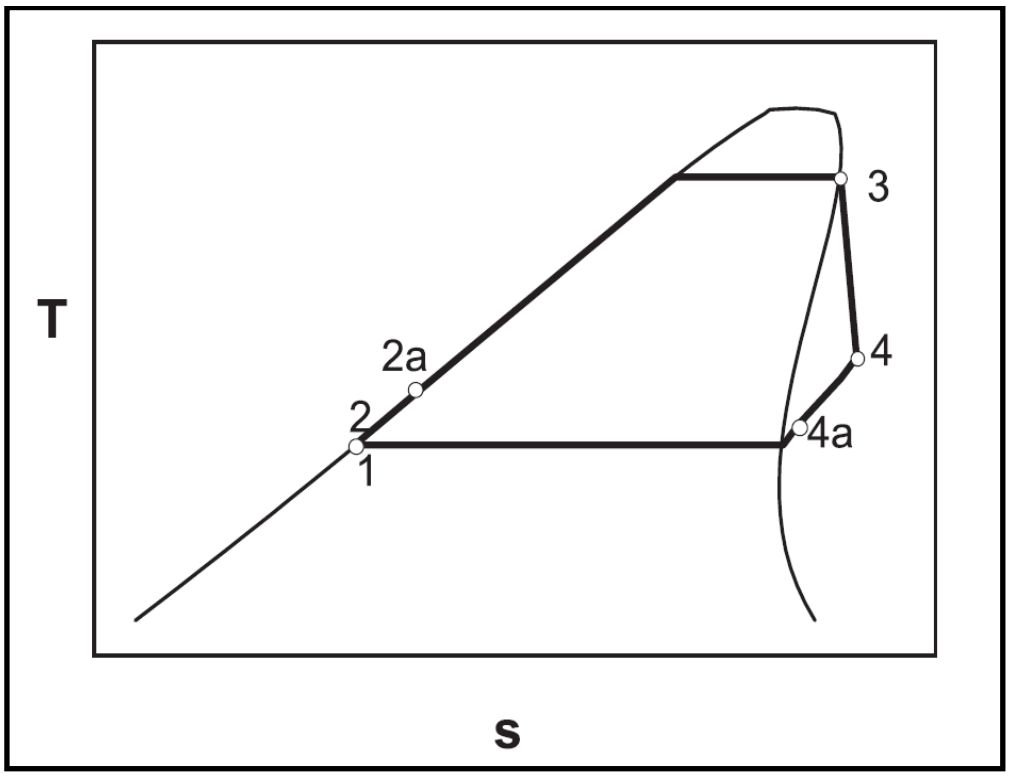

Figure 4.13: T-s diagram of an O_2 Rankine Cycle with an IHE (Lai et al., 2011: p. 201)

Section 4.4.4.3: Supercritical Organic Rankine Cycle

The final cycle type is the supercritical Rankine cycle (**S_2**) and as its name suggests the higher pressure level is above the fluid's critical pressure level. It is schematically represented in Figure 4.14 (Lai et al., 2011: p. 202). In this cycle, the working fluid does not experience a phase transition from liquid to vapour; it rather becomes superheated directly from the liquid phase after passing to the right hand side of the fluid's critical point on the peak of the curve. **S_2** cycles are used when the fluid's critical pressure is relatively low and can potentially maximise the overall efficiency of the cycle, even though not many studies have been made on the topic (Chen et al., 2010: p. 3061). This is quite intuitive, as during the phase transition the fluid absorbs/rejects heat though its specific latent heat capacity under constant temperature. Often the latent heat capacity is much greater than the specific heat capacity of the fluid, which means that the achievement of the maximum temperature and therefore enthalpy of state **3** in Figure 4.13 requires the absorption of larger amounts of heat compared to Figure 4.14. As a result the efficiency of an **O_2** or **O_3** cycle is smaller than the one achieving with a supercritical one.

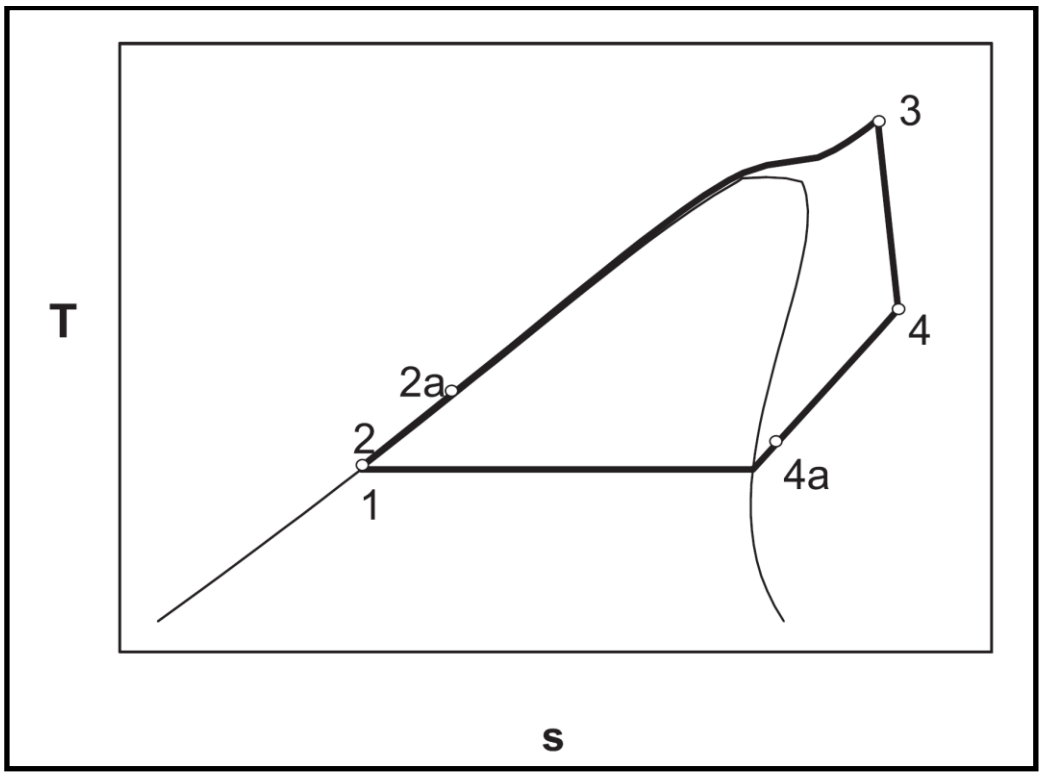

Figure 4.14: T-s diagram of an S_2 Rankine Cycle with an IHE (Lai et al., 2011: p. 202)

Section 4.4.5: Working Fluid Selection Criteria

Apart from chemical stability, a working fluid must also possess appropriate thermodynamic properties between the cycle's operating temperatures and therefore the careful selection of a fluid for a Rankine cycle is a very important task (Chen et al., 2010: p. 3062). This section explains the selection criteria for ORC working fluids, depending on the application.

Chen et al., (2010: p. 3063) proved that a fluid with high specific latent heat and density in conjunction with a low liquid specific heat is very beneficial for the cycle, as these properties contribute to the increase of the turbine work output, hence increasing the efficiency. The authors also support this opinion by citing a paper stating that these properties decrease the required mass flow rate of the cycle that also reduces the energy input for the feed pump. Additionally, the fluid's critical temperature must be well over **300 K** (room temperature) in order to be able to reject thermal energy during the condensation process to the environment, either ambient air or water bodies (Chen et al., 2010: p. 3064). Moreover, for supercritical cycle applications, the critical point should not be extremely high both in

terms of pressure and temperature as they would be difficult to surpass with a low grade energy source. A great example is carbon dioxide (**CO_2**) that has a low critical temperature of **31.1 ºC**, low cost and it does not significantly pollute the environment in case of a leakage. However, its critical pressure level is about **74 bar** (Bao & Zhao, 2013: p. 331), a very high pressure compared to the 20 bar consideration, mentioned in the Section 4.4.2. So, **CO_2** cannot be used for the calculations this project.

In terms of environmental safety, the working fluid should possess at least one hydrogen atom in their molecule that makes them react with hydroxyl (**OH^-**) radicals in the lower atmosphere, thus preventing any leaked amounts of it from reaching the stratosphere and depleting the ozone layer. As far as human safety is concerned, the selected fluids must not be harmful to human health, corrosive or flammable. Even though most organic compounds are at least flammable, the real consideration is around the auto ignition temperature, maximum allowed concentration and explosion limits of each fluid (Chen et al., 2010: p. 3064).

Lastly, apart from the above criteria, one of the most important aspects is cost. The fluid must not be overly expensive or alternatively the designer could simply make trade-offs in efficiency units for a cheaper fluid, such as hydrocarbons, water and in general fluids that exist in large quantities in the marketplace (Chen et al., 2010: p. 3064).

Section 4.4.6: Working fluid candidates

Section 4.4.6.1: Working fluid selection process

This section describes the attributes of five working fluids considered for usage in an ORC to replace water for this project's parameters. Not all three selection criteria where followed as none of compounds presented by Chen et al. (2010: p. 3065) possessed all the attributes of high density and latent heat capacity and low specific heat simultaneously. The list was shortened to 4 compounds that had properties similar to the three physical property criteria and the intention was to have one candidate for each of the **O_2**, **O_3** and **S_2** cycle: **Benzene**, **Toluene**, **Refrigerant – 134a** and **FC-4-1-12**. Benzene and Toluene are very similar compounds with practically identical critical pressure levels and temperatures, as well as very similar specific heat and latent heat capacities. They are both relatively wet fluids, as

seen from their ξ parameter and so one of the two had to be rejected (Chen et al., 2010: p. 3065). Conclusively, Toluene remained in the list as it has been studied by Lai et al. (2011), who utilized its properties for calculating the efficiency of an ORC with and without an IHE. **Toluene**, as a wet fluid is to be used for an **O_3** cycle.

For the supercritical **S_2** cycle the **R – 134a** was initially selected. However, it was rejected eventually as its superheated region data are only available for temperatures up to **200 ºC**, which is very much lower than the desired **390 ºC** for this project and also its critical pressure level is about **40 bar** (Chen et al., 2010: p. 3065 & Moran et al. 2011: p. 911). As for the dry fluid candidate for utilizing in the **O_2** cycle, **FC-4-1-12**'s data are easily accessible in chemistry webbook of NIST (2011).

Due to the initial candidates' lack of the needed data, the project's attention shifted towards alternative solutions for the working fluid. Lai et al. (2011) studied other compounds as ORC working fluids apart from Toluene, for producing a net power output of **1 MW** by dividing the fluids into three groups for each of the **O_2**, **O_3** and **S_2** cycles. The fluids do not change group and in all three cases the cycles operate under the same higher pressure levels, which are **0.9** and **1.2** times the critical pressure of the fluids in **O_3** and **S_2** cycles respectively. The **O_2** cycle assumes for the higher pressure level the saturation pressure at the maximum temperature of the cycle. The three cases operate within various temperature ranges, calculating also the cycle's Carnot efficiency:

a. Case 1: From **85** to **250 ºC** (358 to 523 K) and η_C = **31.5%**
b. Case 2: From **38** to **250 ºC** (311 to 523 K) and η_C = **40.5%**
c. Case 3: From **85** to **300 ºC** (358 to 573 K) and η_C = **37.5%**

With these configurations, they present the results of the three cases (Lai et al. 2011: pp. 206 – 207) and showed that the following fluids had the best overall efficiency with an IHE in ascending order: **Hexamethyldisiloxane** (**MM**, 28.2%), **Toluene** (**T**, 29.0%), **Decamethyltetrasiloxane** (**MD_2D**, 30.0%), **Dodecamethylpentasiloxane** (**MD_3D**, 30.3%) and **Butylbenzene** (**B**, 31.3%). The efficiency factor showed inside the parentheses are the highest achieved with the settings of the second case (311 to 523 K) and these are the final

candidates for the trials of this project. The thermophysical properties of these compounds are presented in Table 4.9 (Lai, 2009: pp. 195 – 196; NIST, 2011 & ECHA, 2010):

Fluid	**α**	**β**	**γ**	**δ**	**ε**
MM (M)	6.3472	8.5604×10^{-2}	-4.6759×10^{-5}	1.0523×10^{-8}	0.0000
Toluene (T)	- 4.7793	7.0821×10^{-2}	-4.7711×10^{-5}	1.4068×10^{-8}	-1.0756×10^{-12}
MD_2D (M2)	10.0356	1.5327×10^{-1}	-8.6846×10^{-5}	2.0222×10^{-8}	0.0000
MD_3D (M3)	12.8945	2.0199×10^{-1}	-1.2386×10^{-4}	3.0840×10^{-8}	0.0000
Butylbenzene (B)	6.4900	1.9080×10^{-2}	1.5665×10^{-4}	-2.2059×10^{-7}	8.8870×10^{-11}
Fluid	**M_r (g/mol)**	**T_c (K)**	**P_c (bar)**	**T_{AI} (ºC)**	
MM (M)	162.3775	518.7	19.25	341	
Toluene (T)	92.1384	591.8	41.09	480	
MD_2D (M2)	310.6854	599.4	11.90	350	
MD_3D (M3)	384.8393	629.0	9.45	430	
Butylbenzene (B)	134.2182	660.1	28.87	510	

Table 4.9: Vapour specific heat function parameters, molar mass, critical temperature and pressure and auto-ignition temperature of the five fluids (Lai, 2009: pp. 195 – 196; NIST, 2011 & ECHA, 2010)

This table presents the five coefficients (**α** to **ε**) of Equations 4.13 to 4.15, the molar mass ($\mathbf{M_r}$) of each fluid, their critical pressure level ($\mathbf{P_c}$), critical temperature ($\mathbf{T_c}$) and finally the auto-ignition temperature ($\mathbf{T_{AI}}$). The auto-ignition temperature is the lowest temperature capable of causing spontaneous combustion to a substance without the aid of a spark and one can observe that all fluids but **MM** possess auto ignition temperature values higher than this project's maximum cycle temperature of about **390 ºC**. However, as the fluids will not operate in the presence of air inside the piping of the cycle, then there is no danger of combustion even if the auto ignition temperature is surpassed, meaning that all fluids are safe for the temperatures of the cycle. Extra caution should be given to any danger of leakage though, but only in the case of **MM**.

As mentioned, water and several other commonly used fluids have been thoroughly studied throughout the years and so their data are readily available for usage and easily accessible, whereas the above fluids, apart from Toluene, are not commonly used and have not been studied by virtually anyone. One of the few sources that contain information regarding these fluids is the PhD Thesis of Lai Ngoc Anh (2009), in which he presents,

among others, the thermodynamic properties of non-common organic compounds called **siloxanes**. More specifically, these compounds are those that have at least one silicon – oxygen – silicon linkage (**Si – O – Si**) (IUPAC Gold Book). The problem with these data is that they are confined to only those at the liquid and vapour saturation points for each temperature from about **300 K** up to their critical temperature and not any data regarding the superheated vapour, the liquid – vapour mixture and subsaturated liquid regions are available. This problem can be overcome by utilizing the following laws of thermodynamics.

Section 4.4.6.2: Specific enthalpy and entropy for the gas phase

The thermodynamic properties of a gas's enthalpy and entropy can be easily determined by means of its isobaric specific heat capacity, $\mathbf{c_p}$. For common substances there are tabulated values of $\mathbf{c_p}$ so that they can be used as they are. However, for uncommon fluids this specific heat is a function of the absolute temperature of the gas, as indicated by Equation 4.13 (Moran et al., 2011: p. 132):

$$\mathbf{c_p(T) = \frac{R}{M_r}(\alpha + \beta T + \gamma T^2 + \delta T^3 + \varepsilon T^4)}$$

Equation 4.13: Polynomial function of the isobaric specific heat of a gas (Moran et al., 2011: p. 132)

where **α**, **β**, **γ**, **δ** and **ε** are the parameters of the function presented in Table 4.9, while **R** is the universal gas constant, equal to **8.314472 J/mol-K**. Lastly, $\mathbf{M_r}$ is the molar mass of each gas measured in **kg/mol** and **T** is the absolute temperature is measured in **K**. As seen from the above equation, the specific heat is heavily dependent on temperature and so the formulae that will be used for calculating the specific enthalpy and entropy of each state within the superheated region are the following two (Moran et al., 2011: p. 134 & 291):

$$\Delta h(T) = \int_{T_a}^{T_b} c_p(T)dT$$

$$\Rightarrow \boxed{\Delta h(T) = \frac{R}{M_r}\left(\alpha\Delta T + \frac{\beta}{2}\Delta T^2 + \frac{\gamma}{3}\Delta T^3 + \frac{\delta}{4}\Delta T^4 + \frac{\varepsilon}{5}\Delta T^5\right)}$$

Equation 4.14: Specific Enthalpy difference between two states of a gas (Moran et al., 2011: p. 134)

where ΔT^n means $(T_b^n - T_a^n)$ and not $(T_b - T_a)^n$, as this may cause a misconception. The entropy difference between two states of a gas is given by Equation 4.15:

$$\Delta s(T) = \int_{T_a}^{T_b} \frac{c_p(T)}{T} dT - \frac{R}{M_r} \ln\left(\frac{P_b}{P_a}\right)$$

$$\Rightarrow \boxed{\Delta s(T) = \frac{R}{M_r}\left[\alpha \ln\left(\frac{T_b}{T_a}\right) + \beta\Delta T + \frac{\gamma}{2}\Delta T^2 + \frac{\delta}{3}\Delta T^3 + \frac{\varepsilon}{4}\Delta T^4 - \ln\left(\frac{P_b}{P_a}\right)\right]}$$

Equation 4.15: Specific Entropy difference between two states of a gas (Moran et al., 2011: p. 291)

where P_a and P_b are the corresponding pressure levels of states **a** and **b** respectively and ΔT corresponds to $(T_b - T_a)$. With these last two equations the needed data of the five fluids within the superheated region can be produced and the problem of non-existing data is therefore surpassed. Additionally, Equation 4.15 is capable of calculating the temperature of state **4s** (T_{4s}) after the theoretical isentropic expansion of the cycles, by setting Δs equal to zero. With T_{4s} calculated the specific enthalpy h_{4s} is also calculated, which assists the determination of the actual expansion state **4**'s temperature and specific enthalpy (T_4 and h_4) as well.

Section 4.4.6.3: Specific enthalpy and entropy for the liquid phase

Since Equations 4.14 and 4.15 can only be used for calculations in the vapour phase of the fluids, they cannot therefore be used for calculating the power consumption of the feed pump. For this task there is another equation that can be used (Moran et al., 2011: p. 120):

$$\Delta h(P,T) = v(P_b - P_a) + c(T_b - T_a)$$

Equation 4.16: Specific Enthalpy difference between two states of a liquid (Moran et al., 2011: p. 120)

where **v** is the specific volume of the liquid at a particular temperature and **c** is the specific heat capacity of the liquid, measured in **m^3/kg** and **J/kg-K** respectively. Since the pump does not add any thermal energy to the liquid and thus any increase in its temperature is negligible, the second term of the Equation 4.16 can be omitted; hence it takes the form of Equation 4.17:

$$\Delta h(P) = v(P_2 - P_1) = \frac{1}{\rho}(P_2 - P_1)$$

Equation 4.17: Specific Enthalpy difference between states 1 and 2 of the working fluid when compressed in feed pump

In contrast, the difference in pressure is not negligible as the difference between the lower and higher pressure levels is in fact more significant than the difference in temperature. The last point for this equation is that the specific volume of a fluid is equal to the reciprocal of its density (**ρ**) and since density data are given along the saturation data of the five fluids in Lai's PhD thesis (2009), the specific enthalpy difference of Equation 4.17 can also be calculated very easily.

Section 4.4.7: Organic Rankine Cycle efficiency calculations

After explaining the background Thermodynamic laws behind the extra work needed to study the five organic compounds, the same calculations done for the original water based Rankine cycle have been conducted for them as well and are presented in Tables 4.12 and 4.14. As mentioned, the most important calculations of this project are those regarding the superheated region and this is the reason why they are based heavily on Equations 4.14 and 4.15. This section analyses the procedures of calculating both the ideal and non-ideal efficiency factors of ORCs, based on the five fluids mentioned above.

Section 4.4.7.1: Ideal (isentropic) efficiency calculations

The first procedure involves the calculation of the cycles' isentropic (ideal) efficiency and it is basically the same one followed for water. In order to compare the thermodynamic capabilities of the five fluids against those of water in a Rankine cycle application, the operational temperature ranges for the five fluids must be the same as the ones used for water. This will result in having the same Carnot efficiency as water (about **45%**). Unfortunately, the first two fluids that are subjected into an **O_2** cycle have as maximum temperature values the highest saturation temperatures available in Lai's PhD Thesis (2009: p. 120 & 153) that correspond to a pressure level below **20 bar (a)**. More specifically, for **MD_2M** the maximum temperature is **580 K** and for **Butylbenzene** is **630 K**. Therefore, for these two fluids only, the Carnot efficiency is equal to **37.9%** and **42.9%**, respectively. The other three fluids are to be superheated to **660 K**, the same maximum temperature as water's.

After making sure that the temperature and higher pressure levels were within the desired limits, the enthalpy and density data were gathered for each state. Table 4.10 begins with the liquid molar density (**ρ_{mollit}**) of each fluid on their saturated liquid curve at **360 K**. The problem is that Lai's PhD Thesis (2009) presents the data in relation to **moles** and **litres** (**dm^3**), not in SI units. For the density data to be used in Equation 4.17, their units must be converted into SI ones with the conversion factors in Table 4.13. As a result, the specific volume of the liquid phase fluid at **360 K** is simply the reciprocal of density in SI units. After that, the values of specific enthalpy of state **1** were added to the table followed by the pressure and temperature values of state **2**. The data that were collected by Lai's PhD Thesis (2009) are the ones in the columns with the subscript "**mol**" and "**g**", where the latter denotes that the value is that of a saturation point. The specific enthalpy of state **2** was calculated using Equation 4.17 and then added to the Table 4.10 also.

Fluid	ρ_{mollit}	v	T_1	P_1	h_{1mol}	h_1	T_2	P_2	h_2	T_{3g}	T_3	P_3
B	6.06	$1.232x10^{-3}$	360.0	0.0430	12.76	95.22	360.0	19.44	97.61	630.0	630.0	19.44
M2	2.56	$1.259x10^{-3}$	360.0	0.0250	32.32	104.00	360.0	9.02	105.2	580.0	580.0	9.02
M	4.267	$1.447x10^{-3}$	360.0	0.6670	19.42	119.90	360.0	17.45	122.33	510.0	660.0	17.45
M3	2.127	$1.222x10^{-3}$	360.0	0.0063	40.88	106.22	360.0	7.64	107.16	610.0	660.0	7.64
T	8.716	$1.246x10^{-3}$	360.0	0.4898	-4.288	-46.55	360.0	21.21	- 43.97	540.0	660.0	21.21

Fluid	h_{3gmol}	h_{3g}	h_3	T_{4s}	P_4	h_{4s}	$\dot{W}_T$	$\dot{m}$	$\dot{Q}_B$	$\dot{Q}_C$	$\dot{W}_P$	η
B	125.1	933.36	933.36	534.8	0.0430	712.6	20.0	$9.06x10^{-2}$	75.7	55.92	$2.17x10^{-1}$	**26.1**
M2	192.3	618.92	618.92	534.4	0.0250	531.1	20.0	$2.28x10^{-1}$	117.1	97.3	$2.59x10^{-1}$	**16.8**
M	88.54	546.54	873.56	613.4	0.6670	766.9	20.0	$1.88x10^{-1}$	140.9	121.3	$4.55x10^{-1}$	**13.9**
M3	265.3	689.32	796.38	614.4	0.0063	698.6	20.0	$2.05x10^{-1}$	141.0	121.2	$1.91x10^{-1}$	**14.0**
T	52.95	574.97	828.55	563.0	0.4898	620.7	20.0	$9.62x10^{-2}$	83.9	64.2	$2.48x10^{-1}$	**23.5**

Table 4.10: Organic Rankine Cycle ideal configuration for calculation of the ideal (isentropic) efficiency for the five fluids

Variable	Description	Units		Variable	Description	Units
T	Temperature	K		s_g	Specific Entropy at saturation point	kJ/kg-K
T_g	Temperature at saturation point	K		s_{gmol}	Specific Entropy at saturation point	kJ/mol-K
T_s	Temperature after isentropic expansion	K		$\dot{W}_T$	Turbine Output Power	kW
P	Pressure	bar		$\dot{Q}_B$	PTSC Input Power	kW
h	Specific Enthalpy	kJ/kg		$\dot{Q}_C$	Condenser Output Power	kW
h_g	Specific Enthalpy at saturation point	kJ/kg		$\dot{W}_P$	Pump Input Power	kW
h_{gmol}	Specific Enthalpy at saturation point	kJ/mol		$\dot{m}$	Mass Flow Rate	kg/s
v	Specific Volume	m^3/kg		ρ_{mollit}	Molar Density	mol/dm^3
s	Specific Entropy	kJ/kg-K		η	Efficiency Factor	%

Table 4.11: Units and Description of the Variables used for the calculations

For state **3**, the saturation temperature and specific enthalpy data were collected and converted into SI units. $\mathbf{T_{3g}}$ for the first two fluids is the same as $\mathbf{T_3}$ since they are not subjected to superheating; for the other three fluids $\mathbf{T_3}$ is the superheated state temperature at the turbine's inlet and it is equal to **660 K**. With this temperature and $\mathbf{T_{3g}}$ from the saturation data, $\mathbf{h_3}$ can be calculated using Equation 4.14 and adding the result to $\mathbf{h_{3g}}$. $\mathbf{T_{4s}}$ is the theoretical temperature of the fluid at the lower pressure level after its isentropic expansion. So in order to determine, it the non-linear Equation 4.15 is solved by setting it to zero and using the values of $\mathbf{T_3}$, $\mathbf{P_3}$ and $\mathbf{P_4}$. After this, Equation 4.14 is used again with $\mathbf{T_{4s}}$, $\mathbf{T_3}$ and $\mathbf{h_3}$, and $\mathbf{h_{4s}}$ is calculated.

Finally, with the desired power output from the turbine set to **20 kW**, the other three power quantities $\dot{\mathbf{Q}}_\mathbf{B}$, $\dot{\mathbf{Q}}_\mathbf{C}$, $\dot{\mathbf{W}}_\mathbf{P}$, mass flow rate $\dot{\mathbf{m}}$ and the overall ideal efficiency $\boldsymbol{\eta}$ of the cycle are calculated. As one can observe, only Butylbenzene surpasses water in terms of efficiency with **26.1%** against **25.6%** (see Table 4.7) both with the same maximum and minimum temperatures. In the next section the non-ideal efficiency calculations with and without IHE for the five fluids are presented and the results are again compared to the respective non ideal data of water.

Section 4.4.7.2: Non Ideal (Actual) efficiency calculations

Calculating the overall cycle efficiency under ideal conditions and without an IHE, proved that only Butylbenzene is capable of slightly improving the cycle's performance compared to water, while the other four did not. However, as the system would operate in the real world its components have loses that are represented by their individual efficiency coefficients, as described in sections 4.3.2.2 and 4.3.2.3. As a result, in order to examine if the cycle can be improved with the usage of an IHE and if so by which amount, the procedure mentioned in Section 4.3.2.4 is assumed for the five organic fluids as well.

Table 4.12 summarizes the results of this simulation procedure and also contains both the overall cycle efficiencies with and without an IHE, along with the ideal efficiency (without IHE) for comparison. It is obvious that an IHE can significantly improve the overall efficiency of the cycle; more specifically it increases the efficiency of the three siloxanes by at least 2.3 times and also the efficiencies of all five of fluids are higher than water's **14.8%**

under non ideal conditions and with an IHE. As mentioned, the best PV cell in the marketplace today has an efficiency factor of **21.5%** (SunPower, 2014; Energy Informative, 2014). It should be noted that a PV domestic system consists of other components as well, apart from the PV collector. As no real component is 100% efficient, the overall efficiency of a PV system would be well under 21.5% meaning that the system of this project with either **Butylbenzene** or **MD_3M** and with the settings contained in Table 4.12 could be more efficient than the best PV system available today.

Fluid	T_1	P_1	h_{1mol}	h_1	T_2	P_2	h_2	h_{2a}	T_{3g}	T_3	P_3
B	360.0	0.0430	12.76	95.22	360.0	19.44	97.61	432.3	630	630	19.44
M2	360.0	0.0259	32.32	104.02	360.0	9.02	105.16	396.5	580	580	9.02
M	360.0	0.6670	19.42	119.90	360.0	17.45	122.33	600.0	510	660	17.45
M3	360.0	0.0063	40.88	106.22	360.0	7.64	107.16	577.7	610	660	7.64
T	360.0	0.4898	- 4.288	- 46.55	360.0	21.21	- 43.97	309.6	540	660	21.21
Fluid	h_{3gmol}	h_{3g}	h_3	T_{4s}	T_4	T_{4a}	P_4	h_{4s}	h_4	h_{4amol}	h_{4a}
B	125.1	933.36	933.36	534.7	538.5	360.0	0.043	712.6	778.79	59.51	444.1
M2	192.3	618.90	618.92	534.4	533.2	360.0	0.025	531.1	557.45	82.81	266.5
M	88.54	546.50	873.56	613.4	606.1	360.0	0.667	766.9	798.90	52.04	321.3
M3	265.3	689.30	796.38	614.4	615.9	360.0	0.0063	698.6	727.93	99.04	257.4
T	52.95	575.00	828.55	563.0	565.9	360.0	0.4898	620.7	683.06	30.34	329.4
Fluid	$\dot{W}_T$	$\dot{m}$	$\dot{Q}_{B-IHE}$	$\dot{Q}_{C-IHE}$	$\dot{Q}_{B+IHE}$	$\dot{Q}_{C+IHE}$	$\dot{W}_P$	η_{Carnot}	η_{Ideal}	η_{R-IHE}	η_{R+IHE}
B	20.0	$1.29x10^{-1}$	154.5	88.45	92.62	45.14	$2.17x10^{-1}$	**42.9**	26.1	**12.7**	**21.3**
M2	20.0	$3.27x10^{-1}$	240.3	148.6	1040	53.20	$2.58x10^{-1}$	**37.9**	16.8	**8.2**	**18.9**
M	20.0	$2.68x10^{-1}$	287.6	181.9	104.7	53.96	$4.55x10^{-1}$	**45.5**	13.9	**6.7**	**18.5**
M3	20.0	$2.92x10^{-1}$	287.8	181.7	91.29	44.18	$1.91x10^{-1}$		14.0	**6.9**	**21.6**
T	20.0	$1.37x10^{-1}$	171.3	100.3	101.9	51.68	$2.48x10^{-1}$		23.5	**11.5**	**19.3**

Table 4.12: Organic Rankine Cycle configuration for calculation of the non-ideal (actual) efficiency for the five fluids with and without an IHE

Quantity	From	To	Multiplier
Density	mol/litre	kg/m^3	M_r*10^3
Specific Enthalpy	kJ/mol	kJ/kg	M_r
Specific Entropy	kJ/mol-K	kJ/kg-K	M_r
Pressure	bar	Pa	10^5

Table 4.13: Unit conversions and their conversion factors

Comparing with water, the five fluids surpassed even the overall cycle efficiency they had under ideal conditions without IHE. The reason is that these fluids are dry, with the exception of Toluene that is wet; however, it is almost critically isentropic in comparison with water. As seen from Table 4.12, this dry nature of the fluids has the effect that all of them reached a significantly higher temperature $\mathbf{T_4}$ after the turbine expansion at the lower pressure level than the **360 K** water had. Since the thermal energy difference from state **4** to state **4a** is transferred back into the fluid from state **2** to **2a**, it meant that state **2a** would be have a temperature similar to that of state **4**'s. This can also be seen in Figures 4.12 to 4.14 where state **2a** has a similar temperature value as state **4**. This fact decreases the heat input demanded by the PTSC, resulting in the phenomenal increase of the cycle's efficiency.

Section 4.4.7.3: Further improvement of the O_2 cycles

Even though section 4.4.3 explicitly mentions that subjecting dry fluids to superheating would be detrimental to the cycle's efficiency, this section attempts to test if the $\mathbf{O_2}$ cycle fluids could be positively affected by superheating in combination with the IHE. As a result, by changing those fluids' $\mathbf{T_3}$ temperature in Table 4.12 to **660 K** the simulation results, shown in Table 4.14, reveal that this is very much possible:

Fluid		Temperature (K)	$\eta_{R_{-IHE}}$ (%)	$\eta_{R_{+IHE}}$ (%)
Butylbenzene	$\mathbf{O_2}$	630	12.7	21.3
	$\mathbf{O_3}$	660	12.3	22.0
MD_2M	$\mathbf{O_2}$	580	8.2	18.9
	$\mathbf{O_3}$	660	7.1	20.8

Table 4.14: Efficiency improvement of Butylbenzene and MD_2M by superheating them to 660 K

Even though the overall cycle efficiency with superheating and without an IHE was expected to be decreasing, the presence of the IHE in this case benefits the efficiency, as extracted from Table 4.14. Moreover, the increase in efficiency seems to be proportionally correlated with the temperature difference between the states **3g** and **3**. One can clearly see that **MD_2M** increased its efficiency within an **80 K** difference more than **Butylbenzene** did that only increased its temperature by only **30 K**, which is very logical. This means that even dry fluids can be superheated for improving the overall efficiency, as long as the system that utilizes them is fitted with an IHE.

Section 4.4.7.4: Non Ideal (Actual) Supercritical efficiency calculations

As Lai (2009) included only the saturation data of the various fluids he studied in his PhD Thesis, superheated and supercritical data are not available for usage. For this reason, Equations 4.13 to 4.17 were used to generate the missing superheated data in order to produce the results of Tables 4.10, 4.12 and 4.14. In the case of this project, both **MD_2D** and **MD_3D** could have been used in a supercritical **S_2** cycle; however, only equations 4.16 and 4.17 can determine supercritical data regarding the subsaturated liquid region on the T-s diagram, in which the specific volume of the fluid is relatively constant. In contrast, in the superheated region the specific volume in the gas phase changes dramatically with pressure. The other reason is that Equations 4.14 calculates only data in the superheated region and only under constant pressure. Since there are no available supercritical data for the fluids, this equation cannot be used either. So, the equation that can be used in this case for generating supercritical data is the following basic one (Çengel & Boles, 2015: p. 348):

$$\mathbf{dh = Tds + vdP}$$

Equation 4.18: Change of specific enthalpy with changes in specific entropy and Pressure (Çengel & Boles, 2015: p. 348)

The equation can be integrated within its boundary conditions to give the total difference of specific enthalpy between the subcritical superheated state **3** and its supercritical counterpart (**3_{sc}**), as shown in Equation 4.19:

$$\Delta h = h_{3_{sc}} - h_3 = \int_{s_3}^{s_{3_{sc}}} T(s)ds + \int_{P_3}^{P_{3_{sc}}} v(P)dP$$

Equation 4.19: Total difference of specific Enthalpy between the subcritical states 3 and supercritical 3_{sc}

where $\mathbf{h_{3sc}}$ is the specific enthalpy of state **3** at supercritical pressure. The equation can be simplified as state **3** and $\mathbf{3_{sc}}$ have exactly the same entropy, hence the first integral term of the equation is equal to zero. The only difference is between the two states' pressure levels and as a result only the second integral term of the equation is necessary. For that, one must determine the specific volume function **v(P)** and substitute it into Equation 4.19. This is an easy task, as he can extract this function by using the Ideal Gas Law under an isothermal process, since the the temperature values of the **3** and $\mathbf{3_{sc}}$ states are the same at **660 K**. With these conditions the specific volume function and total specific enthalpy difference are shown below in SI units:

$$Pv = \frac{RT}{M_r} \Leftrightarrow \boxed{v(P) = \frac{RT}{PM_r}}$$

$$\Longrightarrow \boxed{\Delta h = \frac{RT}{M_r}\int_{P_3}^{P_{3_{sc}}} \frac{dP}{P} = \frac{RT}{M_r}\ln\left(\frac{P_{3_{sc}}}{P_3}\right)}$$

Equation 4.20: Final version of Equation 4.19 for the purpose of this project

Table 4.15 contains the results of superheating the two fluids to their supercritical pressure level of **20 bar (a)** and how this affects the overall efficiency of the cycle.

Fluid		h_3 (kJ/kg)	P_3 (bar)	$\eta_{R_{+IHE}}$ (%)
MD_2M	O_3	782.68	9.02	20.8
	S_2	796.80	20.0	23.6
MD_3M	O_3	796.38	7.64	21.6
	S_2	810.10	20.0	24.5

Table 4.15: Efficiency improvement of MD_2M and MD_3M in a supercritical cycle at 660 K compared with the normal O_3 cycle

where $\mathbf{h_{3sc}}$ and $\mathbf{P_{3sc}}$ have been replaced with the value of $\mathbf{h_3}$ and $\mathbf{P_3}$, respectively in the supercritical cycle $\mathbf{S_2}$. As expected, the table shows that the overall $\mathbf{S_2}$ efficiency increased when the two fluids are subjected to a pressure level of **20 bar(a)** in comparison with their $\mathbf{O_3}$ efficiency. More specifically, $\mathbf{MD_2M}$ and $\mathbf{MD_3M}$ achieved an overall cycle efficiency of **23.6%** and **24.5%** respectively, both of them greater than the $\mathbf{O_3}$ one of **Butylbenzene**. This proves that siloxanes with low critical pressure points could potentially offer an overall supercritical efficiency greater than the efficiency of the best PV cell. Table 4.17 contains all the above modifications and the various quantities' units are found in Table 4.11.

Section 4.4.8: Working fluid toxicity

The toxicity aspect of the system's working fluid is a serious issue and needs to be addressed. This section presents the toxicity characteristics of the three siloxanes (**MM,** $\mathbf{MD_2M}$ & $\mathbf{MD_3M}$) used for this project and also presents the cases of **Butylbenzene** and **Toluene**.

Section 4.4.8.1: Butylbenzene and Toluene

Here, Table 4.16 contains the safety features of **Butylbenzene** and **Toluene** in accordance with the **29 CFR 1910.1200** safety classification standard (Matheson TriGas Inc., 2014a: p. 1; 2014b: p. 1).

	Butylbenzene	**Toluene**
Acute Toxicity	---	Cat. 4
Skin/Eye Damage	Cat. 2/2A	Cat. 2/2A
Acute Central Nervous System (CNS) Damage	Cat. 3	Cat. 1
Acute Respiratory Tract Damage	---	Cat. 3
Chronic CNS, liver and kidney Damage	---	Cat. 2
Hazards to Aquatic Environment	Cat. 1	Cat. 2
Flammability	Cat. 3	Cat. 2

Table 4.16: Safety Features of Butylbenzene and Toluene (Matheson TriGas Inc., 2014a: p. 1; 2014b: p. 1)

As seen from the table, these two fluids are mildly to extremely hazardous when entered into the human body, they cause mild irritations on skin and eyes and also they are mildly dangerous to aquatic ecosystems, while toxic to aquatic life. Additionally, they are highly flammable in both liquid and vapour phase.

Fluid	Cycle	T_1	P_1	h_{1mol}	h_1	T_2	P_2	h_2	h_{2a}	T_{3g}	T_3
B	O_3	360	0.043	12.76	95.220	360	19.44	97.610	499.3	630	660
M2	S_2	360	0.0259	32.32	104.02	360	9.016	105.16	551.6	580	660
M	O_3	360	0.6670	19.42	119.90	360	17.45	122.33	600.0	510	660
M3	S_2	360	0.0063	40.88	106.22	360	7.648	107.16	577.7	610	660
T	O_3	360	0.4898	- 4.288	- 46.55	360	21.21	- 43.97	309.6	540	660
Fluid	**Cycle**	P_3	P_{3sc} (S_2)	h_{3gmol}	h_{3g}	h_3	h_{3sc} (S_2)	T_{4s}	T_4	T_{4a}	P_4
B	O_3	19.44	19.44	125.1	933.36	1008.1	1008.1	563.4	568.5	360	0.0430
M2	S_2	9.016	20.00	192.3	618.92	782.68	796.80	612.0	612.5	360	0.0259
M	O_3	17.45	17.45	88.54	546.50	873.56	873.56	613.4	606.1	360	0.6670
M3	S_2	7.648	20.00	265.3	689.32	796.37	810.10	614.4	615.9	360	0.0063
T	O_3	21.21	21.21	52.95	575.00	828.55	828.55	563.0	565.9	360	0.4898
Fluid	**Cycle**	h_{4s}	h_4	h_{4amol}	h_{4a}	$\dot{W}_T$	$\dot{m}$	$\dot{Q}_{B_{+IHE}}$	$\dot{Q}_{C_{+IHE}}$	$\dot{W}_P$	$\eta_{R_{+IHE}}$
B	O_3	776.2	845.79	59.51	444.1	20.0	$1.23x10^{-1}$	89.55	42.98	$2.94x10^{-1}$	**22.0**
M2	S_2	683.1	712.97	82.81	266.5	20.0	$2.39x10^{-1}$	83.6	38.79	$2.70x10^{-1}$	**23.6**
M	O_3	766.9	798.90	52.04	321.3	20.0	$2.68x10^{-1}$	104.7	53.96	$4.55x10^{-1}$	**18.5**
M3	S_2	698.6	727.94	99.04	257.4	20.0	$2.43x10^{-1}$	80.83	36.81	$2.27x10^{-1}$	**24.5**
T	O_3	620.7	683.06	30.34	329.4	20.0	$1.37x10^{-1}$	101.9	51.68	$2.48x10^{-1}$	**19.3**

Table 4.17: Organic Rankine Cycle configuration for the non-ideal (actual) efficiency on O_3 and S_2 cycle with an IHE

Even though neither fluid has been rendered by the simulation as the best working fluid for the system (see Table 4.12), the above safety issues can be used as additional deterring factors for using them. Any small leakage from the system's pipelines could cause the above problems to the inhabitants of the household. More specifically, in the case of the odourless **Butylbenzene** (Matheson TriGas Inc., 2014b: p. 4), the inhabitants would possibly be inhaling its leaked vapours without their knowledge for long periods of time, causing them health damage from both acute and chronic exposure, especially to the central nervous system. Fire danger is also extreme, as the fluid's undetectable vapour can ignite with a just one cigarette or a match, two very common items in a household.

Section 4.4.8.2: Siloxanes

The same toxicity evaluation procedure as the one for **Butylbenzene** and **Toluene**, according to the **29 CFR 1910.1200** safety classification standard, was followed for the three siloxanes as well and the results are presented in Table 4.18 (SCB, 2010: p. 1; 2011a: p. 1 & 2011b: p. 1).

	MM	**MD_2M**	**MD_3M**
Flammability	Cat. 3	Cat. 1	Cat. 3
Toxicity	Cat. 0	Cat. 0	Cat. 0
Body Contact	Cat. 2	Cat. 2	Cat. 2
Reactivity	Cat. 1	Cat. 1	Cat. 1
Chronic Effects	Cat. 0	Cat. 0	Cat. 2

Table 4.18: Safety data for MM, MD_2M & MD_3M (SCB, 2010: p. 1; 2011a: p. 1 & 2011b: p. 1)

The table shows that all three of siloxanes are not toxic at all, compared to **Toluene** as indicated in Table 4.17, while they cause moderate irritations to the skin, eyes and respiratory tract. Moreover, all three siloxanes are relatively inert in terms of reactivity with the additional property of **MM** and **MD_2M** of causing no health problems with continuous exposure; **MD_3M** is shown to pose a moderate health threat to the human body. More specifically, it can cause respiratory airway problems, including breathing difficulty (SCB, 2010: p. 2).

Apart from the above advantages that siloxanes have against the other two aromatic candidates, a major disadvantage that all organic compounds possess is flammability. With the exception of **MD_2M**, both **MM** and **MD_3M** are highly flammable, according to Table 4.18. However, detection of any possible siloxanes leakage is relatively easy, as all three of them have a mild and characteristic odour and so the addition of an extra odorant agent is not necessary. This task would alter the composition and ultimately the thermodynamic properties of the fluids (Clearco Inc., 2012a: p. 1; 2012b: p. 1 & 2012c: p. 1).

With all the above safety and performance features in mind, the two best candidate working fluids are **MD_2M** and **MD_3M**, as they both have the greatest efficiency factors of the five, **23.6%** and **24.5%** respectively and as siloxanes are not toxic to the human body at all and almost chemically inert. However, **MD_3M** is shown to have chronic moderate chronic health effects and it is highly flammable, whilst **MD_2M** has the lowest flammability risk and also has no chronic effects. Even so, since detection of these compounds is easy and since the auto-ignition temperature of **MD_3M** is over **400 ºC** (according to Table 4.9) **MD_3M** is the most favourable compound for the system's working fluid and its data will be the ones used from this point on.

Section 4.4.9: Sizing the Steam Accumulator (SA)

The Steam Accumulator (SA) is the component used as a buffer between the steam generation side and the turbine side of the concept systems, as this is shown in Figure 4.1. Its role is to collect the generated pressurized Working Fluid Vapour (WFV) that does not have a stable flow rate from the collector side and release it into the main circuit at exactly the mass flow rate $\dot{m}$ calculated with the simulation and shown in Table 4.16, ensuring the production of stable voltage and frequency electricity from the electrical generator.

For this project, the SA's constraint is that it needs to hold one hour's worth of WFV at **660 K** (**390ºC**) and **20 bar (a)** with supercritical specific enthalpy **h_{3sc}**, given again in Table 4.16. Another specification is that the SA needs to be filled with at least with the same rate as it releases WFV into the main circuit, meaning that at the worst case the amount of WFV the SA holds remains constant. In better cases the SA could be filled with a faster rate than the main circuit's mass flow rate, so the flow of WFV from the collector/storage side

would be interrupted until a certain amount of WFV is released. In order to calculate the size of the SA, the cases of charging and discharging are examined below.

Section 4.4.9.1: Discharging the SA – Total mass of stored WFV

Since the SA is designed to hold one hour's worth of WFV, the easiest way to calculate the total mass of that WFV is to use the simple relationship between the calculated mass flow rate of the main circuit, the mentioned WFV total mass and the time it takes to fully discharge the SA. This relationship is given by Equation 4.21 and the results are presented Table 4.19:

$$\dot{m} = \frac{m_{SA}}{t_{SAd}}$$

$$\Leftrightarrow \boxed{m_{SA} = \dot{m} t_{SAd}}$$

Equation 4.21: Total WFV mass the SA needs to hold

Property name	Property	Units	Value
Main system mass flow rate	$\dot{m}$	kg/s	2.43×10^{-1}
Total discharge time of the SA	t_{SAd}	s	3600
Total mass of WFV stored in the SA	m_{SA}	**kg**	**874.5**

Table 4.19: Calculation of the total WFV mass stored in the SA (data from Table 4.16)

For safety reasons and since the charging and discharging of the SA take place with the same flow rates at the worst, it does not need to be fully filled at all times; only in the cases that the flow rate of charging is greater than the one of discharging the SA could be filled up to **90%**. Then the charging could be halted and continue after the SA would have been discharged below a certain level, for example **10%**. These actions are monitored and controlled by the Computerised Control Subsystem (CCS).

Section 4.4.9.2: Charging the SA – Minimum charging power

Even if the Collector, the Thermal Storage Tank or the Natural Gas Boiler are charging the SA, the WFV charging mass rate should be at least the same as the mass flow

rate of discharge as mentioned above. It should be noted that even though the Thermal Storage Tank (ThST) in Concept System 2 and the natural gas Boiler (NGB) of Concept System 3 are capable of feeding their main circuit with a stable flow of WFV, the SA should not be omitted for safety reasons in case the system needs to be evacuated of its working fluid and also for the system to be allowed to operate for an hour more after the solar irradiance is reduced below its reference value or if the collector side of the system is damaged.

With this in mind, this section presents the calculation of the minimum output power (thermal energy rate) of the component charging the SA, while it feeds the main circuit with WFV at the calculated system flow rate $\dot{\mathbf{m}}$, shown in Table 4.16. As a result, the feed in mass flow rate of the SA must be greater or equal to $\dot{\mathbf{m}}$. Furthermore, this suggests that the power output of the collector/storage or NGB must also be greater or equal to the power output of the SA. To calculate this minimum power rating of the WFV (in this case **MD$_3$D**) producing components, Equation 4.22 is used and the results are shown in Table 4.20:

$$\dot{W}_x = \dot{m}_x(h_{3sc} - h_{2a}) \geq \dot{m}(h_{3sc} - h_{2a})$$

Equation 4.22: Generic power output of a WFV generator feeding the SA

where, **x** is the index of the charging component: **Col** for the Collector, **ThST** for the Thermal Storage Tank and **NGB** for the natural gas Boiler. This value is used in the next sections for calculating the size of the ThST of Concept System 2 and the total amount of natural gas of Concept System 3. Moreover, since both the ThST and the NGB are components that are capable of charging the SA with a stable mass flow rate, the inequality can be omitted and Equation 4.22 can be a pure equality. The only case the inequality is necessary is that of the collector charging the SA directly in Concept System 1, as solar irradiance is variable throughout the day.

Property name	Property	Units	Value
Main system mass flow rate	$\dot{m}$	kg/s	2.43×10^{-1}
Specific enthalpy of state 3 (supercritical)	h_{3sc}	kJ/kg	810.10
Specific enthalpy of state 2a	h_{2a}		577.70
Component x's minimum power output	$\dot{W}_x$	kW	56.47

Table 4.20: Calculation of the SA charging component's minimum power output (data from Table 4.17)

Section 4.4.10: Charging the DHW tank – Determining the tank's recovery time

The tank storing the amount of DHW of the household is the final component of Concept System 1 that needs to be sized. As seen in Figure 4.1, there is a Non Storing Calorifier (**NSC**) assuming the role of the system's condenser and a Storing Calorifier (**SC**) that stores and heats the needed amount of DHW. The figure also indicates that the working fluid after exiting the outlet of the ST enters the Bypass Valve, which it diverts it into the SC (when needed) for warming the DHW from **20** to **60 ºC**. Obviously, the working fluid flows through the SC's internal heat exchanger with the main system's mass flow rate for transferring the thermal energy difference between states **4** and **1** (see Table 4.16), so that it becomes fully condensed and passes through the Steam Separator (**SS**) into the CStT. This lost thermal energy from the WFV is transferred into the stored water following the Equation 4.23 below:

$$\dot{Q}_{DHW} = -\dot{m}(h_1 - h_4) = \frac{\rho_w V_{DHW} c_w \Delta T}{t_r}$$

Equation 4.23: DHW Storage Calorifier's duty

At this point it is worth mentioning that a typical DHW storage tank in Cyprus has **150 – 200 litres** capacity (CEA, 2010: p. 5); however this capacity does not include the demand of a clothing washing machine and a dishwasher. So, the typical daily amount of hot water per person used in the UK is a good approximation to the DHW demand of a Cypriot household. As a result, the daily total volume of the DHW is taken to be **225 litres** (5 people x 45 litres per person). All the data needed for this calculation are shown in Table 4.21. After completing all the necessary calculations, the final modified block diagram for Concept System 1 (with the IHE) is presented in Figure 4.15. The numbers in green indicate the thermodynamic state that the working fluid is in at each point of the diagram. It should be noted that the density of water that has been used for this calculation is the maximum one at **4 ºC**. The project's design temperature range of DHW is between **20** and **60 ºC**; at those temperatures the density of water is **0.998** and **0.983 kg/litre**, respectively. This means that at worst (at **60 ºC**) the density of water is smaller only by **1.7%** than the used value, which is a negligible error for this calculation (The Engineering Toolbox, 2014).

Property name	Property	Units	Value
Main system mass flow rate	$\dot{m}$	**kg/s**	2.43×10^{-1}
Specific enthalpy of state 1	h_1	**kJ/kg**	106.22
Specific enthalpy of state 4	h_4		727.94
DHW Storage Calorifier duty	$\dot{Q}_{DHW}$	**kW**	**151.1**
Total daily DHW volume	V_{DHW}	**litres**	225
Specific heat capacity of water	c_w	**kJ/kg-K**	4.19
Density of water	ρ_w	**kg/litre**	1
Design temperature increase of DHW	ΔT	**ºC (K)**	40
Storage Calorifier's Recovery Time	t_r	**s**	**249.57**

Table 4.21: Calculation of the DHW storage tank's recovery time (data from Table 4.17)

In summary, the small scale of a Rankine cycle based system operating at **20 bar(a)** and **400 ºC** cannot utilize water as its working fluid. The reason is that water is a "wet" fluid and even with the usage of an Internal Heat Exchanger (IHE), would have a thermal-to-electrical efficiency factor of about **15%** (see Table 4.8). For this reason, organic "dry" siloxane fluids were studied and that proved that if **MD_3M** would be used as the cycle's working fluid with the same settings as water and the addition of the IHE, it would offer an efficiency factor of about **25%** instead of **15%** (see Table 4.15). This concludes the study of the basic direct WFV generation concept system, which acts as the blueprint for the other two. The next sections describe the methodology for sizing the extra components of the other two concept systems, such as the Thermal Storage Tank (ThST) containing the Thermal Storage Medium (TSM) and the Natural Gas Boiler (NGB).

Section 4.5: Concept System 2 (Direct WFV Generation with Thermal Storage)

Section 4.5.1: Introduction

This section describes the operation of the second concept system of this project, the one appearing in Figure 4.15 and it is fitted with thermal storage. This storage is charged by the PTSC during daytime and that stored energy is being utilized during night time. The section also contains the calculations regarding the sizing of the ThST, depending on the amount of time it is set to provide the system with thermal energy throughout the day.

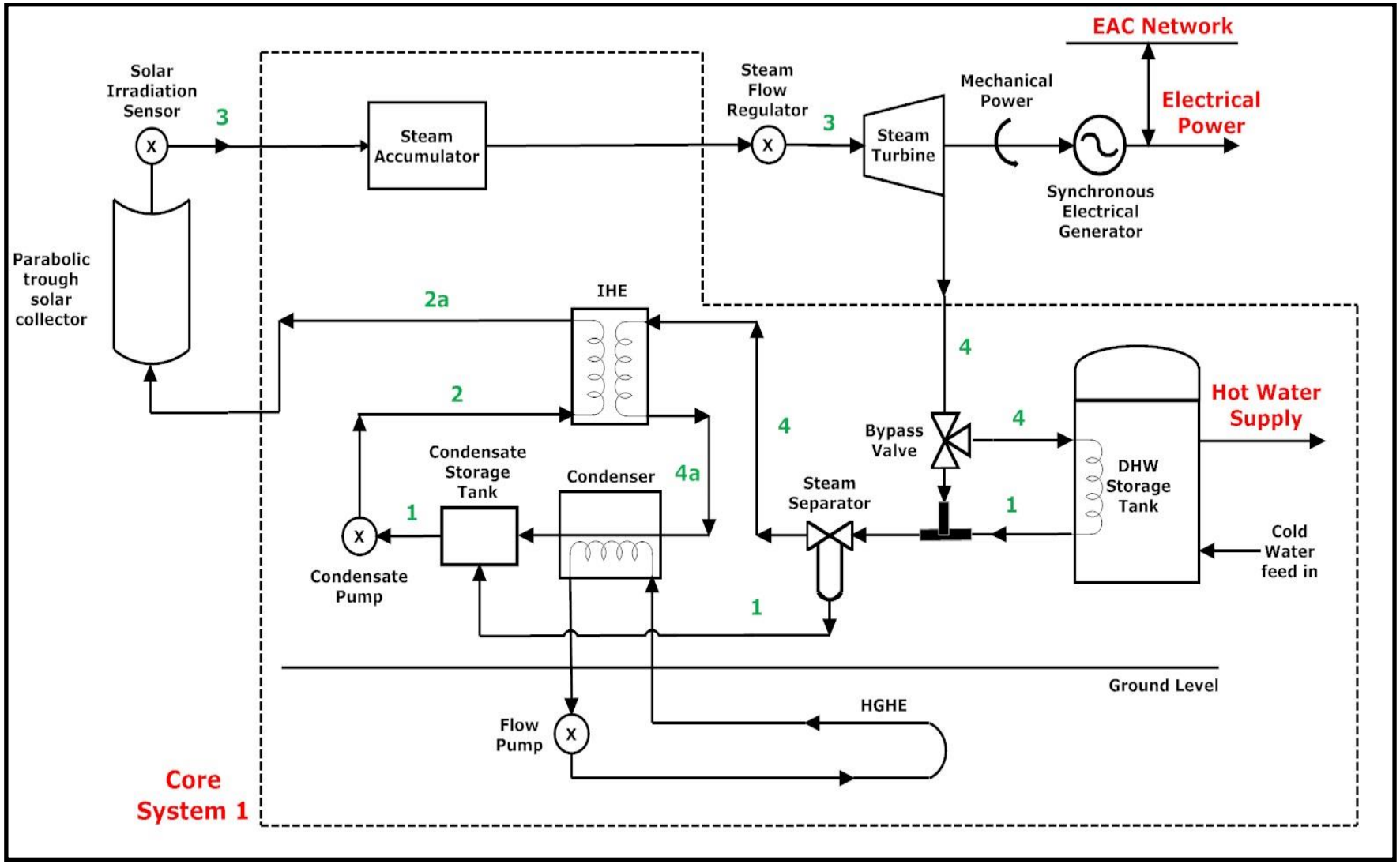

Figure 4.15: Final form of Concept System 1 (with IHE)

Section 4.5.2: Types of Thermal Storage

As mentioned in Section 3.2.2, there are three types of thermal storage, depending on the natural mechanism that the storage material or medium absorbs and/or releases thermal energy into the system, according to Medrano et al. (2010: pp. 37 – 40) and Tian and Zhao (2013: pp. 543 – 545):

a) **Sensible Heat Storage:** In this type, the storage medium absorbs thermal energy from the collector by raising its temperature according to Equation 4.24:

$$\mathbf{Q = m_{TSM} c_{TSM} \Delta T}$$

Equation 4.24: Fundamental law for sensible heat transfer

where, **Q** is the amount of heat being absorbed/released by the storage medium in **J**, $\mathbf{m_{TSM}}$ is the total mass of the Thermal Storage Medium (**TSM**) in **kg**, $\mathbf{c_{TSM}}$ is its specific heat capacity measured in **J/kg-K** and finally **ΔT** is the medium's difference in temperature during the heat absorption/release cycle in **K** or **ºC**. Storage materials for the sensible heat type are in either solid or liquid phase, they operate between **200** and **1200 ºC**, they have great thermal conductivities and they are cheap to purchase. However, they also have low specific heat capacities and this has an impact on the size of the storage tank. Such materials include oils, liquid sodium and molten salts. The use of oils raise serious safety issues as they require high vapour pressure, while liquid sodium has a high thermal conductivity of **71 W/m-K** but it is highly chemically unstable, which also raises safety issues. Molten salts, on the other hand are extremely stable on high temperatures, they are non-toxic, non-flammable and they have high thermal conductivities, making them the most suitable type of medium for solar thermal applications (Tian & Zhao, 2013: p. 544).

b) **Latent Heat Storage:** The second type of thermal storage refers to materials that absorb/release heat by changing their phase, according to Equation 4.25:

$$\mathbf{Q = m_{TSM} L_{TSM}}$$

Equation 4.25: Fundamental law for latent heat transfer

where, $\mathbf{L_{TSM}}$ is the specific latent heat capacity of the TSM measured in **J/kg**. The materials used for this type of thermal storage are called Phase Change Materials (**PCM**) and they are capable of storing greater amounts of energy than the sensible heat type under an almost constant temperature (isothermal process). Their disadvantage is their low thermal conductivities, from about **0.2** to **0.7 W/m-K**, leading to the usage of thermal transfer enhancing materials and techniques for better performance (Tian & Zhao, 2013: p. 544).

Cárdenas & León (2013: pp. 729 – 733) present several techniques that enhance the thermal absorbing/releasing capability of the latent heat storage type. The first technique is employing fins made from graphite, copper, aluminium or steel inside the ThST, which they have high conductivity values, melting points and corrosion resistance when they are in contact with the TSM. These fins allow heat conduction to occur in smaller distances inside the TSM's volume, thus increasing the rate of that conduction according to Equation 4.32 and they are suitable for temperatures below **400 ºC**. Another technique is the usage of a porous metallic or graphite matrix with high conductivity. This matrix, depending on its porosity, would increase the surface area for heat conduction and also it would assist natural convection movement during the melting process. Graphite and metal particle can also be dispersed inside Phase Change Materials, instead of existing on a fixed matrix. This technique is much simpler that the previous one and the matrix's porosity factor is not an issue in this case. The last technique in this list is the usage of multiple PCMs with different melting points. These PCMs are placed in separate layers inside the ThST by decreasing order of their melting points, ensuring that each layer would receive heat under a constant temperature difference, thus increasing the performance and uniformity of energy storage.

c) **Chemical Storage:** The last type of thermal storage is based on the reversibility of their media's chemical reactions, storing or releasing even more thermal energy that the latent heat type with the formation of chemical bonds. Several examples of such reactions are listed in Table 4.22 (Tian & Zhao, 2013: p. 545):

Material Types	Temperature Range (°C)	Energy Density (GJ/m^3)	Chemical Reaction
Iron Carbonate ($FeCO_3$)	180	2.6	$FeCO_3 \rightleftharpoons FeO + CO_2$
Metal Hydrides	200 – 300	4	$xCaH_2 \rightleftharpoons yCaH_2 + (x - y)H_2$
Metal Hydroxides	500	3	$Ca(OH)_2 \rightleftharpoons CaO + H_2O$
Calcium Carbonate ($CaCO_3$)	800 – 900	4.4	$CaCO_3 \rightleftharpoons CaO + CO_2$

Table 4.22: Examples of chemical thermal storage reactions (Tian & Zhao, 2013: p. 545)

As this type of TSM has not been researched thoroughly yet, this technology has many problems needed to be solved before it becomes a reliable adversary of the other two types. The mentioned problems include complicated chemical reactions for a number of media, chemical stability during the reaction and the preservation of the reaction's long term reversible strength (Tian & Zhao, 2013: p. 544 – 545).

Section 4.5.3: Selection of the storage medium and sizing of the ThST

The selection of the TSM is a serious issue as this determines the size of the Thermal Storage Tank (**ThST**) and therefore the financial and spatial cost of it. The TSM should be of **latent heat** type as it would have greater storage density without any temperature variation compared to a sensible heat type material, while a chemical type material would be expensive and certainly it is unreliable for the reasons listed above. In addition, the WFV generation side of the system that utilizes a latent heat type material is much simpler than the sensible heat one, as observed from the Figures 4.16 and 4.17. In the **sensible heat** storage type the TSM is stored inside the ThST and circulates through both the collector and PCHE, whilst in the **latent heat** type the TSM remains inside the ThST and exchanges heat through internal thermal coils. The reason is that if the TSM moving through pipelines solidified, it would leave crystal residue on the inner surface of those pipeline, thus reducing the efficiency of both the collector and the PCHE. So, the collector would collect and transfer heat into the TSM with a sensible heat type medium with a high specific heat capacity.

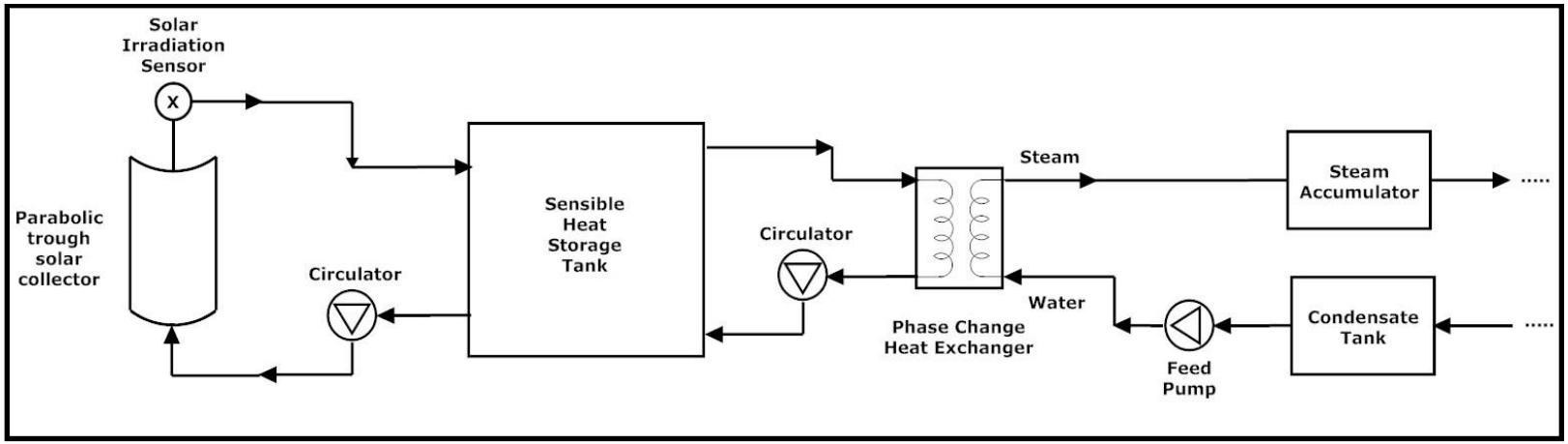

Figure 4.16: WFV generation side when using a sensible heat storage medium

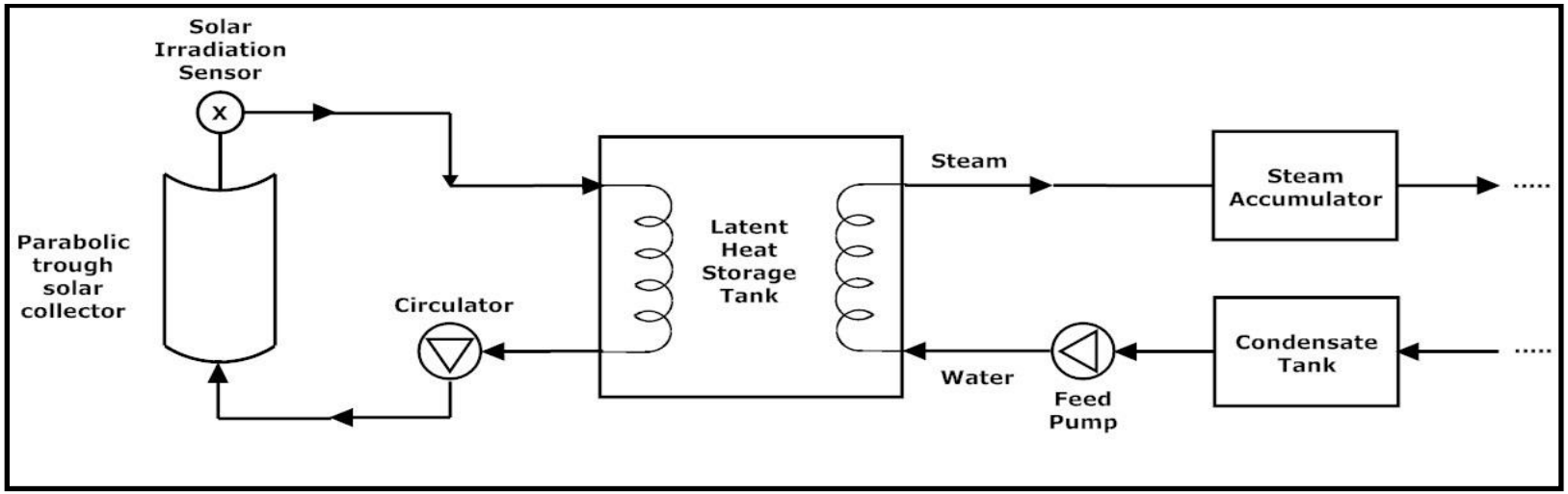

Figure 4.17: WFV generation side when using a latent heat storage medium

Section 4.5.3.1: Selecting the TSM

The selection criteria for the TSM are the following:

a) **High storage density:** The TSM should have the capability of absorbing large amounts of heat per m^3 and so a relatively small volume of material could cover the energy needs of the household

b) **Melting point close to 660 K:** Its melting point should be lower or equal to **660 K** (**390 ºC**) in order to begin melting and store latent heat at that temperature. Moreover, since the heat exchange would occur at that constant temperature, the WFV would possess that temperature value as well.

c) **Cheap:** The price per m^3 should also be as low as possible for reducing the overall cost of the system.

d) **Chemical stability at temperature range:** For reliability and safety purposes, the TSM must not disintegrate and/or decompose around the operating temperatures. This fact also contributes to the TSM having a longer life span. Several authors mention the life span of concentrating solar power plants to be between **20** and **30 years** (Portaspana, 2011: p. 6) and **30 years** (Kuravi et al., 2013: p. 298 & Mathur et al., 2014: p. 910). The durability of the salt is basically dependent on whether the salt mixture remains homogeneous during the charge/discharge cycle and does not create areas of different densities throughout its body.

Naumann and Emons (1989: p. 1010) advocate that salt hydrates are suitable latent heat type of TSMs for solar applications with high storage densities (**200** – **600 MJ/m^3**); however their melting points are lower than **390 ºC** (more specifically they are lower or equal to **120 ºC**) and so they are only suitable for DHW applications and not for the purposes of this project. Moreover, the authors mention that salts in general have a broader storage density range (**150** – **1100 MJ/m^3**) in addition to a variety of melting points (**90** – **1300 ºC**) (Naumann & Emons, 1989: p. 1010) but their entire paper examines only the salt hydrates as potential latent heat type TSMs. Kenisarin (2010), on the other hand, wrote a review paper listing an array of salt eutectic compositions of various alkali and alkaline earth metals at various percentages per mole. He shows that pure salts of the mentioned metals have limited applications, as they

have relatively high melting points (over **400 ºC**) with very few exceptions and specific latent heat capacities that limit their technological application (Kenisarin, 2010: p. 957). He then lists several eutectic compositions of salts that have been developed by various researchers over the years, in which several of them had eutectic melting points below **390 ºC** (**660 K**). So, in order to find the composition ratio of those salts systems for achieving a melting point at exactly **390 ºC** (**660 K**), engineers use the phase diagram of the desired eutectic system. For reasons of data availability and time management one such system was selected and its characteristics as well as its phase diagram are presented in Table 4.23 (Kenisarin, 2010: p. 958, Basin et al., 2008: p. 1510 & Sridharan, 2012: p. 3) and Figure 4.18 (Basin et al., 2008: p. 1510) respectively. From the phase equilibria data in their paper, Basin et al. (2008: p. 1509) also show the numerical values that lead to the construction of the phase diagram and the composition ratio that has a melting point of exactly **390 ºC** (**660 K**) is also shown in Table 4.23. The red circle on the phase diagram indicates this composition.

Property	Units	Value
Salt System	---	LiCl – KCl
Eutectic Point	ºC (K)	348 (618), 352 (622), 355 (625)
Specific Latent Heat Capacity	kJ/kg	170
Composition with melting point of 390 ºC	%mol	45% KCl – 55% LiCl

Table 4.23: Eutectic salt's properties (Kenisarin, 2010: p. 958; Basin et al., 2008: p. 1509 & Sridharan, 2012: p. 3)

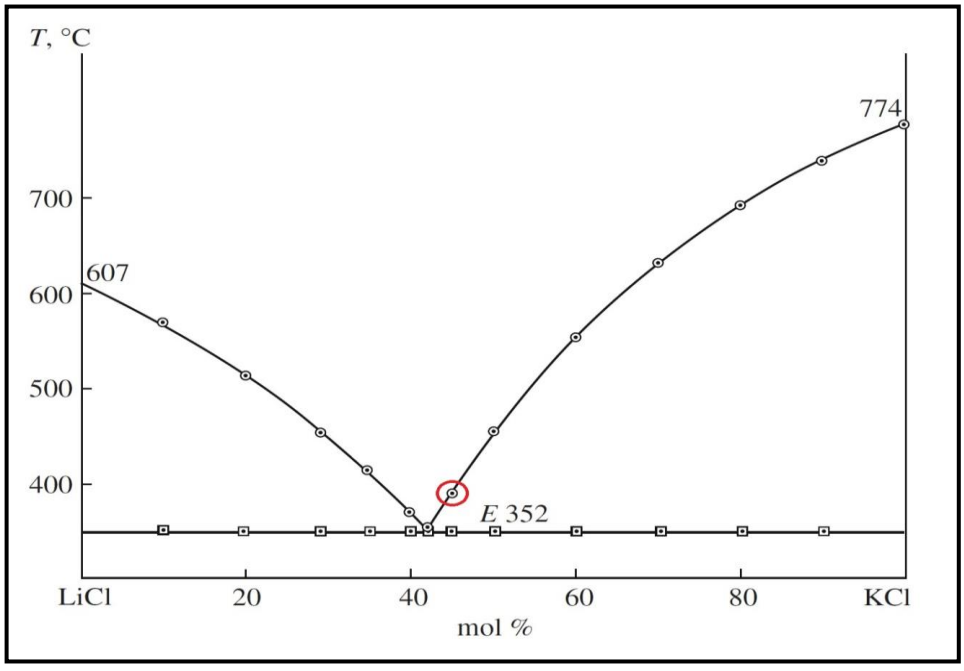

Figure 4.18: LiCl – KCl system phase diagram (Basin et al., 2008: p. 1510)

Section 4.5.3.2: Discharging the ThST – Total mass of TSM

Since the calculations in Section 4.4.9.2 established the minimum thermal energy rate to charge the SA and this rate being essentially the power output of the WFV generation component, this section presents the calculations regarding the total mass of the TSM selected in the previous section. In the case of Concept System 2, the ThST is the one charging the SA and so it is acceptable for the power output of the ThST to be exactly the same as the charging power of the SA. Equations 4.26 and 4.27 determine the total amount of TSM the system needs and the size of the ThST. The results are shown in the Table 4.26.

$$\dot{W}_{ThS} = \frac{m_{TSM} L_{TSM}}{t_{ThS}} = \dot{m}(h_{3sc} - h_{2a}) \Leftrightarrow \boxed{m_{TSM} = \frac{\dot{W}_{ThS} t_{ThS}}{L_{TSM}}}$$

Equation 4.26: Total mass of TSM

$$\rho_{TSM} = \frac{m_{TSM}}{V_{TSM}} \Leftrightarrow \boxed{V_{TSM} = \frac{m_{TSM}}{\rho_{TSM}}}$$

Equation 4.27: Total volume of TSM and the size of the ThST

The density data ρ_{TSM} of the eutectic system mentioned above is given explicitly in William's report (2006: p. 12) and are shown in Table 4.24:

Property	Units	Value
Solid density (at 20 ºC)	kg/m^3	2034
Solid density (at melting point 355 ºC)		1853
Liquid density (at melting point 355 ºC)		1691
Solid – Liquid density difference	%	- 8.8
Solid (at 20 ºC) – Liquid density difference		- 16.9

Table 4.24: Physical properties of the LiCl – KCl system on the eutectic composition (Williams, 2006: p. 12)

However, that data refer to the eutectic composition of the salt system and not to the 45KCl – 55LiCl composition that this project needs. So, given the salt's molar fractions from its chemical formula, the mixture density is calculated using the following procedure. This will also examine how close the density values of the eutectic composition (41.7KCl – 58.3LiCl) are to the slightly different composition mentioned above.

In basic chemistry studies, one learns to use the molar mass $\mathbf{M_r}$ and number of moles **n** of a substance in solving problems instead of using the regular mass **m** of that substance. This makes calculations easier as the chemical formula of that substance represents the ratio of the atoms constituting it and does not need to involve the actual mass of each atom. For example the chemical formula of water ($\mathbf{H_2O}$) states that in each molecule of water there are 2 atoms of hydrogen and 1 atom of oxygen, ignoring the fact that an oxygen atom is heavier that a hydrogen atom. In the case of a mixture compound, in which its components do not react with each other, the chemical formula indicates the **molar fraction** ($\mathbf{x_i}$) of each component that in essence is the molar percentage of that component substance in the mixture. By seeing the composition data of Table 4.23, one can derive that it consists of **45%** of potassium chloride (**KCl**) and **55%** of lithium chloride (**LiCl**). In addition to the molar fraction, there is the related **mass fraction** ($\mathbf{w_i}$) that represents the mass ratio of each component compared to the total mass of the salt. These two types of fraction are mathematically described in Equation 4.28:

$$\boxed{x_i = \frac{n_i}{\sum n_i}}\ (1), \qquad \boxed{w_i = \frac{m_i}{\sum m_i}}\ (2)$$

Equations 4.28: Definition of the molar and mass fraction

The two types of fractions are related to each other. This is proven in the next series of steps, leading to Equation 4.29:

$$m = nM_r \Rightarrow m_i = n_i M_i \Rightarrow \frac{m_i}{\sum m_i} = \frac{n_i M_i}{\sum m_i}$$

$$\Rightarrow w_i = \frac{n_i M_i}{\sum n_i M_i} = \frac{n_i M_i}{\sum (x_i \sum n_i) M_i} = \frac{n_i M_i}{\sum n_i \sum x_i M_i} = \frac{n_i}{\sum n_i} \frac{M_i}{\sum x_i M_i} = x_i \frac{M_i}{\sum x_i M_i}$$

$$\Rightarrow \boxed{w_i = x_i \frac{M_i}{M_r}}$$

Equation 4.29: Relation between mass and molar fractions

where in this case $\mathbf{M_r}$ represents the average weighted molar mass of the compound. After deriving the relationship between the two fraction types, the next stage is to produce an

equation that calculates the overall density of the compound, using Equation 4.29. Before the procedure begins, however, the assumption that the volumes of the individual component salts are **additive** should be made. The steps that follow lead to the determination of the eutectic mixture's overall density, which is shown in Equation 4.30; they are based on the relations derived in Equation 4.29.

$$\rho = \frac{m}{V} \Rightarrow \rho_i = \frac{m_i}{V_i} \Leftrightarrow V_i = \frac{m_i}{\rho_i} = \frac{w_i m}{\rho_i} = \frac{x_i M_i m}{M_r \rho_i}$$

$$V = \sum V_i = \sum \frac{x_i M_i m}{M_r \rho_i} = \frac{m}{M_r} \sum \frac{x_i M_i}{\rho_i} \Rightarrow \rho = \frac{m}{\frac{m}{M_r} \sum \frac{x_i M_i}{\rho_i}} = \frac{1}{\frac{1}{M_r} \sum \frac{x_i M_i}{\rho_i}}$$

$$\Rightarrow \boxed{\rho = \frac{M_r}{\sum \frac{x_i M_i}{\rho_i}}}$$

Equation 4.30: Overall mass density of the eutectic salt in relation with its components' molar masses and fraction

where the variables with the **i** subscript refer to the properties of the eutectic's components, while the variables lacking a subscript refer to the properties of the eutectic compound salt as a whole. The next section concentrates the molar fractions and masses of the salt's components and presents the calculations of the desired overall density of the salt.

The molar fractions of the eutectic salt in Table 4.23 are given by its composition formula; the molar mass of each component can be found in suppliers' websites. The data and calculated quantities are presented in Table 4.25 (FSE, 2012: p. 2 & 2013: p. 3). An additional issue that needs to be addressed before the overall composition density calculation is that since the TSM melts during the energy absorption process, its density decreases from a sudden increase in its volume, as seen in Table 4.24 (Williams, 2006: p. 12). The mentioned change in density is attributed exclusively to the collapse of the crystal lattice, since the temperature is constant during phase change. Therefore, this density decrease of the component salts is independent of temperature and thus the melting point. The solid density result in red of Table 4.25 is compared with the density of the eutectic composition (41.7KCl – 58.3LiCl) in Table 4.24, which they differ only by **0.88%**. So the theoretical data of Table

4.25 are indeed reliable as they are proximate to the experimental data of Table 4.24 (Williams, 2006: p. 12). The liquid density at the melting point (**390 ºC**) of the needed composition (45KCl – 55LiCl) is therefore easily calculated by using the difference percentage between the 20 ºC solid and liquid density of 41.7KCl – 58.3LiCl (**-16.9%**). The liquid density is shown in the last row of Table 4.25, again in red; it is only **0.92**% less than the liquid density of the eutectic composition at the melting point (**355 ºC**).

Property name	**Property**	**Units**	**Value**	
			KCl	**LiCl**
Component molar mass	$\mathbf{M_i}$	**kg/mol**	74.56	42.38
Component molar fraction	$\mathbf{x_i}$	---	0.45	0.55
Component density	$\boldsymbol{\rho_i}$	**kg/m^3**	1987	2060
Overall composition molar mass	$\mathbf{M}$	**kg/mol**	**56.86**	
Overall composition solid density	$\boldsymbol{\rho_{TSMs}}$	**kg/m^3**	**2016.3**	
Overall composition liquid density	$\boldsymbol{\rho_{TSMl}}$		**1675.5**	

Table 4.25: Calculation of eutectic salt's overall density (data from Table 4.23 and FSE, 2012: p. 2 & 2013: p. 3)

After calculating the eutectic salt's overall density, the next step is the calculation of the total mass and volume of the TSM; these figures are useful for estimating the size of the ThST. The last step for this estimation is the total duration of the ThST's usage. In order to ensure the system operates completely and reliably throughout the year $\mathbf{t_{ThS}}$ is assumed to be the time period that solar irradiance is below **200 W/m^2** during the weakest month. The only data useful for this task are those seen in Figure 4.19 (Koroneos et al., 2005: p. 1896); all other data sources for Cyprus show cumulative annual or mean monthly values of both Global Horizontal Insolation (GHI) and Direct Normal Insolation (DNI) in **kWh/m^2** and not solar irradiance (solar radiation flux) ones in **W/m^2**. Figure 4.19 also presents DNI data in **Wh/m^2/h**; however since they are hourly data, the average value of solar irradiance during each hour of day time can be calculated by simplifying the given units to **W/m^2**. So, Figure 4.19 indicates that the worst month for solar irradiance is December and so the total time span that solar irradiance is over **200 W/m^2** is about **3.5 hours** (between 10:00 and 13:30). Subtracting that amount from **24 hours** and $\mathbf{t_{ThS}}$ is taken to be **20.5h**. The rest of the given data are taken from sections 4.4.9.2 and 4.5.3.1 and Table 4.25, while Equations 4.26 and 4.27 are used.

Property name	Property	Units	Value
Thermal Storage power output ability	$\dot{W}_{ThS}$	**kW**	56.5
TSM's latent heat capacity	L_{TSM}	**kJ/kg**	170
Total time span for the ThST to discharge completely	t_{ThS}	**10^3 s**	73.8
Total amount of TSM needed	m_{TSM}	**10^3 kg**	**24.53**
TSM liquid density	ρ_{TSM}	**kg/m^3**	1675.5
Total volume of ThST	V_{TSM}	**m^3**	**14.6**

Table 4.26: Calculation of the ThST's size (data from sections 5.4.9.2 and 5.5.3.1 and Table 4.25)

The calculated figure of about **15 m^3** is basically the volume of a cubic ThST with edge length of about **2.5 m**, a relatively realistic figure for a single household. Some safety space is required for thermal expansion tolerance of the eutectic salt.

Section 4.5.3.3: Charging the ThST – Total collector area

As with the case of SA so the ThST needs to be charged with thermal energy, instead of WFV, with exactly the same principles: the charging procedure should occur at a rate greater or equal to the discharging rate. As the ThST is directly charged by the collector, the inequality of Equation 4.22 must be conserved and the equation itself can be modified as presented in Equation 4.31 and the calculation results are presented in Table 4.26. This issue is not only specific for Concept System 2; it is rather an issue of the basic blueprint of the three scenarios. So, in order to ensure that $\mathbf{A_{Col}}$ is sufficient for the systems to operate the longest throughout day time around the year, an examination of hourly solar irradiance data for every month is needed. These data are capable of assisting the calculation of $\mathbf{A_{Col}}$.

$$\dot{W}_{Col} = \eta_B \dot{W}_B = \eta_B I_b A_{Col}$$

$$\dot{W}_{Col} \geq \dot{W}_{ThS} \Leftrightarrow \eta_B I_b A_{Col} \geq \dot{W}_{ThS}$$

$$\Leftrightarrow \boxed{A_{Col} \geq \frac{\dot{W}_{ThS}}{\eta_B I_b}}$$

Equation 4.31: Minimum total collector surface area

After the examination of Figure 4.19, the worst months in terms of DNI are January and December, registering about **250 W/m^2** as their daily peak irradiance value. As the specifications of the project require that the optimal system should operate effectively the longest throughout the year, it is obvious that it should operate effectively during the periods with the weakest levels of solar irradiance as well. For this reason, Table 4.27 assumes two different minimum values of $\mathbf{I_b}$ for the system to start operating, in order to calculate the minimum surface area of the collector $\mathbf{A_{Col}}$.

Property name	Property	Units	Values	
Minimum required absorbed solar power	$\dot{W}_{Col}$	kW	56.5	
Collector's efficiency	η_B	%	70	
Min. Direct Normal Irradiance for system operation	I_b	W/m^2	100	200
Minimum total surface area of the collector	A_{Col}	m^2	**807.14**	**403.57**

Table 4.27: Calculation of the PTSC's minimum required surface area (data from Section 4.5.3.2 and Figure 4.19)

As seen from the above table, the minimum value of $\mathbf{A_{Col}}$ for a start operation $\mathbf{I_b}$ value of **100 W/m^2** is **807.14 m^2**, which is an unrealistic number for a domestic application. Equation 4.31 shows that the values of $\mathbf{A_{Col}}$ and $\mathbf{I_b}$ are inversely proportional, so by increasing the tolerance of $\mathbf{I_b}$ the $\mathbf{A_{Col}}$ can be reduced. So if $\mathbf{I_b}$ increases to **200 W/m^2** then $\mathbf{A_{Col}}$ is halved and becomes **403.57 m^2**, which is also unrealistic. In other words, one would need to have a flat surface area on his roof large enough to host of about two, **24.5 m** x **7.51 m UltimateTrough** solar collectors or about five, **13.9 m** x **6.0 m SkyTrough** collectors (NREL, 2015: p. 4). Even a typical household in Cyprus with a surface area between **101** and **150 m^2** (see Figure 2.9 in Section 2.3.2) would not be capable of hosting a collector with an area of this size. Improvements for solving this problem are being proposed in Chapter 5.

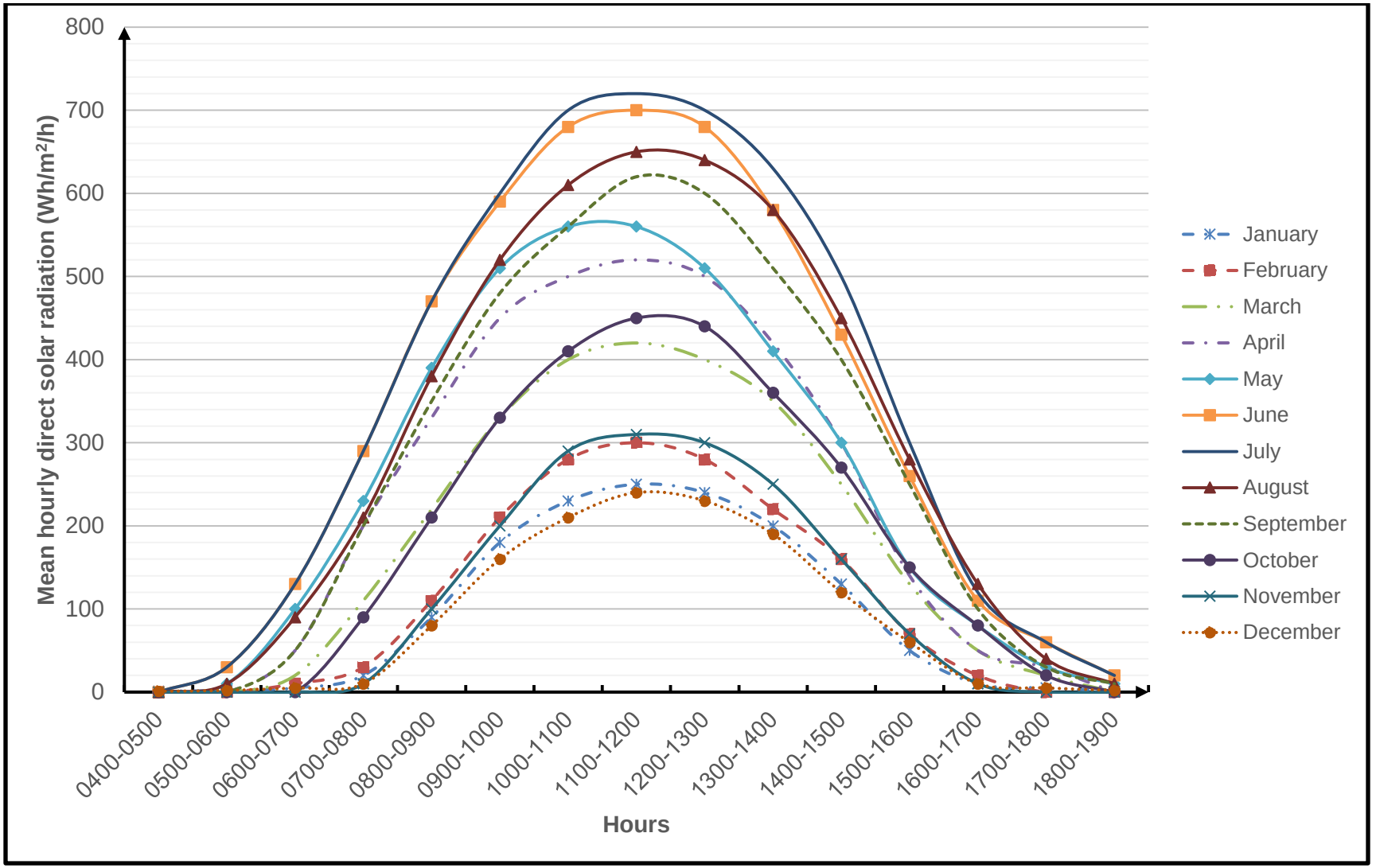

Figure 4.19: Mean hourly direct solar radiation (Koroneos et al., 2005: p. 1896)

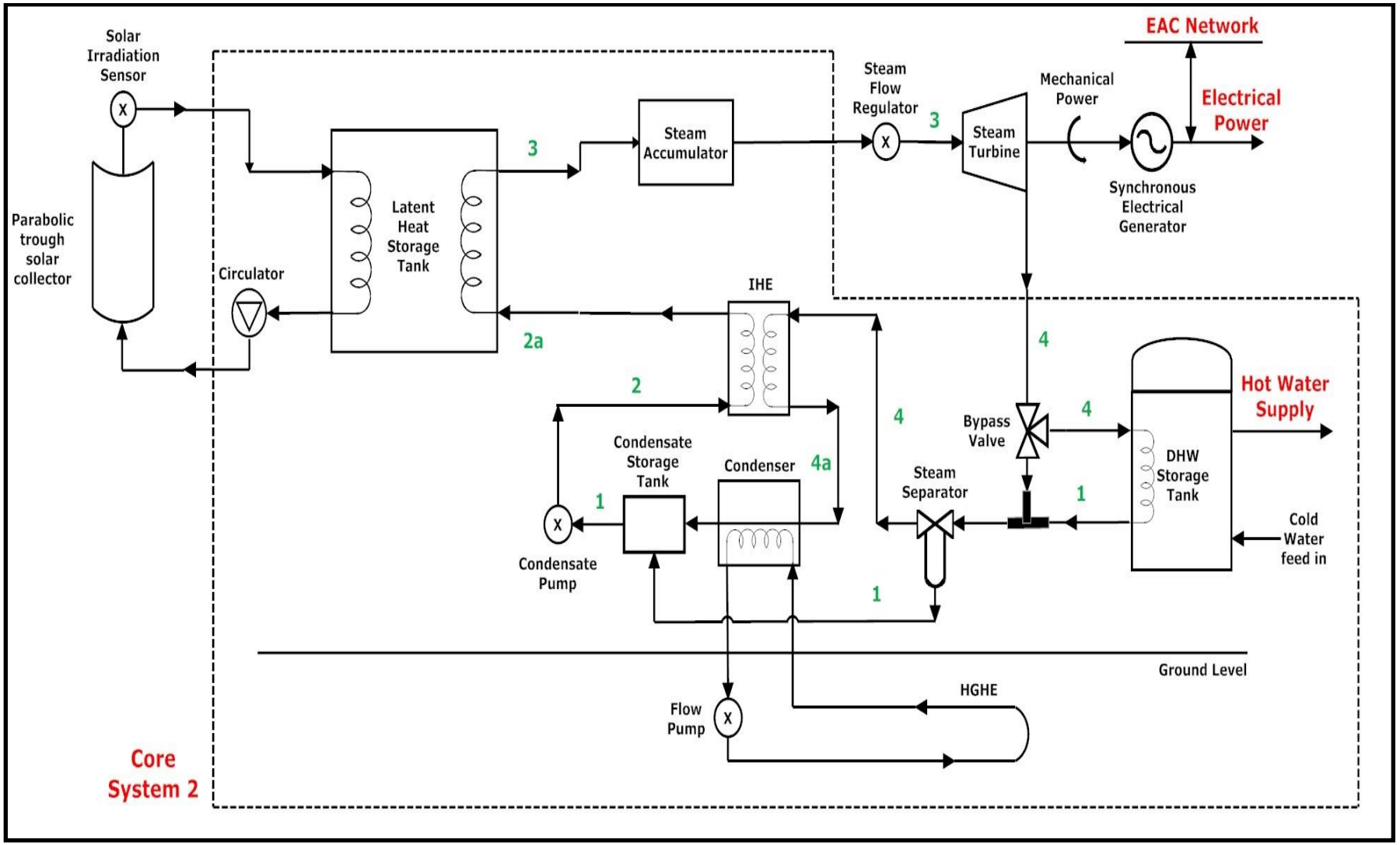

Figure 4.20: Final form of Concept System 2 (with IHE)

Even so, it is still an unrealistic figure and it also reduces the system's operation period from about 10:00 to 13:30 during the winter months. However, the system would be capable of operating for **24 hours** daily during the worst months (3.5 during day time plus 20.5 hours from the stored energy in the ThST) not requiring the usage of the national electrical network to cover the household demand. Additionally, the graph also indicates the months with the highest peak values of $\mathbf{I_b}$, June and July. During these months, the period that $\mathbf{I_b}$ is greater than **200 W/m^2** is 06:30 until 16:00, meaning that the systems daily operation capability becomes **30 hours** (9.5 hours during day time and the 20.5 hours from ThST), eliminating the household's dependency on the national network. Possible reductions of the overall size of the system are examined in Chapter 5. Figure 4.20 shows the final form of this system, in the same format as Concept System 1 in Figure 4.15.

Section 4.5.3.4: Insulating the ThST

The storage tank containing the TSM has an internal temperature of **660 K** (**390 ºC**), which if can cause problems left without insulation. Firstly, this high temperature could cause serious thermal injury to anyone coming in contact with it accidentally, its increases the temperature of the household leading to occupant thermal discomfort and thirdly it would cause a rapid depletion of the stored energy and the TSM would solidify. In order to solve this problem, this section studies the mechanisms of thermal transfer so that the energy losses from the ThST can be reduced to the minimum.

Thermal energy is propagated when there is a difference in temperature with three mechanisms: conduction, convection and radiation. **Conduction** is the method of transferring heat successively from one atom or molecule to the next within an object. Heat increases the kinetic energy of the object's particles, causing them to vibrate more quickly. As a result they collide with their neighbouring and less vibrating particles to increase their kinetic energy and so forth (Serway & Jewett, 2014: p. 608). It is worth mentioning that conduction occurs almost exclusively within solids. On the other hand, **convection** occurs in fluids (liquids and gases) in which their warmer masses expand and thus having a smaller density than cold ones. Less dense masses of a fluid experience greater buoyancy force and so they rise to a greater height. The process is repeated causing a circulatory current of warm masses throughout the fluid's volume (Serway & Jewett, 2014: p. 612). Conduction and convection

occur only in the presence of a medium, as its particles carry and propagate the heat. The difference between them is that while convection occurs with the movement of the more energetic particles inside the medium, conduction occurs without the medium's particles changing their location. The third and last heat transfer mechanism is **radiation**, which does not require a medium to propagate energy; heat is transferred by means of electromagnetic waves and this is how the Earth absorbs heat from the Sun (Serway & Jewett, 2014: p. 613).

Conduction

Energy transfer by conduction is described by Fourier's law, which states that heat transfer rate per unit area $\left(\frac{\dot{Q}}{A}\right)$ is proportional to the temperature gradient to the direction of flow $\left(\frac{\partial T}{\partial x}\right)$, in this case to the x-direction, perpendicular to area **A** (Holman, 2010: p. 2). More specifically Fourier's law appears in the next equation (Holman, 2010: p. 2) and its illustration is shown in the slab diagram of Figure 4.21 (Serway & Jewett: 2014: p. 609):

$$\dot{Q}_x = -kA\frac{\partial T}{\partial x}$$

Equation 4.32: Fourier's law of thermal conduction in the x-direction (Holman, 2010: p. 2)

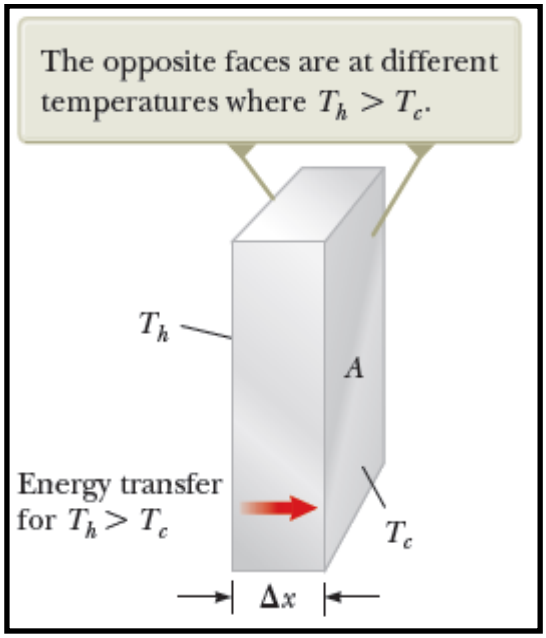

Figure 4.21: Slab diagram for thermal conduction (Serway & Jewett: 2014: p. 609)

It should be noted that the minus sign on the equation exists as in the slope of the temperature profile in regards to x inside the material is negative. Property **k** is called thermal conductivity and it is a characteristic of the material. By integrating Fourier's law over the total thickness of the material, the steady state Equation 4.33 is derived, according to Figure 4.21, considering that **k** is constant (Serway & Jewett: 2014: p. 610):

$$\dot{Q}_x = kA\frac{T_h - T_c}{\Delta x}$$

Equation 4.33: Thermal conduction in the thickness of the material (Serway & Jewett: 2014: p. 610)

When heat is propagated through two or more materials in thermal contact with different thermal conductivities, as Figure 4.22 (Holman, 2010: p. 28) illustrates, Equation 4.33 takes the form shown in Equation 4.34 (Holman, 2010: p. 28):

$$\dot{Q}_x = \frac{T_1 - T_4}{\frac{\Delta x_A}{k_A A} + \frac{\Delta x_B}{k_B A} + \frac{\Delta x_C}{k_C A}}$$

Equation 4.34: Thermal conduction of multiple materials with different thermal resistances (Holman, 2010: p. 28)

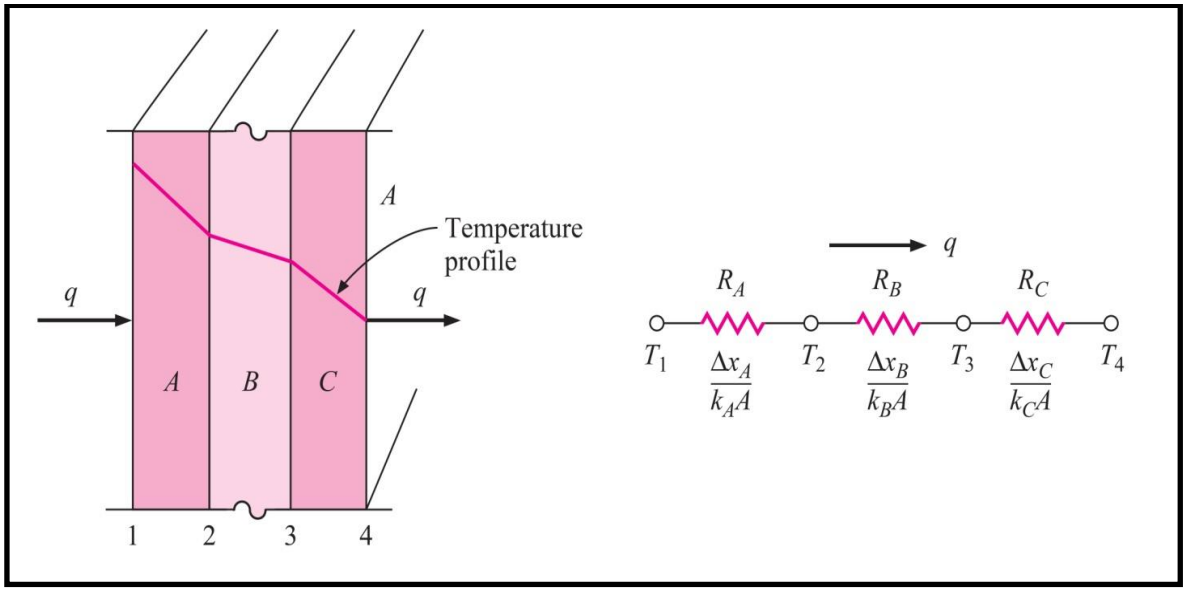

Figure 4.22: Slab diagram of multiple materials in thermal contact and their electrical equivalent (Holman, 2010: p. 28)

As seen from the electrical equivalent in Figure 4.22, each material has its own thermal resistance **R**, equal to $\frac{\mathbf{\Delta x}}{\mathbf{kA}}$, and the problem of conduction can be simplified into an electrical resistance one.

Radiation

As mentioned, heat transfer by radiation occurs as a means of electromagnetic waves without the need of a transfer medium. Thermal radiation obeys the Stefan – Boltzmann law, which states that heat transfer rate per unit area $\left(\frac{\dot{\mathbf{Q}}}{\mathbf{A}}\right)$ is proportional to the fourth power of an object's surface absolute temperature ($\mathbf{T^4}$). More specifically, the law has the form shown in Equation 4.35 (Serway & Jewett: 2014: p. 613):

$$\dot{\mathbf{Q}}_{\mathbf{rad}} = \boldsymbol{\varepsilon\sigma \mathbf{A} \mathbf{T}^4}$$

Equation 4.35: Stefan-Boltzmann's law of thermal radiation (Serway & Jewett: 2014: p. 613)

The factor **ε** is called the emissivity of the object's surface and can be between **0** and **1**, while **σ** is the Stefan – Boltzmann constant. However, an object does not only emit radiation heat; it also absorbs heat from its surroundings with the same difficulty as it emits. So, instead of Equation 4.35 this project uses Equation 4.36, as the former is primarily used for interstellar objects, where the contribution of their surrounding is negligible (Serway & Jewett: 2014: p. 614):

$$\dot{\mathbf{Q}}_{\mathbf{rad}} = \boldsymbol{\varepsilon\sigma \mathbf{A}\left(\mathbf{T}_{\mathbf{out}}^4 - \mathbf{T}_{\mathbf{surr}}^4\right)}$$

Equation 4.36: Stefan-Boltzmann's law with significant contribution from the object's surroundings (Serway & Jewett: 2014: p. 614)

where, $\mathbf{T_{out}}$ and $\mathbf{T_{surr}}$ are absolute temperatures of the object's outside envelope and its surroundings, respectively.

Thermal loss calculations

In order to solve the problem of insulating the ThST, a set of assumptions must be stated first:

1. The absolute temperature of the eutectic salt, mentioned in Table 4.23, inside the ThST is kept constant at **660 K** (**390 ºC**). This is not an assumption; it is rather a statement since the type of the storage material is of latent heat and so the temperature of that material does not change with the addition or subtraction of energy.

2. The surrounding temperature of the ThST is room temperature (**300 K**), as it would be enclosed in a special compartment at the basement of the household so that it would not be exposed to the ambient atmospheric conditions.

3. Finally, the calculations determine the total rate of energy loss by conduction $\dot{\mathbf{Q}}_{\mathbf{con}}$ and radiation $\dot{\mathbf{Q}}_{\mathbf{rad}}$ from the ThST for various values of the desired $\mathbf{T}_{\mathbf{out}}$ and insulation thickness, $\mathbf{L}_{\mathbf{ins}}$. $\dot{\mathbf{Q}}_{\mathbf{con}}$ is considered constant, since both $\mathbf{T}_{\mathbf{in}}$ and $\mathbf{T}_{\mathbf{out}}$ are time invariant.

Thermal energy is transferred from the TSM to the surroundings through the insulation by conduction, as explained in Section 4.5.3.4.1. The manufacturers of insulation materials are showing in their online datasheets that their products' thermal conductivity is dependent on temperature (Acoustiblok, 2012: p. 1; Knauf Insulation, 2014: p. 3; Pittsburgh Corning, 2014 & RTI, 2012). So, since the conduction mechanism deploys a thermal gradient across the material's thickness as seen in Equations 5.32 and 5.33 and in Figure 4.22, it means that each elementary slice inside the insulation with a different temperature has a different value of thermal conductivity. As a result, the calculation of the total energy loss by conduction $\dot{\mathbf{Q}}_{\mathbf{con}}$ must take into account the significant temperature gradient between **660** and **300 K**. For this reason there are several methods that can be used for this purpose:

a) **R-values or U-values:** According to Holman (2010: pp. 28 – 29, 34) a commonly used method for determining building envelope composite insulation is by utilizing the insulating material's **R-value** (not to be confused with thermal resistance **R** explained in Section 4.5.3.4.1) or its overall heat transfer coefficient (**U-value** or heat flux per unit area), which is the reciprocal of the **R-value**. These figures exist in tabulated form for each material.

Moreover, this method considers small changes in temperature and so the thermal conductivity of each material is assumed to be constant.

b) **Arithmetic average:** The simplest method for single and composite materials is using the arithmetic average of the materials' conductivity values that correspond to the temperature difference across each insulating layer. This method is used when the mentioned temperature difference is not small and so the material's thermal conductivity cannot be assumed to be constant.

c) **Boundary condition with multiple dimensions:** This category of methods contains the conduction problems in one dimension and multiple dimensions. For steady state and one dimension with variable thermal conductivity problems, Fourier's Law of Equation 4.32 becomes a **separation-of-variables** differential equation problem. For steady state and multiple dimensions, the problem becomes very complicated and closed form solution is almost unachievable. So, numerical methods of partial differential equations are used, such as the **finite-difference approximation** (Holman, 2010: p. 88) and the **Gauss-Seidel iteration** (Holman, 2010: p. 99). For transient analysis problems, methods include the **lumped-heat-capacity** method (Holman, 2010: p. 141) and the **forward and backward** techniques (Holman, 2010: p. 172).

In the case of this project, the problem is basically a single dimension one with variable thermal conductivity, since there is a significant temperature difference across the ThST's wall and so it is included in the third category mentioned above. The solution is a simple separation-of-variables method of Fourier's Law analysed below and leads to Equation 4.37:

$$\dot{Q}_{con} = -Ak(T)\frac{dT}{dx} \Leftrightarrow \dot{Q}_{con}dx = -Ak(T)dT$$

$$\Rightarrow \int_0^{L_{ins}} \dot{Q}_{con}dx = -\int_{T_{in}}^{T_{out}} Ak(T)dT \Rightarrow \dot{Q}_{con}\int_0^{L_{ins}} dx = -A\int_{T_{in}}^{T_{out}} k(T)dT$$

$$\Rightarrow \dot{Q}_{con}L_{ins} = -A[K(T_{out}) - K(T_{in})]$$

$$\Rightarrow \boxed{\dot{Q}_{con} = \frac{A[K(T_{in}) - K(T_{out})]}{L_{ins}}}$$

Equation 4.37: Derivation of the ThST's energy loss rate when thermal conductivity is dependent on temperature

where **K(T)** is the integral of thermal conductivity function in regards to temperature. For this purpose, three commercial materials (Aerogel, FoamGlass and ProRoxSL) have been selected that their manufacturer provided thermal conductivity data in regards to temperature in their brochures (Acoustiblok UK, 2012: p. 1; Pittsburgh Corning, 2014 & RTI, 2012). These data were exponentially interpolated to produce a reliable function of thermal conductivity **k(T)**. The plots, equations and the fitting R^2-values of the mentioned interpolated functions are shown in Table 4.28 and Figure 4.23.

Temperature		Thermal Conductivity (W/m-K)		
°C	K	Aerogel	FoamGlass	ProRoxSL
-160	110	---	0.021	---
-80	190	---	0.029	---
0	270	0.0131	0.040	---
10	280	---	0.041	---
25	295	0.0136	---	---
50	320	0.0143	---	0.040
75	345	0.0153	---	---
100	370	0.0164	0.057	0.044
125	395	0.0177	---	---
150	420	0.0193	---	0.050
175	445	0.0210	---	---
200	470	0.0230	---	0.057
220	490	---	0.085	---
250	520	---	---	0.064
300	570	---	---	0.073
350	620	---	---	0.084
400	670	---	---	0.094
500	770	---	---	0.119
600	870	---	---	0.148
700	970	---	---	0.182
Interpolation function k(T)		$0.0058e^{0.0029T}$	$0.0144e^{0.0037T}$	$0.0186e^{0.0024T}$
R^2-value		0.9871	0.9977	0.9986
Integrated interpolation function K(T)		$2.0000e^{0.0029T}$	$3.8919e^{0.0037T}$	$7.7500e^{0.0024T}$

Table 4.28: Thermal conductivity data for 3 commercial insulating materials (Acoustiblok UK, 2012: p. 1; Pittsburgh Corning, 2014 & RTI, 2012)

As seen from the fitting R^2-values, the interpolation functions are greatly reliable as they are about equal to 1. So, these thermal conductivity functions **k(T)** in green can now be used with Equation 4.37 to calculate $\dot{Q}_{con}$; this task is presented in Table 4.29, where $\dot{Q}_{con}$ and $\dot{Q}_{rad}$ are calculated for various values of T_{out} and arbitrary values of L_{ins}:

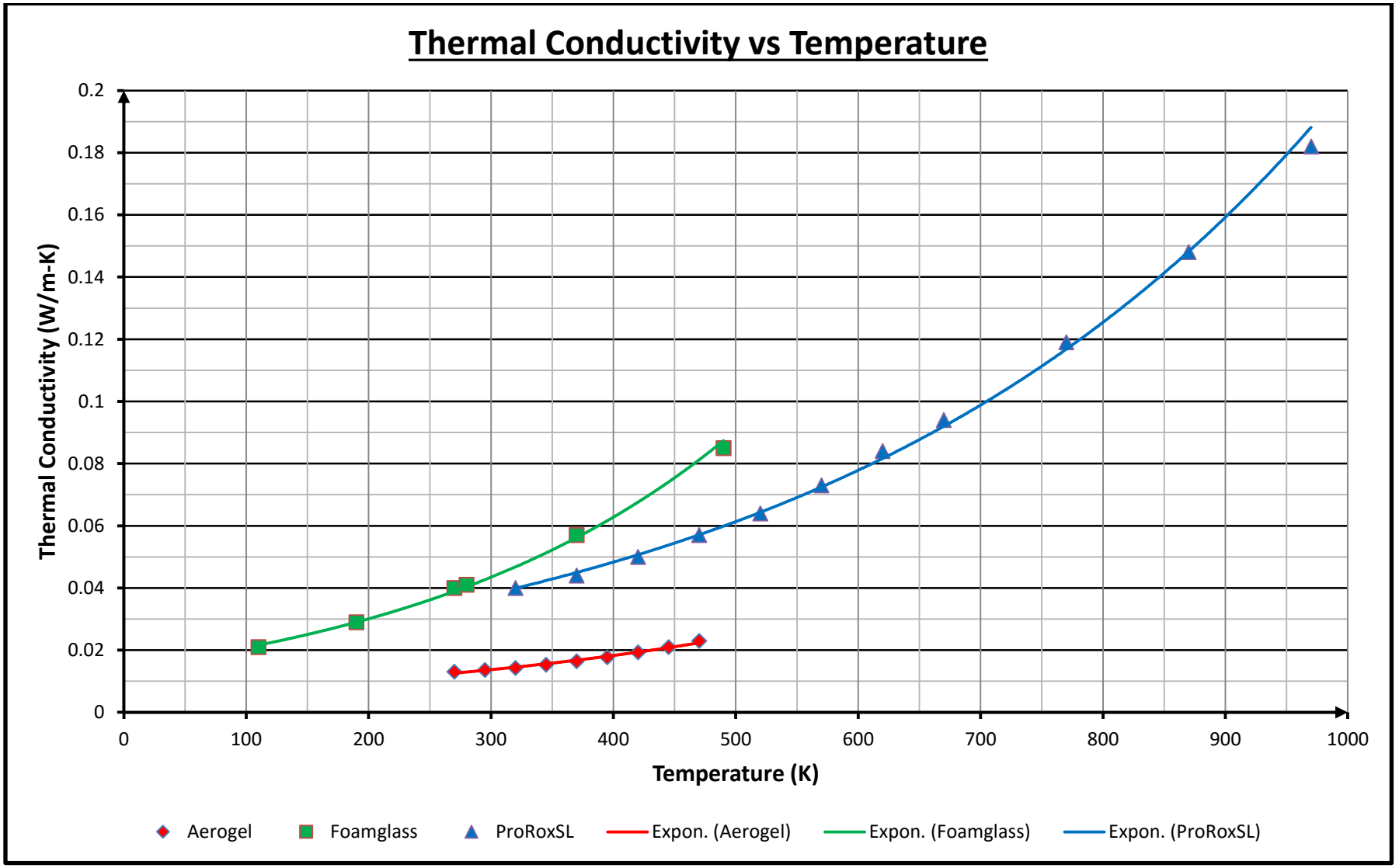

Figure 4.23: Thermal conductivity plots of the 3 insulating materials in Table 4.28 (Acoustiblok UK, 2012: p. 1; Pittsburgh Corning, 2014 & RTI, 2012)

Material	L_{ins} (m)	$\dot{Q}_{con}$ (kW) for various T_{out} (K) for whole tank			
		330	300	295	290
Aerogel	0.10	3.2818	3.4446	3.4703	3.4957
	0.15	2.1879	2.2964	2.3136	2.3305
	0.18	1.8232	1.9136	1.9280	1.9421
	0.20	1.6409	1.7223	1.7352	1.7479
	0.25	1.3127	1.3778	1.3881	1.3983
	0.30	1.0939	1.1482	1.1568	1.1652
	0.40	0.8205	0.8611	0.8676	0.8739
	0.50	0.6564	0.6889	0.6941	0.6992
FoamGlass	0.10	12.462	12.982	13.063	13.143
	0.15	8.3080	8.6546	8.7087	8.7618
	0.18	6.9233	7.2122	7.2573	7.3015
	0.20	6.2310	6.4909	6.5315	6.5714
	0.25	4.9848	5.1928	5.2252	4.9848
	0.30	4.1540	4.3273	4.3544	4.1540
	0.40	3.1155	3.2455	3.2658	3.1155
	0.50	2.4924	2.5964	2.6126	2.6285
ProRoxSL	0.10	8.0939	8.5397	8.6109	8.6813
	0.15	5.3960	5.6931	5.7406	5.7875
	0.18	4.4966	4.7443	4.7838	4.8229
	0.20	4.0470	4.2698	4.3054	4.3406
	0.25	3.2376	3.4159	3.4444	3.4725
	0.30	2.6980	2.8466	2.8703	2.8938
	0.40	2.0235	2.1349	2.1527	2.1703
	0.50	1.6188	1.7079	1.7222	1.7363
		$\dot{Q}_{rad}$ (kW) for various T_{out} (K) for whole tank			
		330	300	295	290
		7.2257	0.0000	-1.0123	-1.9744

Table 4.29: Conduction and radiation energy loss rates from the ThST as a whole based on the data of Table 4.28

Constant	Constant's name	Units	Value
σ	Stefan-Boltzmann constant	$W/m^2\text{-}K^4$	5.67×10^{-8}
T_{in}	Temperature inside the tank	K	670
T_{surr}	ThST surroundings temperature		300
a	ThST edge length	m	2.5
ε	Average ThST's paint emissivity	---	0.904

Table 4.30: Constants used for Equations 4.36 and 4.37 to produce the data in Table 4.28 (ETB, 2015)

As expected, increasing of $\mathbf{L_{ins}}$ would decrease the conduction energy losses $\mathbf{\dot{Q}_{con}}$, while decreasing the desired $\mathbf{T_{out}}$, $\mathbf{\dot{Q}_{con}}$ increases. In contrast, $\mathbf{\dot{Q}_{rad}}$ decreases significantly only by decreasing $\mathbf{T_{out}}$, as radiation does not depend on the type of insulation, rather only on the colour the ThST's outer surface is painted. This colour is capable of adjusting the ThST's emissivity to a desired value. For this case the emissivity coefficient appearing in Table 4.30 is the average of five different paint types' emissivity (Black silicone paint, black epoxy paint, black enamel paint, lampblack paint and oil paint) (ETB, 2015). Moreover, radiation can also be absorbed as indicated by the negative values in the last row of Table 4.29. This is because the ThST's surroundings have greater temperature ($\mathbf{T_{surr}}$) than that of its outer wall ($\mathbf{T_{out}}$). So, if the desired $\mathbf{T_{out}}$ is either **290** or **295 K**, the ThST can actually absorb energy and for several $\mathbf{L_{ins}}$ values there is no energy loss from the ThST to the surroundings. More specifically this occurs for $\mathbf{T_{out}}$ of **290 K** and insulating material **Aerogel** or **ProRoxSL** with $\mathbf{L_{ins}}$ greater than **0.18 m** and greater than **0.40 m** respectively. If $\mathbf{T_{out}}$ is **295 K**, then only **Aerogel** can accomplish no energy leakage for $\mathbf{L_{ins}}$ values greater than **0.30 m**.

Section 4.5.3.5: Selecting the thermal medium for the PTSC to charge the ThST

The last aspect of this concept system is which material should be used on the left side of the ThST on Figure 4.20, in other words the material that would receive the absorbed solar energy from the PTSC so that it charges the ThST. This material must be liquid and of sensible heat type, as it guarantees that it would remain in its liquid state during operation and it would not create small crystals, causing fouling effects inside the piping of PTSC and ThST.

According to Gil et al. (2010: p. 38), there are several liquid sensible heat type materials utilized by the power production industry, with molten salts to be the most preferred ones since they have high volumetric specific heat capacities and thermal conductivities and they are cheaper per thermal kWh than other materials (Gil et al., 2010: pp. 37 – 38). However, if a PCM has a low melting point, this would guarantee that no solidification would occur when its temperature becomes smaller than the operating temperature of **390 ºC**. So, a commercially available organic compound (**A22H**) with a melting point of **22 ºC** from the

PCM Products company (2013: p. 4) can be used to solve this issue. The properties for this material are presented in Table 4.31 (PCM Products, 2013: p. 4).

In order to calculate the mass flow rate of the **A22H** compound that would absorb thermal energy from the PTSC to charge the ThST, the following equation is used. The results of the calculations are also presented in Table 4.31:

$$\dot{Q}_{sen} = \dot{m}_{sen} c_{sen} \Delta T$$

Equation 4.38: Sensible heat transfer law

Property	Property Name	Units	Value
$\dot{Q}_{sen}$	Absorbed power from PTSC	**kW**	56.5
c_{sen}	Specific heat capacity	**kJ/kg-K**	2.85
ΔT	Operation temperature range	**°C**	390 – 400
T_{max}	Maximum operation temperature		400
$\dot{m}_{sen}$	**Charging mass flow rate**	**kg/s**	**1.98**

Table 4.31: Total volume and mass flow rate of A22H used to charge the ThST (PCM Products, 2013: p. 4)

The small temperature difference **ΔT** is due to the fact that since this material transfers sensible heat its temperature must not become lower than **390 °C**, as thermal energy would not be transferred into the ThST, rather back into **A22H**. In addition, the highest temperature achievable for the PTSC of this project is **400 °C**, thus creating the upper limit of the temperature range for **A22H**, which is also the maximum allowed temperature for the material. It should be noted that the total amount of the material needed for the system depends on the length and thickness of the pipelines connecting the PTSC with the ThST.

Section 4.6: Concept System 3 (Direct WFV generation with a NGB)

Section 4.6.1: Introduction

The third concept system scenario of this project examines the replacement of the ThST with a Natural Gas Boiler (NGB) so that WFV continues to be generated after the PTSC ceases to absorb enough solar irradiance for driving the system by itself. This section

analyses the sizing procedure for the NGB, which is same followed in the previous sections for the ThST and SA.

Section 4.6.2: Calculating the natural gas consumption of the NGB

Section 4.6.2.1: Calorific value of natural gas and diesel

In order to calculate the demanded consumption rate and total mass of natural gas for Concept System 3, data about the calorific value of natural gas and diesel in Cyprus today need to be explained. These data are also useful for calculating the carbon footprint of the three concept systems in Chapter 5. First of all, fuels are presented to have both a **Lower Heating Value (LHV)** or **Net Calorific Value (NCV)** and a **Higher Heating Value (HHV)** or **Gross Calorific Value (GCV)**. Various sources give different net and gross values for each type of fuel and for this reason the various calorific values of both natural gas and diesel are presented in Table 4.32 along with their respective source. Additionally, as the calorific values of natural gas are provided by the sources in **MJ/m^3** (**CV$_{(V)}$**, volumetric calorific value), Table 4.32 also contains the respective values in **MJ/kg** comparing the two fuels together. The density $\boldsymbol{\rho_{NG}}$ of natural gas can be found in the Engineering Toolbox website to be between **0.7** to **0.9 kg/m^3** in Standard Temperature and Pressure (**0 ºC, 1 atm**) (ETb, 2014b). So the average density of **0.8 kg/m^3** is used to convert the units according to Equation 4.39:

$$\boldsymbol{\rho_{NG} = \frac{m_{NG}}{V_{NG}}}$$

$$\boldsymbol{\left[CV_{(m)}\right] = \frac{MJ}{kg}\ ,\ \left[CV_{(V)}\right] = \frac{MJ}{m^3}\ \Rightarrow\ \rho = \frac{CV_{(V)}}{CV_{(m)}}}$$

$$\boldsymbol{\Rightarrow\ \boxed{CV_{(m)} = \frac{CV_{(V)}}{\rho}}}$$

Equation 4.39: Conversion between the volumetric and regular calorific value

Natural gas					Diesel oil (Low – sulphur)		
Source	MJ/m³		MJ/kg		Source	MJ/kg	
	LHV	HHV	LHV	HHV		LHV	HHV
(DECC, 2014)	35.7	39.7	44.6	49.6	(DECC, 2014)	42.6	45.3
(ETb, 2014a)	---	43.0	---	53.8	(ETb, 2014a)	43.4	44.8
(USDE, 2011: p. 201)	42.1	52.2	52.7	65.3	(USDE, 2011: p. 201)	42.6	45.6
Average	38.9	45.0	48.7	56.2	Average	42.9	45.2

Table 4.32: Calorific Values of diesel and natural gas

As observed from Table 4.32, natural gas has in all cases a higher Calorific Value (CV) than diesel in the respective categories; this makes natural gas a fuel of greater quality compared and consequently a more preferred one in usage for energy production. The average NCV of diesel calculated in this table is also confirmed in the most recent Annual Report of EAC, which states that the average CV of diesel used during 2012 was **42960 kJ/kg** and during 2011 was **42963 kJ/kg** (**42.96 MJ/kg**) (EAC, 2012: p. 24). The diesel data listed in the above table are used for comparison purposes in this section and they are only needed in Chapter 5 for the calculations of a power station's fuel consumption per household.

Section 4.6.2.2: Determining the total monthly natural gas demand per household

Better quality can be also explained by means of fuel consumption in the NGB of Concept System 3, the configuration of which is shown in Figure 4.24. Equation 4.40 summarizes the boiler's thermodynamic behaviour in the system:

$$\dot{W}_{NGB} = \eta_{NGB}\, \dot{m}_{NG}\, CV_{NG(m)}$$

Equation 4.40: Thermodynamic Equation of a Natural Gas Boiler

In order to determine the consumption rate of the boiler, Equation 4.39 can be rearranged into Equation 4.41:

$$\dot{m}_{NG} = \frac{\dot{W}_{NGB}}{\eta_{NGB}\, CV_{NG(m)}}$$

Equation 4.41: Fuel consumption rate of a Natural Gas Boiler

As shown in Section 4.5.3.2, $\dot{W}_{Col}$ is the minimum required energy rate of the PTSC and it is equal to **56.5 kW**. The NGB must also have the same power output, so it is capable to effectively replace the PTSC during the hours the latter is not in operation. In other words, $\dot{W}_{Col}$ needs to be equal to $\dot{W}_{NGB}$. The value of natural gas's $CV_{NG(m)}$ is assumed to be the average LHV for conservative calculations. Finally the efficiency of the gas boiler varies depending on its energy class. According the Seasonal Efficiency of Domestic Boilers in the United Kingdom (SEDBUK) rating, boilers are categorised into seven energy classes (**A** to **G**) with class **A** to include all the boilers with **90%** efficiency and above, while **G** includes all those with **70%** efficiency and below (HHG, 2014). The boiler is assumed to be of class **A** with the lowest **90%** rating. With these assumptions, Table 4.33 contains the desired natural gas consumption rate.

Property name	Property	Units	Value
Required power output of the NGB	$\dot{W}_{NGB}$	kW	56.5
NGB efficiency (Class A)	η_{NGB}	%	90
Average Lower Heating Value of natural gas	$CV_{NG(m)}$	MJ/kg	48.7
NGB consumption rate	$\dot{m}_{NG}$	10^{-3} kg/s	**1.289**

Table 4.33: Calculation of the NGB's consumption rate (data from Tables 5.16 and 5.26 and HHG, 2014)

Following the calculations of the natural gas consumption rate is the calculation of its containing tank's size. This is given by Equation 4.42:

$$\dot{m}_{NG} = \frac{m_{NG}}{t_{NG}}$$

$$\Rightarrow \boxed{m_{NG} = \dot{m}_{NG}\, t_{NG}}$$

Equation 4.42: Natural gas total mass over a period of time

For this case, three scenarios are studied: the first assumes that the boiler operates for one month nonstop, so t_{NG_1} is equal to **24 h**, the second assumes that the boiler operates in the hours the PTSC receives less than **200 W/m²** during January and December, while the third scenario is exactly as the second one but for June and July instead. As calculated in Section

4.5.3.3, the mentioned durations are **20.5** (24 hours minus 3.5 hours) and **14.5 hours** (24 hours minus 9.5 hours) respectively, so these are the values of $\mathbf{t_{NG_2}}$ and $\mathbf{t_{NG_3}}$ correspondingly. The next table presents the calculated daily amount of natural gas that Concept System 3 would need to consume for each of the three scenarios. Moreover, the final form of Concept System 3 is presented in Figure 4.25.

Property name	Property	Units	Value
NGB consumption rate	$\dot{\mathbf{m}}_{\mathbf{NG}}$	$\mathbf{10^{-3}}$ **kg/s**	1.289
Consumption time span (24 hours)	$\mathbf{t_{NG_1}}$	$\mathbf{10^6}$ **s**	2.592
Consumption time span (for winter)	$\mathbf{t_{NG_2}}$		2.214
Consumption time span (for summer)	$\mathbf{t_{NG_3}}$		1.566
Total consumed amount of NG (for $\mathbf{t_{NG_1}}$)	$\mathbf{m_{NG_1}}$	**tonnes**	**3.34**
Total consumed amount of NG (for $\mathbf{t_{NG_2}}$)	$\mathbf{m_{NG_2}}$		**2.85**
Total consumed amount of NG (for $\mathbf{t_{NG_3}}$)	$\mathbf{m_{NG_3}}$		**2.02**

Table 4.34: Calculation of the three cases' total monthly natural gas consumption (data from Section 4.5.3.3 and Table 4.27)

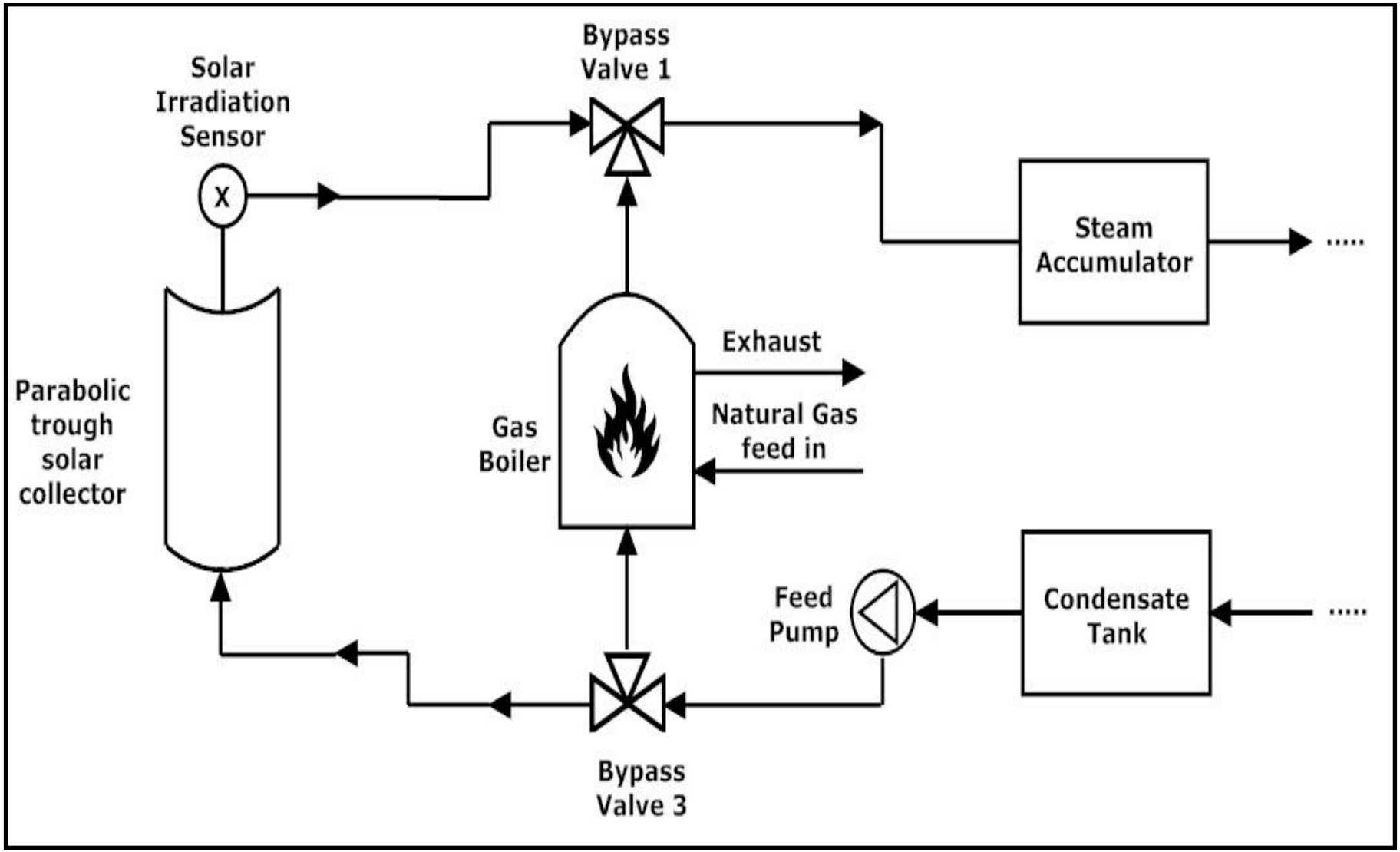

Figure 4.24: WFV generation side when using a NGB

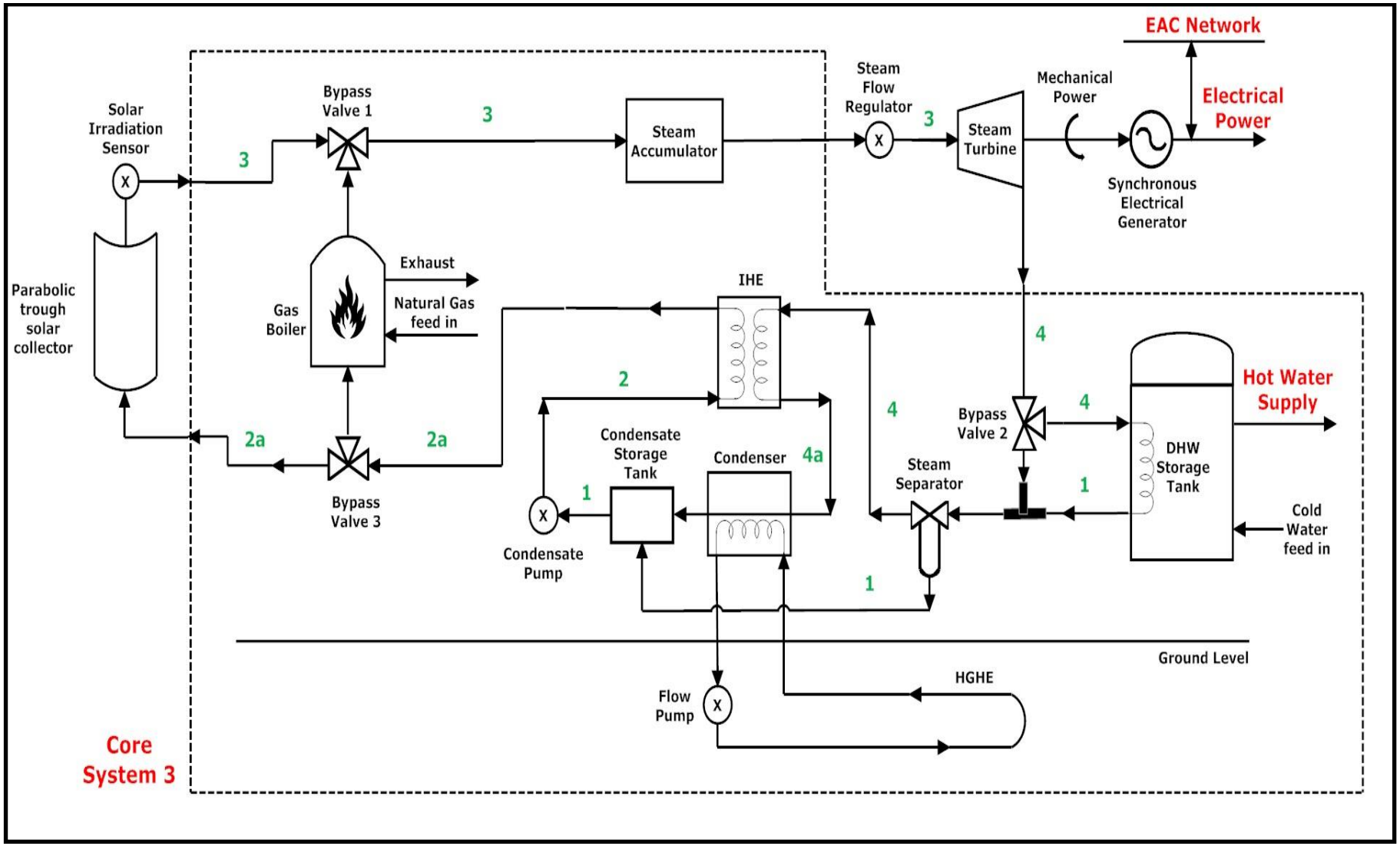

Figure 4.25: Final form of Concept System 3 with state numbers

Reference List

Acoustiblok UK Ltd. (2012) ***ThermablokSP Aerogel Insulation Blanket Datasheet.*** [Online].Available at: http://www.thermablok.co.uk/wp/wp-content/uploads/2012/07/thermabloksptechdata.pdf [Accessed: 25 January 2015].

Avallone, E. A.; Baumeister, T. & Sadegh, A. K. (2007) ***Marks' Standard Handbook for Mechanical Engineers*****, 11th edn., New York: McGraw-Hill.**

Bao, J. & Zhao, L. (2013) 'A review of working fluid and expander selections for Organic Rankine cycle', ***Renewable and Sustainable Energy Reviews*****, 24, pp. 325–342.**

Basin, A. S.; Kaplun, A. B.; Meshalkin, A. B.; & Uvarov, N. F. (2008) 'The LiCl–KCl Binary System', ***Russian Journal of Inorganic Chemistry*****, 53(9), pp. 1509 - 1511.**

Cárdenas, B. & León, N. (2013) 'High temperature latent heat thermal energy storage: Phase change materials, design considerations and performance enhancement techniques', ***Renewable and Sustainable Energy Reviews,*** **27, pp. 724-737.**

Çengel, Y. A. & Boles, M. A. (2011) ***Thermodynamics: An Engineering Approach*****, 7th edition. New York: McGraw-Hill.**

Chen, H.; Goswami, D. Y. & Stefanakos, E. K. (2010) 'A review of thermodynamic cycle and working fluids for the conversion of low-grade heat', ***Renewable and Sustainable Energy Reviews*****, 14, pp. 3059–3067.**

Clearco Products co., Inc. (2012a) ***Material Safety Data Sheet PSF-0.65cSt HMDS Silicone Fluid*****.** [Online]. Available at: http://www.clearcoproducts.com/pdf/msds/pure-silicone/msds-psf-0-65cSt.pdf [Accessed: 27 June 2014].

Clearco Products co., Inc. (2012b) ***Material Safety Data Sheet PSF-1.5cSt Silicone Fluid Decamethyltetrasiloxane*****.** [Online]. Available at: http://www.clearcoproducts.com/pdf/msds/pure-silicone/msds-psf1-5-cSt.pdf [Accessed: 27 June 2014].

Clearco Products co., Inc. (2012c) ***Material Safety Data Sheet PSF-2cSt Pure Silicone Fluid Dodecamethylpentasiloxane*****.** [Online]. Available at: http://www.clearcoproducts.com/pdf/msds/pure-silicone/MSDS-PSF-2cSt.pdf [Accessed: 27 June 2014].

Cyprus Energy Agency (CEA) (2010) ***Solar Thermal Systems: Domestic Applications*** **(In Greek).** [Online]. Available at: http://www.cea.org.cy/TOPICS/Renewable%20Energy/Solar%20thermal%20systems.pdf [Accessed: 22 January 2014].

Electricity Authority of Cyprus (EAC), (2012), *Annual Report 2012*. [Online]. Available at: https://www.eac.com.cy/EN/EAC/FinancialInformation/Documents/2012%20-eng.pdf [Accessed: 13 October 2014]

Electricity Authority of Cyprus (EAC) (2014) *New Supplies* [Online]. Available at: https://www.eac.com.cy/EN/customerservice/electricitysupplyinformation/Pages/NewSupply.aspx [Accessed: 16 May 2015]

Energy Informative (2015) *What Are the Most Efficient Solar Panels? Comparison of Mono-, Polycrystalline and Thin Film*. Available at: http://energyinformative.org/best-solar-panel-monocrystalline-polycrystalline-thin-film/ [Accessed: 16 May 2015]

The Engineering Toolbox (ETB), (2014), *Density and Specific Weight of Water - SI Units*. Available at: www.engineeringtoolbox.com/water-density-specific-weight-d_595.html [Accessed: 01 December 2014]

The Engineering Toolbox (ETB), (2015), *Emissivity Coefficients of some common Materials*. Available at: http://www.engineeringtoolbox.com/emissivity-coefficients-d_447.html [Accessed: 10 March 2015]

European Chemical Agency (ECHA) (2010) *Decamethyltetrasiloxane (Exp Key Auto flammability.001)*.
Available at:
http://apps.echa.europa.eu/registered/data/dossiers/DISS-dcee8151-4078-1afc-e044-00144f67d031/AGGR-606c3bc8-95e7-462d-b958-e11bda1b062f_DISS-dcee8151-4078-1afc-e044-00144f67d031.html#AGGR-606c3bc8-95e7-462d-b958-e11bda1b062f [Accessed: 01 June 2015]

Fisher Science Education (FSE) (2012) *Material Safety Data Sheet (Potassium Chloride)*.
[Online]. Available at:
http://static.fishersci.com/cmsassets/downloads/segment/ScienceEducation/pdf/Chemicals/MSDS/S25484_PC1050.pdf [Accessed: 09 February 2015]

Fisher Science Education (FSE) (2013) *Material Safety Data Sheet (Lithium chloride)*. [Online]. Available at: *https://www.fishersci.ca/viewmsds.do?catNo=L121500&lang=en* [Accessed: 04 March 2015]

García, D.; González, M. A.; Prieto, J. I.; Herrero, S.; López, S.; Mesonero, I. & Villasante, C. (2014) 'Characterization of the power and efficiency of Stirling engine subsystems', *Applied Energy*, 121, pp. 51 – 63.

Gil, A.; Medrano, M.; Martorell, I.; Lazaro, A.; Dolado, P.; Zalba, B. & Cabeza, L. F. (2010) 'State of the art on high temperature thermal energy storage for power generation. Part 1—Concepts, materials and modellization', *Renewable and Sustainable Energy Reviews,* 14, pp. 31-55.

Holman, J. P. (2010) *Heat Transfer*, 10th edn., New York: McGraw-Hill.

Hoyle, R. & Clarke, P. H. (1973) ***Thermodynamic cycle and Processes*****. London: Longman Group Ltd.**

IUPAC Gold Book (2014) ***Siloxanes*****.** [Online]. Available at: http://goldbook.iupac.org/S05671.html [Accessed: 28 April 2014]

Kenisarin, M. M. (2010) 'High-temperature phase change materials for thermal energy storage', ***Renewable and Sustainable Energy Reviews,*** **14, pp. 955–970**

Knauf Insulation Ltd. (2014) ***Earthwool® DriTherm Cavity Slabs Datasheet.*** [Online]. Available at: http://www.knaufinsulation.co.uk/media/809608/kine1514dat-earthwool-dritherm-cavity-slabs-glass-datasheet.pdf [Accessed: 25 January 2015]

Koroneos, C.; Fokaidis, P. & Moussiopoulos, N. (2005). 'Cyprus energy system and the use of renewable energy sources'. ***Energy,*** **30(10), pp. 1889 – 1901**.

Kutscher, C.; Burkholder, F. & Stynes, K. (2010) ***Generation of a Parabolic Trough Collector Efficiency Curve from Separate Measurements of Outdoor Optical Efficiency and Indoor Receiver Heat Loss*****. U.S. Department of Energy, Office of Energy Efficiency & Renewable Energy: National Renewable Energy Laboratory (NREL).**

Kuravi, S.; Trahan, J.; Goswami, D. Y.; Rahman, M. M. & Stefanakos, E. K. (2013) 'Thermal energy storage technologies and systems for concentrating solar power plants', ***Progress in Energy and Combustion Science,*** **39, pp. 285 – 319.**

Lai, N. A. (2009) ***Thermodynamic Data of Working Fluids for Energy Engineering*****, PhD Thesis, Universität für Bodenkultur Wien.**

Lai, N. A.; Wendland, M & Fischer, J. (2011) 'Working fluids for high-temperature organic Rankine cycles', ***Energy*****, 36, pp. 199-211.**

Matheson TriGas Inc. (2014a) ***Safety Data Sheet (Toluene)*****.** [Online]. Available at: http://www.chemadvisor.com/Matheson/database/msds/mat23590000800003.PDF [Accessed: 25 June 2014]

Matheson TriGas Inc. (2014b) ***Safety Data Sheet (Butylbenzene)*****.** [Online]. Available at: http://www.chemadvisor.com/Matheson/database/msds/mat03530000800003.PDF [Accessed: 25 June 2014]

Mathur, A.; Kasetty, R.; Oxley, J.; Mendez, J. & Nithyanandam, K. (2014) 'Using encapsulated phase change salts for concentrated solar power plant', ***Energy Procedia,*****49, pp. 908 – 915.**

Medrano, M.; Gil, A.; Martorell, I.; Potau, X. & Cabeza, L. F. (2010) 'State of the art on high-temperature thermal energy storage for power generation. Part 2—Case studies', ***Renewable and Sustainable Energy Reviews*****, 14, pp. 56 – 72.**

Moran, M. J.; Shapiro, H. N; Boettner, D. D. & Bailey, M. B. (2011) ***Fundamentals of Engineering Thermodynamics*****, 7th edition. New Jersey: John Wiley & Sons, Inc.**

Müller, I. & Müller, W. H. (2009) ***Fundamentals of Thermodynamics and Applications*****, Berlin: Springer.**

National Institute of Standards and Technology (NIST) (2011) ***Thermophysical Properties of Fluid Systems*****.** Available at: http://webbook.nist.gov/chemistry/fluid

Naumann, R. & Emons, H. H. (1989) 'Results of thermal analysis for investigation of salt hydrates as latent heat-storage materials', ***Journal of Thermal Analysis*****, 35, pp. 1009 – 1031.**

National Renewable Energy Laboratory (NREL) (2015) ***Parabolic Trough Collector Cost Update for the System Advisor Model (SAM).*** [Online]. Available at: http://www.nrel.gov/docs/fy16osti/65228.pdf [Accessed: 18 January 2015].

Portaspana, J. P. (2011) ***Master Thesis: High temperature thermal energy storage systems based on latent and thermo-chemical heat storage.*** [Online]. Available at: http://upcommons.upc.edu/bitstream/handle/2099.1/14566/MasterThesisjennifercarrasco.pdf [Accessed: 15 January 2015].

PCM Products Ltd (2013) ***PlusICE® Phase Change Materials.*** [Online]. Available at: http://www.pcmproducts.net/files/PlusICE%20Range-2013.pdf [Accessed: 18 March 2015]

Pittsburgh Corning (UK) Ltd. (2014) ***FOAMGLAS® T4+ Datasheet.*** [Online]. Available at: http://global.foamglas.com/__/frontend/handler/document.php?id=2090 [Accessed: 01 September 2015]

Rockwool Technical Insulation (RTI) (2012) ***ProRox SL 980UK Datasheet.*** [Online]. Available at: http://rwiumbracortiny-en.inforce.dk/media/929396/prorox_sl_980uk.pdf [Accessed: 25 January 2015]

Santa Cruz Biotechnology (SCB), Inc. (2010) ***Dodecamethylpentasiloxane (Material Safety Data Sheet)*****.** [Online]. Available at: http://datasheets.scbt.com/sc-227958.pdf [Accessed: 26 June 2014]

Santa Cruz Biotechnology (SCB), Inc. (2011a) ***Decamethyltetrasiloxane (Material Safety Data Sheet)*****.** [Online]. Available at: http://datasheets.scbt.com/sc-239653.pdf [Accessed: 26 June 2014]

Santa Cruz Biotechnology (SCB), Inc. (2011b) ***Hexamethyldisiloxane (Material Safety Data Sheet)*****.** [Online]. Available at: http://datasheets.scbt.com/sc-250106.pdf [Accessed: 26 June 2014]

Serway, R. A. (1990) ***Physics: For Scientists and Engineers, Volume III*****, 3rd (Greek) edn., Athens: A. Chondrorizos & Sia O.E..**

Serway, R. A. & Jewett, J. W. (2014) ***Physics for Scientists and Engineers with Modern Physics*****, 9th edn., Boston, USA: Brooks/Cole.**

Siemens A.G. (2011) ***Steam turbines for CSP plants*****.** [Online]. Available at: http://www.energy.siemens.com/co/pool/hq/power-generation/steam-turbines/downloads/new/steam-turbine-for-csp-plants-siemens_en.pdf [Accessed: 27 March 2014]

Siemens A.G. (2013) ***Pre-designed Steam Turbines*****.** [Online]. Available at: http://www.energy.siemens.com/co/pool/hq/power-generation/steam-turbines/downloads/new/steam-turbines-45kW-12MW_en.pdf [Accessed: 30 March 2014]

SkyFuel Inc. (2010) ***SkyTrough Thermal Efficiency*****.** [Online]. Available at: http://www.skyfuel.com/downloads/SkyTroughEfficiency(SkyFuel).pdf [Accessed: 30 March 2014]

SkyFuel Inc. (2011) ***Parabolic Trough Concentrator SkyTrough*****.** [Online]. Available at: http://www.skyfuel.com/downloads/brochure/SkyTroughBrochure.pdf [Accessed: 08 October 2014]

Spirax – Sarco Ltd. (2014) ***Steam Tables*****.** Available at: http://www.spiraxsarco.com/Resources/Pages/steam-tables.aspx#close [Accessed: 01 September 2015]

Sridharan, K. (2012) ***Thermal Properties of LiCl-KCl Molten Salt for Nuclear Waste Separation*****, University of Wisconsin, Madison: U.S. Department of Energy, Nuclear Energy University Programs.**

SunPower (2014) ***Facts about Solar Technology from SunPower***. [Online] Available at: http://us.sunpower.com/solar-panels-technology/facts [Accessed: 03 December 2014]

Tian, Y. & Zhao, C. Y. (2013) 'A review of solar collectors and thermal energy storage in solar thermal applications', ***Applied Energy*****, 104, pp. 538 – 553.**

TimeandDate.com, (2014), ***Nicosia, Cyprus — Sunrise, sunset and daylength, December 2014*****,** Available at: http://www.timeanddate.com/sun/cyprus/nicosia?month=12&year=2014 [Accessed: 7 September 2014]

United Kingdom, Department of Energy & Climate Change (DECC), (2014), ***DUKES: Calorific values*****.** Available at: https://www.gov.uk/government/publications/dukes-calorific-values [Accessed: 5 September 2014]

Williams, D. F. (2006) ***Additional Physical Property Measurements and Assessment of Salt Compositions Proposed for the Intermediate Heat Transfer Loop.*** [Online]. Available at: http://nuclear.inl.gov/deliverables/docs/salt_property_measurements_ltr-06-033.pdf [Accessed: 03 March 2015].

Chapter 5: Environmental impact of the three systems and possible further improvements

Section 5.1: Introduction

An analysis of some crucial economic aspects is a very significant part of every design project as this offers the latter a realistic foundation and renders it more feasible for implementation. Even though this chapter may not cover fully the financial costs of acquiring and maintaining the components of the three Concept Systems, as some of those components do not exist today, it nevertheless presents some environmental economics and comparisons with the current electricity production situation in addition to comparing natural gas and diesel from a financial acquisition and sheer energy density perspective. This will allow the examination whether the systems could truly benefit the host household as well as Cyprus's economy and natural environment, thus assisting the state to achieve its goals and responsibilities towards the EU and world environmental policies by exploiting the relative abundance of solar energy the country receives. This chapter will also allow the determination of the best of the three scenarios and provide the capability of proposing further study in this field.

Section 5.2: Calculating the environmental impact of the three systems

The following three sections calculate the concept systems' environmental impact and consequently the possible financial cost in the cases the systems are not capable of operating 24 hours per day and the national network undertakes the task of supplying the household with electricity.

Section 5.2.1: Concept System 1

Since the first concept scenario is the one without any form of storage, it means that it is capable of operating during day time and more specifically between the hours that the solar irradiance absorbed by the PTSC is greater or equal to **200 W/m^2**, as mentioned in section 4.5.3.3. The best and worst case scenarios in terms of hours of daily continuous operation according to Figure 4.19 occur during the summer months of June and July and during the winter months of December and January, with a total of **9.5 hours** (from 06:30 until 16:00) and **3.5 hours** (from 10:00 until 13:30), correspondingly. This means that for about **14.5 hours** during the above summer months and **20.5 hours** during the mentioned

winter months, Concept System 1 would cease to operate and the household would need to absorb electricity directly from the national network.

So, in order to make conservative calculations about the environmental impact of Concept System 1 and consequently that of the other two, the chapter assumes that:

a) All national electrical power is produced by Vasilikos Power Station, which is state-of-the-art (EAC, 2014a) as it is fitted with the most recent and energy efficient equipment,

b) All losses from transmission lines are negligible. More specifically, according to the Annual Report of EAC (2012: pp. 26 – 27) the losses from Transmission and Distribution were **136.55 GWh** in 2012, while the total net production sent to the consumers were **4443.1 GWh**, thus if one calculates the percentage of those losses to the supply for the public the losses are equal to only **3.1%**, a very small percentage that can easily be omitted from the conservative calculations.

c) Both the national and concept systems produce energy at their peak demand continuously for comparison purposes and for making the calculation processes easier. In reality the large electricity power stations operate in accordance with the demand at each moment, by having the slow-start equipment to operate on "base load" mode throughout the day and the more "quick response" equipment to operate at times of steep changes in the demand of the day.

Taking into account the above assumptions, a national power station needs to provide each household with **16.5 kW** of electricity throughout the year 24 hour a day, 7 days a week, if it is utilizes three phase voltage. For this case, the monthly consumption of diesel and emissions for a single household are presented in this section, so the three systems would be compared with each other on their dependency to the national network. For the purposes of these calculations, the properties of Vasilikos power station are used as mentioned. The efficiency of the whole power station is given by Equation 5.1:

$$\eta_{PS} = \frac{\dot{W}_C}{\dot{Q}_{PS}}$$

Equation 5.1: Efficiency of a Power Station

where, $\boldsymbol{\eta_{PS}}$ is the average efficiency of the power station, $\boldsymbol{\dot{W}_C}$ is the consumer's power demand in **kW** and $\boldsymbol{\dot{Q}_{PS}}$ is the thermal energy input of the power station in **kW**. In addition, as there are no known data regarding the upper and lower operating temperature limits of Vasilikos Power Station in order to determine its Carnot efficiency, $\boldsymbol{\eta_{PS}}$ is determined as the weighted mean efficiency of its component units. The weighted mean efficiency formula is given by Equation 5.2:

$$\bar{\eta}_{PS} = \frac{\sum \eta_{u_i} \dot{W}_{u_i}}{\sum \dot{W}_{u_i}}$$

Equation 5.2: Mean weighted efficiency of a Power Station

where, $\boldsymbol{\eta_{u_i}}$ is the dimensionless efficiency of power station unit **i**, $\boldsymbol{\dot{W}_{u_i}}$ is the i-th unit's power rating in **kW** and finally $\boldsymbol{\bar{\eta}_{PS}}$ is the needed mean weighted efficiency of the power station. For the purpose of calculating $\boldsymbol{\bar{\eta}_{PS}}$, Table 5.1 presents the power rating and efficiency factor of each individual unit of Vasilikos Power Station (EAC, 2007; 2014) so they can be substituted to Equation 5.2.

Type of Unit	Number of Units	Unit Power Rating (MW)	Unit Efficiency Factor (%)
Steam	3	130	35.1
Gas Turbine	1	38	29.0
Combined Cycle No.4	1	220	46.1
Combined Cycle No.5	1	220	46.7

Table 5.1: Power rating and efficiency factors of Vasilikos Power Station's component units (EAC, 2007; 2014)

Using the data from Table 5.1 and Equation 5.2 $\boldsymbol{\bar{\eta}_{PS}}$ is determined to be **40.6%**. Additionally, the consumer demands **16.5 kW** of electricity constantly and so the thermal input for one household $\boldsymbol{\dot{Q}_{PS}}$ is equal **40.6 kW**. The next step is to calculate the amount of diesel consumed throughout a month's time when the household is supplied full time by the national network

and this followed by the consumption calculation when the household is fitted with Concept System 1. Equation 5.3 calculates that mentioned monthly amount of diesel per household.

$$\mathbf{m_{D_i} = \frac{\dot{Q}_{PS} t_{PS_i}}{\eta_{DB}\, CV_{D(m)}}}$$

Equation 5.3: Total fuel consumption mass of a diesel Boiler

where, $\mathbf{m_{D_i}}$ is the total mass of diesel consumed in **kg** over each period of $\mathbf{t_{PS_i}}$ in **s**, while $\boldsymbol{\eta_{DB}}$ is the efficiency of the power station's diesel boiler and $\mathbf{CV_{D(m)}}$ is diesel's regular Net Calorific Value from Table 4.32 of Chapter 4 in **kJ/kg**; the thermal efficiency of Vasilikos' diesel boilers $\boldsymbol{\eta_{DB}}$ is approximately **90%** (EAC, 2007: p. 5) and as for the $\mathbf{t_{PS_i}}$ three cases are examined, the same as in section 4.6.2.2 of Chapter 4 with the difference that the fuel in this case is natural gas instead of diesel. So once again $\mathbf{t_{PS_1}}$ is **2.592 x 10^6 s**, $\mathbf{t_{PS_2}}$ is **2.214 x 10^6 s** while $\mathbf{t_{PS_3}}$ is **1.566 x 10^6 s**. The results of this data on Equation 5.3 are presented in Table 5.2.

The next step is to determine the amount of CO_2 that $\mathbf{m_{D_i}}$ data produces after being completely burned inside the Vasilikos' boiler. According to Martinez (2014: p. 5), diesel is a mixture of aromatics, alkanes and alkenes with mean molecular formulae that include $C_{11}H_{21}$, $C_{12}H_{23}$, $C_{12}H_{26}$, $C_{16}H_{26}$ and $C_{14}H_{30}$. For the purposes of this study, **dodecane** (**$C_{12}H_{26}$**) is assumed to be the mean formula of diesel. For calculating the emissions products from the combustion of $C_{12}H_{26}$, its combustion chemical equation is needed, just as with natural gas, given by Equation 5.4:

$$\mathbf{2C_{12}H_{26} + 37O_2 \xrightarrow{comb} 24CO_2 + 26H_2O}$$

Equation 5.4: Complete combustion reaction of $C_{12}H_{26}$

After simplifying the equation, it is observed that **1 mole** of $C_{12}H_{26}$ produces **12 moles** of CO_2 or alternatively, **170 g** of diesel produce **528 g** of CO_2. Equation 5.5 calculates of the total mass of CO_2 taking into account the total mass of diesel consumed as determined in the previous paragraph:

$$\left.\begin{matrix} 170g\ C_{12}H_{26} \rightarrow 528g\ CO_2 \\ m_{C_{12}H_{26_i}} \rightarrow m_{C_{12}H_{26}\rightarrow CO_{2_i}} \end{matrix}\right\} \Rightarrow m_{C_{12}H_{26}\rightarrow CO_{2_i}} = \frac{528 m_{C_{12}H_{26_i}}}{170}$$

$$\Rightarrow \boxed{m_{C_{12}H_{26}\rightarrow CO_{2_i}} = m_{C_{12}H_{26_i}} \frac{264}{85}}$$

Equation 5.5: Calculation of CO_2 mass produced by the $C_{12}H_{26}$

where, $m_{C_{12}H_{26}\rightarrow CO_{2_i}}$ is the total mass of CO_2 produced by diesel and $m_{C_{12}H_{26_i}}$ is the mass m_{D_i} from Equation 5.3, both measured in **tonnes**. The results are also presented in Table 5.2 below.

	With Concept System 1		**Without System**
	14.5 hours	**20.5 hours**	**24 hours**
Total Fuel Consumption m_{D_i} (tonnes)	1.65	2.33	2.73
Total CO_2 Emissions $m_{C_{12}H_{26}\rightarrow CO_{2_i}}$ (tonnes)	5.12	7.24	8.48

Table 5.2: Total monthly power station consumption and emissions production per household with and without Concept System 1

As expected, the more time a household demands supply from the power station, the more fuel is being consumed and thus the more emissions are released into the atmosphere. Additionally, on average, even Concept System 1 that is plain without storage or an NGB is capable of reducing the overall dependency on the national network supplied electricity and the emissions per household to about **85.3%** up to **60.4%**. The next section examines the cases of the other two concept systems that utilize extra equipment for further reductions in the previous two domains.

Section 5.2.2: Concept System 2

After calculating the environmental impact of Concept System 1, the same calculations regarding the second concept system may imply that it is more environmentally

friendly, since the presence of the thermal storage reduces dramatically the dependency on the national network.

As with the first concept system, the amount of time the system would not be operational is the main factor to specify the amount of emissions produced by the power stations for that household. According to section 4.5.3.2.2 of Chapter 4, Concept System 2 is capable of continuously operating for **24 hours** during December and January and for **30 hours** during June and July; this means that Concept System 2 is capable of producing electricity for the household throughout the year and the household would not rely on the network at all. So, no amount of diesel is spent for this case and thus the household's demand accommodation produces no emissions. These results are also presented in Table 5.3 along with the results of the other two for comparison.

As expected, the environmental performance of Concept System 2 is better than the one of Concept System 1. Clearly thermal energy storage is a significant addition to the core Concept System 1 since it increases the system's operation time, rendering it capable of also being completely independent from the national network for a few months of the year. In addition, the carbon footprint of the household is also reduced to zero, since the energy source is completely renewable, while the thermal storage technology is simple and therefore allows the complete household demand coverage for the entire year.

Section 5.2.3: Concept System 3

Since the last concept scenario is fitted with the NGB, is completely independent from the national network by default, so its carbon footprint is entirely based on the consumption of natural gas and not diesel. As it was presented in Table 4.32 of Chapter 4, natural gas has a greater average CV (net and gross) than diesel making it a better quality fuel. This section analyses the performance of Concept System 3 by making the same calculations as previously, but using natural gas instead of diesel.

Natural gas is a mixture of simple hydrocarbons, mostly **methane** (**CH_4**), which has many uses both in industry and at a domestic level. The environmental impact of any fuel is measured by its amount of emissions to the atmosphere after its usage and so this section and the next contain calculations of the amount of **carbon dioxide** (**CO_2**) being produced by

burning natural gas and diesel, respectively. Then, a comparison is made between the two fuels to identify which of the two has the smallest impact to the country's environment, based on its emissions and the amount of time this fuel is used.

More specifically, natural gas is typically **95% per mole** CH_4, about **2.5** to **3.2%** **ethane** (**C_2H_6**) and others, such as **propane** (**C_3H_8**), **butane** (**C_4H_{10}**), **hydrogen** (**H_2**) and **nitrogen** (**N_2**) in much smaller proportions (UnionGas, 2014; Enbridge, 2014). As the components with the most significant proportions of the fuel are CH_4 and C_2H_6, only the emissions caused by those two are significant enough to be calculated. Equations 5.6 and 5.7 show the combustion chemical reactions of the two gases respectively in the air:

$$\mathbf{CH_4 + 2O_2 \xrightarrow{comb} CO_2 + 2H_2O}$$

Equation 5.6: Complete combustion reaction of methane

$$\mathbf{2C_2H_6 + 7O_2 \xrightarrow{comb} 4CO_2 + 6H_2O}$$

Equation 5.7: Complete combustion reaction of ethane

As observed, a mole of CH_4 produces one mole of CO_2 and a mole of C_2H_6 produces two moles of CO_2. Considered that the standard average atomic masses of hydrogen, carbon and oxygen according to IUPAC are **1.008**, **12.01** and **16.00 g/mol**, respectively, then **16 g** of CH_4 produce **44 g** of CO_2 and **30 g** of C_2H_6 produce **88 g** of CO_2 (IUPAC, 2014).

The next step is to calculate the actual mass of each component in the total mass of natural gas consumed every time in the boiler. As the proportions of natural gas's components are given in molar percentages, in order to calculate the actual mass proportions of each one based on the Equations 5.6 and 5.7, the law of partial volumes or Amagat's Law needs to be used. According to this law, every gas component in a gas mixture follows the Ideal Gas Law as if that component it was pure under the same temperature and pressure conditions (Moran et al., 2011: p. 711). As a result the volume (and therefore the actual mass) of each component in a mixture is proportional to its molar proportion (molar percentage) in the mixture as shown by Equation 5.8:

$$V_x = \frac{n_x RT}{P} \quad , \quad V_{tot} = \frac{n_{tot} RT}{P}$$

$$\Rightarrow \frac{V_x}{V_{tot}} = \frac{n_x RT}{P} \frac{P}{n_{tot} RT} = \frac{n_x}{n_{tot}} = y_x$$

$$\Rightarrow V_x = y_x V_{tot} \quad , \quad \rho = \frac{m}{V} \Leftrightarrow V = \frac{m}{\rho}$$

$$\Rightarrow \frac{m_x}{\rho_x} = y_x \frac{m_{tot}}{\rho_{tot}}$$

$$\Rightarrow \boxed{m_x = y_x \rho_x \frac{m_{tot}}{\rho_{tot}}}$$

Equation 5.8: Actual mass of a gas mixture component based on its molar percentage in the mixture

where **m** is the mass of a gas in **kg** and **ρ** is its density in **kg/m^3**. All variables with the subscript "**x**" refer to the properties of component x and those with the subscript "**tot**" refer to the properties of the mixture and y_x is the molar percentage of component x. So in order to calculate the actual mass of **CH_4** and **C_2H_6** in the natural gas mixture, not only the respective molar percentages and total mass of natural gas being consumed are needed, but also the densities of the mixture and each of the components. As mentioned in the beginning of this section, the density of natural gas ρ_{tot} is equal to **0.8 kg/m^3** while the density at **1 atm** and **15 ºC** and molar proportion of CH_4 ρ_{CH_4} and of C_2H_6 $\rho_{C_2H_6}$ are equal to **0.68** and **1.28 kg/m^3** with **95%** and **2.9%** respectively (Air Liquide, 2013a; 2013b). For this case also, the total mass of natural gas according to the three duration scenarios are equal to those calculated in Section 4.6.2.2 of Chapter 4; the values of m_{NG_i} are **3.42**, **2.92** and **2.06 tonnes** for monthly usage. After substituting the above to Equation 5.8, the total mass of **methane** is between **2.76**, **2.36** and **1.66 tonnes**, whilst **ethane's** total mass is between **0.159**, **0.135** and **0.096 tonnes**.

After calculating the mass of each of the two most significant components of natural gas, it is now possible to calculate the emissions range for the two usage scenarios using Equations 5.9 and 5.10:

$$\left.\begin{matrix} 16g\ CH_4 \rightarrow 44g\ CO_2 \\ m_{CH_4} \rightarrow m_{CH_4 \rightarrow CO_2} \end{matrix}\right\} \Rightarrow m_{CH_4 \rightarrow CO_2} = \frac{44 m_{CH_4}}{16}$$

$$\Rightarrow \boxed{m_{CH_4 \rightarrow CO_2} = m_{CH_4} \frac{11}{4}}$$

Equation 5.9: Calculation of CO_2 mass produced by the CH_4

$$\left.\begin{matrix} 30g\ C_2H_6 \rightarrow 88g\ CO_2 \\ m_{C_2H_6} \rightarrow m_{C_2H_6 \rightarrow CO_2} \end{matrix}\right\} \Rightarrow m_{C_2H_6 \rightarrow CO_2} = \frac{88 m_{C_2H_6}}{30}$$

$$\Rightarrow \boxed{m_{C_2H_6 \rightarrow CO_2} = m_{C_2H_6} \frac{44}{15}}$$

Equation 5.10: Calculation of CO_2 mass produced by the C_2H_6

where $\mathbf{m_{x \rightarrow CO_2}}$ is the mass of **CO_2** produced by component x in kg and $\mathbf{m_x}$ is the actual mass of component x. By substituting the above numbers into Equations 6.9 and 6.10 the masses of CO_2 from both **CH_4** and **C_2H_6** is **7.59**, **6.49** and **4.57 tonnes** and **0.466**, **0.396** and **0.282 tonnes** respectively. As a result, the total amount of CO_2 that Concept System 3 emits for both usage scenarios is **8.06**, **6.89** and **4.85 tonnes**.

Section 5.2.4: Comparison of the three concept systems

After making all the fuel consumption and carbon emission calculations in the previous three sections, for reasons of clarity, Table 5.3 concentrates all the calculated results regarding the three concept systems. Specifically, the first three columns represent the amount of diesel consumed the power station per household and the emissions because of diesel, while the far right column contains the consumption data and emissions of natural gas (NG) used by Concept System 3.

	Without System	With Concept System 1		With Concept System 2		With Concept System 3 (NG)		
	24 hours	**14.5 hours**	**20.5 hours**	**0 hours**	**0 hours**	**14.5 hours**	**20.5 hours**	**24 hours**
Total Fuel Consumption $\mathbf{m_{D_i}}$ or $\mathbf{m_{NG_i}}$ (tonnes)	2.73	1.65	2.33	0.00	0.00	2.06	2.92	3.42
Total CO_2 Emissions (tonnes)	8.48	5.12	7.24	0.00	0.00	4.85	6.89	8.06

Table 5.3: Total monthly fuel consumption and emissions production per system

As seen from the above table, Concept System 1 simply reduces the amount of time a power station supplies the host household with electricity, thus the power station consumes less amount of diesel per household and therefore emits smaller amounts of CO_2. This simple scenario is undoubtedly helpful, however the whole purpose of a renewable energy system is attempt to reduce the usage of fossil fuel to the greatest extent possible and Concept System 1 reduces diesel consumption by **39.5%** during the two summer months and only by **14.7%** during the two winter months. Additionally, a renewable system without storage is not a good financial investment, as that system would have a longer payback period.

In contrast, Concept System 2 is capable of achieving over **100%** of fossil fuel independence for its host household even during the winter months, due to ThST being designed to store thermal energy for sustaining the production WFV for **20.5 hours** after solar irradiance levels decrease below **200 W/m^2**. During those months, solar irradiance remains over the mentioned limit for **3.5 hours** meaning that the system alone is capable of covering the demand of the household without the need to absorb extra electricity from the national network, so for that household the power stations would not have to spend fuel and therefore the emission caused by the household are also zero.

As the previous two concept systems partial or total dependency on the national network, Concept System 3 is by default independent since it is equipped with the NGB that give it the characteristics of stability and reliability of fossil fuel systems. Table 5.3 actually shows in the "Concept System 3" column the total amount of natural gas in the being consumed but that system in order to cover its household's needs beyond the hours of sufficient solar irradiance. The column also contains the consumption data of a hypothetical **24 hour** NGB usage for comparison with the "Without System" power station consumption

scenario. As observed, the amount of natural gas consumed during the winter months (**20.5 hours**) is greater than the **24 hours** amount per household of the power station and therefore the same can be said in the case of "Concept System 3 (**24 hours**)"; this is only due to the fact that the mean weighted efficiency of the power station is about **41%** as mentioned in Section 5.2.1, while Concepts System 3's efficiency on natural gas operation mode becomes about **32%** instead of **24.5%** on Solar operation mode (see Table 4.17, Chapter 4). The financial comparison of the two fuels are analysed in Section 5.3 below. On the other hand, the emissions created by natural gas, even in the **24 hour** scenario, are less than those of the "Without System" diesel scenario by about **5%**. This fact is essential for the officials of Cyprus to know, as the power stations of the country could consume natural gas for the national electricity production instead diesel and fortunately the Vasilikos Power Station is fitted with two Combined Cycle Gas Turbine units that are can be converted to operate on natural gas.

In all cases, the three systems are responsible for fewer emissions than the "Without System" scenario as the consumption of diesel per household due to the first two systems is reduced and also natural gas produces a smaller amount of **CO_2 per kg** than diesel.

Section 5.3: Comparing the financial cost of using natural gas or diesel

This section compares the acquisition cost of both natural gas and diesel per unit energy and per unit mass in order to examine which fuel is financially more economical for usage per household in Cyprus. The natural gas prices, however, are not the ones used in Cyprus as the country's market does not currently provide its citizens with natural gas commercially; instead the prices below are those of the UK for being able to make comparisons with diesel consumption by the power stations. As a consequence, if Cyprus would use natural gas in a similar fashion as in the UK, the price per kWh would most probably be greater that the UK one, as natural gas would be imported to Cyprus. Moreover, since the prices of fossil fuels are not constant over time, in order to have a reliable price for each fuel, Table 5.4 contains the standard tariffs of various providers in the UK to calculate an average value for natural gas price. On the other hand, the price of diesel has been taken directly from the website of Cyprus's Ministry of Commerce, Industry and Tourism and it is

the average monthly price of August 2014 (MCIT, 2014a). That price is also registered into Table 5.4.

The conversion between both the price of natural gas in **British pence per kWh** and the price of diesel in **Euros per m^3** to **British pence per kg**, need to be executed before filling the table. Equations 5.11 and 5.12 execute the conversions by using the average low **CV$_{(m)}$** of the two fuels from Table 4.32 of Chapter 4:

$$\mathbf{E_{(kWh)} = 3.6\,\frac{MJ}{kWh}}$$

$$\mathbf{\left[Pr_{(m)}\right] = \frac{£p}{kg}\ ,\quad \left[Pr_{(kWh)}\right] = \frac{£p}{kWh}}$$

$$\mathbf{\left[E_{(kWh)}\right] = \frac{MJ}{kWh}\ ,\quad \left[CV_{(m)}\right] = \frac{MJ}{kg}}$$

$$\mathbf{\Rightarrow \boxed{Pr_{(m)} = \frac{Pr_{(kWh)}\,CV_{(m)}}{E_{(kWh)}}}}$$

Equation 5.11: Conversion between the price of natural gas per kWh to price per kg

$$\mathbf{\left[Pr_{(m)}\right] = \frac{£p}{kg}\ ,\quad \left[Pr_{(E)}\right] = \frac{€}{t}\ ,\quad \left[C_{(€\rightarrow £p)}\right] = \frac{£p}{€}}$$

$$\mathbf{\Rightarrow \boxed{Pr_{(m)} = 10^{-3} Pr_{(E)}\,C_{(€\rightarrow £p)}}}$$

Equation 5.12: Conversion between the price of diesel in Euros per m^3 to British pence per kg

where, **Pr$_{(m)}$** and **Pr$_{(kWh)}$** are the prices in pence of fuel per kg and kWh respectively, **Pr$_{(E)}$** is the price in **Euros per tonne**, **C$_{(€\rightarrow £p)}$** is the conversion factor of Euros to British pence and **E$_{(kWh)}$** is the conversion factor from **kWh** and **J**, which is basically the definition of the kWh. Lastly, the price of 1 **British penny per Euro** on the 22nd of September 2014 was **78.5 £p/€** (XE, 2014).

Natural gas			Diesel oil		
Source	Price		Source	Price	
	$Pr_{(kWh)}$ (£p/kWh)	$Pr_{(m)}$ (£p/kg)		$Pr_{(E)}$ (€/10^3 kg)	$Pr_{(m)}$ (£p/kg)
(British Gas, 2014)	5.18	68.78	(MCIT, 2014a)	880	69.08
(CAE, 2014)	4.80	63.73			
(EDF Energy, 2014)	4.79	63.60			
(nPower, 2014)	4.98	66.12			
(Scottish Power, 2014)	4.78	63.47			
Average	4.91	65.19			

Table 5.4: Domestic natural gas and industrial diesel prices in the UK from various sources

The table indicates that the **retail price** of natural gas in the UK is about **4 pence** smaller than the **wholesale price** of diesel in Cyprus even though wholesale prices are smaller than retail ones for the same item, as this is the benefit of purchasing in bulk. By combining the data from Tables 5.3 and 5.4 it becomes clear that per household, the consumer would pay fuel costs between about **£1140** to **£1610** per month by using the Concept System 1, **£0** if he is using Concept System 2 and from **£1343** to **£1904** if he consumes natural gas with Concept System 3. The 24 hour case of Concept System 3 would cost **£2230** per month to the consumer compared to **£1886** of continuous national network usage; the reason for this last price difference is that, even though natural gas is a cheaper fuel than diesel with a better CV, the amount of natural gas in the 24 hour scenario of Concept System 3 would be greater by **25.3%**, due to the fact that the system is less efficient than the power station. The other reason for the price difference is that the fuel data come from two different countries with Cyprus having lower fuel prices than the UK. For example, the average retail price diesel in Cyprus in September 2014 was **£1.123 per litre** (MCIT, 2014b), while the respective price in the UK on the 23 of September 2014 within a two mile radius from Manchester city centre **£1.313 per litre** (Petrol Prices, 2014). This means that if natural gas was used in Cyprus at a district level today, its retail price maybe would have been smaller than the average **65.19 £p/kg** currently being sold in the UK.

It should be noted that the above calculations of fuel costs for the three concept systems have been conducted assuming that the systems operate at maximum capacity (**20 kW**) throughout the month; in reality the consumer does not demand **20 kW** from the network constantly. Moreover, since all three of the systems are assumed to be connected to

the national network, the annual network connection costs charged by the EAC are omitted, as it would be the same for all three of them. The above calculations were conducted for comparing only the fuel cost to the consumer depending on the concept system and as a result, the calculated prices are indicative for the purposes of this project.

Section 5.4: Average power consumption of a typical household in Cyprus

The electrical load profile of a household is an important tool for predicting its demand in electrical energy from the national network and eventually from its subscripted power company (in the case of Cyprus the state's Electricity Authority is the sole provider). Moreover, the load profile could also assist the reduction of demand and the overall improvement of the household's electrical system by showing the possible periods of high consumption and thus revealing its peak value. The usage of daily real time measurements of a household's load could also indicate whether there is unnecessary "leakage" or not useful consumption of electricity due to design flaws, damage or due to the usage of low efficiency appliances. This section presents and analyses a rough load profile of a typical, 5-occupant Cyprus household and possible improvements this could suggest to the basic Concept System 1 design.

Section 5.4.1: Average power consumption of typical appliances

Before the typical load profile is presented, this section concentrates the average consumption rating of the most common household appliances. After that, Section 5.4.2 presents the consumption of the household over a **24 hour** period, one for winter and another for summer. With these two profiles, the peak value and overall electricity demand can be determined and further improvements to the basic concept system core design can be made. These calculations assume that the household is fitted with recently developed appliances with relatively high efficiency or low consumption without any electric heating or air conditioning. These figures are presented in Table 5.5 (Energy.gov, 2014; Philips, 2014; Bosch, 2015).

Appliance Name	Abbr.	Power Consumption (W)	
		Typical Range	Average
Ceiling Fans	CF	65 – 175	120
Clothing Dryer	CD	1800 – 5000	3400
Clothing Washing Machine	WM	350 – 500	425
Coffee Maker	CM	900 – 1200	1050
Compact Fluorescent Lights	CFL	8 – 27	18
Hair Dryer	HD	1200 – 1875	1540
Hobs (Induction – Bosch)	H	---	6850
Microwave Oven	MW	750 – 1100	900
Laptop	L	---	50
Refrigerator	R	---	725
Spotlights (LED)	SP	4 – 18	11
Television (Flat screen)	T	---	120
Toaster	TS	800 – 1400	1100
Vacuum Cleaner	VC	1000 – 1440	1220

Table 5.5: Energy consumption rating of common household appliances (Energy.gov, 2014; Philips, 2014; Bosch, 2015)

Section 5.4.2: Electrical load profile estimation

With the average consumption values in Table 5.5, the summer and winter typical household consumption schedules are shown in Table 5.6, followed by a chart representation in Figure 5.1.

Hour	Schedule		Cumulative Consumption (W)	
	Summer	Winter	Summer	Winter
00:00 – 01:00	R + 4CF	R	1205	725
01:00 – 02:00				
02:00 – 03:00				
03:00 – 04:00				
04:00 – 05:00				
05:00 – 06:00				
06:00 – 07:00	R + T + TS + CM	R + T + TS + CM + 4CFL	2995	2617
07:00 – 08:00	R	R	725	725
08:00 – 09:00				
09:00 – 10:00				
10:00 – 11:00				
11:00 – 12:00				
12:00 – 13:00				
13:00 – 14:00				
14:00 – 15:00	R + T + H + CF	R + T + H	7815	7695
15:00 – 16:00	R + 4CF + 4L	R + 4L	1405	925
16:00 – 17:00				
17:00 – 18:00	R + MW + T + CD	R + MW + T + 3CFL + CD	5145	5199
18:00 – 19:00				
19:00 – 20:00	R + T + 3CFL + H	R + T + 3CFL + H	7749	7749
20:00 – 21:00				
21:00 – 22:00	R + T + 4CFL + 4L	R + T + 5CFL + 4L	1117	1135
22:00 – 23:00	R + 4CF	R	1205	725
23:00 – 24:00				

Table 5.6: Summer and winter consumption schedule

As observed, Table 5.6 presents the amount of appliances most probably used per hour in a household and also the electricity demand in order the appliances can operate normally. Moreover, Figure 5.1 presents the mentioned electricity demand in a chart form, which indicates clearly the peak demand periods of the day and how much is the peak demand. In the typical case the peak demand does not exceed **8.5 kW** around the year and this means that the core system's goal electricity production can be reduced from **20 kW** to **10 kW**. The reason that the core system's electricity production capability is chosen to be **10**

kW is that to have a margin of error in case the system needs to provide more electrical power than the typical situation described in Figure 5.1. As a result, the basic Concept System 1 can be scaled down even more and so the energy input from the sun and/or the natural gas boiler is reduced by **50%**, since the power production demand $\dot{W}_T$ is halved. Further calculations appear in the following sections.

Another solution due to this fact is to have the system being shared by two households instead of one, since each household typically needs **10 kW** of peak load. This solution maybe more feasible than scaling down the system from **20** to **10 kW** as the two household could split the expenses of acquisition and maintenance and most importantly, they could more easily share the total number of the PTSC in their properties. This solution may be safer in case one of the households needs to exceed the consumption of electricity beyond the 10 kW on occasion, while the connection with the main power stations and the national network would ensure that the system would not fail if both households wish to exceed their demand in an extreme case. In addition to the sharing of the PTSC, the ThST can become a modular unit instead of one large tank so that it could become large enough to cover the needs of the household throughout the year and not only during the summer months, as mentioned in Section 5.2.4.

Section 5.4.3: Further improvements using the electrical network's coincidence factor

The previous section presents the average consumption profile of a typical household in Cyprus, which does not utilize the properties of the national electrical network; meaning that the **10 kW** system operates on a standalone basis and occasionally injects energy into the network. This system has the advantage of operating in "islanded" mode and as a result it does not need to be connected to the network. The problem with this system as explained previously is that for the time being several its components, mainly the turbine, do not exist or its installation on the premises of a typical household in Cyprus may not be feasible. More specifically, the PTSC's surface area of about **400 m^2**, as it has been calculated in Section 4.5.3.3, is an unrealistically high figure for installing in the rooftop of a household.

If, on the other hand, the household's system is connected on the network and does not operate in "islanded" mode, it then becomes part of the network and thus sharing the properties of the network. It is a common practice to assume that not all consumers of an

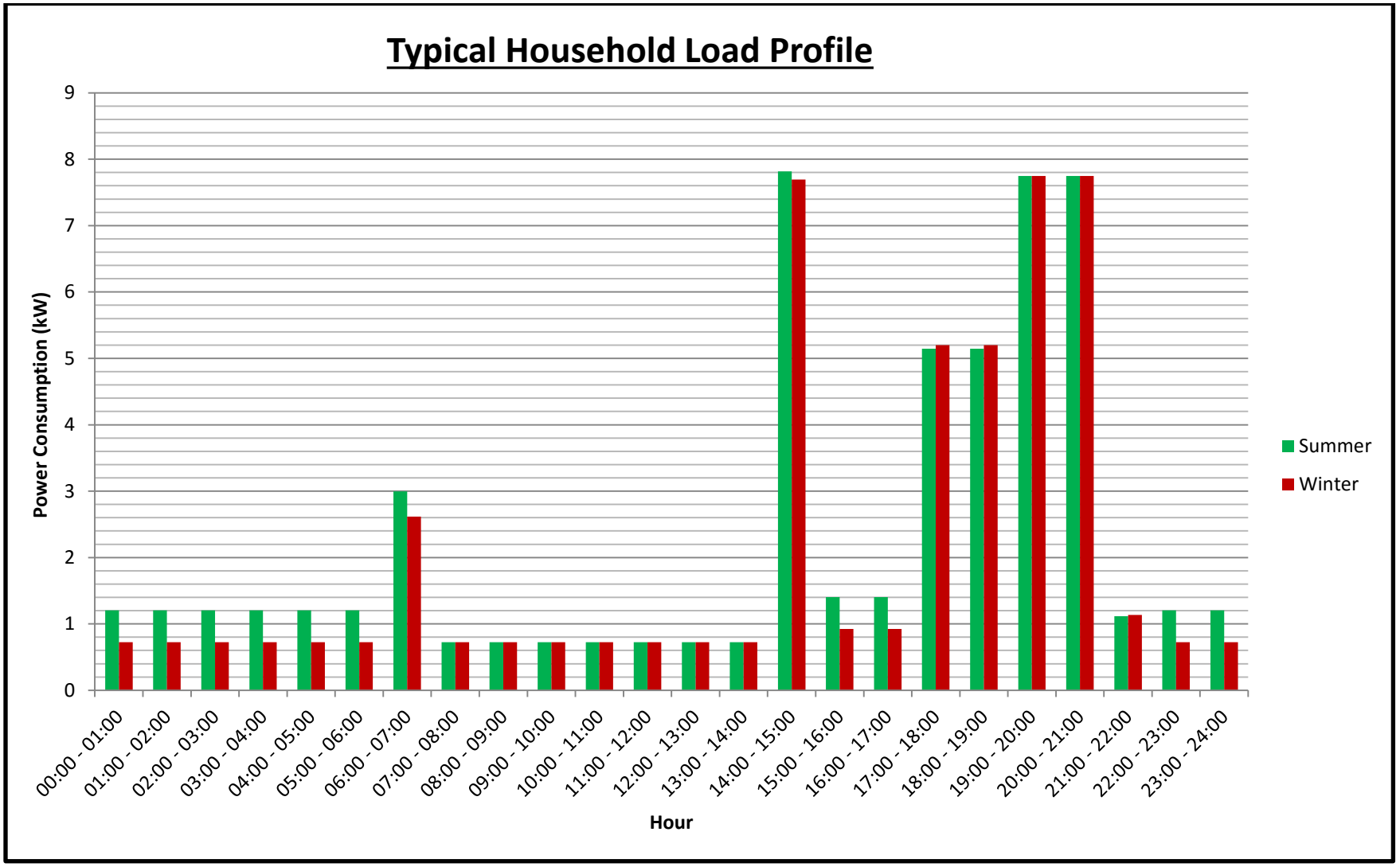

Figure 5.1: Typical household daily load profile

electrical network would exert their peak demand simultaneously at any given time. Thus electrical installation designers calculate the **simultaneity** or, more commonly, **coincidence factor** (**k_s**), thus estimating the apparent peak power supply that each consumer would require (Schneider Electric, 2010: p. A16). Depending on the total number of consumers connected on the network, the coincidence factor is less than or equal to 1 (Navarro et al., 2012: p. 2; Good, 2015: p. 206), meaning that interconnected consumers would have a smaller demand from the provider than their total installed load. In the case of this project, if there is a large number of network consumers fitted with the project's optimal system, then the coincidence factor allows the reduction of the system's power output even further from **10 kW** and thus reducing its components' size.

More specifically, Navarro et al. (2012: pp. 1-2), created models of UK residential loads with one-minute resolution and with randomly allocated numbers of occupants and available appliances. Based on a specific two-occupant UK summer model example, shown in Figure 5.2 (Navarro et al., 2012: p. 2), they calculated several quantities including the coincidence factor of the model. In addition, they examined the granularity effect on the

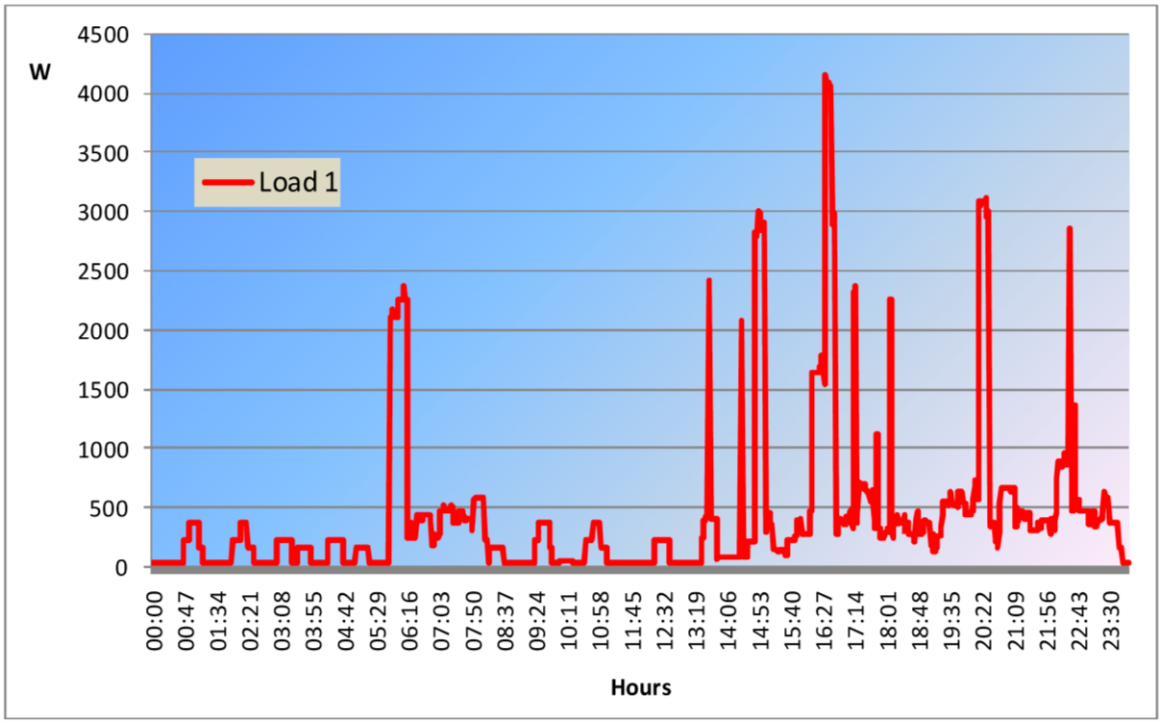

Figure 5.2: Example of a UK residential load model with two occupants with one minute resolution (Navarro et al., 2012: p. 2)

extracted quantities by calculating the average power demand of the mentioned example model for every **5**, **10**, **15**, **30** and **60 minutes** and then produced the graph of coincidence factor curves, shown in Figure 5.3 (Navarro et al., 2012: p. 2).

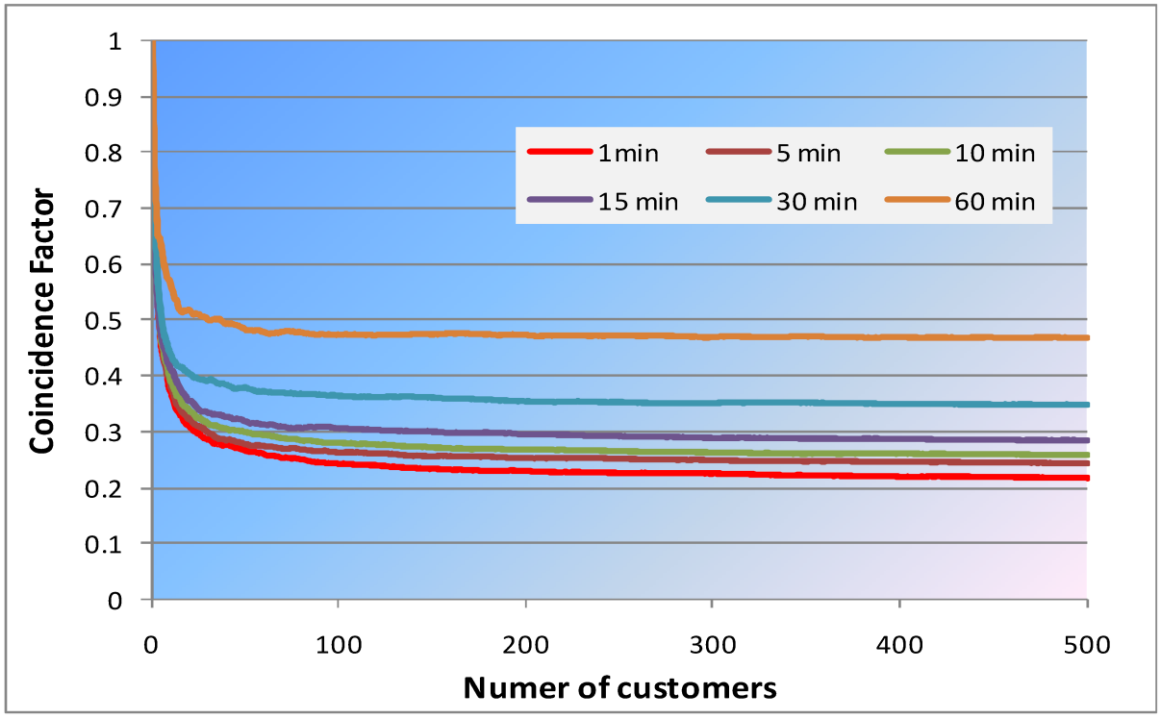

Figure 5.3: Coincidence factor curves indicating the granularity effect on the one-minute resolution example model of Figure 5.2 (Navarro et al., 2012: p. 2)

As observed, the coincidence factor is reduced significantly with the addition of a few customers and then it is reduced asymptotically to its final value with the cumulative addition of several hundred customers. Moreover, the resolution of the model has a significant impact on the calculation accuracy of the coincidence factor, as the one-minute resolution produces a coincidence factor of just over **0.2**, while the 60-minute resolution produces a coincidence factor of just under **0.5**, both for **500** customers. Based on these two observations, it is clear that the coincidence factor of a large number of interconnected customers would be between **0.2** and **0.5**, depending on the resolution of the demand data. In addition the summer demand profile of the 5-occupant Cyprus household example in Figure 5.1 is similar to the 2-occupant UK household example in Figure 5.2 with the exception that the one in Figure 5.1 has been created using the data of low consumption LED lighting technology, induction cooking hobs and of ceiling cooling fans. Moreover, increasing the number of occupants may not increase the total demand of the household linearly, as cooking, washing and watching television are

examples of activities that can reduce the usage time of energy consuming appliances when they are utilized to cover the needs of a greater number of occupants than one or two.

Consequently, as the EAC is the only electricity provider in Cyprus and also owns the islanded national electrical network of the country, it is safe to assume that all consumers in Cyprus are connected on the national network and they amount more than **500**. Thus, since the calculated coincidence factors shown in Figure 5.3 approach values between **0.2** and **0.5** asymptotically, these values can be used in this section for improving the demand profile of more than 500 interconnected customers in Cyprus as well. As a result, the **10 kW** peak demand of a standalone household – producer, as it was calculated in section 5.4.2, can be reduced to between **2** and **5 kW** per household connected to the network. The effects of this reduction to the size of Concept System 2's components are shown in Table 5.7 for a turbine power production of **1**, **2** and **5 kW**. The used data and formulae are found in Tables 4.17, 4.19, 4.21, 4.26 & 4.27 and Equations 3.9, 4.21, 4.23 & 4.31:

h_{3sc} (kJ/kg)	810.10	h_{2a} (kJ/kg)	577.70
h_4 (kJ/kg)	727.94	h_2 (kJ/kg)	107.16
h_{4a} (kJ/kg)	257.40	h_1 (kJ/kg)	106.22
t_{ThS} (s)	73.8×10^3	ρ_{TSM} (kg/m^3)	1675.5
L_{TSM} (kJ/kg)	170.00	$I_{b,\,min}$ (W/m^2)	200
$\dot{W}_T$ (kW)	**1**	**2**	**5**
$\dot{m}$ (kg/s)	12.2×10^{-3}	24.3×10^{-3}	60.8×10^{-3}
$\dot{Q}_{B_{+IHE}}$ (kW)	4.05	8.07	20.19
$\dot{Q}_{C_{+IHE}}$ (kW)	1.84	3.67	9.19
$\dot{W}_P$ (kW)	11.5×10^{-3}	22.8×10^{-3}	57.2×10^{-3}
$\dot{W}_{ThS}$ (kW)	2.84	5.65	14.13
m_{TSM} (kg)	1.32×10^3	2.45×10^3	6.13×10^3
V_{TSM} (m^3)	0.79	1.46	3.66
A_{Col} (m^2)	20.25	40.35	100.95
t_r (s)	4991.4	2495.7	998.3
m_{SA} (kg)	43.9	87.5	218.9

Table 5.7: Recalculation of Concept System 2's size based on the reduced electricity output that is improved by the coincidence factor (data from Tables 4.17, 4.19 4.21, 4.26, 2.27)

From these values, one can conclude that the project's optimal solution is more feasible to be installed in a typical household in Cyprus if its size is between **1** and **5 kW**, instead of **20 kW**. The first and most apparent benefit is that the collector's area is reduced by between **20** and **4 times** respectively; so if one decides to install a **2 kW** system, then he would need to reserve only about **40 m^2** on the household's rooftop rather than **400 m^2**. The size of all components is reduced as well, thus reducing the amount of latent heat Thermal Storage Medium, the size of the Thermal Storage Tank, the size of the Steam Accumulator and most importantly the size of the turbine. The only disadvantage of this improvement is that the amount of recovery time (**t_r**) it takes to heat the **225 litres** of Domestic Hot Water is instead increased by between **4** and **20 times**. This means that the system producing **1 kW** of electricity would also need about **84 minutes** to increase the temperature of DHW from **20** to **60 ºC**. So, the better improved scenario of the three presented in Table 5.7 is the one producing **2 kW** of electricity, as it needs only about **40 m^2** of solar collector area and has about **42 minutes** of total recovery time for the DHW tank.

Section 5.5: Examining existing equipment based on the new concept system 2 size and comments on cost

Since the optimal Concept System 2's size was reconsidered in Section 5.4.3, the next step is to re-examine if suitable equipment based on the values of Table 5.7 currently exist in the marketplace. The major components of this system are: the three-phase synchronous alternator; the parabolic trough solar collector and the heat engine (in the case of this project, the steam turbine). The secondary components would be: the steam accumulator; the DHW storage tank; the TSM storage tank; the heat exchangers and the condensate pump.

The alternator is a component readily available, as the synchronous electrical machine technology is well established and it is the protagonist in nearly all large scale power systems today, either they are based on fossil fuel or not. After establishing contact with several suppliers, one particular Chinese company Fuzhou Jet Electronic Machinery Co., Ltd. indicated the availability of single-phase (ST-) and three-phase (STC-) synchronous alternators, ranging from **2** to **20 kW** (single-phase) and between **3** and **50 kW** (three-phase); their respective price range is between **106** to **385** United States Dollars (USD) and from **129** to **746** USD. These prices include the shipping price to either Cyprus or the UK; however, the company mandates a minimum order quantity of **100** pieces in order to ship the

equipment, indicating that the mentioned prices are wholesale. This is a problem, as an individual household would not need **100** units, instead it only one for its system. Therefore, acquisition of the alternator may not be feasible from an individual client's standpoint. On the other hand, if there would be a supplier company in Cyprus importing the equipment and selling individual units to local customers, then the acquisition of alternators would be achievable.

The parabolic collector is the second major component that is significantly improved according to Table 5.7. An Italian company, Soltigua Concentrating Solutions offers two types of small scale collectors, the **PTMx** type and the **FLT** type. The former type is a parabolic trough collector that is available in 4 versions depending on the collector's length: **PTMx-18**, **PTMx-24**, **PTMx-30** and **PTMx-36** with lengths of **20.7**, **27.2**, **33.2** and **39.6** m respectively and effective collector area of **41**, **54**, **68** and **82 m^2**, correspondingly (Soltigua Concentrating Solutions, 2016a: p. 3). The FLT type includes 5 Fresnel solar collectors with effective surface areas ranging from **148.5** to **445.5 m^2** and corresponding lengths between **25.02** and **74.34** m (Soltigua Concentrating Solutions, 2016b: p. 4). It is obvious that the most suitable type for domestic applications is the **PTMx** one, as those collectors are available in smaller surface areas and they can easily fit on the rooftop of a household. More specifically, the **PTMx-18** collector is the most suitable for this project, as its effective surface area is **41 m^2**. Even though the company states that these collectors are suitable for ORC electricity generation applications, their maximum operating temperature is **280 ºC**, which much lower than the maximum operating temperature of Concept System 2 at **390 ºC** (Soltigua Concentrating Solutions, 2016a: p. 3). Moreover there is no indication of the collector's maximum operating pressure in the collectors' booklet, which means that the usage of such collector is not feasible.

Lastly, it is the examination of the heat engine and as already mentioned small scale steam turbines do not exist today. In contrast, there are commercially available engine-generator packages that produce electrical power under **100 kW**. Two characteristic examples of such packages are the **GENIOUS Stirling generator** by the Swedish company INRESOL (INRESOL, 2016) and the **Rank LT** model by the Spanish company Rank® (Rank, 2016). The GENIOUS engine produces **5 kW** (**10 kW** peak) of AC electricity at between **600** to **1200 rpm**, which is then rectified to **565 V_{DC}** and then inverted to three-

phase **400 V_{AC}**. The primary problem with this product is that it is an engine-generator package, whereas this project only requires an engine for driving the synchronous generator. Secondly, electricity produced by this product needs to pass through a rectifier and an inverter to become useful and thus becoming unsuitable for network injection. Moreover, operation of the product commences after the heat source has exceeded **600℃**, whereas the project demands a maximum temperature of **390℃** from the parabolic collector. The fourth and most important issue is that the thermal-to-electrical efficiency of the package lies between **22** and **34%**, as expected of a Stirling engine based product (INRESOL, 2016: p. 4). The **Rank LT** is also a complete package, capable of receiving heat energy from various renewable and waste heat sources for producing **25** to **50 kW** of electricity with an activation temperature at **85℃**. It is unknown if the prime mover of the package is a Stirling engine; however it is stated that the package is based on the ORC. The waste heat from the electricity production process can be used for industrial processes, DHW heating and absorption cooling. As with the INRESOL package, the major problem of this engine-generator package is its low thermal-to-electrical efficiency of about **6.25%**, which is much lower than the INRESOL one's. In addition, the electricity power output of this package is between **12.5** and **25 times** greater than the **2 kW** output of the project's scaled down optimal system and also further details about the production of this electrical power, such as voltage and frequency and number of phases are not mentioned (Rank, 2016: p. 2).

In summary, even with the reduction of Concept System 2 in scale and even though heat engines and the parabolic solar collectors exist in the marketplace today, they are not within the specifications of this project. Additional problems are caused by the wholesale policy of synchronous alternator suppliers, as they require the purchase of a large amount of units from them in order to ship the products to Europe. In other words, existing components still cannot be used for constructing the system into the real world. Secondary components, such as Steam Accumulators, even though they exist in the marketplace they also are not within the specifications; however, such components are simple devices and it would be easier to be designed and manufactured. So, further research and development is needed at this stage for the optimal system of this project so that prototypes are constructed and tested before they are mass produced. This means that at this stage the project is in no position to make any comments about acquisition nor maintenance costs and thus making comparisons with similar sized PV systems.

Reference List

Air Liquide, (2013a), *Gas Encyclopedia – Ethane*. Available at: http://encyclopedia.airliquide.com/Encyclopedia.asp?LanguageID=11&CountryID=19&Formula=&GasID=28&UNNumber=&EquivGasID=41&VolLiquideBox=&MasseLiquideBox=&VolGasBox=&MasseGasBox=&RD20=29&RD9=8&RD6=64&RD4=2&RD3=22&RD8=27&RD2=20&RD18=41&RD7=18&RD13=71&RD16=35&RD12=31&RD19=34&RD24=62&RD25=77&RD26=78&RD28=81&RD29=82 [Accessed: 13 September 2014]

Air Liquide, (2013b), *Gas Encyclopedia – Methane*. Available at: http://encyclopedia.airliquide.com/Encyclopedia.asp?GasID=41#GeneralData [Accessed: 13 September 2014]

Bosch UK, (2015), *Home Appliances – Induction Hobs* (Instruction Manuals) Available at: http://www.bosch-home.co.uk/products/cooking-baking/hobs.html [Accessed: 01 September 2015]

British Gas, (2014), *Compare energy tariffs*. Available at: http://www.britishgas.co.uk/products-and-services/gas-and-electricity/our-energy-tariffs/compare-energy-tariffs.html#gas-Standard-til [Accessed: 19 September 2014]

Confused About Energy (CAE), (2014), *Fuel Prices*. Available at: http://www.confusedaboutenergy.co.uk/index.php/domestic-fuels/fuel-prices [Accessed: 19 September 2014]

EDF Energy, (2014), *Tariff Information Label (TIL) – Standard (Variable)*. Available at: https://my.edfenergy.com/gas-electricity/tariff-information-labels/view-label?region=G&division=02&paytype=01&tariff=STD&product=GRC1_CORE&showpaymentmethoddesc=true [Accessed: 19 September 2014]

Electricity Authority of Cyprus (EAC), (2007), *Vasilikos Power Station*. [Online]. Available at: https://www.eac.com.cy/EN/EAC/NewsAndAnnouncements/Informative%20Leaflets/VASILIKOS%20POWER%20STAT-ENG.pdf [Accessed: 14 September 2014]

Electricity Authority of Cyprus (EAC), (2014a), *Generation*. Available at: https://www.eac.com.cy/EN/EAC/Operations/Pages/Generation.aspx [Accessed: 19 September 2014]

Electricity Authority of Cyprus (EAC) (2014b) *Daily System Generation (MW) (Sunday, 9 November 2014)*, Available at: http://www.dsm.org.cy/nqcontent.cfm?a_name=graphing_load_1&lang=l2 [Accessed: 9 November 2014]

Enbridge, (2014), *Components of natural gas*. Available at: https://www.enbridgegas.com/gas-safety/about-natural-gas/components-natural-gas.aspx [Accessed: 12 September 2014]

Energy.gov, (2014), *Estimating Appliance and Home Electronic Energy Use*. Available at: http://energy.gov/energysaver/articles/estimating-appliance-and-home-electronic-energy-use [Accessed: 9 September 2014]

Good, N.; Zhang, L.; Navarro, A. & Mancarella, P. (2015) 'High resolution modelling of multi-energy domestic demand profiles', *Applied Energy*, 137, pp. 193-210.

Home Heating Guide (HHG), (2014), *SEDBUK (Seasonal Efficiency of Domestic Boilers in the UK) Rating*. Available at: http://www.homeheatingguide.co.uk/sedbuk-rating.html [Accessed: 6 September 2014]

Innovative Renewable Energy Solutions (INRESOL) (2016) ***GENIOUS Solar and CHP Stirling Solutions.*** [Online]. Available at: http://www.inresol.se/pdf/GENIOUS_datasheeet_stirling_engine.pdf [Accessed: 13 February 2016]

Isidoro Martinez, (2014), ***Fuel Properties,*** Available at: http://webserver.dmt.upm.es/~isidoro/bk3/c15/Fuel%20properties.pdf [Accessed: 14 September 2014]

Moran, M. J.; Shapiro, H. N; Boettner, D. D. & Bailey, M. B. (2011) ***Fundamentals of Engineering Thermodynamics*****, 7th edition. New Jersey: John Wiley & Sons, Inc.**

Navarro, A.; Ochoa, L. F. & Mancarella, P. (2012) 'Learning from Residential Load Data: Impacts on LV Network Planning and Operation', ***Transmission and Distribution: Latin America Conference and Exposition (T&D-LA), 2012 Sixth IEEE/PES*****, pp. 1-8.**

nPower, (2014), ***Tariff Comparison Rate (TCR).*** Available at: https://www.npower.com/at_home/Applications/product_comparison/Tariff.aspx/TcrResults?productTerm=Long [Accessed: 19 September 2014]

Petrol Prices, (2014), ***Petrol station prices within 2 miles from M1 5QD.*** Available at: http://www.petrolprices.com/search.html?search=M1+5QD [Accessed: 23 September 2014]

Philips UK, (2014), ***Lamps – Product Catalogue.*** Available at: http://www.ecat.lighting.philips.co.uk/l/lamps/23079/cat/ [Accessed: 9 September 2014]

Rank® (2016) ***Rank®: Your trusted partner.*** [Online]. Available at: http://www.rankweb.es/files/file1277_Diptic_Rank_MAIL.pdf [Accessed: 13 February 2016]

Republic of Cyprus, Ministry of Commerce, Industry and Tourism (MCIT), (2014a), ***Sale prices of petroleum fuels in Cyprus's market (in Greek).*** [Online]. Available at: http://www.mcit.gov.cy/mcit/mcit.nsf/All/232E1DCBE183F78AC2257D4A0025AB87/$file/AUG%202014%20OIL%20PRICES.pdf [Accessed: 23 September 2014]

Republic of Cyprus, Ministry of Commerce, Industry and Tourism (MCIT), (2014b), ***Observation of petroleum products' retail prices (in Greek).*** [Online]. Available at: http://www.mcit.gov.cy/mcit/mcit.nsf/dmloilnew_gr/dmloilnew_gr?OpenDocument [Accessed: 22 September 2014]

Scottish Power, (2014), ***Scottish Power – Standard Tariff.*** Available at: http://www.scottishpower.co.uk/tilpdf/G-PPLUS-BDM-GAS.pdf [Accessed: 19 September 2014]

Schneider Electric S. A. (2010) ***Electrical installation guide 2010 - According to IEC international standards*****, France: AXESS.**

Soltigua Concentrating Solutions (2016a). ***A new horizon for solar energy: Soltigua presents PTMx, the parabolic solar collector for a wide range of applications.*** [Online]. Available at: http://www.soltigua.com/wp-content/uploads/2014/09/Soltigua-PTMx_ENG.pdf [Accessed: 11 February 2016].

Soltigua Concentrating Solutions (2016b). ***A world of opportunities: Soltigua's linear Fresnel collector FLT is the ideal solution for solar process heat and air conditioning on ground and rooftop installations.*** [Online]. Available at: http://www.soltigua.com/wp-content/uploads/2015/04/Soltigua_FLT_ENG_4pg.pdf [Accessed: 11 February 2016].

The Engineering Toolbox (ETb), (2014a), ***Fuels – Higher Calorific Values*****.** Available at: http://www.engineeringtoolbox.com/fuels-higher-calorific-values-d_169.html [Accessed: 4 September 2014]

The Engineering Toolbox (ETb), (2014b), ***Gases – Densities*****.** Available at: http://www.engineeringtoolbox.com/gas-density-d_158.html [Accessed: 5 September 2014]

The Engineering Toolbox (ETb), (2014c), ***Fuels – Densities and Specific Volumes*****.** Available at: http://www.engineeringtoolbox.com/fuels-densities-specific-volumes-d_166.html [Accessed: 22 September 2014]

The International Union of Pure and Applied Chemistry (IUPAC), (2013), ***IUPAC Periodic Table of the Elements*****.** Available at: http://www.iupac.org/fileadmin/user_upload/news/IUPAC_Periodic_Table-1May13.pdf [Accessed: 12 September 2014]

UnionGas, (2014), ***Chemical Composition of natural gas.*** Available at: https://www.uniongas.com/about-us/about-natural-gas/chemical-composition-of-natural-gas [Accessed: 12 September 2014]

U.S. Department of Energy (USDE), (2011), ***Biomass Energy Data Book*****, 4th edn., Oak Ridge, Tennessee: Oak Ridge National Laboratory.**

XE Currency Converter, (2014), ***Conversion of GBP to Euros*****.** Available at: http://www.xe.com/currencyconverter/convert/?Amount=1&From=GBP&To=EUR [Accessed: 22 September 2014]

Chapter 6: Conclusions and discussion

Section 6.1: Summary and Conclusions

This final section contains the project's conclusions along with a discussion part for future projects and improvements regarding the meeting of electricity demand in Cyprus based on Renewable Energy Sources (RES).

Section 6.1.1: Summary

This project explores the question of whether there is an alternative method to the usage of Photovoltaics for harnessing the free and renewable solar energy in an effective way in buildings for the island state of Cyprus. The aim of the project is to design a system capable of harnessing thermal solar energy in order to produce electricity and domestic hot water at a residential level. This main idea is divided into two main objectives:

1. Design and simulate three alternative concept systems. This is the main core of the project, the one that has to do with the conception, design and virtual implementation of three system scenarios, Concept Systems 1, 2 and 3, each examining the a different way of producing or storing energy to cover the needs of the host household and from those the optimal system could be declared. An initial calculation of the household's electricity and Domestic Hot Water needs set the designing targets and after the three concept systems were illustrated in block diagrams the sizing calculations of their components were realised. The concepts were then mathematically simulated with the usage of the Engineering Equation Solver software package.

2. Analyse the economic aspects of the project. After sizing each of the systems' components, some economic aspects needed to be addressed, mainly the environmental impact each concept would have in Cyprus and how they would financially benefit the owners of the household in terms of electricity bill reduction, which ultimately are the main factors of determining the optimal system to be eventually mass manufactured. The project however does not contain an in-depth economic analysis for determining the length of the investment's payback period along with the overall acquisition and maintenance costs, as several of the systems' components do not exist in the marketplace today at appropriate capacities and they are only conceptualised for the purposes of this project.

Following the project's objectives is a summary of each chapter:

Chapter 1: It is the introductory chapter that states the project's aim and objectives.

Chapter 2: This is the Literature review chapter that contains background information about the socioeconomic life of Cyprus that give a general idea about the various issues regarding the demands of energy, leading to the need and the essence of seriously exploiting the RES.

Chapter 3: This chapter analyses several fundamental topics of Thermodynamics, before it explains the study of the three different concept systems. This is the basis for the objectives and aim of the project to design a Solar Thermal (STh) electricity production system at a domestic level that also has the capabilities of heating up Domestic Hot Water (DHW).

Chapter 4: Here, the actual design process for three concept STh systems is described in detail and step by step. Originally, the thought was to design a medium sized, district level Trigeneration (or CCHP) STh system; however, that system was proven too large for a single PhD project to handle as it had a large number of parameters. So, the aim and objectives of the original project shifted into designing three, domestic level, concept systems for examining three different configurations and operation scenarios: The first one is the core system that absorbs solar energy, heats up the compressed working fluid into superheated vapour, expands it into a steam turbine producing the needed electricity and DHW and lastly it is liquefied through a condenser, repeating the cycle. The second system adds thermal storage to the first core system so that its operation is extended during the hours that solar energy is not enough to drive the system. The third and last concept system replaces the thermal storage with a natural gas boiler that assumes the task of driving the system after hours. The usage of water as the systems' working fluid was the first choice, but it turned out not to be suitable for a small scale system and so a "dry" organic siloxane compound (**Dodecamethylpentasiloxane,** or **MD_3D**) was selected to act as the working fluid, as it offered the system greater efficiency.

Chapter 5: After chapter 4 explains the technical aspects of the project, this next chapter analyses the impact of the three systems to the host household, by showing which one is capable of reducing the electricity expenses to the minimum. Moreover, it contains the impact of each one to the environment, by indicating which is causing less emission production either by reducing the amount of fossil fuels used by a power station per household or by its own operation. Additionally, the chapter presents a calculation of a typical household's load profile to examine whether there is a way of scaling down the system even further, in order to reduce the acquisition costs and that the equipment would become easier to be fitted in the grounds of a household. Chapter 5 ends with another improvement to the size of the optimal system. In this case the system does not operate on a standalone basis, but as a part of the national electrical network, which allows the peak demand of the host household to be reduced from about **10 kW** to **2 kW** due to the coincidence factor of the network that considers that the customers of the network almost never ask for their peak demand simultaneously. As a result the system's components can be further reduced in size, thus offering a more realistic size for installing in a single household in Cyprus. However, even with the latest improvement, the necessary components either do not exist or they are not within the specifications of the project thus actual financial acquisition costs could not be presented and the project's investment financial analysis could not be realised.

Section 6.1.2: Conclusions

1. This projects presents that Cyprus has an overall problem of increasing electricity demand per annum and therefore increasing emission levels in the atmosphere. The possible reasons for these increasing trends are the increase in population, the number of households, the amount of private passenger vehicles and lastly because electricity in Cyprus is produced almost exclusively by using fossil fuel. Moreover, **55%** of residential buildings, which most of them are single family households, are not fitted with any type of insulation. This fact increases the demand for space heating and cooling during winter and summer respectively, which leads to the excessive usage of fossil fuel based central heating systems and air conditioning split units. Increased dependency on fossil fuel for energy production and elevated emission levels oppose the Directives of the EU, especially the EUETS and its 20-20-20 target by 2020, meaning that Cyprus will be obligated to pay an annual fine for not complying with this target.

2. On the other hand, Cyprus possesses the largest proportion of solar collector area per capita amongst the EU members and nearly all residential buildings are fitted with a solar water heating system. This means that the Cyprus population has an established positive mentality towards exploiting renewable energy. This opinion is reinforced, as several households are fitted with additional photovoltaic collectors for partial electricity demand coverage.

3. However, photovoltaic technology has several serious disadvantages, including low module efficiency, the need for complementary power electronic components, decrease of modules' power output with temperature, usage of hazardous materials during their manufacturing process and the fact that electricity cannot be stored easily. For these reasons, the project investigates the utilization of solar thermal technology instead to avoid these disadvantages and also for offering an alternative solution to photovoltaic systems. The advantages of solar thermal systems are: simpler design; longer lifespan; greater overall system efficiency; easier energy storage; dispatchablity; direct production of AC electricity and capability of reducing the carbon footprint and net energy demand of the building to zero.

4. The project examines three concept system designs for this purpose, based on a solar thermal system template. The PTSC was deemed as the most suitable collector type for this template and in the case of energy storage for after-hours operation, the latent heat type was selected. The systems are capable of producing stable, three-phase voltage that ensures the safe and reliable electricity injection into the national network, if necessary. In addition, the systems use the ground for condensing their working fluid by utilizing a horizontal ground heat exchanger.

5. Traditional large scale power stations are based on the Rankine thermodynamic cycle, using water as their working fluid. Even though being abundant and well-studied, water is not suitable for usage in the three domestic scale systems, as there are safety constraints regarding temperatures and pressure levels and it also offers an overall system efficiency factor of about **14.8%**, under non-ideal conditions. For this reason, an organic working fluid was selected and used instead called **Dodecamethylpentasiloxane** (**MD_3D**),

which increases the non-ideal efficiency to **24.5%**, greater than the best acclaimed efficiency of a photovoltaic solar collector today (**21.5%**).

6. The three concept system configurations are: direct working fluid vapour generation; direct working fluid vapour generation with thermal storage and direct working fluid vapour generation with a companion NGB. The first system vaporizes the working fluid through the PTSC directly from the sun for its ORC operation and it does not have any storage for night time operation. The second system, in addition to the PTSC, vaporizes the working fluid by using latent heat stored in the eutectic salt compound **45KCl – 55LiCl** and it is capable of operating on a 24-hour basis, without any support from the national network. Lastly, the third system also has the 24-hour operation capability; however it is fitted with a NGB instead of a thermal storage. The project proved that the second concept system is the optimal one, as it supplies its host household with renewable energy constantly, reducing its carbon emissions to zero, as it does not depend on the national network to operate, thus saving fossil fuel from the power stations' operation and it also does not have a natural gas operating boiler.

7. As the original thought for this project was for the optimal system to produce **20 kW** of electricity on a standalone basis, the final size of it proved to be unrealistically large for a single household. The most characteristic example was the **400 m^2** of needed surface area for the PTSC. As a result, the estimation of the household's electricity demand profile for both winter and summer proved that the system's maximum capacity could be reduced to **10 kW** instead, which assists the reduction of its components' sizes by half. One more solution takes into consideration the coincidence factor of the network and since the nearly all consumers in Cyprus are connected on the EAC network, the coincidence factor could reduce the average demand of each household to about **20%** of the original peak demand. This means that by sacrificing the benefits of a standalone system and exploiting the properties of the network, the optimal system can be further reduce in producing **2 kW**. Consequently, this system's size can be reduced by **90%** of the original **20 kW** system size allowing for a need of **40 m^2** of collector's surface area, which is much more realistic for installing on household's rooftop. The only disadvantage is that the recovery time for the DHW tank is increased by ten times to about **42 min**, as the demand for hot water remained constant to **225 litres**.

Section 6.2: Discussion – Proposal of future projects

Section 6.2.1: Project benefits

As renewable energy is free and inexhaustible, there are several benefits that offer to a country's economy and environment. More specifically for the optimal system of this project the benefits revolve mainly around the domains of national electricity production, environment and financial economics of Cyprus.

1. Firstly, the electricity production on a national scale would be directly affected since the optimal system is capable of operating exclusively on solar energy. The country's three power stations would be kept operational for other functions, such as public lighting and also in the case where households are incapable of producing their own electricity, either because they are too small for hosting a system the size of the optimal one's or they are not fitted with any other system based on renewable energy. This will enable the power stations to operate on **Base Load** mode, which is basically having their boilers operate on minimum capacity. The reason why power stations should not be turned off completely is that the boilers and steam turbines need several hours to operate on full capacity once turned on, as they have a low response time. So, the **Base Load** operation is in place around the day and when extra capacity is demanded, the turbines with much quicker response time would be connected onto the network to cover the extra demand.

2. The **Base Load** mode automatically means the reduction of fossil fuel consumption per day and generally per year. In addition, households' electricity bills would be reduced as well, since their demand would be covered directly from solar energy, without the dependency on the national network around the day. Consequently, this will reduce the greatest proportion of national expenditure, possibly leading to a reduction in fuel taxation. Less fuel consumption means reduced annual emissions levels, allowing the country to comply with its EU responsibilities and thus avoiding paying extras fines due to the 20 – 20 – 20 target of the EUETS (see section 2.5.2).

3. National network independency also means the decentralization of electricity production, raising the reliability of the whole national system of Cyprus even further. As being isolated, Cyprus' electrical system is susceptible to power interruptions if one of the

three stations gets damaged, such as the Vasilikos power station's case in 2011. As a result, if the EAC also acts as the arbiter of the renewable electricity being injected into the national network, its stability and sustainability could be more secured.

4. One other possible and long term benefit of such a system is the creation of new engineering and technician job positions in Cyprus, responsible for assembling, installing and maintaining these systems on a large scale. New industrial units could also be created to accommodate the assembly processes, improving the country's economy and position in the international stock markets.

Section 6.2.2: Proposals for further research

Every research projects contributes to the increase and improvement of human intellect, while aiding the human life to become better and also preserve the natural environment. So, the second task of every researcher is not only to reach his project's goals, but to motivate and promote the creation of new research topics. This spawns new generations of individuals for getting involved with research in order to bring fresh ideas and approaches on how to solve humanity's problems. This section concentrates several topics that could be assumed from this project for further research and development.

1. The most important topic is for mechanical engineers to design and manufacture the small scale equipment to accommodate the system capacities that this project designed. Additionally, these engineers could improve the steam (and/or organic WFV) turbine technology in terms of higher isentropic efficiency by attempting to remove the irreversibilities described in section 4.3.2.2 of Chapter 4. These developments would not only assist the increase of research positions for young engineers, but also would lead to the reduction of fossil fuel demand and therefore greenhouse emissions.

2. Another research topic derived from this project is for mechanical engineers to identify other organic fluids with similar thermodynamic properties as water in combination with the additional benefits of dry fluids (see section 4.4.3 of Chapter 4). In parallel, the project also could create new chemical engineering research positions for synthesising new organic compounds with better thermodynamic properties, for acting as organic working fluids for the optimal system. Furthermore, researchers could also study the utilization of

safer and abundant fluids (such as **CO_2**) for supercritical applications in medium and large scale systems, in which there are no safety concerns about high pressure levels in the **S_2** ORC. Better properties assist the increase of the system's overall efficiency, thus reducing its overall size and cost. Therefore, the optimal system would become more affordable to the public and maybe motivate the government to offer higher subsidies for promoting this technology.

3. The PTSC is another area of interest that needs improvement. Mechanical engineers could develop new collector geometric designs with greater surface area per module than current designs have for harnessing greater amounts of solar energy per unit area. Additionally, theυ could develop special coatings for the collector's reflective area in order to increase its reflectivity index even higher; the coating could simultaneously have a low friction coefficient as well so that dirt particles would slide away from the reflective area and therefore not reducing the thermal efficiency of the PTSC. Engineers could also designs domestic size collectors capable of reaching temperatures greater than **400 ºC** (**670 K**) so that the working fluid could reach a state of higher specific enthalpy value and thus increasing the efficiency of the system.

4. Another possible research topic is the development of more environmentally friendly electronic components based on safer semiconductor and other materials and at the same time attempt to increase the efficiency of PV panels. The possible environmental, health and safety (EHS) hazards are mentioned in section 3.3.1 of Chapter 3.

Section 6.2.3: Discussion

The project set out to examine if solar thermal energy can be utilized effectively for electricity production at a domestic level. One of the reasons that the project focused on designing a solar thermal system is to also to give an alternative feasible solution to PV, since a PV system has very small efficiency (**21.5%** is the acclaimed highest efficiency of a PV collector and not of an entire system) they are expensive to acquire and maintain and also electricity itself cannot be stored easily. On the other hand, the STh optimal system of this project has an overall efficiency of about **25%**, so it is more efficient than a PV system of the same size. Furthermore, the only EHS consideration about the project's optimal system

is the safe containment of its chemical compounds (sensible and latent heat storage salts along with siloxane working fluid) in order to prevent leakages (Tsoutsos et al., 2005: p. 291).

In order to avoid using the dangerous chemicals mentioned in the previous paragraph, researchers have developed **Organic Photovoltaics (OPV)**, also called "plastic solar cells" that have additional advantages including being light weight, semi-transparent, they have mechanical flexibility over their semiconductor counterparts and most importantly their production processes require less energy consumption and demand of scarcely found materials, such as Indium (**In**), Tellurium (**Te**) and Gallium (**Ga**). On the other hand, compared with semiconductor based PV, the lifespan of **OPV** devices is a few years, their payback periods are about double (**2** to **4 years**) and their achieved device efficiencies are about half (maximum **10%**) of normal PV. So, since the OPV technology is at its infancy, its position is disadvantageous; however, it is very promising as it has important advantages over semiconductor PV and it would eventually replace them (Zimmermann et al. 2012: p. 129).

In summary, even though Photovoltaic technology (semiconductor or organic) is arguably very appealing, due to its capability of directly converting solar energy into electricity, its disadvantages outweigh the advantages. In comparison, even though having more parts and potentially be more expensive to acquire, the proposed optimized system of this project is simpler in design and selection of materials, its overall system efficiency is greater than even the best PV panel today, its EHS considerations are lower and it has a much longer lifespan if maintained properly. As for its size, it may be too large for a single household, whereas PV are being already installed on top of Cypriots' households with ease, and maybe a STh system could be even more effective if constructed at a medium scale to cover the needs of a small community or neighbourhood, instead of a single household. It would be able to utilize a larger land area for increased solar energy absorption and it could therefore operate at greater temperatures and pressure levels without the safety constraints of a household. Photovoltaic technology has the potential of becoming even more appealing at some point in the future, as it is currently improving according to NREL (2015), while young researchers with fresh ideas continuously assist the industry in designing and producing all the more efficient and reliable systems. The de facto improvement of the various PV

technologies throughout the years is shown in Figure 6.1 (NREL, 2015). However, STh technology and systems similar to this project's would not become obsolete for the reasons listed the sections 3.1.1 and 3.1.2. It will also evolve alongside PV technology and as a result, these two competing technologies would offer a much broader array of products to individual consumers and governments to choose from, based on their needs and preferences.

It is also understandable that during the course of this project, new statistics and new technology will emerge with more up-to-date data and upgraded technological products. The most characteristic issue is the statistical data from the various official government services of Cyprus that have been used in the background information Chapter 2 of the project. A distinct example is the information gathered about the Vasilikos Power Station's operation state after its accidental damage in the summer of 2011. The project started in September of that year and the latest information at the time was that the power station was under repair and restoration and that the overall network capacity had become just over the peak demand load during the next several months. Currently, the network has been restored completely with a total capacity of about **910 MW** (on the 9th of November 2014) (EAC, 2014). Nevertheless, changes in data regarding the sectors of house stock, climate, usage of fossil fuels, energy and emissions would not be significant within the project's four-year execution period.

In conclusion, the project succeeded in its technical aim of presenting the design and simulation of three domestic scale STh concept systems in the quest for an alternative solution to domestic PV systems. After gathering raw data from the government's official websites, the project identified the reasons behind Cyprus' energy and emissions problem: the heavy dependence on fossil fuel for electricity production; the Cypriots' tendency to live in large households the vast majority of the being constructed before 2004 and thus lacking proper insulation; the near lack of public transport and the large numbers of privately owned passenger vehicles. The next step was the design and mathematical simulation of the three concept systems, which indicated that the optimal solution of them was Concept System 2 that has the capability of producing renewable electricity throughout the year by storing thermal energy in a latent heat storage tank. The estimation of a typical household's demand profile and the making the system part of the network further improved the optimal solution

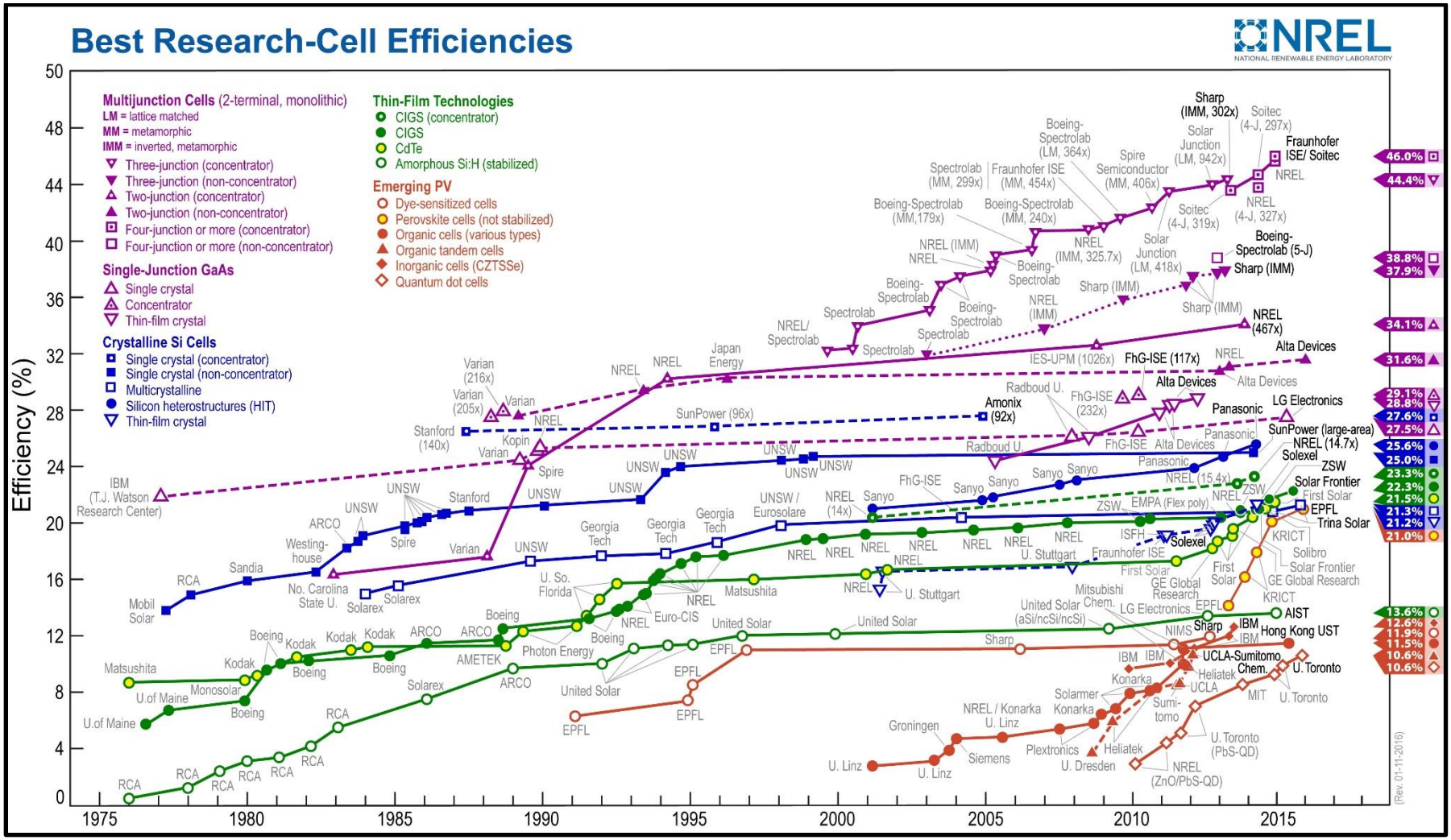

Figure 6.1: Improvement of various PV module technologies (NREL, 2015)

by allowing its reduction in size thus making it more feasible for installation in a typical household in Cyprus. As a result, the novelty aspect of domestic scale installation feasibility was achieved, at least at a theoretical and technical standpoint. The system design also successfully combined the novelty aspect of electricity production with the heating of DHW, by using the waste heat of the electricity production process of the Rankine cycle. The last novelty aspect of using an organic "dry" siloxane compound for the Rankine cycle's working fluid in combination with an IHE succeeded in raising the thermal-to-electrical efficiency of the optimal system to around **25%**. This overall efficiency percentage proved that STh system at temperatures as low as **400℃** could be more efficient than the acclaimed most efficient PV solar collector (around **21%**), rendering STh a potential competitor of PV in the domestic sector.

Overall, the positive contribution of this project is that it indicated the most important problems that cause the increase of electricity demand and emissions in Cyprus that the government could address. Moreover, exploiting the already existing EAC national network the project indicated that it is feasible for a domestic STh system to be installed in the typical household in Cyprus and operate around the year, reducing the emission levels and demand in fossil fuel per household. The system proved to be more efficient than current PV systems and probably less complex. However, the project failed in making financial comparisons between the optimal solution and a similar sized PV system. Even if with the reduced size after the using the network's coincidence factor, the main components (PTSC, turbine and synchronous alternator) for assembling the optimal system either do not exist or they are not within the project's specification. For this problem to be solved, a group of researchers would need to develop prototypes of the system's components, conduct tests and then mass produce and install in actual households under real conditions. For this reason, this project could not contain any acquisition/maintenance cost and investment analysis thus it could not conclude if its optimal STh system is more economical than a similar sized PV system. More research and development is needed beyond the scope of this PhD Thesis.

Reference List

Electricity Authority of Cyprus (EAC), Operations (2014) ***Generation.*** [Online] Available at: https://www.eac.com.cy/EN/EAC/Operations/Pages/Generation.aspx [Accessed: 06 April 2015].

National Renewable Energy Laboratory (NREL) (2015) ***Best Research-Cell Efficiencies.*** Available at: http://www.nrel.gov/ncpv/images/efficiency_chart.jpg [Accessed: 14 January 2016]

Tsoutsos, T.; Frantzeskaki, N. & Gekas, V. (2005) 'Environmental impacts from the solar energy technologies', ***Energy Policy*****, 33, pp. 289 – 296.**

Zimmermann, Y. S.; Schäffer, A.; Hugi, C.; Fent, K.; Corvini, P. F. X. & Lenz, M. (2012) 'Organic photovoltaics: Potential fate and effects in the environment', ***Environment International*****, 49, pp. 128 – 140.**